A STUDY OF FRACTIONAL EXTRACTION IN A SCHEIBEL COLUMN

By

GURASHI ABDALLA GASMELSEED

A Thesis Submitted to the University of Aston in Birmingham for the Degree of Doctor of Philosophy.

Department of Chemical Engineering
University of Aston in Birmingham

July 1985

DEDICATION

To My Father, My Mother and

My Beloved Country, The Sudan.

THE UNIVERSITY OF ASTON IN BIRMINGHAM

S U M M A R Y

A STUDY OF FRACTIONAL EXTRACTION IN A SCHEIBEL COLUMN

GURASHI ABDALLA GASMELSEED

PhD - JULY 1985

A study of liquid-liquid equilibria for both ternary and quaternary combinations of the quaternary system, water-acetic acid-n-butanol-n-hexane have been made and correlated. The literature pertaining to the liquid phenomena, and contactors, liquid-liquid equilibrium equations such as the NRTL, the UNIQUAC and the UNIFAC as well as the relevant mathematical models have been reviewed.

Experiments were then carried out to investigate and study the column hydrodynamics without mass transfer in order to specify the experimental conditions for further work.

Based on the results obtained from the column hydrodynamics without mass transfer, a two-level factorial experiments were made to study the effects of the various factors that have the greatest influence on the column performance, these factors are mainly: The speed of agitation, feed concentration, phase ratio and feed flow rate.

Having specified the column hydrodynamics for non-mass-transfer and the statistical data made accordingly, further investigations were designed to settle any doubt raised by the statistical analysis, through the proper choice of the range of the levels of the relevant factors. The factors needed to be further investigated were the agitator speed and the feed flow rate.

The overall efficiency, the drop size, drop size distribution and the hold-up volume of the dipersed phase were investigated at various levels of speeds of agitation and feed flow rates. The drop size in both, with/without mass transfer experienced an appreciable decrease with the speed of agitation, but with larger size in the absence of mass transfer at the same conditions. The hold-up volume was also affected by the presence of solute transfer and it was lower in absence of solute transfer than that in the presence thereof at the same experimental conditions. On the other hand the overall efficiency reached a maximum value at a certain speed and then decreased, this decrese in efficiency after a maximum value thereof was realised in all runs, with different feed flow rates at a speed of (650-750 r.p.m.).

Key words: Scheibel Column,
Fractional Extraction,
Overall Efficiency.

ACKNOWLEDGEMENTS

I wish to express my gratitude and thanks to Professor G V Jeffreys, the Head of the Department of Chemical Engineering, and Professor M A Fahim of Kuwait University, Chemical Engineering Department, for their invaluable supervision, support, constructive criticism and encouragement.

I also wish to thank Dr C J Mumford for his supervision and interest, and my former students at Kuwait University for their help and co-operation.

CONTENTS

CHAPTER 4 MASS TRANSFER FUNDMENTALS

CHAPTER 5 FRACTIONAL EXTRACTION

CHAPTER 6 LIQUID-LIQUID EQUILIBRIA

CHAPTER 7 EXPERIMENTAL DETERMINATION OF LIQUID-LIQUID EQUILIBRIA

CHAPTER 8 MATHEMATICAL MODELS

CHAPTER 9 EXPERIMENTAL INVESTIGATION

CHAPTER 10 MASS TRANSFER STUDIES

CHAPTER 11 CONCLUSION AND RECOMMENDATION

LIST OF TABLES

LIST OF FIGURES

CHAPTER ONE

INTRODUCTION

1.0 INTRODUCTION

Fractional extraction is a process employing counter-current flow to separate two solutes dissolved in a solvent by means of another suitable solvent partially miscible in the former. Recently fractional extraction has made steady progress, new types of columns have been designed, old types have been further investigated and improved to allow better selection of an extractor that is most suitable for a specific separation problem. Columns with mechanical energy input, such as, the Scheibel Column, are generally preferred as they improve the dispersion quality and give a large interfacial area, hence improving the separation efficiency. Investigations have been directed to contactors with centrally positioned agitators, wherein packing or plates are installed to separate the fluid dynamics and mass transfer as well as to minimise the backmixing effect between the adjacent stages. The Scheibel Column consists of alternative calming and mixing sections with a centrally located shaft mounted with agitators. The packing between the stages gives additional extraction and a stage is considered to consist of a mixing and calming section, thus the efficiency of such stage can be better than one theoretical stage, provided that perfect mixing is realised.

Multi-component liquid/liquid extraction is defined as the unit operation in which either:

1. The added solvents are mixtures.
2. The feed contains two or more components.
3. The feed solution and the solvents are at least partially immiscible.

Although mixed solvents are practically used, they could be treated as a single solvent, except in cases wherein the concentration of the solutes are very high and their effect on miscibility is considerable. Multi-component liquid/liquid extraction is an important industrial extraction operation, and the equilibria of the multicomponent chemical system provides an important basis for the design of industrial extraction process. Over the years, ternary and quaternary liquid/liquid equilibria have been well investigated, but the methods of representation were rather tedious and cannot be directly inserted into the computer for stage-to-stage calculation. Hence correlation models, based on the experimental equilibrium tie line data have been developed. The single binary quaternary model, coupled with Hand's equation is used in this work for correlation of the quaternary system undertaken. The correlation models were used in the calculation of the stage-to-stage composition.

Column hydrodynamics have a considerable effect on performance, and as flooding conditions are the limiting maximum that should only be approached within a suitable working limit, they must be specified at various speeds, feed flow rates and phase ratios. The drop size, drop size distribution and the dispersed phase hold-up must be investigated and related to the performance of the column at the prevailing operating conditions.

In this work, the equilibrium data of the chemical system undertaken were determined and correlated. The flooding limits were specified at different operating conditions and the effect of the various factors were investigated and their significance on the column performance and efficiency was studied.

CHAPTER TWO

LIQUID-LIQUID EXTRACTION EQUIPMENT

2.0 LIQUID-LIQUID EXTRACTION EQUIPMENT

2.1 Equipment Selection

In the absence of prior experience the selection of a suitable contactor to achieve a given duty involves a complex decision whether on a pilot plant or full scale basis. The difficulty of selection arises from the availability of a wide range of contactors and the large number of design variables. An attempt to rationalise the selection procedure is Pratt's scheme wherein numerical ratings were allocated to each extractor against each design requirement. More recently Oliver (9) has discussed the general criteria for the selection of contactors and Hanson (10) has made a single form of chart that provides broad guidance to selection.

A modified and updated version of Pratt's selection chart (8) is presented in Table 2.1 and a summary of the features and field of industrial application of commercial contactors as given by Lo (10) is presented in Table 2.2

However, industrial liquid-liquid contactors may be classified in compliance with the construction and the operating chracteristics, into two major types:

(1) Stagewise contactors, in which the liquids are mixed, extracted and settled. Examples of this type are the mixer-settler, the sieve plate and the Scheibel columns.

TABLE 2.1 : EXTRACTOR SELECTION CHART

Design Requirements	Gravity-Separated Extractors: Continuous Contact: Non-Mechanical			Gravity-Separated Extractors: Continuous Contact: Mechanical		Gravity-Separated Extractors: Discontinuous Contact: With Settling: Without Inter-Stage Settling: Mechanical			Gravity-Separated Extractors: Discontinuous Contact: With Settling: Non-Mechanical	Gravity-Separated Extractors: Discontinuous Contact: With Settling: Mechanical			Gravity-Separated Extractors: Discontinuous Contact: With Settling: Mixer-Settlers: Horizontal		Gravity-Separated Extractors: Discontinuous Contact: With Settling: Mixer-Settlers: Vertical		Centrifugally Separated: Continuous Contact		Centrifugally Separated: Mixer Settler	
Ref. Description	A1 Spray Column	A2 Baffle Plate Column	A3 Packed Column	B1 Pulsed Column	B2 Raining Bucket Contactor	C1 Rotary Agitated Columns	C2 Reciprocating Plate Column	C3 Pulsed Plate Column	D1 Perforated Plate Column	E1 Sheibel Column	E2 ARDC Column	E3 Rotary Film Contactor	F1 Pump Settler	F2 Agitated Mixer-Settlers	G1 Pump-Settler	G2 Agitated Mixer-Settlers	H1 Perforated Plate	H2 Film Flow Type (deLaval)	J1 LUWESTA	J2 ROBATEL
1 Total throughput																				
0.25m^3/hr	3	3	3	3	3	3	3	3	3	3	3	1	0	1	0	1	3	1	0	0
0.25-25m^3/hr	3	3	3	3	3	3	3	3	3	3	3	3	1	3	1	3	3	3	1	1
2.5-25m^3/hr	3	3	3	3	3	3	3	3	3	3	3	3	3	3	3	3	3	3	3	3
25-250m^3/hr	3	1	3	3	1	3	1	1	3	1	1	1	3	3	3	1	0[a]	0[a]	0[a]	0[a]
250m^3/hr	1	0	1	1	0	1	0	1	1	0	0	1	5	5	1	1	0[a]	0[a]	0[a]	0[a]
2 NTS																				
1.0	5[b]	3	3	3	3	3	3	3	3	3	3	3	3	3	3	3	3	3	3	3
1-5	1[c];0	3	3	3	3	3	3	3	3	3	3	3	3	3	3	3	3	3	d[d]	3
5-10	0	3	3	3	3	1	3	3	3	3	3	1	3	3	3	3	1[a]	1	0[a]	3
10-15	0	1	1	3	1	1	3	3	1	3	1	1	3	3	1	1	0[a]	0[a]	0[a]	0[a]
15	0	1	1	1	1	1	1	1	1	1	1	0	2	3	1	1	0[a]	0[a]	0[a]	0[a]

Table continued/over

Table 2.1 - Continued

3 a)Physical Properties[g] $(\sigma/\Delta\rho g)^{\frac{1}{2}} > 0.60$	1	1	1	3	1	3	3	3	1	1	3	3	3	3	3	3	5	5	5	5
b)Density Difference $0.05(\Delta\rho) > 0.03 g/m^3$	3	3	3	0	3	0	0	0	1	0	1	3	1	1	1	1	5	5	5	5
c)Viscosity μ_c and/or $\mu_d > 20cP$	1	1	1	1	1	1	1	1	1	1	1	1	1	1	1	1	1	1	1	1
4 Slow Heterogeneous Reaction $k_1 < 4 \times 10^{-5}$ m/s	0	1	1	3	1	3	3	3	1	3	3	0	0	3	0	3	3	3	3	3
5 Slow Homogeneous Reaction $t_{\frac{1}{2}}$=0.5-5 min >5 min	0	0	0	0	1	0	0	0	1	0	0	0	3	5	3	3	0	0	0	0
6 Extreme Phase Ratio F_d/F_c <0.2 or >5	1	1	1	1	3	1	1	1	3	1	1	3	1	5[e]	1	5[e]	3	3	3	3
7 Short Residence Time	0	0	0	1	0	1	1	1	0	0	0	0	0	0	0	0	5	5	3	3
8 Ability to Handle Solids Trace(< 0.1%in feed)	3	3	1	1	5	3	3	3	1	1	1	5	3	3	3	3	1	1	1	1
Appreciable (0.1%in feed)	1	1	1	1	3	3	3	3	0	0	0	5	1	1	1	1	1	1	1	1
Heavy (>1%in feed)	1	1	0	0	1	1	1	1	0	0	0	5	1[f]	1[f]	1[f]	1[f]	0	0	1	1

Table continued/over

Table 2.1 - Continued

9 Tendency to Emulsify																						
Slight	3	3	1	1	3	1	1	1	3	1	1	3	1	1	1	1	5	5	5	5		
Marked	1	1	1	0	1	0	0	0	1	0	0	1	0	0	0	0	3	3	3	3		
10 Limited Space Available																						
Height	0	1	1	1	5	1	1	1	1	1	1	3	5	5	0	0	5	5	5	5		
Floor	5	5	5	5	0	5	5	5	5	5	0	0	0	5	5	5	5	5	5	5		
11 Special Materials Required (Metals stainless steel, Ti, etc.)	5	3	5	5	3	3	3	3	3	3	3	3	3	3	3	3	5	5	5	5		
Nonmetals	5	3	5	1	1	0	0	1	1	0	0	1	1	5	1	1	0	0	0	0		
12 Radioactivity Present Weak																						
(Weak mainly α , β)	5	5	5	3	1	1	1	3	3	1	1	1	3	5	3	1	1	1	1	1		
(Strong, γ)	5	5	5	3	0	0	0	3	3	0	0	0	3	5	1	0	0	0	0	0		
13 Ease of Cleaning	5	3	1	1	3	3	3	3	1	1	3	5	3	3	3	3	1	3	3	1		
14 Low maintenance	5	5	5	3	3	3	3	3	5	3	3	3	3	3	3	3	1	1	1	1		

KEY:
a Multiple Units in series and/or parallel can be used.
b For immeasureably fast homogeneous reaction.
c For diameters < 15C.
d Two or three stages only in single machine.
e With recirculation of separated phase to mixer.
f Requires provision for solids removal from settler.
g See text for effect of direction transfer.

TABLE 2.2

SUMMARY OF FEATURES AND FIELDS OF INDUSTRIAL APPLICATION OF COMMERCIAL EXTRACTORS[a].

Types of Extractors	General Features	Fields of Industrial Use
Unagitated Columns	Low capital cost, low operating and maintenance cost, simplicity in construction, handles corrosive material.	Petrochemical, Chemical.
Mixer-Settlers	High stage efficiency, handles wide solvent ratios, high capacity, good flexibility, reliable scale-up, handles liquids with high viscosity.	Petrochemical, nuclear, fertiliser, metallurgical.
Pulsed Columns	Low HETS, no internal moving parts, many stages possible.	Nuclear, petrochemical, metallurgical.
Rotary-Agitation Columns	Reasonable capacity, reasonable HETS, many stages possible, reasonable construction cost, low operating and maintenance cost.	Petrochemical, metallurgical, pharmaceutical.
Reciprocating-Plate Columns	High throughput, low HETS, great versatility and flexibility, simplicity in construction, handles liquids containing suspended solids, handles mixtures with emulsifying tendencies.	Pharmaceutical, petrochemical, metallurgical, chemical.
Centrifugal Extractors	Short contacting time for unstable materials, limited space required, handles easily emulsified material, handles systems with little liquid density difference.	Pharmaceutical, nuclear, petrochemical.

(2) Differential contactors, wherein continuous contacting between the phases is realised and the phase compositions change continuously. Examples of this type of equipment are the packed columns and the mechanically agitated contactors.

2.2 The Scheibel Column

The schematic diagram of a typical Scheibel column is shown in Figure 2.1. The column consists of alternate calming and mixing sections with a centrally located shaft upon which are mounted the agitators. The calming section generally consists of a woven wire mesh which acts as an entrainment separator for the two liquids. The heavier phase is introduced at the top of the column and flows downwards through the packing to the mixing chamber where it is brought into intimate contact with the lighter liquid by agitation in the chamber. It then passes downwards through the packed calming/coalescing section counter-currently to the lighter liquid which is introduced at the bottom of the column and flows upward there through. The detailed study of flow indicates that if perfect contact is obtained in the mixing section, and total coalescence of the dispersed phase is achieved in the packing the stage efficiency may approach unity through enhanced mass transfer resulting from the reformation and

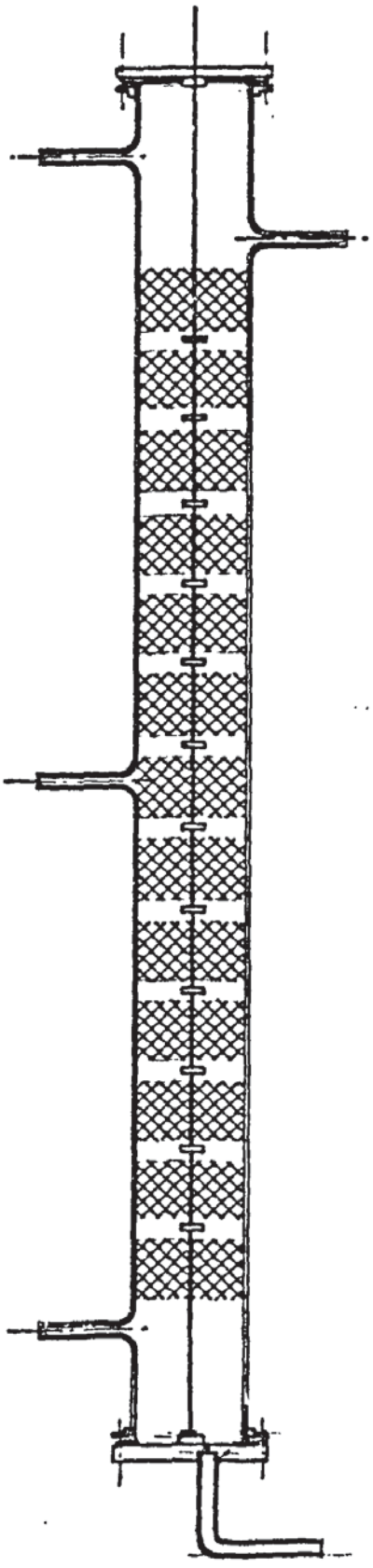

Figure 2.1 A Typical Scheibel Column

subsequent coalescence of drops of the dispersed phase. That is, by considering a stage as being composed of a single mixing and packed section, the efficiency of such a stage might easily be expected to be greater than one theoretical stage (11, 12).

The scheibel extraction column was patented in 1950 (12) by Hoffman-La Roche Company. The first unit that was constructed consisted of a single mixing chamber in a 5.08cm glass column with a 8.16cm height packing above and below the mixing chamber and this unit gave 1.3 theoretical stages on a simple extraction operation. This efficiency was based on the assumption that a mixing section and a packing section comprised one stage.

Generally, in the interally agitated columns the height required for a theoretical stage increases with diameter. Scheibel (11) reported performance data 0.2×10^{-2}m and a 30.5×10^{-2}m diameter column and concluded that the HETS on this type of column varies with the square root of the diameter. This indicated that the flow pattern follows a geometrically similar shape when scale-up is undertaken on the basis of dimensional similitude.

There are different designs and arrangements of scheibel columns, and these are discussed below.

2.2.1 The First Scheibel Column

The first (1) scheibel column design is the one shown in Figure 2.2. In this column the counter-current liquid phases are contacted in the mixing chambers with flat bladed turbine agitator and separated in the packed calming sections. The column is a typical design of the first concept wherein the wire mesh packing isolates the agitator flow patterns between the adjacent mixing chambers in order to prevent the loss of efficiency due to backmixing, it also provides the necessary baffling to remove the rotational motion imparted to the liquid mixture by agitation. The packing could be made of any conventional tower packing, but the smaller void volume restricts the flow through such packing and reduces the baffling effect.

The vertical components of the flow pattern in the mixing chamber is indicated in Figure 2.3. This figure shows the difficulties involved in scale-up of the relevant design. However, if the diameter of the column is doubled, the solvent capacity, which is a function of the cross-sectional area, would be increased four times, but if the geometry of the flow pattern is retained, the volume of the packing required will increase eight times (10). Hence an economic problem arises, as the wire mesh packing will increase, in fact it becomes the most expensive item in the larger

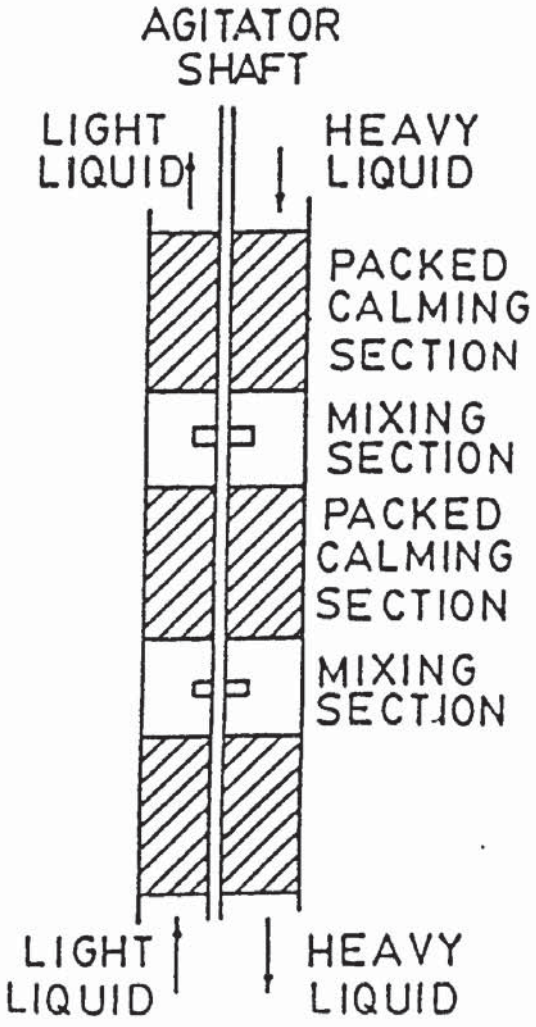

Figure 2.2 Schematic Diagram of the First Scheibel Column

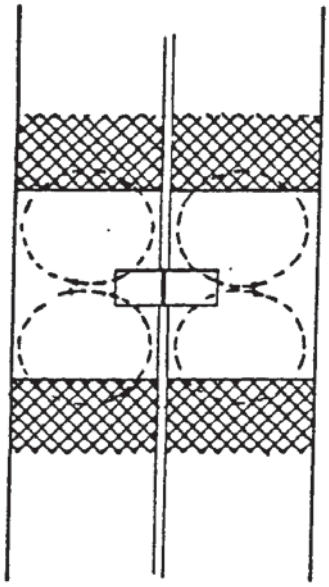

Figure 2.3

Vertical Components of Flow Pattern in Mixing Stage of First Scheibel Column.

diameter columns. When scale-up is to be made, this fact makes this type of column non-commercial on a large scale, and the largest scheibel column constructed is believed to be 1.0 meter in diameter (12).

However, the simplicity and high efficiency makes this type of design most suitable for pilot plant and laboratory columns of up to 3.0×10^{-2}m in diameter, it is available in sizes down to 2.5×10^{-2}m diameter, which makes it suitable for research and process development studies in laboratories and pilot plants.

2.2.2 The Second Schiebel Column

Due to the economic problem pertaining to scale-up of the first type of scheibel extractor, a modified column was developed to provide baffling in the mixing chamber and at the same time minimises the height of a large-diameter multistage column with a given number of theoretical stages (12). The modified model is shown in Figure 2.4, wherein the vertical flow of the phases in the mixing chambers is diverted by horizontal annular baffles at the wall of the column, thereby preventing mixing with the circulation in the adjacent mixing chambers. In order to eliminate the rotational motion and to ensure complete mixing across the column, the liquid mixture is pumped between two inner annular

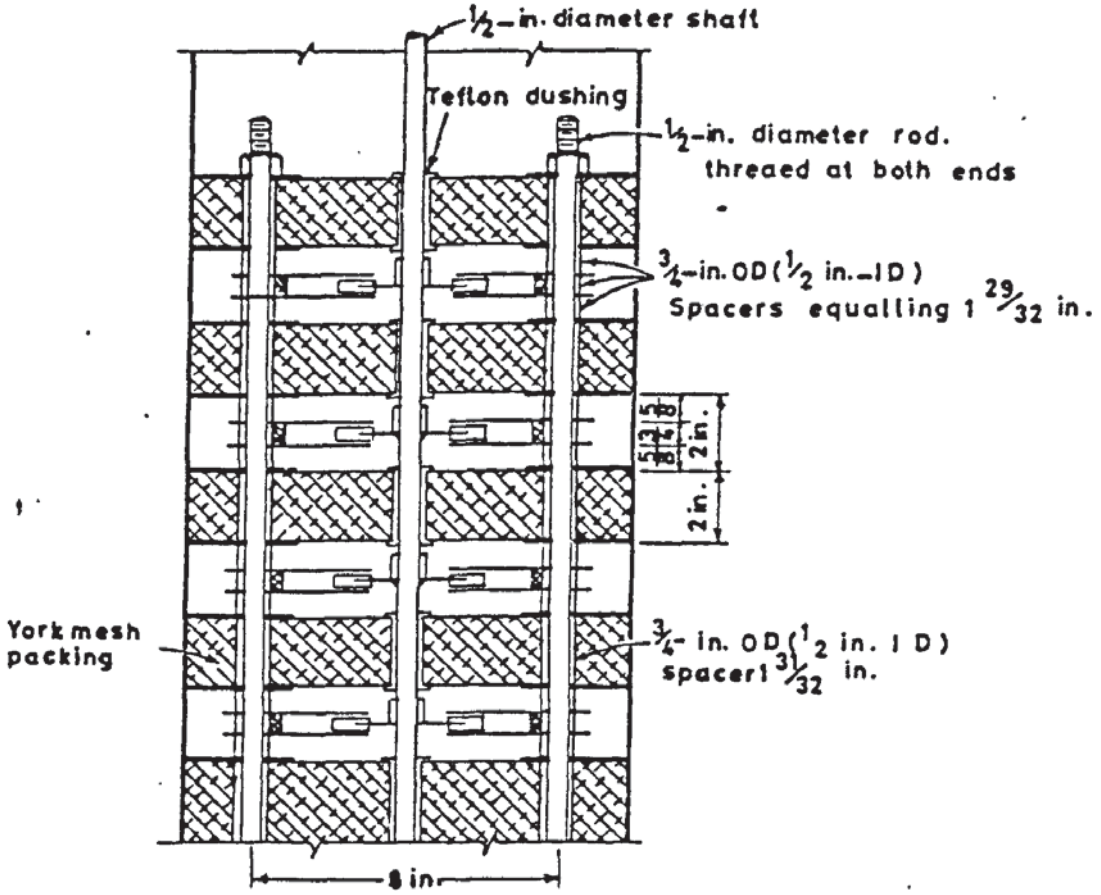

Figure 2.4

Modified Extraction Column with Baffled Mixing Stages and Intermediate Mesh Sections.

baffles with several layers of wire mesh between them at the discharge of the impeller blades. This mesh has a dual purpose, it does not only eliminate the rotational motion imparted by the impeller, but also serves to break-up the liquid droplets, hence increasing mass transfer between the relevant phases. The amount of such wire mesh must be adequate to affect the baffling, and would increase in amount when the relevant liquid phases require high speed agitation to provide complete mixing. This design reduces the amount of wire mesh required between the mixing stages to a minimum, and for liquid systems with low interfacial tension, it is economical up to 1.0 meter in diameter (11-13).

2.3 Application of the Scheibel Column

In all extraction columns a compromise is made between capacity and efficiency. The concept of a theoretical stage is based on mixing the counter-current phases to achieve equilibrium and then separating them completely. The first step requires a large contacting surface area or a long contacting time or both. The smaller the droplets size in the dispersed phase, the greater the interfacial area and probably the rate of mass transfer between the relevant phases, but according to Stokes law relationships, smaller drops will move more slowly counter-currently to the continuous phase, thus

reducing throughput and increasing contact time. However, the use of external power for mixing can provide the full range of capacity up to suitable emulsion formation. The residence time of the dispersed phase in an agitated column is a function of the power input. High power inputs increase the approach to equilibrium between the phases by increasing:

(1) The interfacial area thereby assisting mass transfer rate,

(2) The residence time of the droplets in the mixing and calming sections.

Effect (2) reduces the capacity of the column, and excessive speed of agitation at any given throughput will result in a flooding condition where a second liquid interface may appear in the column at the end of the column opposite to that at which it is being controlled. Alternately, phase inversion may occur in one of the stages that will ultimately result in the second interface forming at the opposite end of the column. The capacity of an agitated extraction column is very sensitive to the interfacial properties of the relevant system. The presence of surfactants or insoluble materials that collect at the interface will tend to stabilise emulsion and require a longer time for phase separation. Flooding velocities are functions of the power input such that the extractors will have a high

efficiency and low throughput at high agitator speeds and a low efficiency and high throughput at low agitator speeds. For column diameters greater than 5.0×10^{-2}m (10), throughput in the range of 20-40 m^3/m^2 of column cross-section will normally result in maximum stage efficiencies. Optimum column performance is always obtained by dispersing the phase flowing at the smaller volume rate, but it may be practical to sacrifice some capacity and efficiency to operate at constant conditions then to periodically vary the agitator speed between cleanings.

If sufficient packing is provided and if the power input is increased, the packing will serve to prevent the overlapping of the flow patterns in the mixing steps and also will provide sufficient volume for complete phase separation between the stages. The stage efficiency varies with packing height as shown in Figure 2.5 made in a 2.5×10^{-2} m diameter extraction column, for extracting acetic from water with methyl-isobutylketone, a typical system that has a low interfacial tension (11,12), also shown in Figure 2.5 are the data for dehydration of ethyl alcohol with the use of both methyl n-amyl ketone-glycol and xylene-glycol solvent systems, which are typically high interfacial tension systems, and higher viscosity.

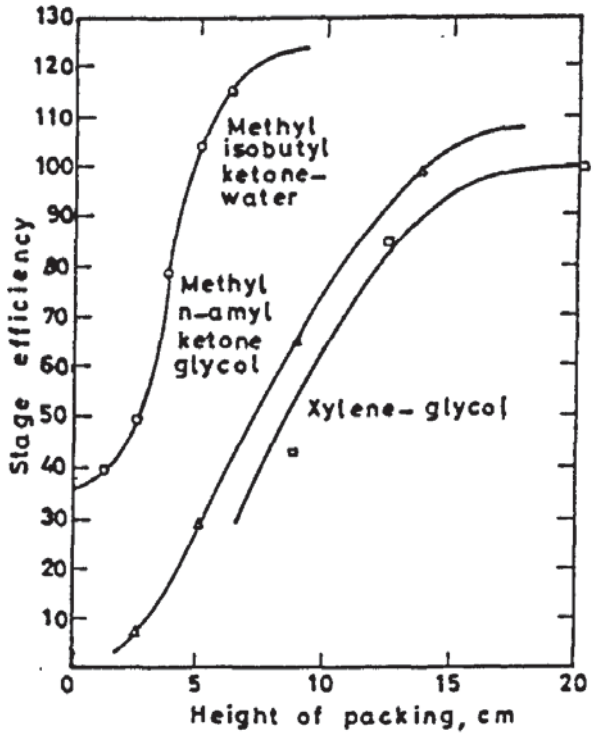

Figure 2.5

Variation of Stage Efficiency With Height of Packing.

It has been reported by Hanekamp and Burkhart (14) that when the agitator was operated at very low speed, the scheibel column was not as effective as the packed column, confirming the fact that the wire mesh packing eliminates the rotation flow and isolates the individual flow patterns in the mixing stages. Mass transfer was believed to be mainly due to the coalescence and reformation of the droplets in the packing. Honekamp and Burkhart (14) also reported that the dispersed phase hold-up increased with increasing agitator speed and was very proportional to the dispersed phase flow rate at constant continuous phase flow rate.

2.4 The Scale-Up Procedure

For scale-up it is required to provide the performance data of throughput and column efficiency. In general the smaller the capacity of the laboratory column, the greater will be the scale-up factor. The usual scale-up procedure is based on providing the same stage efficiency in the test column and adjusting the power input accordingly. If the test column contains sufficient stages, it can also be used to confirm the process design as well as provide the ncessary scale-up data. If the same power input per unit volume of fluids is maintained in the larger diameter columns, the radial velocities in the mixing stages will be greater in the larger-diameter columns.

This factor limits the diameter/height ratio in large columns. The larger residence time in the mixing stages permits operation at lower power inputs, and this is a prime factor in providing greater throughput capacity (10).

Pilot scale testing is an inevitable preliminary study to a full-scale extractor design for any new commercial process. The pilot test provides the following qualitative and quantitative piece of information for scale-up and design of the relevant extractor:

(1) Total throughput and agitation speed.

(2) HETS or H.T.U.

(3) Stage efficiency.

(4) Hydrodynamic conditions i.e. drop size, droplet dispersion, phase separation, flooding, phase inversion and drop size distribution.

(5) Slection of dispersed phase or mass transfer direction.

(6) Solvent feed ratio.

(7) Material of construction and its wetting characteristics.

Pilot-scale performance and tests should be carried out under similar process conditions in an extractor of design and material of construction similar to those of a large-scale contactor. It is important that actual process feed and solvent be used in the

tests because the process streams usually contain impurities. Samples and measurement of extractor parameters should be taken only after the steady state has been established in each run. Pilot-scale studies should cover a wide range of flow rates and phase ratios and provision should be made for solvent recovery and solvent recycle. The study should be concluded with extended runs, carried out to confirm and specify the optimum proccess.

The factors that affect scale-up are:

- properties of the chemical system
- total throughput
- solvent-feed ratio
- Mass transfer direction
- phase to be dispersed
- Materials of construction and its wetting effects.
- Degree and type of mechanical agitation
- Drop size and drop size distribution
- Rate and boundary effects
- Axial-mixing or longitudinal dispersion

However, upon designing a large-scale contactor, pilot-scale data should be carefully examined, as the relevant particulars on drop size, drop size distribution and axial mixing are sometimes excluded or estimated. These data are most important for the design of some extractors and depend more strongly on the scale of the relevant equipment, the size of the agitator and its height between each compartment and location.

CHAPTER THREE

FUNDAMENTALS OF COLUMN DESIGN AND PERFORMANCE

3.1 Internal Geometry

Scheibel multistage extraction columns can be designed to satisfy specific application requirements. Design emphasis is on versatility and economy. All Scheibel columns consist of a central vertical shaft to which are attached agitators that are mounted between wire mesh sections to affect counter-current mixing and phase separation with the result that all operations in a multi-stage mixer-settler extraction system are incorporated in a single column. Baffling action and phase separation are achieved by the wire mesh packing.

Simple designs (12) have diameters 2.5×10^{-2}m with any number of stages. Early studies on the use of vertical baffles in the mixing sections of such a column indicated that, although these baffles eliminated the rotational motion of the fluids and probably improved the mixing, they transformed this motion into a vertical motion and necessitated an even greater packed height to isolate the flow patterns of the individual mixing section. It then becomes obvious that horizontal baffles were essential for the best performance of an internally agitated extractor.

In general, however, in internally agitated extractors the height required for a theoretical stage increases with column diameter because of the

tendency of the flow pattern in the mixing section to follow a geometrically similar shape when scale-up is made on the basis of dimensional similitude.

The Scheibel column used in this study is 7.6×10^{-2}m diameter and 1.83m high. Each stage was composed of a calming section of 0.125m high and mixing section of 3.2×10^{-2}m high. The nominal capacity of the column is 38.0 L/hr and the column possessed nine actual stages. The packing is made of wire mesh which provides two effects, firstly it isolates the agitator flow patterns between adjacent mixing zones to prevent the loss of efficiency due to back-mixing, and secondly it provides the necessary baffling to remove the rotational motion imparted to the liquid mixture by the agitator. The packing section is filled with knitted wire mesh packing and it is self supporting.

Coalescence in the calming section is maximised when the dispersed phase preferentially wets the packing surface (15) and coalesces to form liquid films or drops that flow through the voids of packing. Knitted wire mesh packing made of single material are commonly used in Scheibel extractors for coalescence of fine dispersions in the separation zone. The material may be stainless steel or plastic and is selected so as to be wetted by the dispersed phase. Such packing affects partial coalescence of the droplets while allowing counter-current flow of the continuous and dispersed phases.

Figure (2.1) shows the schematic diagram of the Scheibel column, wherein the counter-current liquid phases are contacted in mixing zones and separated in the calming sections. The light phase passes upwards into the mixing stage above while the heavy phase passes down to the stage below. Figure (2.3) shows the vertical components of the flow pattern in the mixing stage wherein rotational motion and consequently mixing is realised depending on the degree of agitation, and the diameter of the agitator blade.

3.2 Packing Material Wetted by the Dispersed Phase

Piper (15) used knitted wire mesh made of propylene that was wetted by the kerosine dispersed phase. On the study of the flow regime pertaining to his systems Piper observed that the drops wetted the packing and coalesced inside the packing, creating a second continuous phase, and left the packing surface in the form of a continuous stream at high flow rate and by a drip-point mechanism at low flow rates. He concluded that the limiting flow was higher when compared with that obtained for packing wetted by the continuous phase.

3.3 Packing Material Non-Wetted by the Dispersed Phase

Lewis et al. (16) observed that there was a critical size of packing above which the exit droplet size was independent of the packing size and type. Bonnet (17) claimed that the exit droplet size was independent of the size of the inlet drop, and that large inlet drops were gradually broken down to some equilibrium size while small inlet drops grew in size by coalescence to attain the same equilibrium drop size. Gayler et al. (18) developed an expression for the critical packing size, thus:-

$$(d_p)_{critical} = 2.42 \left(\frac{\sigma}{\Delta\rho g}\right)^{0.5} \qquad (3.1)$$

Gayler and Pratt (19) correlated the Sauter mean diameter for some organic-aqueous chemical systems in a 1.83m packed section wherein the packing size was greater than the minimum as:

$$d_{32} = 0.92 \left(\frac{\sigma}{\Delta\rho g}\right)^{0.5} \left(\frac{\bar{v}_o \varepsilon \phi_D}{V_D}\right) \qquad (3.2)$$

Where:

$\bar{v}_o$ = Characteristic velocity, defined as the vertical limiting mean droplet velocity at zero continuous phase and at very low dispersed flow rate.

The equation that defined $\bar{v}_o$ (19) is:-

$$\frac{V_d}{\phi D} + \frac{V_c}{1-\phi D} = \bar{t}_{vo}\,(1 - \phi D) \qquad (3.3)$$

It was concluded that the drop size in a Scheibel column is determined by the relevant drop size in the mixing compartment, which mainly depends on the agitator speed and the chemical system properties as well as the mass transfer direction. It is said that the behaviour of the Scheibel column at constant stirrer speed, as far as hold-up is concerned, closely paralled to a packed extraction column.

Piper (15) used 7.6×10^{-2}m packing section made of stainless steel knitted wire mesh packing in a 7.6 cm diameter Scheibel column, essentially wetted by the continuous phase. The packing had 98.75% voidage and the flow characteristics and flooding was studied. Pipers data was correlated by Bonnet (17) who concluded that the data could be represented by straight lines indicating that a general flooding rate correlation could be made from the plot of ($V_c^{0.5}$ vs. $V_D^{0.5}$). Jeffreys et al. (20) extended the previous investigation pertaining to the characteristic drop size in the wire mesh packing by studying droplet break-up and coalescence on different wire mesh packing sections in a 7.6×10^{-2}m Scheibel column. They observed that droplet size distribution in the packing consisted of three groups:

(1) Small droplets passing from one mixing section to the other without being affected.

(2) Droplets that are slightly larger than (1), but less in size than the voids of packing, these are slightly altered when passing from one mixing section to the other.

(3) Droplets that are larger than the mesh size, which collect at the interface of the packing unitl they coalesce to sufficient size to break away, leaving sufficient liquid on the mesh to enhance coalescence.

They also observed the significant effect of void space on flooding velocity of the column using kerosine water chemical systems.

3.4 Power Requirements

Scheibel (13) made the first study on the column using the system MIBK-water-acetic acid and reported that, at low agitator speeds, the stage efficiency was greater at the low throughputs and at high agitator speeds the efficiency was greater at high throughputs. This indicated that there is an optimum power input per unit volume of liquids flowing through the column.

The power input to the agitator shaft was calculated from the speed and torque, and it was found to vary as the cube of the speed, as has been observed for fully baffled tanks at high Reynolds numbers.

Reman (21) considered power requirements on the basis of mixing and he correlated the power number with the disc Reynolds number for the R.D.C. extractor. Scheibel (12) made a general correlation for the power consumption for internal baffled multistage extraction columns as:

$$P = 1.85 \frac{D^5 \rho N^3}{g} \qquad (3.4)$$

And with average density in the mixing section based on about one third hold-up of the dispersed phase. The following equations were made to calculate the power consumed per stage:

$P = 0.132\ N^3$ for water dispersed in O-xylene,

$P = 0.140\ N^3$ for O-xylene dispersed in water,

$P = 0.128\ N^3$ for water dispersed in MIBK,

$P = 0.136\ N^3$ for MIBK dispersed in water,

suggesting that on average $P \simeq 0.134\ N^3$, (Figure 3.4) gives a correlation of stage efficiency of the mixing section as a function of power input and phase ratio. Figure (3.1) shows that the use of excessive power in the mixing stage (13) reduces the efficiency. This is due to the increase in backmixing between the stages that result from both overlapping of the flow patterns and the formation of small droplets that do not coalesce and are entrained to the next stage with the relevant continuous phase. Successive agitation causes back-mixing of the continuous phase and high liquid phase ratios produce backmixing of the dispersed phase.

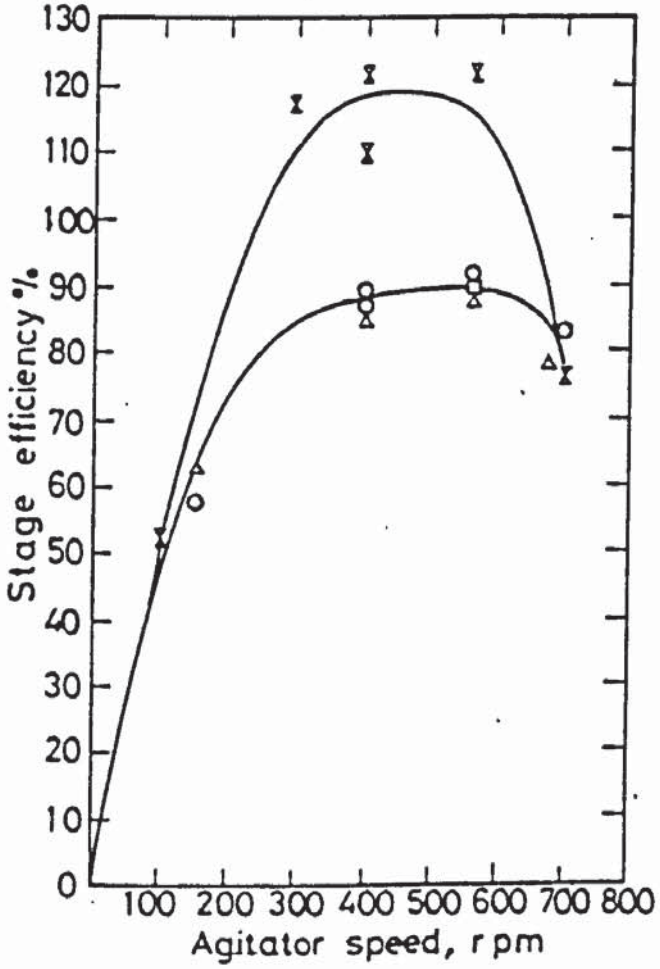

Figure 3.1

Variation of Stage Efficiency with Power Input.

3.5 Column Hydrodynamics

3.5.1 Hold-Up Volume

In order to determine the interfacial area of the dispersion for mass transfer rate estimation ($a = \frac{6\phi_D}{d}$) the following must be specified:

(1) Residence time of the drop in the contactor.

(2) The dispersed phase hold-up.

Usually the phase that preferentially wets the column internals is the continuous phase so that the dispersion consists of discrete (10) droplets moving freely within the continuous phase. If the wetting phase is dispersed this flows as streams or uneven chunks producing a poor dispersion with unpredictable hydrodynamics. The volume of droplets in the contactor during steady state operation is termed as the operational hold-up of the dispersed phase and is generally expressed as a fraction of the total volume or of the effective volume of the column. However, the static hold-up blocked at the junction or elsewhere by the contactors internals has little effect on mass transfer, and it is the operational hold-up that plays the major part. Also as it is easy to determine, hold-up is used rather than the drop residence time for the interfacial area determination.

Several methods are available for the estimation of the hold-up (ϕ_D). The shut-off or displacement method is the simplest known. In this method all feeds and exit lines are simultaneously closed, then the fractional volume of the dispersed phase is measured. Recently a novel sampling technique has been developed (17). This technique consists of suddenly draining a part of the contents of the extraction section to determine the fraction of the dispersed phase after the settlement of the relevant sample. The sampling device could be a probe inserted inside the dispersion (17) or sampling points at different locations, or side tubes fitted along the column may also be used. The size of the sample withdrawn is important as a small sample reduces the precision of the observed hold-up while a large sample may affect the column contents. This method was adopted by Bonnet (17) and more information can be obtained therefrom. Gayler (18) reported that the drop size increases with the phase ratio, and so does the hold-up as the latter is a function of the drop size.

3.5.1.1 Characteristic Velocity

The hold-up has been correlated on the basis of Steinour's analysis (22). The slip velocity concept was reported by Lapidus and Elgin (23) while the relative velocity concept was proposed by Pratt et al. (8). The slip or relative velocity U_s is given by:

$$U_s = \frac{U_c}{1-\phi D} + \frac{U_d}{\phi D} = \bar{U}_o\,(1-\phi D) \qquad (3.5)$$

Where $\bar{U}_o$ = the characteristic velocity and may be identified with the average terminal velocity $(U_t)_{av}$ of the droplet.

However, Bonnet (17) correlated the hold-up with respect to the mean drop size, local energy input per unit mass, Reynold's number of the impeller and the Weber number and reported that:-

$$\frac{d_{32}}{D_1} = K_1(\phi D)\ (Re_1)\ \ (We)\ \ \left(\frac{H_p}{H_M}\right) \qquad (3.6)$$

$$d_{32} = K_1 \times 10^{(1+K_2\phi D)} \times (\bar{t})^{K_3} (HP)^{K_4} \qquad (3.7)$$

where,

$$We = \frac{D_1^3 N^2 \rho_c}{\sigma}$$

$$Re = \frac{D_1^2 N \rho_c \pi}{\mu_c}$$

$$E\bar{t} = \frac{4.4 N^3 D_1^5 \rho_c}{\frac{\pi De^2}{4} H_m \rho}\ ,$$

the above equations can be correlated to determine the constants (K_1, K_2, K_3, K_4 and K_5).

The Figure 4.4 represents the value of the power number for fully developed turbulent flow in a baffled agitated vessel (24). Thus one may predict the hold-up for any given system by determining the parameters specified in the preceding equations using a Linear regression analysis. It is important to observe that the direction of mass transfer affects the droplet coalescence characteristics as well as the mean drop size, hold-up and the characteristic velocity within the contactor due to Marangoni effect and other interfacial instabilities.

3.5.2 Flooding

Regarding counter-current columns, steady operation is possible when the rate of arrival of the droplets does not exceed the coalescence rate at the main interface otherwise droplet build up occurs at the interface, gradually extending over the entire column and leading to flooding (25). Flooding is observed when an interface appears in the column at the opposite end from which it is being controlled. A column floods when the relevant throughput is greater than that can be handled by the column at a specified agitator speed. Flooding can be eliminated by either reducing the agitator speed or reducing the throughput. It should be observed that when a column is operating close to flooding, a sudden upset in the

conditions such as rapid adjustment of the interface may produce an appearance of flooding which will gradually disappear when the disturbing influence is removed.

The value of the limiting flow velocity of both the dispersed and continuous phases, known as flooding points are rather important in column design for the estimation of column diameter. Flooding, if allowed to occur will lead to the entrainment of the dispersed phase with the continuous phase and phase inversion wherein the dispersed phase changes into the continuous and vice versa with the formation of a second interface below the packing section. Flooding rate correlation in packed columns has been well established and many investigators have made correlations predicting flooding rates therein (26).

No successful attempts have so far been made to correlate flooding points for the Scheibel column similar to that made for packed columns (27). The difficulty and reason for failure to obtain similar correlation is that the Scheibel is not a packed column; in fact it is a stagewise contactor similar to the mixer-settler and bubble cap columns.

3.5.3 Phase Inversion

This hydrodynamic effect refers to the interchange of phases in such a manner that the dispersed phase becomes continuous and the continuous phase becomes dispersed. M. Arashmid and Jeffreys (28) reported that the variation in drop size with hold-up confirmed with the Thornton-Bouyatiotes (29) correlation close-up to the phase inversion concentration, but at the vicinity of phase inversion, the drop size increased rapidly with very small additions of the dispersed phase.

When phase inversion takes place in an agitated vessel and the volume fraction at inversion is plotted against the rotor speed (30), a hysteresis effect results, defined by two curves covering a meta-stable or ambivalent region, as shown in Figure (3.2). Figure (3.2) represents inversion characteristics for toluene-water system (30). In this Figure the system can exist as water dispersed only/organic continuous as indicated above curve 1, water continuous only/organic dispersed as below curve 2 and in between the two curves either configuration is possible. If at constant rotor speed the organic phase is added to the organic/water dispersion, inversion would take place on reaching the upper curve and on adding water to water/organic dispersion, inversion will be shown at the lower curve.

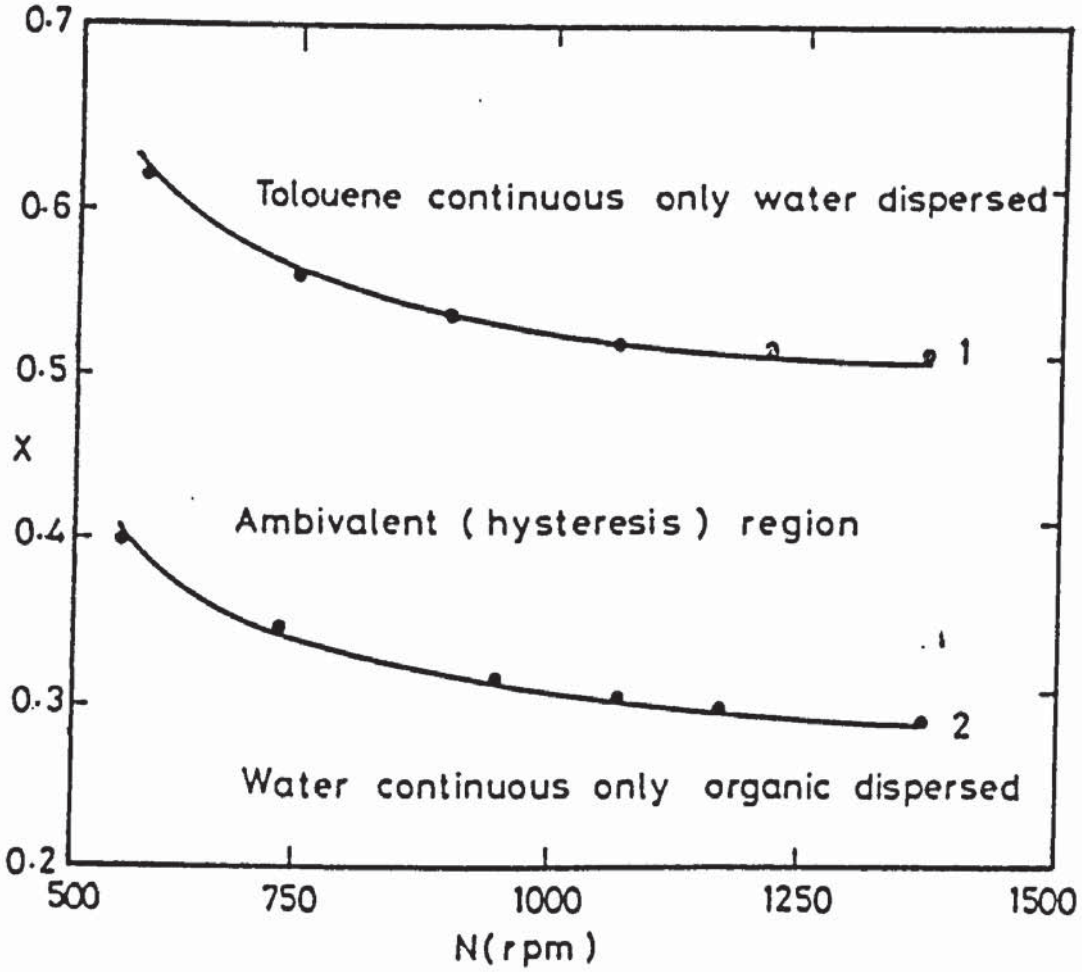

Figure 3.2

Inversion Characteristics For Toluene/Water System (1).

In a later investigation, Luhning et al. (31) showed that the width of the hysteresis gap was critically affected by the interfacial tension and that the lower the interfacial tension, the wider was the hysteresis gap i.e. the greater was the resistance of the relevant system to phase inversion.

Further, Clark et al. (30) studied the effect of the presence of solutes on phase inversion and they claimed that the presence thereof in equilibrium between the phases increased the resistance of the dispersion to phase inversion. This is due to the fact that the solute might lower the surface tension and widen the hysteresis gap. Quinn and Sigloh (32) reported that for a fixed rotor speed, the inversion concentration expressed as volume fraction of the organic phase was given by:

$$\phi = \phi_o + a/p \qquad (3.8)$$

Where ϕ_o = constant

P = power input

3.5.4. Axial Mixing

Pure plug flow of the phases is realised only in extractors in which the phase separation between the stages is virtually complete as in discrete - stage mixer-settler and perforated plate column. However, the performance of other types of extractors is influenced

adversely by departures from plug flow pattern. The factors that contribute to this departure of performance are complex, but can be identified as follows (33):-

(1) Circulatory flow of continuous phase arising from the dissipation of the potential energy of the dispersed phase droplets or films.

(2) Transport and shedding of the continuous phase in wakes attached to the rear of the dispersed phase droplets.

(3) Molecular and turbulent diffusion of the continuous phase in both axial and radial directions along concentration gradients.

(4) Circulation of continuous phase and consequent entrainment of dispersed phase in mechanically agitated contactors.

(5) Chanelling and consequent maldistribution due to the particular characteristics of the relevant contactor geometry.

(6) Non-uniform velocity profiles of one or both phases due to frictional drag of the stationary surfaces.

(7) Variation of droplet velocities as a result of the range of droplet diameters present.

The above first two factors indicate pure backmixing of the continuous phase, but wake shedding stated in factor two occurs only at high Reynolds number of the dispersed phase (Re_d > 150 - 200) and approximated to only 5-10% of the circulatory flow (34). Factors three and four lead to backmixing, particularly the latter is responsible for backmixing of the dispersed phase as well.

Factor six is a consequence of the velocity profile that exists in single phase flow between a stationary surface, wherein the velocity is zero, and the centre of the stream wherein it is a maximum. This effect leads to the distribution of residence times of the fluid elements, which may be also expected to influence the performance of the extractor adversely. Combination of the various effects is more accurately termed axial dispersion.

Axial dispersion can be determined by several methods, such as tracer techniques or concentration profile sampling. Models are then constructed and solved for such effects. Two distinct types of models have been proposed, namely:- The diffusion of solute superimposed on plug flow of the phase (35) and the back flow model, with well-mixed non-ideal stages between which back flow occurs (36). More details with regard to the aforesaid models are discussed in Chapter Eight.

3.6 Droplet Phenomena

The drop size and drop size distribution depend on the method of drop formation, the nature of the interactions between the droplets, the internal geometry of the relevant contactor, the physical properties of the chemical system and the relevant phase ratios.

3.6.1 Drop Break-Up

The change in drop shape or deformation thereof occurs due to the energy supplied by the agitator that circulates and mixes the relevant phases causing impact against the wall of the contactor and between the drop themselves. In agitated columns the break-up of drops may occur when:-

(1) The magnitude of the dynamic pressure acting on the drop counteracts the cohesive surface forces; and

(2) The drop remains for a sufficient period of time in the vicinity of high shear zone.

In compliance with Kolmogoroff (37) theory of local isotropy which states that, in turbulent flow, instabilities in the main flow amplify the existing disturbances and produce primary eddies that have a wave length similar to that of the main flow. Hinze (38) characterised the fundamentals of the droplet break-up by the following two dimensionless groups:-

(a) Weber number $N_{We} = \frac{P}{\sigma/d}$ (3.9)

(b) Viscosity Group $N_{vi} = \frac{Ud/d}{(\rho_d \sigma/d)^{\frac{1}{2}}}$ (3.10)

and that deformation increases with increase in Weber number until, at a critical value of N_{We}, the break-up of the relevant droplet occurs. For break-up to occur from viscous stress the drop size should be small compared with the region of viscous flow (39).

Hinze (38) claimed that, when he studied the droplet break-up due to dynamic pressure fluctuation, changes in velocity over a distance equal to the drop diameter causes development of a dynamic pressure, and that such pressure determines the magnitude of the largest drop pressure. Hinze modified Kolmogoroffs theory (37) to predict the size of the maximum stable drop in a turbulent field to be:-

$$d_{max} = C \left(\frac{g_c \sigma}{\rho_c}\right)^{0.6} \bar{\varepsilon}^{-0.4} \qquad (3.11)$$

where C is a constant, whose value could be determined in accordance with the specific condition prevailing in the relevant mass transfer process and the tendency of the drop to break-up or coalesce, as suggested by Strand et al. (33).

Droplet break-up mechanism in a given hydrodynamic field may be considered in terms of energy dissipation (40). If the drop size is greater than the minimum eddy size, the break-up rate depends mainly on the energy dissipation rate per unit mass of fluid as related by equation (3.9) derived by Hinze. Table (3.1) summarises the relationship for E (which is the power dissipated per unit mass of fluid) for some known type of contactors.

3.6.2 Droplet Coalescence

3.2.6.1 Single Drop Coalescence

This pertains to coalescence without having the complexities interdroplet interactions. The process occurs in successive sequences as follows (10):-

(1) The drop and the interface are deformed as the drop approaches thereto.

(2) Oscillation of the drop at the interface is dampened and a film of continuous phase is held between the drop and its bulk phase.

(3) The film is thinned by a drainage and then ruptured, initiating the drop coalescence process. The rupture hole expands and the drop contents flow either completely or partially into the main phase.

(4) The mean time t, also termed the rest time comprises the mean of several observations of the total time taken for stages 1-3. The time taken for stage 1 is called the predrainage time and that for stage 2 and 3, the drainage time. The coalescence time denotes the sum of predrainge and drainage time. The time taken for film removed in stage 4 is found to be small (0.06 - 0.08 secs) and therefore could be neglected (112). Most of the coalescence time is occupied by the process of drainage, and the rate of coalescence is controlled by the drainage and rupture of the film of continuous phase held between the drop and the interface. The diameter of this film (d_f) is related to the drop diameter (d):

$$\frac{d_f}{d} = 0.707 \left(\frac{d^2 \Delta\rho g}{\gamma}\right)^{0.5} \qquad (3.12)$$

Rupture of the film occurs after an elapse of a time (t_o) at some minimum thickness (h_o), which depends on the physical properties of the relevant system.

The interdrop coalescence in the agitated zone is one factor determining the equilibrium drop size in the extractor and also the drop size required at the interface near the dispersed phase outlet must be such

as to realise phase separation. In the agitated zones the drop size depends on the balance between interdrop break-up and coalescence. The size of the drop so formed determines the interfacial area and drop rise velocity.

The coalescence of a liquid drop at a flat interface is controlled mainly by:-

(1) Drop size,

(2) Distance of fall of the drop to the relevant interface,

(3) Curvature of the drop size interface.

(4) Density difference between the phases

(5) Viscosity of the phases,

(6) Interfacial tension effects,

(7) Temperature effects.

(8) Solute transfer effect, i.e. , direction of mass transfer.

Jeffreys et al. (10) suggested the following correlation on the basis of dimensional analysis of the major controlling variables.

$$\frac{\gamma \bar{t}}{d\mu_c} = 1.32(10)^5 \left(\frac{L}{d}\right)^{0.18} \left(\frac{d^2 \Delta\rho g}{\gamma}\right)^{0.32} \qquad (3.13)$$

3.6.2.2 Drop-Drop Coalescence

Drop-drop coalescence is a complex process and the knowledge thereof is rather limited. However, various models have been proposed (42) and with some omissions the most significant is the effect of internal circulation of the drops on the coalescence time or film thinning process. Neilsen et al. (43) measured coalescence time of drops at a flat interface, and claimed progressive increase of coalescence time with surfactant concentration. The surfactant stabilises the drop and damps out circulation and reduces the film drainage rate as well.

Groothius et al. (44) demonstrated the effect of solute transfer on the coalescence of pairs of drops held at nozzle tips opposite to each other within a tank holding the continuous phase. They indicated that coealscence was promoted by the solute transfer from the dispersed phase to the continuous phase and that when the solute diffused from the continuous phase to the droplets coalescence was strongly inhibited. Treybal (45) showed that the interfacial tension is reduced by the presence of the solute; hence, for dispersed to continuous (d → c) transfer there is a region of low interfacial tension as shown in Figure (3.3a) leading to promotion of film drainage and rapid coalescence. On the other hand, for transfer from the continuous phase

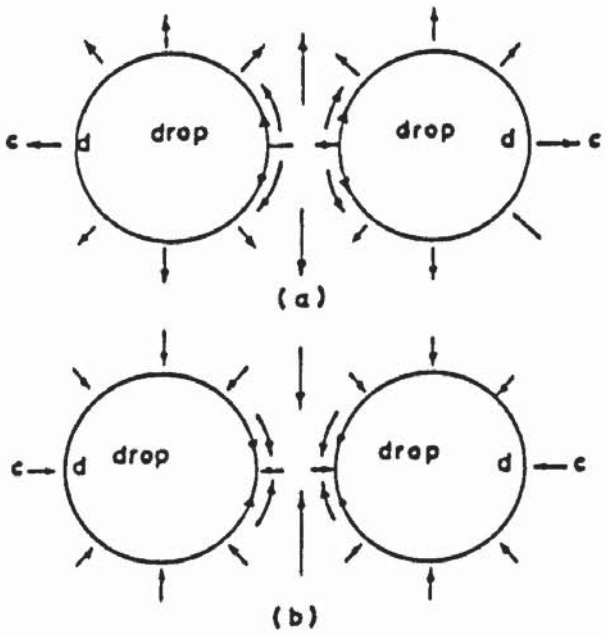

Figure 3.3

Effect of Solute Transfer on Interdrop Coalescence:

(a) d → c

(b) c → d

to the dispersed phase (c → d) as shown in figure (3.3b), the film becomes depleted of solute and the higher interfacial tension has the effect of drawing in the continuous phase and counter-acting the drainage tendency of the film.

3.7 Drop Size Measurement and Drop Size Distribution

For practical reasons and simplicity the drops are assumed to be spherical in shape. Mean drop size may be estimated by photography. The success of photographical method depends on the proper choice of the location of the dispersion within the extractor. The distribution of the photographed images must truely represent the mean distribution of drops in the entire column after correcting the distortion and magnification, particularly when microphotography is used (46-48). However, for non-spherical drops the minor and major axes for the drop images should be measured and reduced to the actual value d_1 and d_2 taking into consideration the magnification factor. The equivalent size of the drop d_e can then be calculated using the method proposed by Lewis et al. (16) as:

$$d_e = (d_1^2 \, d_2)^{1/3} \qquad (3.14)$$

For spherical drops, the drop diameter is taken as d_e. On the basis of the number of drops (clear image) counted in the photographs and their d_e values, the

mean drop size usually calculated as sauter mean diameter d_{32} of the relevant drop, can be obtained as:

$$d_{32} = \frac{\sum_{1}^{n} d_e^3}{\sum_{1}^{n} d_e^2} \qquad (3.15)$$

The value of the Sauter mean drop size is used to calculate the interfacial area, thus:

$$a = \frac{6\phi_D}{d_{32}} \qquad (3.16)$$

The drop size distribution consists of several sizes in accord with, the generation of new drops as a result of drop break-up and droplet coalescence due to interaction between the drops. The relevant size distribution is governed by an upper limit or maximum stable drop size, which would be specified, in the absence of coalescence by the size of the nozzle or distributor and a lower limit to minimum size, which could be estimated by the size entrained with the continuous phase (49).

There are various approaches regarding the drop size distribution curve in an agitated extractor. Some of these use a normal distribution (50) and others use the log-normal distribution (51). It has been

reported that for a fixed volumetric throughput (52) the normal distribution wherein the mode is equal to the mean size, is preferable to a log-normal distribution It was claimed by Chartes et al. that Olney's (53-54) conclusion which states that the drop size distribution in an R.D.C. is evident and that the relevant distribution follows the upper limit proposed by Mugele and Evans (55):

$$\frac{dv}{dr} = \frac{\delta}{\pi} \exp\ (-\delta^2 r^2) \qquad (3.17)$$

where $r = \ln\left(\frac{a'd}{d_m - d}\right)$

The upper limit distribution is a modified log-normal distribution that can be compared with the standard form of the log-normal distribution.

$$\frac{dv}{dr} = \frac{\delta}{\pi} \exp\ (-\delta^2 r^2) \qquad (3.18)$$

where $r = \ln \frac{d}{d_{vg}}$

d_{vg} is the geometrical mean drop diameter.

Olney (56) indicated that the Sauter mean diameter (d_{32}) may not be the proper mean drop size to represent the transfer rate to or from the total drop population

and claimed that the upper limit distribution will represent the drop size distribution in an R.D.C. Korchinsky and Azinadeh Khateylo (57) found that the upper limit distribution actually represented the drop size distribution in an Oldshue-Rushton column. Recently, Jeffreys et al. (28) confirmed the accuracy of representation of the upper limit density distributions of Mugele and Evans (55) for the drop size distribution in a large R.D.C. In their work, they compared the Sauter mean diameter (d_{32}) calculated by the volume surface diameter.

$$d_{32} = \frac{\sum_1 n_i d_i^3}{\sum n_i d_i^2} \qquad (3.19)$$

And the value of d_{32} as obtained from Mugele and Evans:

$$d'_{32} = \frac{dm}{1+a'e^{0.25}} \delta^{-2} \qquad (3.20)$$

They claimed that both d_{32} and d'_{32} showed very good agreement.

In a recent study Bonnet (17) used the Sauter mean diameter which was calculated from several photographs taken from all the mixing compartments in the Scheibel column. The values of d_{32} obtained were used in correlations taking into consideration, the diameter of the agitator, the Reynolds number, the Weber number and

the hold-up volume of the dispersed phase. He concluded that the Sauter mean diameter d_{32} is directly proportional to the agitator speed and influenced by mass transfer direction:

$$d_{32} \alpha N^{-0.8} \quad \text{dispersed} \rightarrow \text{continuous}$$

$$d_{32} \alpha N^{-1.8} \quad \text{continuous} \rightarrow \text{dispersed}$$

Figure 3.4

Correlation of Mixing Stage Efficiency With Power Input and Liquid Flow Rates.

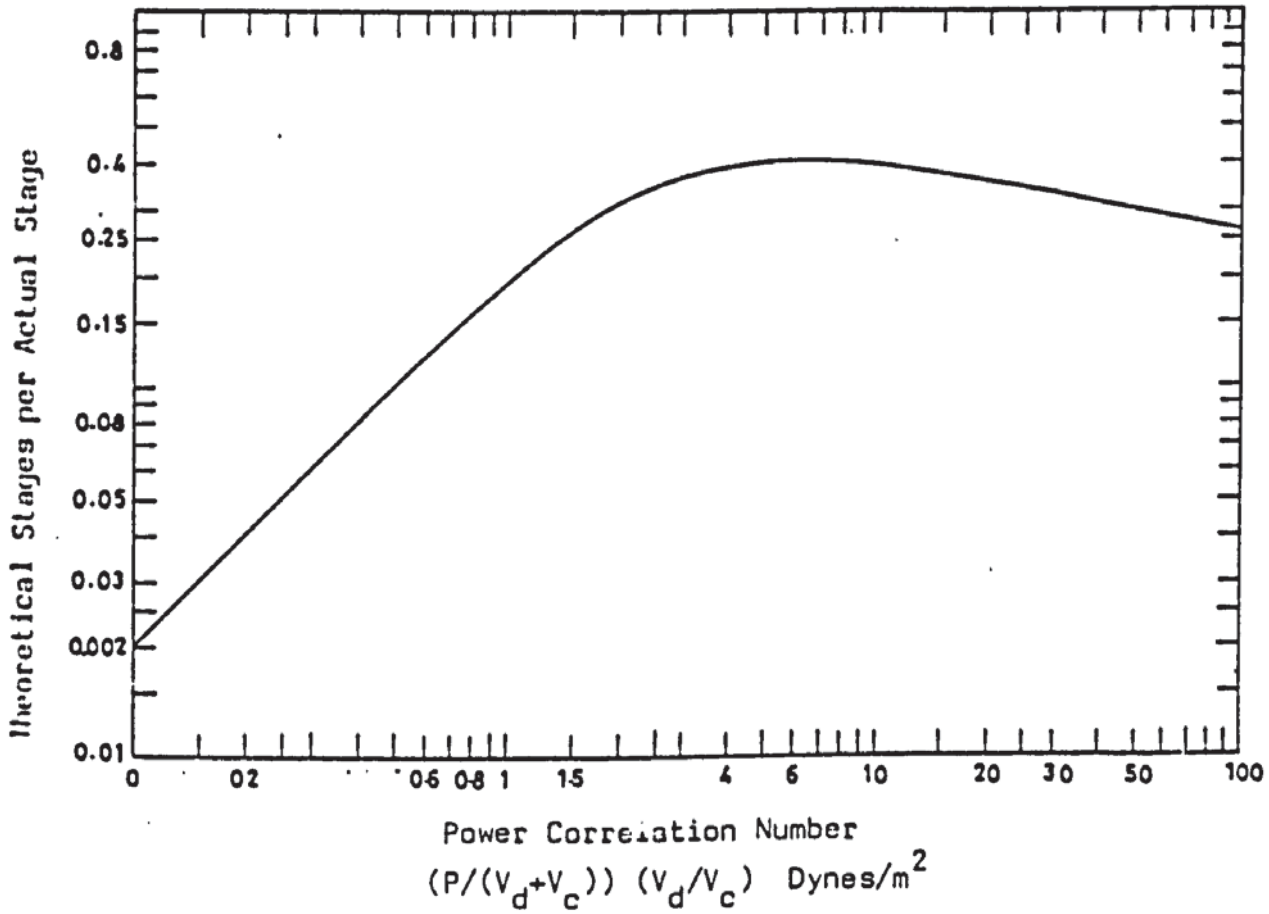

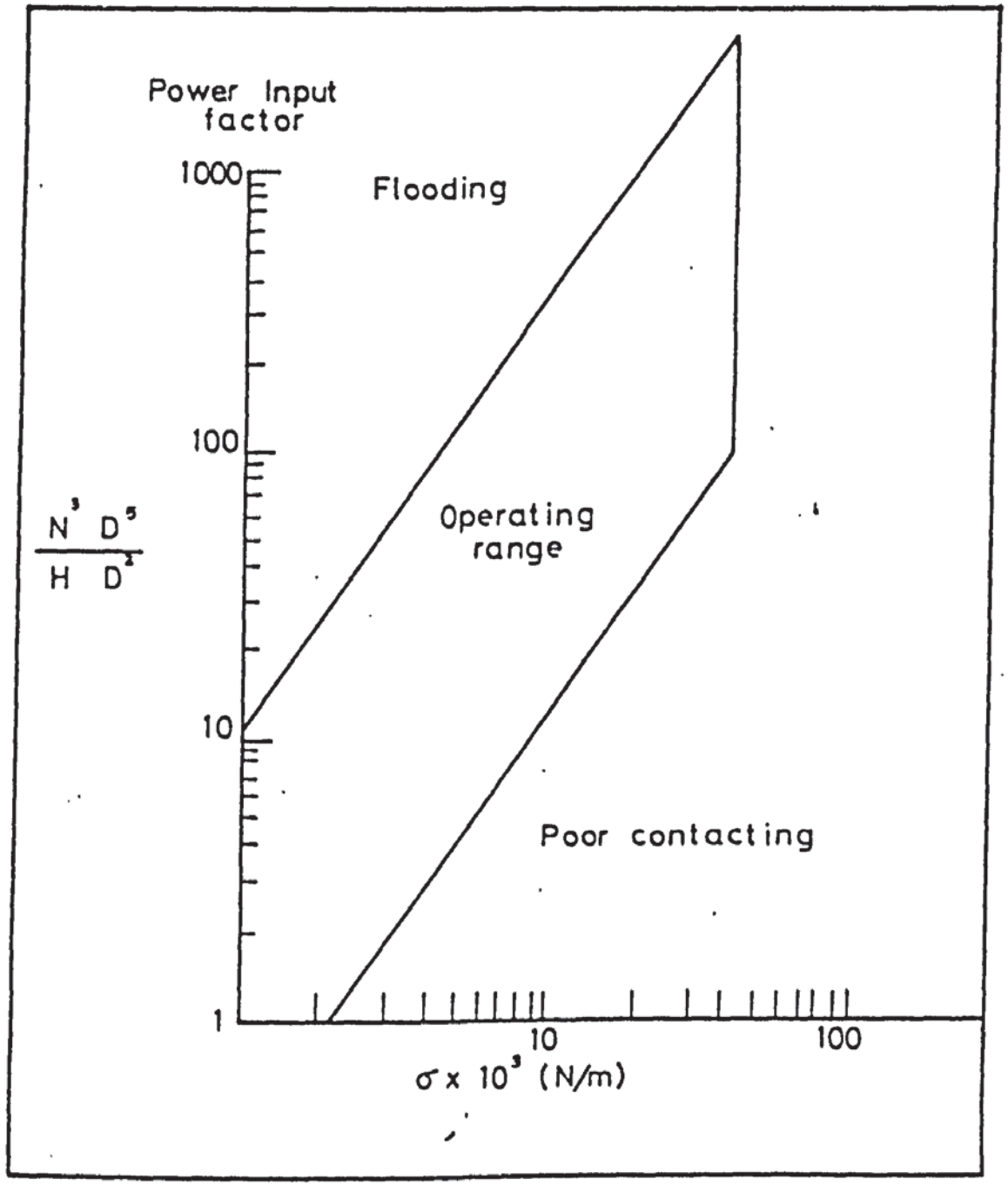

Figure 3.5 R.D.C. Power Input Operating Range (1)

Table 3.1 Relationships For ε For Some Contactors

Contactor and Reference	Relationship	Equation Number	Remarks.
Spray Column	$\varepsilon = u_d g \frac{\Delta\rho}{\rho_c}$	(3.21)	Assuming that entire energy is dissipated in the continuous phase.
Plain Disk R.D.C.	$\varepsilon = N_{po} \frac{4 N^3 D^5 R}{\pi n_c Z_c D^2_T}$	(3.22)	$N_{po} = 0.03$ for Re 10^5; C_1=0.4-0.6 (Organic dispersed), C_1=0.8-1.2 (Aqueous dispersed),
Pulsed Sieve Plate Columns	$\varepsilon = \frac{\pi^2 n_c (S_t/S_N)^2 - 1 (Af)^3}{2 g_c c_N^2 Z_T}$	(3.23)	Predicts low ε for low S_t/S_N ratios (0.35).
Oldshue-Rushton Columns	$N_{po} = 4.4$	(3.24)	In equation (3.22) above.
Scheibel Columns	$N_{po} = 1.85$	(3.35)	In equation (3.22) above.

CHAPTER FOUR

MASS TRANSFER FUNDAMENTALS

4.1 Introduction

Phase dispersion and coalescence are important in liquid-liquid extraction equipment for both stagewise and differential contactors. Systems with high interfacial tension require applied mechanical agitation in order to achieve adequate dispersion, and that the amount of turbulence is the criterion controlling drop size. Systems with low interfacial tension may be handled in non-agitated gravity columns, whereas agitated dispersions will require an additional volume for phase separation, such as in the mixer-settler and Scheibel column. For difficult separation systems with emulsification tendency having low density difference between the relevant phases, centrifugal extractors provide the force required for phase separation.

The break-up of liquid jets issuing from orifice distributors results in spread of drops, rise velocities, and contact times for the drops as the drops move through the continuous phase. The presence of column internals and the application of additional mechanical energy further affect the dispersion characteristics. The mean drop size in a contactor is controlled by coealescence-redispersion phenomena. Large drops entering the contactor emerge as smaller droplets, whereas smaller droplets after coalescence emerge as large droplets of an equilibrium size. A dynamic

equilibrium is established between the continuous break-up and the coalescence process occurring in the contactors. The mean equilibrium drop size depends on the mode of operation of the contactor and the type and extent of agitation as well as the physical properties of the liquid phases. High agitation energies cause break-down of drops, producing high interfacial areas, but this advantage is greatly offset by the absence of oscillation, or circulation in the smaller drops. In large drops, interfacial phenomena such as circulation, oscillation interfacial turbulence and spontaneous emulsification considerably influence the coalescence rates. These effects are sensitive to trace contamination and the presence of surfactants. However, when polar organic solvents, which have a low interfacial tension compared to that of water are used, the drop break-up and coalescence process form clear interfaces while much of mass transfer is occurring, as such types of solvents are less sensitive to contaminant adsorption (43).

4.2 Mass Transfer in the Dispersed Phase

4.2.1 Mass Transfer During Drop Formation

Drop formation at a nozzle occurs in two hydrodynamic regions (59-61) depending on the terminal velocity range of drops. As the nozzle size is increased, the size of the drops produced also increases, until a

size is reached beyond which the drop terminal velocity remains almost independent of drop size. The following simple relations give a useful estimate (62-65) of peak drop size d_p, above which drops are broken down and below which the drops could be either stable or could coalesce to give the peak terminal velocity u_p:

$$d_p = 1.38 \left(\frac{\gamma}{\Delta\rho g}\right)^{\frac{1}{2}} \tag{4.1}$$

$$u_p = 1.59 \left(\frac{\gamma \Delta\rho g}{\rho}\right)^{\frac{1}{4}} \tag{4.2}$$

The drop size and terminal velocity above and below this peak condition may be related in terms of the gravity group:

$$G = (g_{\Delta\rho}\ \rho_c\ d_e^3/\mu_c^2) \tag{4.3}$$

and the Property group:

$$P = (\gamma^3\ \rho_c^2/\Delta\rho g \mu_c^4) \tag{4.4}$$

In addition to the drop Reynolds Number:

$$Re = (d_e\ u_t\ \rho_c/\mu_c) \tag{4.5}$$

and that:

$$\frac{G^{0.54}}{P^{0.25}} = C \left(\frac{Re}{P^{0.25}}\right)^n \tag{4.6}$$

Where the constants C and n vary according to the region of operation as follows:

Region 1:

$$\frac{Re}{p^{0.25}} < 0.22 \qquad (4.7)$$

$$n = 1.0$$

$$c = 1.225$$

Region 2:

$$\frac{Re}{p^{0.25}} > 0.22 \qquad (4.8)$$

$$n = 1.33$$

$$c = 0.94$$

The mean size of drops released at a nozzle, at flow rates up to the low setting velocity may be estimated by following equation of Devatta (66):

$$d_e \left(\frac{\gamma}{\Delta\rho g}\right)^{-\frac{1}{2}} = 2.3 \left(\frac{d_N^2 \Delta\rho}{\gamma}\right)^{0.235} \left(\frac{U_N^2}{2g\, d_N}\right)^{0.022} \qquad (4.9)$$

In equation (4.9) the last term on the right hand side is always small and it is only the second term on the right hand side which is dominant. It is also clear that this equation has completely neglected the effect of viscosity, indicating its inpractibility for high viscous fluids.

Many investigators (65-66) show that extraction during drop formation before drop release from the dispersing nozzle is a considerable fraction of the total amount extracted. The phenomena of drop formation in agitated columns is independent of the speed of agitation and dispersed phase hold-up but depends on the linear velocity of the dispersed phase. The amount of mass transfer that occurs during droplet formation and coalescence, has usually been determined by varying the column height and extrapolating the amount of mass transfer to zero height. In some cases special provision has been made to minimise the effect of droplet coalescence as this would not usually occur at the nozzle tips where the drops formed. An alternative method has also been used (67) in which drops are successively formed and withdrawn at the same nozzle, without release. Drops are assumed to grow as a sphere and K_{df} is based upon the time of drop formation t_f and the surface area at the point of drop release.

The rate of mass transfer to a forming droplet can be expressed in terms of the Higbie (68) penetration theory, allowing for the increase of area during growth. From the penetration theory:

$$J = -D \left(\frac{dc}{dz}\right)_{z=o} = (C_i - C_b) \sqrt{\frac{D}{\pi t}} \qquad (4.10)$$

From equation (4.10) the amount (dM) transferred during time dt is given by:

$$dM = \Delta C_A \left(\frac{D}{\pi}\right)^{\frac{1}{2}} t^{-\frac{1}{2}} dt \qquad (4.11)$$

where:

ΔC is the driving force

A is the area of contact, which in terms of full grown droplet is given by:

$$A = A_f (t/t_f)^{2/3}$$

and t_f = time of formation

and the dispersed phase mass transfer coefficient k_{df} is correlated as follows:

$$K_{df} = \frac{M}{A_f t_f \Delta c} = \frac{6}{7} \left(\frac{D}{\pi}\right) t_f^{-\frac{1}{2}} \qquad (4.12)$$

Several alternative mechanisms have been proposed, all of which lead to similar expressions.

4.2.2 Mass Transfer During Drop Travel Through the Continuous Phase.

The shape of travelling drops in liquids is dependent on the force balance between the hydrodynamic pressure exerted on account of the relative velocities of the continuous phase on the drops and the pressure

of the field liquids as well as the surface forces which tend to return the drop into a sphere.

Many investigations have been made regarding the nature of local transfer process in the vicinity of a drop in addition to the overall effect around the drop (10). The estimation of the overall mass transfer coefficients to be used in the design of liquid-liquid extraction columns calls for a knowledge of the dispersed phase and continuous phase coefficients. Mass transfer between a single drop and the surrounding fluid may be divided into two categories:

(1) Mass transfer within the drop dominated by the dispersed phase mass transfer coeficients.

(2) Mass transfer outside the drop, dominated by the continuous phase mass transfer coefficients.

4.2.3 Mass Transfer within the Drop

The drop travels through the continuous phase and the drag forces at the interface tend to set up internal circulation of the contents thereof. Such circulation increases with the droplet diameter and with the ratio of viscosity of the continuous phase to that of the dispersed phase (6). The internal circulation is also influenced by the interfacial tension difference between the dispersed and continuous phases. The nature

of the interface such as polarity of the solvent droplet in the aqueous phase, spontaneous emulsification, and Marangoni instability.

Mass transfer rate within the drop depends on both the molecular motion and the process of fluid mixing. Small droplets are assumed to be stagnant, and mass transfer rate takes place by molecular diffusion. Drops that have intermediate size will develop a laminar toroidal internal circulation, which reduces the length of path of molecular diffusion. However, in large drops, the laminar circulation is replaced by violent internal mixing resulting in drop oscillation. Drop circulation occurs in most liquid drops wherein the Reynold number is greater than 50 (76-78). It was reported by Rose and Kintner (79) that droplet oscillations which break up the internal circulation streamlines and turbulent internal mixing is thus realised.

Recently, it was reported by Al-Hassan (34) that the Reynolds number is not enough to explain the hydrodynamic state of the relevant drop, and that the complex interactions must be taken into consideration with the Reynolds number. The droplet Reynolds number may be used only as a rough estimate to determine the hydrodynamic conditions of the drop such as:

(1) Stagnant or rigid droplets $\leq$ 10

(2) Circulating droplets 10 $\leq$ Re 200

(3) Oscillating droplets Re $\geq$ 200

The mechanism of mass transfer for the above type of drops would be covered below:

4.2.4 Stagnant Drops

Usually these drops are small and the diameter is less than 1.0 mm. They do not experience internal circulation and mass transfer is by molecular diffusion throughout. Rigid drops are the limiting case applicable only to very small drops. This process is one of entire molecular diffusion, represented by Newman (82) model:

$$E_m = \frac{C_o - C_f}{C_o - C^*} = 1 - \frac{6}{\pi^2} \sum_{n=1}^{\infty} \frac{1}{n^2} \exp\left(-n^2 \pi^2 \frac{D_{dt}}{a^2}\right) \qquad (4.13)$$

This expression can be further reduced (82) to:-

$$E_m = \pi \left(\frac{D_{dt}}{a^2}\right)^{\frac{1}{2}} \qquad (4.14)$$

Treybal (83) reported the mass transfer coefficient (82) for rigid drops based on a linear driving force concentration:

$$K_d = \frac{4\pi^2 D_d}{3a} \qquad (4.15)$$

4.2.5 Circulating Drops

The Reynolds number is generally considered as the criteria for laminar circulation within the drops. The effect of circulation within the drop on the rate of mass transfer is that it is increased compared to

that of a rigid drop, and for situations wherein the circulation is fully developed, mass transfer rates are reported to be 1.5 times that of a rigid drop.

For the laminar flow regime wherein Re $\leq$ 10 Kronig and Brink (84) developed the diffusion model to obtained an expression for transfer which may be approximated by:-

$$K_d = \frac{17.9D}{d} \qquad (4.16)$$

4.2.6 Oscillating Drops

The drop oscillation is expected to prevail in most cases where the drop Reynolds number is within the range of 200-1000 (79). The rate of mass transfer for oscillating drops have been reported to be much greater than circulating drops. When a drop reaches a specific size it starts to oscillate about an ellipsoidal shape. The cause of oscillation has been explained by Gunn (87) that oscillations would occur when the periodic force produced by detaching the wake eddies, have the right frequency to produce such oscillations. Rose and Kintner (79) developed a mass transfer model for the case of oscillating drops which can be expressed by:

$$K_d = 0.450\ (Dw)^{\frac{1}{2}} \qquad (4.17)$$

where the frequency of oscillation is predicted from the Schoeder and Kintner (88) equation, which is a modification of the Lamb (89) equation.

$$\omega^2 = \frac{\sigma b}{r^2} \quad \frac{n(n+1)(n-1)(n+2)}{[(n+1)\rho_d + n\rho_c]} \qquad (4.18)$$

where,

$$b = \frac{d_p^{0.225}}{1.242} \qquad (4.19)$$

Garner and Tayeban (89) reported that for a specified drop size, oscillation was greater for chemical systems that have a low continuous phase viscosity, low surface tension and with low dispersed phase viscosity, and that the period of oscillation depends on the properties of the system.

4.3 Mass Transfer in the Continuous Phase

An extraction process requires the transfer of solutes from the bulk raffinate phase to the interface and then into the bulk of the solvent. The rate of this process depends on the resistance to diffusion, the interfacial area, and the driving force. The internal drops hydrodynamics have a significant effect on the mass transfer coefficient (K_c) in the continuous phase. The overall mass transfer process between the continuous and dispersed phase, comprises the contribution of mass transfer in the continuous phase.

As this is difficult to specify due to the wake behind the droplets, the process is generally described by the overall process for the whole drop, based on the continuous mass transfer coefficient. The coefficient is determined in terms of the resistance of the film surrounding the drop across which mass transfer occurs and the diffusion resistance is a series of resistance prevailing at:

(1) inside the drop,

(2) at the interface, and

(3) in the liquid surrounding the drop.

The relationship between the overall and individual mass transfer coefficient were derived on the basis of the two-film theory (10).

$$\frac{1}{K_c} = \frac{1}{k_c} + \frac{1}{mk_d} \qquad (4.20)$$

For very large values of the distribution coefficient ($m \gg 1$) equation 4.20) becomes:

$$K_c = k_c \qquad (4.21)$$

In which case, the overall mass transfer coefficient is equal to the continuous phase mass transfer coefficient.

The continuous phase mass transfer coefficient may be evaluated from the molecular diffusion:

$$k_c = D_c/X_c \qquad (4.22)$$

where X_c is the continuous phase fictitious film thickness and is a function of the system Reynolds number:

$$X = f(Re) \qquad (4.23)$$

Mass transfer in the continuous phase also experiences the process of different forms of drop hydrodynamics i.e. rigid or non-rigid.

4.3.1 Mass Transfer to and From Drops

4.3.1.1 From and To a Rigid Drop

Many investigators reported that it is difficult to estimate the contribution to mass transfer from the wake of a drop. Hence, the phenomena is sometimes expressed as an overall process for the whole drop. Garner and Jenson (90) used the boundary layer theory to develop the following model for mass transfer from or to a rigid sphere:

$$Sh = A + C\ Re^m\ Sc^n \qquad (4.24)$$

where,

A, C, m and n are constants.

However, Linton and Sutherland (91) correlated the overall transfer unit as the following:-

$$Sh = 0.582\ (Re)^{\frac{1}{2}}\ (Sc)^{1/3} \qquad (4.25)$$

Bayadzhiev and Elenkov (36) made the following model for the mass transfer coefficient for the continuous phase for the turbulent regime in an extraction tube, where the dispersed phase drops act as rigid spheres:

$$k_c = 0.65 \left(\frac{D\mu}{d}\right) \left(\frac{D}{\nu}\right)^{1/6} \qquad (4.26)$$

The most recognised model was that correlated by Kinard and Manning (71) in which the effect of the various factors on the overall process were considered:

$$Sh = 2.0 + (Sh)_n + 0.450\ Re^{\frac{1}{2}}\ Sc^{1/3} + 0.0484\ (Re)(Sc)^{1/3} \qquad (4.27)$$

where,

2.0 indicates the effect of diffusion

$(Sh)_n$ takes care of the natural convection

The third term takes account for the contribution at the front, and the last term allows for the contribution of the wake effect at the rear of the drop.

4.4 Mass Transfer During Coalescence

Liquid-liquid extraction equipment performance is largely affected by the way by which coalescence takes place in:

(1) The settling zone, such as the calming section in the Scheibel column or the settler in the mixing settler contactor, referred to as interface coalescence.

(2) The mixing section, depending on the speed of agitation which takes place in the form of drop-drop coalescence.

Coalescence occurs in accordance with two basic stages:

(a) The process of drainage of the continuous phase from the dispersed fluid droplets until a critical film thickness is obtained.

(b) Then the rupture of such a film.

The mechanism of the coalescence process is highly influenced by the drop size, the duration of the falling or rising period, the curvature of the interface towards the relevant drops and the inter-facial tension of the system. These factors affect the drainage and the relevant film rupture and thus they control coalescing process. Other factors, such as the phase ratio, density difference between the dispersed and continuous phase, temperature, speed of agitation, presence of surfactants, and mass transfer direction also affects the mechanism of coalescence with regard to coalescing time and coalescence control.

Few particulars are available with regard to the effect of coalescence on mass transfer. Skelland et al. (79) reported that the amount of mass transfer during coalescence is rather insignficant compared with that taking place during drop formation, and therefore can be neglected. This is due to the fact that the drainage of the relevant drop-contents directs the continuous phase therefrom and stops the entrainment. In addition to the fact that the coalescence time is relatively short (3×10^{-2} sec) (92). However, coalescence generally increases the drop size and thereby reduces the surface area of contact resulting in reduction of mass transfer rate, if any.

In agitated columns it is reported that interdrop coalescence is insignificant at the hold-up of the dispersed phase up to 10% (93-94), but Misek claimed that at high hold-up of 18% or more drop-drop coalescence occurred.

However, coalescence mostly occurs at the interface of phase separation at the top of the column near the dispersed phase exit. If coalescence does not occur readily at such interface, the residence time will be increased and the capacity of the relevant column is thus reduced. Coalescence time is correlated to the rate at which drops arrive at the interface, as well as diameter, thus:-

$$R \alpha \cdot d/t \qquad (4.28)$$

where,

R = rate of arrival

t = coalescence time

d = drop diameter

Coalescence rates are greatly influenced by mass transfer and mass transfer direction. It is reported (83) that mass transfer enhances coalescence when the solute is transferred from the dispersed to the continuous phase, and reduces rate of coalescence when the transfer of the relevant solute is from the continuous to the dispersed phase. This is in compliance with the Marangoni effect, whereby the generation of motion at a fluid interface occurred due variation in surface tension with concentration gradient, this is only true if the relevant solute decreases the interfacial tension, but if increases the interfacial tension, the opposite would be true (83).

4.5 Overall Mass Transfer Coefficients

The overall mass tranfer coefficient is usually calculated from the theory of additive resistance. As the mass transferred rate N is the same for both films, it follows that:

$$N = K_x(C_{xb}-C_{xi}) = K_y(C_{yi}-C_{yb}) \qquad (4.29)$$

where, C_{xb}, C_{xi}, C_{yb} and C_{yi} are the concentration in either phase (x,y) at the bulk and interface respectively.

$$\text{Therefore} \quad -\frac{K_x}{K_y} = \frac{C_{yi} - C_{yb}}{C_{xi} - C_{xb}} \tag{4.30}$$

It is also convenient to define the overall mass transfer coefficient K_{ox} and K_{oy} as follows:

$$N = K_{ox}\,(C_{xb} - C_x^*) = K_{oy}(C_y^* - C_{yb}) \tag{4.31}$$

The driving force $(C_{yi} - C_{yb})$ in equation (4.29) can be expressed as:

$$m_y\,(C_{xi} - C_x^*) \tag{4.32}$$

where m is the distribution coefficient.

Therefore Equation (4.29) becomes:

From Equation (4.29)

$$C_x - C_{xi} = N/K_x$$

$$C_{xi} - C_x^* = \frac{N}{mK_y}$$

$$\text{Therefore} \quad (C_{xb}-C_{xi}) + (C_{xi}-C_x^*) = \frac{N}{K_x} + \frac{N}{mK_y}$$

$$\text{Therefore} \quad (C_{xb}-C_x^*) = N\left(\frac{1}{K_x} + \frac{1}{mK_y}\right) \tag{4.33}$$

The overall driving force with respect to the X-Phase is:

$$C_{xb} - C_x^*$$

Therefore the overall mass transfer rate is:

$$N = K_{ox} (C_{xb} - C_x^*)$$

but from equation (4.33)

$$C_{xb} - C_x^* = N \left(\frac{1}{K_x} + \frac{1}{mK_y}\right)$$

Therefore $$N = K_{ox} N \left(\frac{1}{K_x} + \frac{1}{mK_y}\right)$$

$$\text{Therefore} \quad \frac{1}{K_{ox}} = \frac{1}{K_x} + \frac{1}{mK_y} \tag{4.34}$$

Similarly for the Y-Phase:

$$\frac{1}{K_{oy}} = \frac{m_x}{K_x} + \frac{1}{K_y} \tag{4.35}$$

This indicates that either phase could be used. However, a criterion to which phase is to be used depends on the knowledge of the time for a droplet to attain 60% or 90% solute concentration, with either phase to be dispersed, and the phase required the larger time is to be used. This time (θ) may be estimated as follows:

For the dispersed phase,

$$Q_t/Q_o = 1-\exp\left(-2.25\left(\frac{4D_d\pi^2\theta}{d^2}\right)\right) \qquad (4.36)$$

And for the continuous phase,

$$\frac{Q_t}{Q_o} = 1 - \operatorname{erf}\left(\frac{X}{\sqrt{4D_c\theta}}\right) \qquad (4.37)$$

4.6 Effect of Surface Active Agents

Although the addition of surfactants cause an increase of the interfacial area, it reduces the rate of mass transfer per unit area in extraction systems wherein there is no chemical reactions. Thus surfactants suppress the physical properties which affect circulation, oscillation and the instabilities of the system at the interphase. It has been reported that surfactants make the droplet more rigid and can cause the mass transfer rate to approach that of the stagnant drop (94), because the relevant system becomes more stable and internal circulation and oscillation will be reduced. It has been reported by Garner et al. (95) that the addition of small quantities (of 0.015% by volume) to water reduce the extraction rate of diethylamine from toluene drops to 45% of its original value.

Therefore the relevant investigations should be carried out with pure materials and should be free from contaminants, this means that purity checks should be made with regard to the chemical system used or upon washing the equipment with some detergents.

TABLE 4.1

Empirical Models For Continuous Phase Mass Transfer Coefficient

Authors	Equation	Comments
1. Linton and Sutherland (69)	$Sh = 0.582\ (Re)^{\frac{1}{2}}\ (Sc)^{1/3}$	Solid sphere.
2. Rowe et al. (70)	$Sh = 2 + 0.76\ (Re)^{\frac{1}{2}}\ (Sc)^{1/3}$	Solid sphere, transfer by diffusion.
3. Kinard et al. (71)	$Sh = 2 + (Sh)_n + 0.45(Re)^{\frac{1}{2}}(Sc)^{1/3} + 0.0484\ (Re)(Sc)^{1/3}$	Solid sphere, transfer by diffusion, convection etc.
4. Boussinesq (cited in ref 72)	$Sh = 1.13\ (Re)^{\frac{1}{2}}(Sc)^{\frac{1}{2}}$	Non-rigid drop.
5. Garner and Tayeban (73)	$Sh = 0.6\ (Re)^{\frac{1}{2}}(Sc)^{\frac{1}{2}}$	Non-rigid drop.
6. Garner and Tayeban (78)	$Sh = 50 + 0.0085\ (Re)\ (Sc)^{0.7}$	Oscillating drop.
7. Hughmark (74)	$Sh = 2 + 0.084\ [Re^{0.484} Sc^{0.339}((dg^{1/3}/D^{2/3})0.072)3/2$	Oscillating drop.

CHAPTER FIVE

FRACTIONAL EXTRACTION

5.0 FRACTIONAL EXTRACTION

5.1 Fractional Extraction with Two Immiscible Liquid Solvents

In fractional liquid extraction with a single solvent, two pure products can be produced only if the solute preferentially soluble in the solvent is partially immiscible. For fractional liquid extraction with two solvents the only requirement is that the two solvents be at least partially immiscible in each other.

When the distribution coefficients of the two solute components are close to each other, a fractional extraction system is used to separate them. The light solvent enters at the bottom of the cascade, flows successively through the various stages, and leaves the system from the top. The heavy solvent enters the system at the top, flows down through the various stages, and leaves the system from the bottom. The two solvent streams may enter the column free of any solute, or they may contain small quantities of solvent due to incomplete separation in the solvent recycle systems. The feed mixture to be separated is fed to some stage in the middle of the column. The solute feed stream could contain one of the solvent components or it could be free. However, it is unusual to contain both solvents; if the solvent flow rates are adjusted such that the extraction factor

(E) is greater than unity for one solute component, but less than unity for the other solute component, this type of arrangement can be made to effect a sharp separation between the two solutes, with one leaving the system predominantly with the heavy solvent from the bottom stage.

The extraction section of a fractional extraction column, below all feed stage is a simple counter current cascade in which the light solvent scrubs most of component C and some of the component B from the heavy solvent stream, assuming that the extraction factor $E_C > 1$ and $E_B < 1$, this indicates that the bottom product contains very little of component C, but richer in component B. The scrubbing section, above the feed stage, is a simple counter current cascade in which the heavy solvent scrubs most of component B and some of component C from the light solvent stream, assuming that $1/E_C < 1$ and $1/E_B > 1$, this results in a top product containing very little of component B, but richer in component C. The two solutes are simultaneously distributed between the two insoluble solvents and thus form a quaternary system and if B and C are the solutes, the distribution coefficients would be:

$$m_B = X_{BA}/X_{BD} \qquad (5.1)$$

$$m_C = X_{CA}/X_{CD} \qquad (5.2)$$

The selectivity in such quaternary system would then be:

$$\beta_{B,C} = m_B/m_C = \frac{X_{BA}/X_{BD}}{X_{CA}/X_{CD}} \qquad (5.3)$$

$$= \frac{X_{BA}\ X_{CD}}{X_{CA}\ X_{BD}} \qquad (5.4)$$

and for the more favourable selectivity $m > 1$.

Solvent Capacity

In addition of having a high selectivity, the relevant solvent should have a large capacity to dissolve relatively large quantities of the preferential solute, otherwise it would not be recommended for use because of the large quantity that would have to be circulated through the cascade. A large value of m_B is not only required, but also a large value of X_{BA}. Thus a solvent with a relatively higher selectivity and lower solubility would not be selected in preference to one with a lower selectivity and higher solubility.

5.2 Independent Solute Distribution

5.2.1 The Ideal Systems

This term refers to solvents wherein the distribution coefficients for the solutes are independent of concentrations. If the solutions are sufficiently dilute, the relevant distribution coefficients can be considered constant and hence classified as ideal over a limited

concentration range. In fractional extraction, if we assume constant flow rates of both the heavy phase (A) and the light phase (D) over the two individual sections of the column, the following equations can be derived, Figure (5.1):

$$Y_{n+1} = (A/D\ m_n)\ Y_n + Y_p \qquad (5.5)$$

$$X_{m+1} = (Dm_n/A)\ X_m + X_B \qquad (5.6)$$

For an ideal system for each component, the distribution coefficients are considered constant in each stage and the coefficients of the Y_n and X_n terms are constant. The $D\ m_n/A$ is defined as the extraction factor, E and is dimensionless.

For any separation to be effective, it is necessary that the solvent ratio must be selected so that $E_1 > 1$ and $E_2 < 1$ where 1 and 2 refer to each solvent, where 1 is favoured.

To determine the optimum solvent ratio, the solvents ratios were plotted against the number of theoretical stages (NTS) as shown in Figure (5.2). This shows that there is an optimum solvent ratio at which a specified separation can be obtained in fewer stages than at any other solvent ratios.

Van Dijeck and Schaafsma (114) used the geometrical mean of the limiting values:

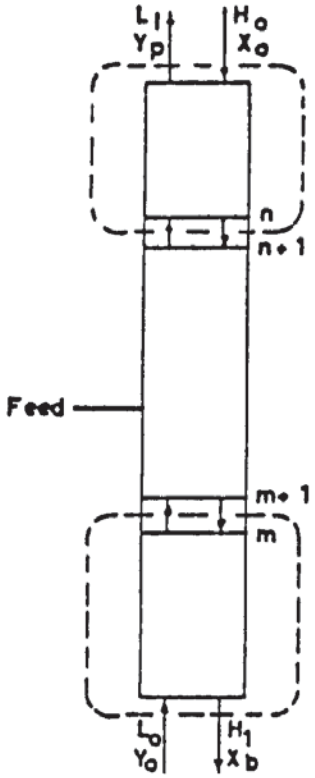

Fig.5.1. Schematic diagram of material balances in two-solvent fractional liquid extraction.

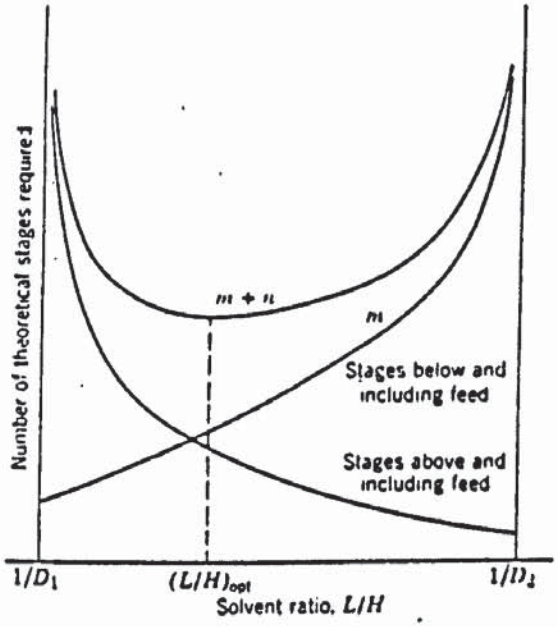

Effect of solvent ratio on stages required in two-solvent fractional liquid extraction. (114).

Figure 5.2

$$A/D = \sqrt{m_1 m_2} \qquad (5.7)$$

and if the solvent selectivity is defined as:

$$\beta = m_1/m_2 \qquad (5.8)$$

equation (5.8) becomes:

$$A/D = m_1/\sqrt{\beta} \qquad (5.9)$$

and at this solvent ratio

$$A/m_2\ D = \frac{1}{\sqrt{\beta}} \qquad (5.10)$$

Therefore, $E_1 = \sqrt{\beta}$ (5.11)

$$E_2 = 1/\sqrt{\beta} = \frac{1}{E_1} \qquad (5.12)$$

However, if the two solutes interact with each other, the equilibrium relationship should be correlated on either the activity coefficient models or any other suitable correlations. The number of theroetical stages would then be based on the operating values and relevant concentrations. Graphical methods could also be used, but it is tedious and requires trial and error as will be shown later on in Chapter 10.

5.3 Dependent Solute Distribution

5.3.1 The Non-Ideal Systems

These systems may be classified into two types. In the first type, the distribution coefficient varies with the concentration of one or both components of the mixture, but the solvent quantities may be considered constant over the entire range of operation. In the second type, the mutual solubility of the solvents varies appreciably with solute concentration so that the solvent quantities cannot be considered constant throughout the operation (13).

When the two solvents are sufficiently immiscible such that their mutual solubilities are not affected by solute concentrations, the solvent quantities can be considered constant. Scheibel (13) used this concept in the design of his fractional liquid extraction column. He expressed concentrations on the basis of a unit quantity of solvent rather than on the basis of mole or weight fractions, as the quantities of each solvent in the column are constant whereas the total quantities of solutions vary with the concentrations. He plotted the amount of each component extracted by stage numbers above and below the feed and from the graphical construction, the feed stage was located and so were the number of theoretical stages and the stage efficiency.

When the distribution coefficients of the componets vary with the concentration of both components, the equilibrium data can be represented by a series of curves representing the concentration of the same solute in the light phase. Other components are represented on different curves and trial and error techniques which match the concentrations of both solutes at the equilibrium conditions in each stage would be applied. This becomes extremely difficult if more than four components are used in the extraction system.

5.4 Graphical Representation of a Fractional Extraction Cascade

Rigorous stagewise calculations for quaternary system could be carried out graphically in three-dimensions, similar to the two dimensional technique applied to the ternary diagram. The entire computation and graphical technique may be made, stage by stage in exactly the same way as the ternary systems. For a larger number than four components the situation obviously becomes more complex, but some simplification results if the principal solvents are immiscible. The technique is quite cumbersome and would be impossible with multicomponent systems of more than four components.

The first requirement for evaluating an extraction is based on liquid-liquid equilibrium data. Details of obtaining these data are to be discussed in Chapter Six.

As the driving force for mass transfer is increased, fewer theoretical stages are required. In extraction an increase in driving force for mass transfer means selecting a solvent with a higher distribution coefficient, m, and with a relatively higher capacity as well as increasing the solvent to feed ratio. The last point should be economically evaluated as solvent recovery adds more expenses. The stagewise computation of liquid-liquid extraction has much in common with the stagewise calculation of vapour-liquid separations. However, in liquid-liquid extraction, the concept of solute-free solvents can be used to simplify the calculations similar to McCabe-Thiele method. The concentrations are then given as the ratio of solute to the light extraction solvent Y and the ratio of solvent to the heavy solvent X. The equilibrium curves are then constructed for each solute and the relevant operating lines are afterwards constructed. The theoretical stages can be stepped off in the conventional manner for each section of the extractor, starting at the extract end as stage 1 and proceeding toward the feed stage, then restarting at the raffinate end and proceeding towards the feed stage, the same procedure would be repeated for the other component, as shown in Figure (5.3) and Figure (5.4).

The feed stage number can be located by matching the individual flow rates at the point of feed introduction. This is obtained by plotting the stage number versus the

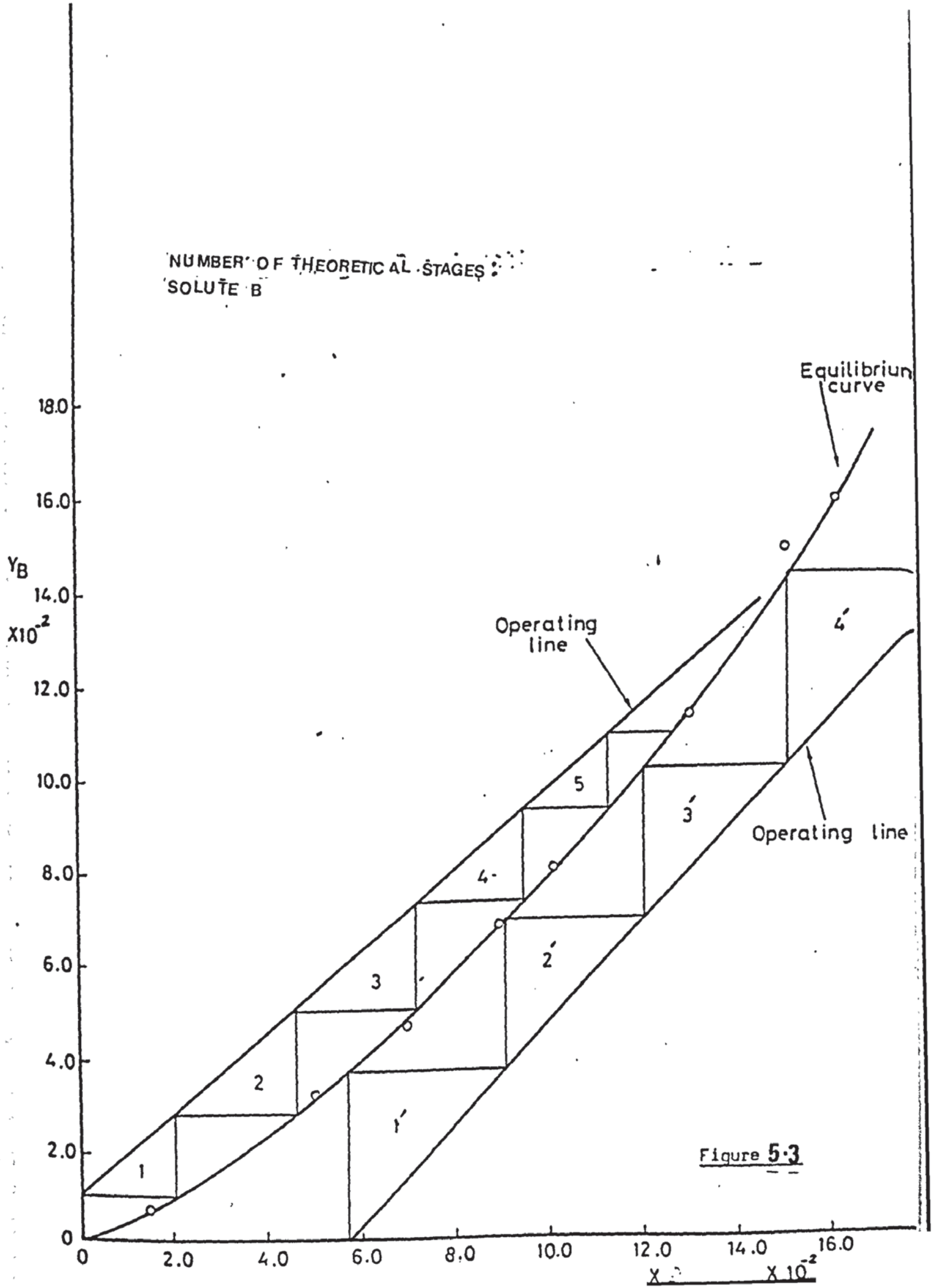
NUMBER OF THEORETICAL STAGES
SOLUTE B
Equilibrium curve
Operating line
Operating line
Y_B
$X10^{-2}$
18.0
16.0
14.0
12.0
10.0
8.0
6.0
4.0
2.0
0
0
2.0
4.0
6.0
8.0
10.0
12.0
14.0
16.0
X_B
$X\ 10^{-2}$
1
2
3
4
5
1'
2'
3'
4'

Figure 5·3

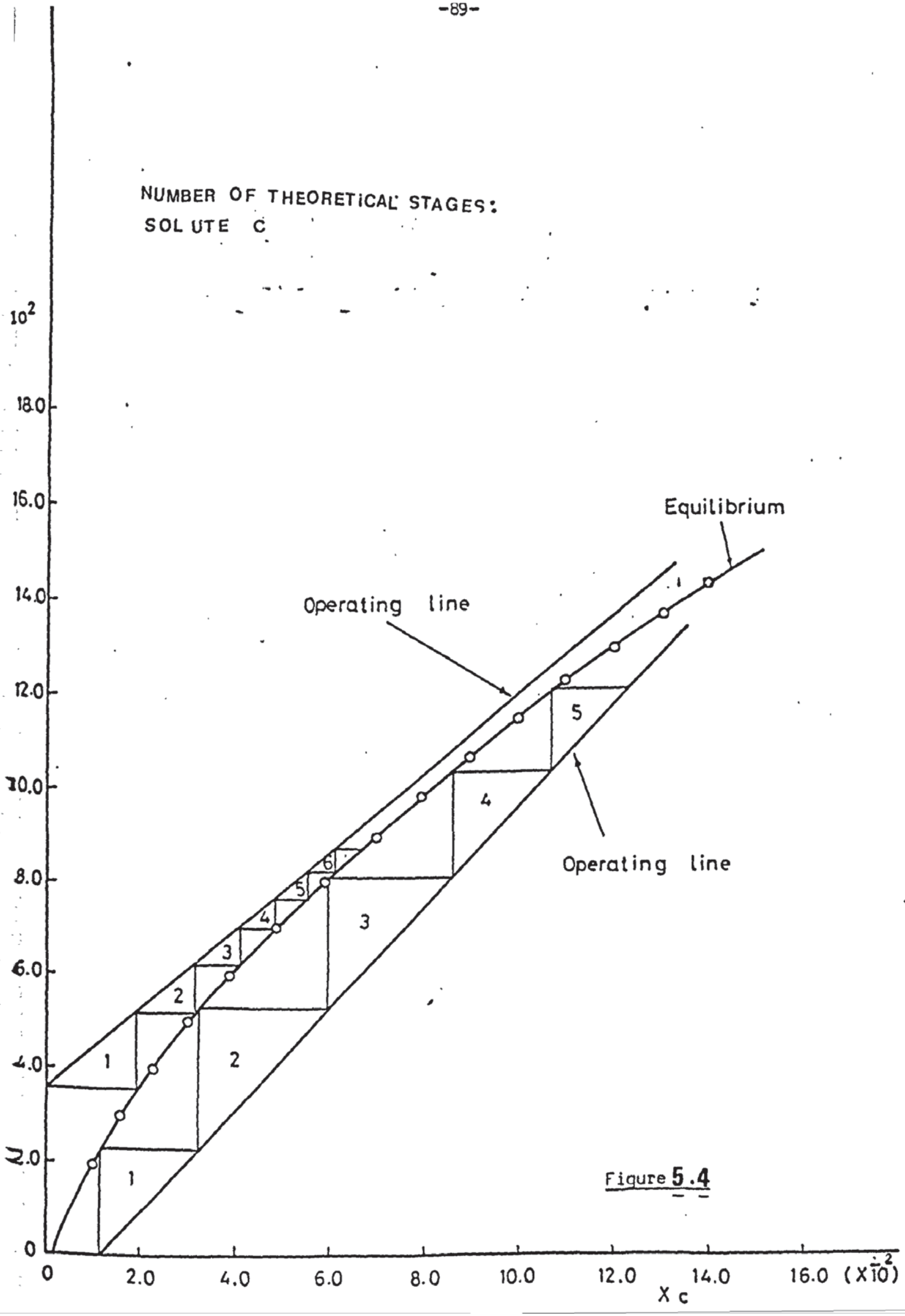
NUMBER OF THEORETICAL STAGES:
SOLUTE C
Equilibrium
Operating line
Operating line
Y
Xc
(X10⁻²)
0
2.0
4.0
6.0
8.0
10.0
12.0
14.0
16.0
18.0
10²
1
2
3
4
5
6

Figure 5.4

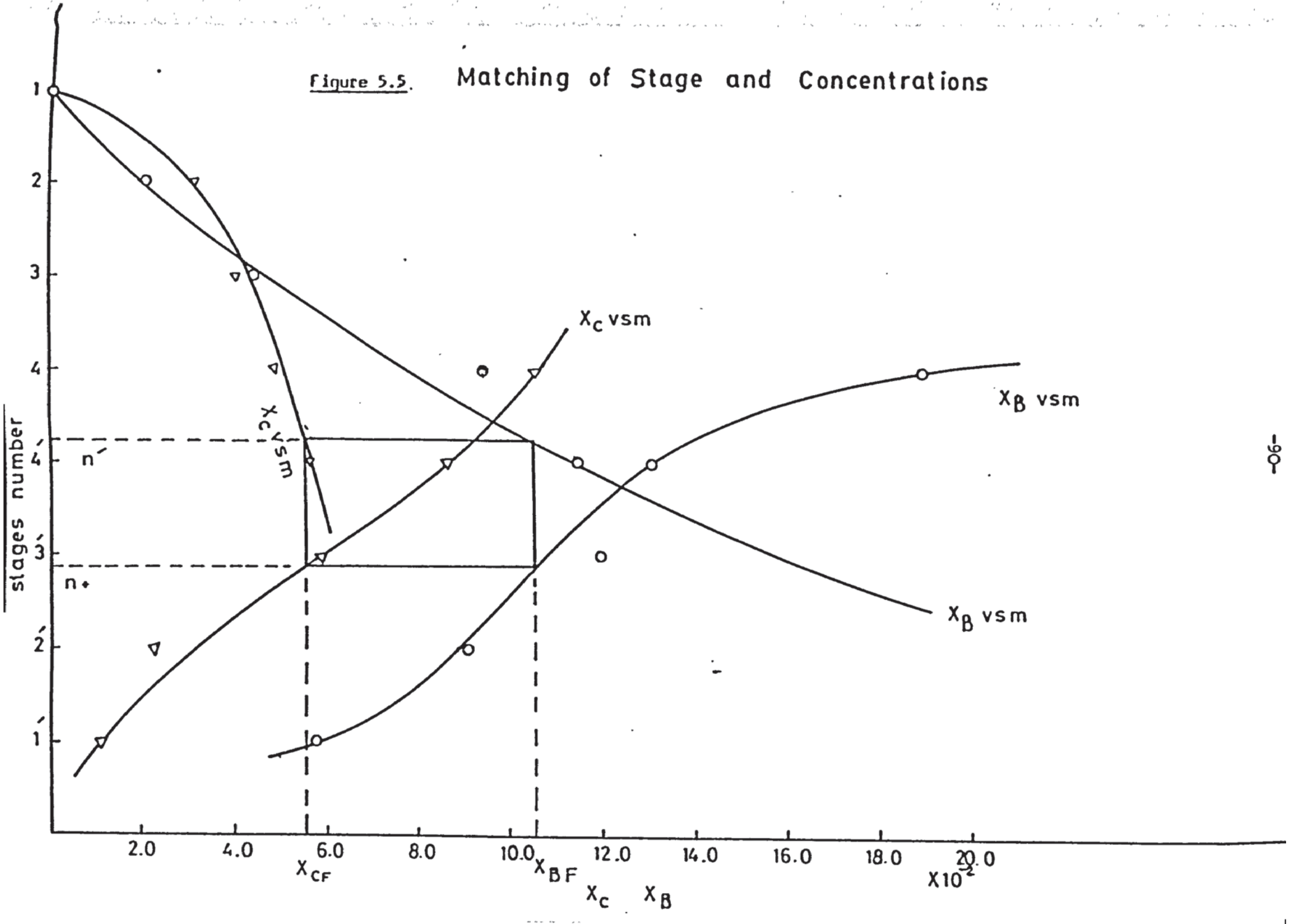
Figure 5.5. Matching of Stage and Concentrations
stages number
1
2
3
4
1'
2'
3'
4'
n'
n+
X_C vsm
X_B vsm
X_B vsm
2.0
4.0
6.0
8.0
10.0
12.0
14.0
16.0
18.0
20.0
X_{CF}
X_{BF}
X_C X_B
$X10^2$

component flow rate of each component in the heavy phase (X) as shown in Figure (5.5). The total number of theoretical stages in the column would then be determined by subtracting one stage from the sum of the stages from both sections, as the feed stage is counted twice. It could be shown that the feed concentrations to be highest at the feed stage and also that the concentrations at the feed stage increase with the number of stages. The amount of solvent used must be sufficiently high so that solute solubilities are not exceeded at the feed stage.

5.5 Stage Calculations

Many methods have been proposed for the correlation of tie-line data, and the relevant correlations or models were used for prediction of equilibrium data. Most of these models are based on activity coefficients, others are based on theories discussed in Chapter Six, Section 6.3.

If the product compositions of both the heavy and light phases are known or could be estimated, and if the equilibrium data could be obtained from any relevant model, the stage calculations would be carried out without the need of making graphical representation. Stage calculations are made from both ends of the column towards the centre. A match of component flow rate is made by trial and error preferably through a computer program until the component flow rate from the scrubbing section matches that of the extracting section; a condition which determines the feed stage location.

Equations that include both material balances and equilibrium relationship required to define the steady-state performance of a liquid-liquid extraction column are non-linear, as the activity coefficients or distribution ratios in the equilibrium relationships are function of composition. However, some approximations to the activity coefficients or distribution ratios can be made and when such approximations are incorporated into the equilibrium relationship and material balances as that a set of linear simultaneous equations is obtained. These equations could be derived from Figure (5.6) as follows:

Material balance round stage n:

$$F_n + D_{n+1} + A_{n-1} = D_n + A_n \tag{5.13}$$

Component balance:

$$F_n X^F_{i,n} + D_{n+1}\, Y_{i,n+1} + A_{n-1}\, X_{i,n-1} = D_n Y_{i,n} + A_n X_{i,} \tag{5.14}$$

$$A_n X_{i,n} - A_{n-1}\, X_{i,n-1} + D_n\, Y_{i,n} + A_n X_{i,n} - D_{n+1}\, Y_{i,n+1} = F_n\, X^F_{i,n} \tag{5.15}$$

The equilibrium Relationship:

$$Y_{i,n} = m_{i,n}\, X_{i,n} \tag{5.16}$$

Substitute equation (5.16) into equation (5.16):

$$-A_{n-1}X_{i,n-1}+D_n m_{i,n}X_{i,n}+A_n X_{i,n}-D_{n+1}m_{i,n+1}X_{i,n+1} = F_n\, X^F_{i,n} \tag{5.17}$$

Multifeed Model

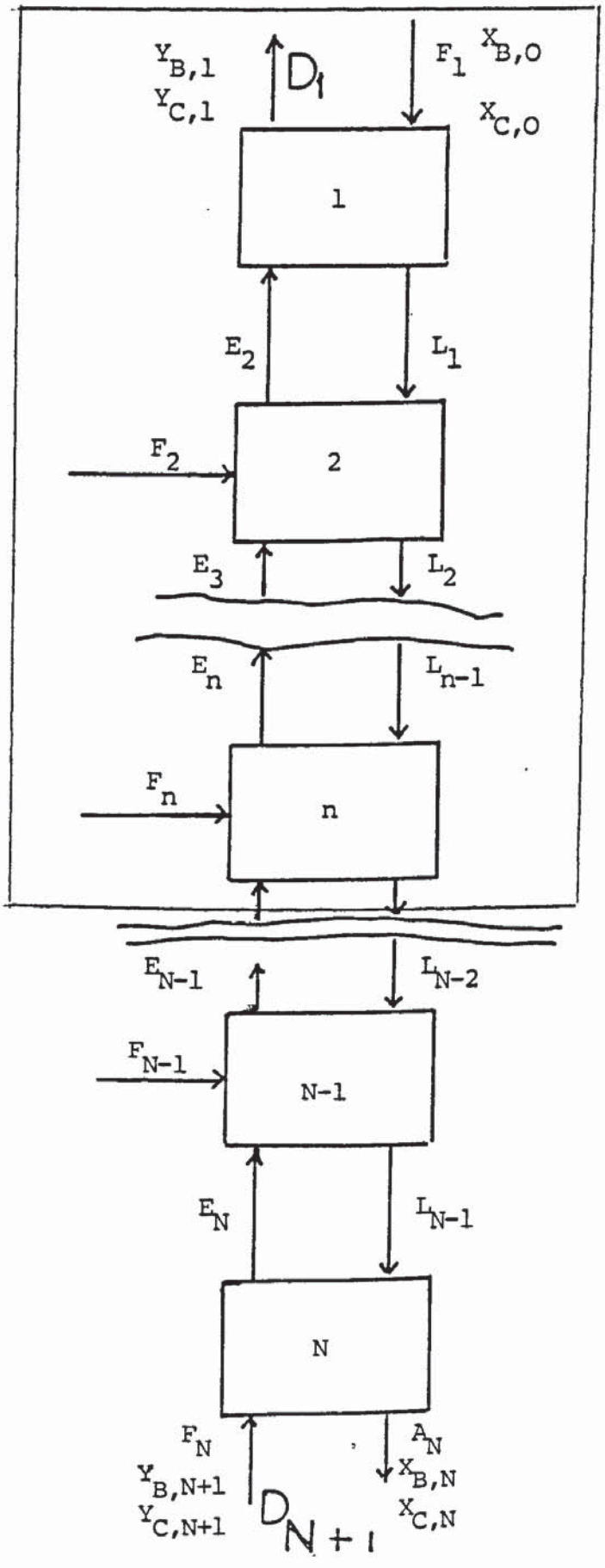

(1)

Figure 5.6

Material Balance round stage (N-1):

$$F_{N-1} + D_N + A_{N-2} = D_{N-1} + A_{N-1} \qquad (5.18)$$

$$-A_{N-2} + D_{N-1} + A_{N-1} - D_N = F_{N-1} \qquad (5.19)$$

Component balance:

$$-A_{N-2}\, X_{i,N-2} + D_N\, m_{i,n}\, X_{i,N} + A_{N-1}\, X_{i,N-1} - D_N\, m_{i,N}\, X_{i,N} = F_{N-1}\, X^F_{i,N-1} \qquad (5.20)$$

Equations (5.17) and (5.20) represent the scrubbing and extraction sections respectively.

5.6 Operation with a Single Solute Feed Stream

A fractional extraction solumn with a single feed stream can be treated in the same manner as multiple feed stream cascade. The only difference is that all feed streams except one would be equated to zero in equations (5.17) and (5.20). In most cases the entering solvents are pure, but sometimes a solute may be present due to the use of recovered solvents. The solutes to be separated will be in solution, in one of the solvents or if they are solids, they may be first dissolved in one of the solvents to facilitate their introduction into the column. If the solvents entering at the ends of the column are pure, the operating lines start on the X and Y axis respectively and if the feed contains no solvent, all operating lines will be parallel. The number of theoretical stages required would be determined graphically, or by

stage-to-stage calculations, when the component flow rates at either section of the cascade match each other approximately, at the feed stage as shown in Figure (5.5).

5.7 Operation with a Multiple Feed Stream

When several feed streams are introduced into the column, whether in solution with one of the relevant solvents or without any solvent therein, the graphical method becomes very complicated and in fact would in most cases be impossible to carry out. In such a case, equations (5.17) and (5.20) would be employed for each solute. The number of theoretical stages would be made in the same manner as for single feed stream by the comparison of the component flow rates from either section of the cascade. The method of multiple feed streams is unusual in liquid extraction particularly if only two solutes and two solvents are used. If more than two solutes and solvents with varying distribution coefficients are used, they may be introduced as multiple feed streams.

CHAPTER SIX

LIQUID-LIQUID EQUILIBRIA

6.0 LIQUID-LIQUID EQUILIBRIA

6.1 Ternary Equilibria Correlations

The design of liquid-liquid extraction equipment depends upon a knowledge of the distribution or relative solubility of a solute between two solvents that are not completely miscible with each other. Many methods have been developed for correlation of the equilibrium data. The ternary triangular diagram, wherein each corner represents a pure solvent and the solute, is used to represent the mutual solubility curve and tie lines. Any composition inside the binodal curve separates into two liquid phases, while composition outside the mutual solubility curve (binodal curve) are in the homogenous region and do not separate into two phases. Graphical methods are still used for representing equilibrium and tie lines data (96) by both ternary and quaternary systems, however, these methods are tedious and cannot be directly used in cases requiring computer analysis. Hence, methods for the correlation of tie lines data have been developed.

6.1.1 The Distribution Law

The solute is distributed between two immiscible solvents to attain equilibrium in such a manner that the ratio of the concentrations of the solute in the two phases at specified temperature is constant. Hence;

$$m = X_{CD}/X_{CA} \qquad (6.1)$$

However, this simple distribution coefficient law is applicable only for ideal linear cases and fails for high concentrations, and also when the distributing solute associates or dissociates in either of the phases.

The equilibrium data can also be represented by a distribution curve obtained by plotting the equilibrium compositions of the solute in the heavy phase against that in the light phase, and the relevant slope gives the value of the distributing coefficient m, at any point on the curve. The curve is located above the 45° line indicating that the distribution ratio is more than unity and that the solute favours the light phase, the opposite is true for the heavy phase. The curve tends to be straight at low concentrations near the origin.

The variation of the distribution coefficient ratio, m has been found to be linear at low (45) concentrations for most systems, and hence any variation in the solute concentrations due to transference does not affect the equilibrium distribution ratio considerably. However, at high concentrations of the solute the extraction equilibria are very much affected by the wide variation of the distribution coefficient ratio. Therefore correlating methods of tie lines data have been introduced.

6.1.2 Campbell's Method

Campbell (97) suggested an equation of the following form to correlate the data for most of the distribution ratios in the ternary systems:

$$m = X_{CD}^{n}/X_{CA} \qquad (6.2)$$

However, it was observed that some curvature appeared near the plait point indicating the difficulty in correlation by this method in the plait point region. However, Banker Hunter and Nash (98) suggested plotting the diluent concentations in the diluent phase (X_{AA}) against the concentrations of the solvent phase (X_{DD}), but again this procedure resulted in a correlation with pronounced curvature. Bachman (99), from the study of the results of Banker et al. (112) observed that the straight line correlation could be directly obtained if Banker's correlation was modified to:

$$X_{DD}\, X_{AA} = a'\, X_{DD} + b'\, X_{AA} \qquad (6.3)$$

or

$$X_{AA} = a' + b'\, X_{AA}/X_{DD} \qquad (6.4)$$

where a' and b' are constant. Howver, the preceeding correlation gave no consideration of the solute concentrations. Later on Bancroft (100) modified the Nernst's model which applied only to limiting cases to the following:

$$|X_{CA}/X_{AA}|^n k = |X_{CD}/X_{DD}| \qquad (6.5)$$

where the constant n takes care of the increase in mutual solubility due to the addition of the solute and the contant k is related to the ratio of the concentration of the consolute in the two phases in equilibrium with each other.

6.1.3 Othmer and Tobias' Correlation

Othmer and Tobias (101) derived their correlation form a consideration of Nernst's law. They also showed that Bachman's correlation, when applied to the limiting case of completely immiscible liquids A and D with no solute involved and with a tie line represented by the base of the triangular plot, would give values for $X_{AA} = 1$ and $X_{DD} = 1$ and hence the constant b' in equation (6.4) would be equal to (1 - a'). The following equations would be obtained on substitution and rearrangement:

$$\frac{1 - X_{DD}}{X_{DD}} = k \frac{1 - X_{AA}}{X_{AA}} \qquad (6.6)$$

or, in terms of the relevant solute and solvents:

$$\frac{X_{CD} + X_{AD}}{X_{DD}} = k \frac{X_{CA} + X_{DA}}{X_{AA}} \qquad (6.7)$$

The preceeding equation shows that the ratio of the sum of the solute and diluent to the solvent in the solvent rich phase is proportional to the ratio of the sum of the solute and solvent to the diluent-rich phase. The quantities $(X_{CD} + X_{AD})/X_{DD}$ when plotted with $(X_{CA} + X_{DA})/X_{AA}$ on a log-log graph give a straight line with a slope equal to unity for systems in which the mutual solubility of the non-consolutes is negligible in the absence of solute component. As other systems with high initial solubilities between the non-consolute pair are quite common, a more generalised model is applied by introducing an exponent on one of the graphs:

$$\text{Log}\left(\frac{X_{CD} + X_{AD}}{X_{DD}}\right) = n \log\left(\frac{X_{CA} + X_{DA}}{X_{AA}}\right) + k'' \qquad (6.8)$$

where k" is constant.

The above equation can also be written in terms of the solvent and diluent concentrations:

$$\text{Log}\left(\frac{1 - X_{DD}}{X_{DD}}\right) = n \log\left(\frac{1 - X_{AA}}{X_{AA}}\right) + k'' \qquad (6.9)$$

The values of the constants n and k" depend on the relevant system.

6.1.4 Hand's Correlation

Hand (102) showed that a logarithmic plot of (X_{CD}/X_{DD}) against (X_{CA}/X_{AA}) of the conjugate phases gives generally a rectilinear plot. Hand's equation for the correlation of tie-lines data is:

$$X_{CD}/X_{DD} = k \left(\frac{X_{CA}}{X_{AA}}\right)^{n} \qquad (6.10)$$

where k and n are constants.

The above model has been recently used by Al-Saadi and Jeffreys (1) and its application was made on various ternary systems. The same model is to be used in this work for all ternary terms and will also be used for the calculation of the ternary terms (x_{BA}/x_{AA}) and (x_{CB}/x_{DD}) in the quaternary correlations from the corresponding quaternary concentrations (X_{BA}/X_{AA}) and (X_{CD}/X_{DD}).

6.2 Quaternary Equilibria Correlation

Four dimensional geometrical models are required to represent four component systems and a regular tetrahedron is used. A single binary quaternary system is formed when two solutes are distributed between two solvents and geometrical correlations deduced for quaternary tie lines and the saturation obtained from the different ternary data. The three and four dimensional plots are non-flexible and difficult to deal with. However, recently a mathematical correlation was used by Al-Saadi and Jeffreys (1) for the single binary quaternary system. The correlation utilised a limited ternary experimental data that correlated through Hand's equation using the mutual solubility data of the relevant quaternary system. The following correlations are generally applicable for the two solutes (B, C) and the corresponding two solvents A,D:-

For Component B:

$$\frac{X_{BA}/X_{AA}}{X_{BD}/X_{DD}} = \frac{x_{BA}/x_{AA}}{x_{BD}/x_{DD}} + k \left[\frac{X_{BA}}{X_{AA}} + \frac{X_{BD}}{X_{DD}} \right]^{m} \left[\frac{X_{CA}}{X_{AA}} + \frac{X_{CD}}{X_{DD}} \right]^{n} \qquad (6.11)$$

For Component C:

$$\frac{X_{CA}/X_{AA}}{X_{CA}/X_{DD}} = \frac{x_{CA}/x_{AA}}{x_{CD}/x_{DD}} + k' \left[\frac{X_{BA}}{X_{AA}} + \frac{X_{BD}}{X_{DD}} \right]^{m'} \left[\frac{X_{CA}}{X_{AA}} + \frac{X_{CD}}{X_{DD}} \right]^{n'} \qquad (6.12)$$

where k, k', m, m', n and n' are constants.

Hand's equation and the correlation made by Al-Saadi and Jeffreys were applied for both the ternary and quaternary tie lines data respectively in this work. A regression analysis has been used for the determination of the above constants, the same was applied to the data reported (1) and an agreement was obtained. The advantage of using these models is that they are comparatively easy and could be fed to the computer for the relevant necessary design data such as the number of theoretical stages and stage-to-stage calculations.

6.3 Prediction of Multicomponent Liquid-Liquid Equilibrium From Binary Parameters

It is assumed that the binary intermolecular interactions predominate the macroscopic properties of the mixtures, and that for a liquid system having two phases in equilibrium at constant temperature and pressure the activity of any component therein has to be the same in both liquid phases. Hence the composition of the conjugated phases would be calculated, if the excess free energy data are available in terms of Gibbs energy (G^E). This is because at a fixed temperature and pressure a stable state mixture is that which has a minimum Gibbs energy. Hence, a liquid mixture will split into two phases to minimise its free energy. In the binary system the equations to be solved are:

$$(\gamma_1 X_1)^I = (\gamma_1 X_1)^{II} \tag{6.13}$$

$$(\gamma_2 X_2)^I = (\gamma_2 X_2)^{II} \tag{6.14}$$

Generally for multicomponent system:

$$(\gamma_i X_i)^I = (\gamma_i x_i)^{II} \tag{6.15}$$

$$\Sigma X_i^I = 1 \tag{6.16}$$

$$\Sigma X_i^{II} = 1 \tag{6.17}$$

Subject to the restrictions:

$$0 \leq X_i^I \leq 1 \tag{6.18}$$

$$0 \leq X_i^{II} \leq 1 \tag{6.19}$$

This indicates that, it is the value of the activity coefficient, which if determined by any suitable method would lead to the prediction of the equilibrium. The method that should be used must contain an equation relating the excess molar free energy (G^E) of the mixture to the overall composition (X_1, X_2 .....X_i), so as corresponding expressions for the activity coefficients (γ_1, γ_2,..... γ_i) can be obtained.
In calculating liquid-liquid equilibria, small inaccuracies in activity coefficients can lead to serious errors, and regardless of which model is used, much care must be provided in determining the relevant parameters from experimental data. Whenever possible, such parameters should come from binary mutual-solubility data. It is claimed that binary vapour-liquid data could also be used for liquid-liquid, if the same correlation can be extrapolated to the operating temperature. However, when parameters are estimated from reduction of vapour-liquid data, the relevant experimental data should be of very high accuracy, and for reliable results it is usually necessary to incorporate some liquid-liquid equilibrium data with the binary vapour-liquid data.

6.3.1 Single Equilibrium Stage

In this operation, a feed for multi-feed streams enter a separation stage and mixed together for a sufficient time and then allowed to settle into two streams of different compositions in equilibrium with each other. The process may consist of single equilibrium stage or of a cascade of equilibrium stages. Figure (6.1) showed a typical equilibrium feed stage.

Mass Balance:

$$F_1 + F_2 = M = \Sigma F_i \tag{6.20}$$

$$\Sigma F_i = R + E \tag{6.21}$$

Component Balance:

$$\Sigma F_i \, x_i^F = R x_i^{I\,I} + E \, x_i^I \tag{6.22}$$

$$x_i^F = \frac{R}{\Sigma F_i} x_i^{I\,I} + \frac{E}{\Sigma F_i} x_i^I$$

From Equation (6.21):

$$R = \Sigma F_i - E \tag{6.23}$$

$$\text{Therefore } x_i^F = \frac{\Sigma F_i - E}{\Sigma F_i} x_i^{I\,I} + \frac{E}{\Sigma F_i} x_i^I \tag{6.24}$$

$$\text{Therefore } x_i^F = \left(1 - \frac{E}{\Sigma F_i}\right) x_i^{I\,I} + \frac{E}{\Sigma F_i} x_i^I \tag{6.25}$$

let $\frac{E}{\Sigma F_i} = \theta'$ fraction of the total feed going to phase 1.

Figure 6.1

Typical Equilibrium Stage.

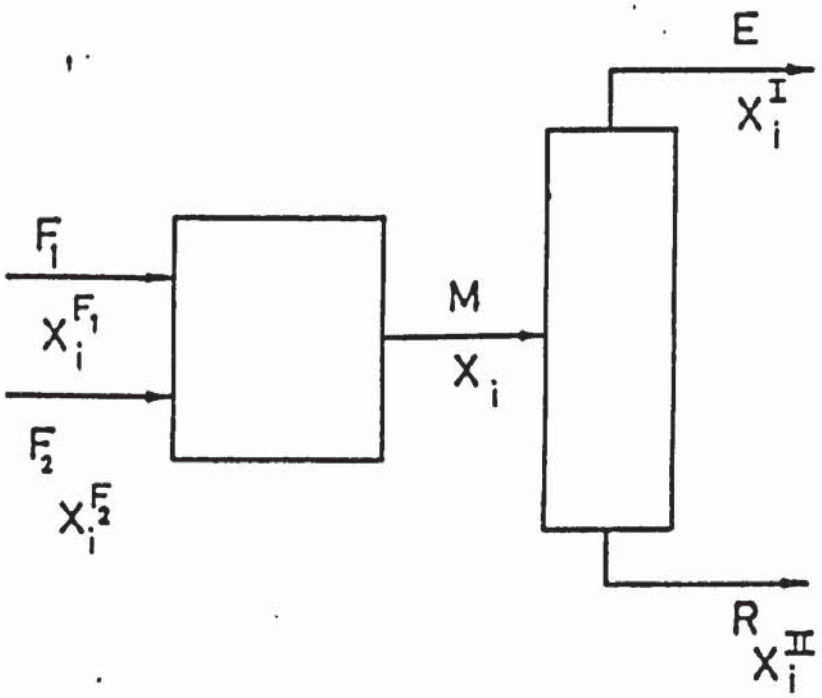

Therefore $x_i^F = (1- \theta') x_i^{II} + \theta' x_i^I$ (6.26)

At equilibrium:

$$\sum_{i=1}^{n} x_i^I = 1.0 \quad (6.27)$$

$$\sum_{i=1}^{n} x_i^{II} \quad (6.28)$$

$$x_i^I/x_i^{II} = m_i = \frac{\gamma_i^{II}}{\gamma_i^I} \quad (6.29)$$

$$x_i^I = \frac{\gamma_i^{II}}{\gamma_i^I} x_i^{II} = m_i x_i^{II} \quad (6.30)$$

Therefore, $x_i^F = (1 - \theta') x_i^{II} + m_i \theta' x_i^{II}$ (6.31)

$$x_i^{II} = \frac{x_i^F}{1 + (m_i-1)\theta'} \quad (6.32)$$

$$x_i^I = \frac{x_i^F m_i}{(m_i-1)\theta'+1} \quad (6.33)$$

Thus, if two liquid phases exist a solution of equation (6.31) must be obtained for which $\Sigma X_i^I = 1.0$. If this holds, then $\Sigma x_i^{II} = 1.0$.

To solve the above equations one normally assumes an initial value of x_i^I and an initial value of θ'. Then x_i^{II} values are calculated by equation (6.26). Then γ_i^I and γ_i^{II} values are calculated from the compositions thus obtained using a suitable activity

coefficient model whose parameters have been previously determined. The distribution coefficients from both the compositions (X_i^I, X_i^{II}) and the activity coefficients (γ_i^I, γ_i^{II}) obtained from the relevant models are compared and if not equal within a certain limit of accuracy new values of X_i^I and X_i^{II} are calculated. If equation (6.24) is not satisfied the value of θ' will be improved until convergence.

The Newton-Raphson Technique is used:

Let:

$$\phi = \Sigma X_i^{II} - 1 \qquad (6.34)$$

$$\frac{d\phi}{d\theta'} = \Sigma \frac{d X_i^{II}}{d\theta'} \qquad (6.35)$$

The value of $dX_i^{II}/d\theta'$ is obtained by differentiating equation (6.33), neglecting the dependence of m_i on composition:

$$\frac{dX_i^{II}}{d\theta'} = \frac{(m_i - 1)x_i^F}{[1+(m_i-1)\theta']^2} \qquad (6.36)$$

Since it is wished to make $\phi = 0$, the Newton Raphson technique gives successive estimates of θ by:

$$\theta'_{new} = \theta'_{old} - \frac{\phi}{d\phi/d\theta} \qquad (6.37)$$

$$\theta'_{new} = \theta'_{old} - \frac{(\Sigma X_i - 1)[1+(m_i-1)\ \theta']^2}{(m_i - 1)\ X_i^F} \qquad (6.38)$$

6.4 The Activity Coefficient Models

Most previous attempts for calculating quaternary liquid-liquid equilibria used geometrical correlations of ternary data (Banker 1940) or empirical equations of ternary data (Prince, 1954). All these methods have two problems in common: they are not readily generalised to more than four components and they are not easily adaptable to computer execution. In an effort to overcome these problems numerous proposals have been made for correlating the excess free energy to liquid composition. Activity coefficient models are algebraic equations which attempt to correlate the activity coefficient of a component in a solution to the composition of that solution. Renon and Prausnitz, 1968, have derived (3) equations from fundamental considerations of molecular forces. Wilson, Deal (103) and then Derr and Deal in the 1960s, presented methods based on treating a solution as a mixture of functional groups instead of molecules. Abrams and Prausnitz derived a model (104) called UNIQUAC (universal quasi-chemical) based on local concentrations. Fredenslund et al. (105), Jones and Prausnitz developed (113) the UNIFAC (UNIQUAC Function-Group Activity Coefficients) group contribution model. The UNIFAC model is theoretically based on the UNIQUAC model wherein the molecular volume and area parameters are replaced by terms relating the number of functional groups in the molecule and the volume area

parameters. In most works, the equilibrium data of multicomponent, ternary and quaternary systems were determined experimentally, the same were predicted using several models, some of them are based on composition relationship and the other are based on activity coefficients equations in order to demonstrate their workability and to compare the result obtained against the experimental values, and agreement was always claimed to be very good.

6.4.1 The NRTL and Its Applications

The NRTL (Non Random Two Liquids) is a function of mole fractions, it was proposed by Renon (3) (1968) and it contains a three-constant parameter for liquid solutions. For a multicomponent system of i components:

$$\ln \gamma_i = \frac{\sum_{j=1}^{N} \tau_{ji} G_{ji} x_j}{\sum_{k=1}^{N} G_{ki} x_k} + \sum_{j=1}^{N} \frac{x_j G_{ij}}{\sum_{k=1}^{N} G_{kj} X_k}$$

$$\tau_{ij} - \frac{\sum_{i=1}^{N} x_i \tau_{ij} G_{ij}}{\sum_{k=1}^{N} G_{kj} x_k} \qquad (6.39)$$

Equation (6.39) involves only the liquid mole fractions and the binary parameters.

For a binary mixture equation (6.39) reduced to the following:

$$\ln \gamma_1 = x_2^2 \left(\frac{\tau_{21} G_{21}^2}{(X_1+X_2G_{21})^2} + \frac{\tau_{12}G_{12}}{(X_2+X_2G_{12})^2}\right) \qquad (6.40)$$

$$\ln \gamma_2 = x_1^2 \left(\frac{\tau_{21} G_{12}^2}{(X_1+X_2G_{12})^2} + \frac{\tau_{12}G_{21}}{(X_2+X_2G_{21})^2}\right) \qquad (6.41)$$

where:

$$G_{12} = \exp(-\alpha_{12}\,\tau_{12})$$

$$G_{21} = \exp(-\alpha_{12}\,\tau_{21})$$

$$\tau_{12} = (g_{12} - g_{22})/RT$$

$$\tau_{21} = (g_{21} - g_{11})/RT$$

Equation (6.40 - 6.41) contain two temperature dependent parameters $(g_{12} - g_{22})$ and $(g_{21} - g_{12})$, in addition to a nonrandomness parameter (α_{12}), which to a good approximation does not depend on temperature and can often be estimated from the nature of the component 1 and 2 (Renon and Prausnitz, 1968). As the NRTL is not sensitive to the nonrandomness parameter variations, the relevant parameters could be specified by the rules set by Renon (3) depending on their binary solubility, in this case only the energy parameters have to be adjusted. The application of the NRTL equation for the prediction of liquid-liquid equilibrium for isothermal conditions and constant pressure would be made as follows:

1. Find the pure components vapour pressure at the specified temperature.

2. Either determine experimentally or obtain from the literature few data points for both the liquid phase (x_i) and the vapour phase in equilibrium therewith (Y_i) at the specified operating pressure.

3. For each data point calculate the activity coefficient γ_i for each binary using the following set of equations:

$$\gamma_1 = Y_1 \, P/x_1 \, P_1^S \qquad (6.42)$$

$$\gamma_2 = Y_2 \, P/x_2 \, P_2^S \qquad (6.43)$$

4. For each data point calculate the molar Gibbs excess energy g^E:

$$g^E = RT \, (X_1 \ln \gamma_1 + X_2 \ln \gamma_2) \qquad (6.44)$$

5. Calculate g^E from the NRTL:

$$g^E_{NRTL} = RT \, x_1 x_2 \left(\frac{\tau_{21} \, G_{21}}{x_1 + G_{21}} + \frac{\tau_{12} \, G_{12}}{x_2 + x_1 G_{12}}\right) \qquad (6.45)$$

6. Adjust the parameters in equation (6.45) to minimise the deviation between g^E and g^E_{NRTL}. The parameters are thus specified and can be used for the prediction of multicomponent equilibrium data. The activity coefficient in step (3) may also be calculated by Flory-Huggins equation (10) and from activity coefficients at infinite dilution. Other methods for parameters determination in application of the NRTL may be made using mutual solubility data.

6.4.2 The UNIQUAC Model

The reason and justification to use any correlation is that it should fit the experimental data and that it should be useful by virtue of its generality and accuracy in prediction of the relvant data, and as the activity coefficients of a component is used to describe the thermodynamic behaviour of the distribution of that solute in a liquid, its value should be determined experimentally or made available through any reliable correlation method.

The UNIQUAC equation gives good representation of both vapour-liquid and liquid-liquid equilibria for binary and multicomponent mixtures containing a variety of nonelectrolytes such as hydrocarbons, ketones, esters, water, amines, alcohols.... etc. In a multi component mixture, the UNIQUAC equation for the activity coefficient of component i is:

$$\ln \gamma_i = \ln \gamma_i^C + \ln \gamma_i^R \qquad (6.46)$$

C = combinatorial part

R = residual part

Both equations of the Combinatorial and Residual parts may be obtained from (113).

6.4.3 The UNIFAC Equation

In the UNIFAC equation, the combinatorial part of the UNIQUAC equation is used directly, and the parameters r_i and q_i are calculated as the sum of the group volume and area parameters R_k and Q_k (113).

The residual part of equation (6.46) is replaced by the following equation:

$$\ln \gamma_i^R = \sum_k \nu_k^{(i)} (\ln \Gamma_k - \ln \Gamma_k^{(i)}) \qquad (6.47)$$

where: Γ_k = Group residual activity coefficient

$\Gamma_k^{(i)}$ = The residual activity coefficient of group k in a reference solution containing only molecules of type i.

Both Γ_k and $\Gamma_k^{(i)}$ have the same form as residual terms:

$$\ln \Gamma_k = Q_k \left[1 - \ln\left(\sum_m \theta_m \psi_{mk}\right) - \sum_m \frac{\theta_m \psi_{mk}}{\sum_n \theta_n \psi_{nm}} \right] \qquad (6.48)$$

where: θ_m = area fraction of group m, given by,

$$\theta_m = \frac{X_m Q_m}{\sum_n X_n Q_n} \qquad (6.49)$$

$$X_m = \frac{\Sigma_j \nu_m^{(i)} X_i}{\Sigma_j \Sigma_n (\nu_k^{(i)} X_j)} \qquad (6.50)$$

$$T_{mk} = \exp\left(\frac{amk}{T}\right) \qquad (6.51)$$

$$Q_{mk} \neq a_{km}$$

The application of the UNIFAC Model lies between the determination of the activity coefficient and the prediction of liquid-liquid equilibrium. The basic steps are:

1. Draw the structural formula of the chemical involved.

2. Determine the kind and the number of structural groups corresponding to those represented in (113).

3. Calculate γ_1, γ_2, q_1 and q_2 using equations in (113), then R_k and Q_k values from (113).

4. Calculate L_1 and L_2.

5. Calculate ϕ_1, ϕ_2, θ_1 and θ_2 and note that:

   $\phi_1 + \phi_2 = 1$

   $\theta_1 + \theta_2 = 1$

6. Calculate γ_1^C and γ_2^C from equations (6.46 and 6.47).

7. Calculate θ_m and x_m for each group from equation (6.44 - 6.50), and note that:

$$\Sigma\ \theta_m = \Sigma\ X_m = 1$$

8. Calculate $\phi_{m,n}$ for each group using the value of a_{nm} in (113) and equation (6.52), where m and n are sub-group numbers.

9. Calculate T_k and $T_k^{(i)}$ for each group using equation (6.48).

10. Calculate ln γ_1^R and ln γ_1^R using equation (6.47).

11. Calculate γ_1 and γ_2.

CONCLUSION

The application of the NRTL to liquid-liquid system equilibria was investigated by Renon and Prausnitz (3). Their investigation indicated tht the NRTL Model could predict quite well the equilibrium composition of multicomponent systems involving one completely miscible binary pair, if the non-randomness parameters (α_{ij}) are set by the rules made by Renon and Prausnitz as well as the binary interaction parameters ($g_{ij} - g_{jj}$). The value of ($g_{ji} - g_{ii}$) are calculated from mutual solubility

data for partially miscible binary pairs. For multi-component systems involving more than one completely miscible binary pair, the value of (α_{ij}) are highly significant, particularly at the plait point, hence ternary data are (3) recommended to be used to specify the value of α_{ij}.

The two adjustable UNIQUAC paramters (U_{ij}-U_{jj}) and (U_{ji} - U_{ii}) could be determined from mutual solubility data for each partially msicible binary pair. Parmeters for miscible binary pairs would be obtained by curve fitting of experimental equilibrium data points. Either the UNIQUAC or the UNIFAC model may be used, but the UNIFAC model is good in predicting whether or not phase separation will occur.

The application of the NRTL for prediction of the concentration profile is shown in Appendix (VII).

CHAPTER SEVEN

EXPERIMENTAL DETERMINATION OF LIQUID-LIQUID EQUILIBRIA

7.1 Experimental Procedure

The experimental technique (2) to obtain the mutual solubility and tie-line data used the Smith Bonner Cell. The properties of the materials used in these experiments are shown in Table (9.1). The analysis of the samples were made at controlled temperature using the ABBE Digital Refractometer made by American optics. Other analysis such as gas-liquid chromatogrphy (G.L.C.) type 5840A, Hewlett Packard and electric photo-refractometer type HP 8415A, Hewlett Packard were also used for checking, and it was decided that the refractometer was the most easy and quickest. A titration method with 0.1 N NaOH was employed for the determination of acetic acid in the aqueous phase using phenolpthalein indicator.

7.2 Experiments on Ternary Systems

7.2.1 Mutual Solubilities

A specified amount of acetic acid and distilled water were introduced into the Smith Bonner cell and agitated at 25°C. This temperature was maintained constant by circulating water from a thermostat. The mixture was then titrated slowly with n-hexane until turbidity or cloudiness was observed. The same was repeated at different compositions.

7.2.2 Equilibrium Tie Lines Determination

A mixture of specified amounts made of n-hexane, distilled water and acetic acid was introduced into the Smith Bonner Cell and agitated continuously for at least three hours, then allowed to settle and separated for the relevant analysis. Various mixture compositions were prepared and used to give different data points. The same procedure was used for a mixture of n-hexane, distilled water and n-butanol. The results are shown in Tables (7.2) and (7.3).

7.3 Experiments on Quaternary Sytems

7.3.1 Mutual Solubilities

A specified amount of the two solutes (acetic acid, n-butanol) and distilled water at various compositions were introduced into Smith Bonner Cell at 25°C with continuous agitation and titrated with n-hexane to turbidity. The same was repeated by titrating the mixture of n-hexane, n-butanol and acetic acid with distilled water. The results are shown in Tables (7.4) and (7.5).

7.3.2 Equilibrium Data on Quaternary Sytems

A known amount of acetic acid, n-butanol, distilled water and n-hexane were introduced into Smith Bonner Cell with continuous agitation at 25°C for at least three hours, then allowed to settle and separated for the required analysis. The results are shown in Table (7.6).

7.4 Cleaning Procedure

The Smith Bonner Cell, the glass mixer and all containers were washed well with normal Fairy Liquid. As the surface active agents affect the mass transfer, extra care was taken to ensure that the containers were rinsed well of the liquid used for cleaning.

The Smith Bonner Cell was filled with 4-5% solution of the Fairy Liquid, run for 30 minutes and emptied, then filled with distilled water and circulated for 15 minutes, drained and rinsed with distilled water three times. This was repeated until the surface tension of distillated water was obtained. The equipment was then dried in the oven at a temperature of 98-100°C.

7.5 Method of Analysis

The relevant analysis was carried out using the ABBE Digital Refractometer, the G.L.C. and the electric photometer. Then titration was made uisng 0.1 sodium hydroxide for the determination of acetic acid (see Appendix I)

7.6 Results

The mutual and tie-line equilibrium data for the ternary systems water-acetic acid n-butanol and water-n-butanol-n-hexane are shown in Tables (7.6) and (7.7).

The quaternary mutual solubility and equilibrium data for the system water-acetic acid n-butanol-n-hexane were arranged as shown in Tables (7.8) and (7.9).

Table 7.1

Equilibrium Data of the Ternary System Water-acetic acid n-hexane, at 25°C Wt.% Saturation Composition.

ORGANIC PHASE			AQUEOUS PHASE		
Water	Acetic Acid	n-Hexane	Water	Acetic Acid	n-Hexane
1.7	73.3	25.0	89.9	10.0	0.1
2.0	78.0	20.0	34.6	64.0	1.4
2.7	82.3	15.0	22.0	76.0	2.0
3.2	84.3	12.5	49.51	50.0	0.49
4.4	85.6	10.0	38.9	60.00	1.0
6.7	86.0	7.3	59.68	40.0	0.32
9.8	85.2	5.0	69.7	30.0	.30
10.5	84.0	5.5	77.8	20.0	.2

Table 7.2

Equilibrium Data of the Ternary System Water-n-Butanol n-Hexane, at 25°C Wt.% Saturation Composition.

AQUEOUS PHASE			ORGANIC PHASE		
Water	Butanol	n-Hexane	Water	Butanol	n-Hexane
93.58	6.4	.0	8.00	64.7	72.7
92.4	7.6	.02	4.8	51.5	43.71
19.8	80.2	0	2.72	38.6	58.68
12.4	74.6	13.00	2	36	62
11.00	73.3	15.7	1.5	20	78.5
9.69	70.3	20.10	.1	10	98.9

Table 7.3

Equilibrium Data of the Ternary System Water-acetic acid n-hexane, at 25°C Wt.% Saturation Composition. Composition of Equilibrium Phases Wt%

AQUEOUS PHASE COMPOSITION WATER LAYER			ORGANIC PHASE COMPOSITION HEXANE LAYER		
Water	Acetic Acid	n-Hexane	Water	Acetic Acid	n-Hexane
87.99	12.0	.01	0.0	0.19	99.9
81.05	18.8	.15	0.0	0.39	99.7
72.99	26.85	.16	0.0	0.78	99.4
65.68	34.1	.22	0.0	1.00	99.0
57.80	41.9	.30	0.0	1.5	98.5
48.00	51.4	.6	0.0	2.2	97.8
38.00	61.0	1.0	0.0	3.3	96.7
27.00	71.0	2.0	0.0	5.7	94.30
15.00	81.8	3.2	0.0	12.0	87.96
0.89	68.0	31.4	0.0	68.0	31.11

Table 7.4

Equilibrium Data of the Ternary System Water-n-Butanol -hexane, at 25°C Wt.% Saturation Composition.

Composition of Equilibrium Phases Wt%

AQUEOUS PHASE COMPOSITION WATER LAYER			ORGANIC PHASE COMPOSITION HEXANE LAYER		
Water	Butanol	n-Hexane	Water	Butanol	n-Hexane
93.13	6.87	0.0	2.9	45.0	52.1
93.21	6.79	0.0	2.3	35.9	61.8
93.41	6.59	0.0	1.7	25.45	72.85
93.72	6.28	0.0	0.9	14.58	84.52
94.15	5.85	0.0	0.6	9.79	89.61
94.8	5.20	0.0	0.3	5.58	94.12
96.1	3.90	0.0	0.2	3.94	95.86
97.0	3.00	0.0	0.0	0.58	99.42
97.85	2.15	0.0	0.0	0.38	99.62

Table 7.4 (continued) Hand's Correlation for Water-Acetic Acid-Hexane

x_{BA}	x_{AA}	x_{BD}	x_{DD}	$\frac{x_{BA}}{x_{AA}}$	$\frac{x_{BD}}{x_{DD}}$	Y Log $\frac{x_{BA}}{x_{AA}}$	X Log $\frac{x_{BD}}{x_{DD}}$
0.2	4.888	0.00316	1.1616	0.041	0.00272	-1.3872	-2.5654
0.313	4.5027	0.0065	1.159	0.0695	0.0056	-1.1580	-2.2518
0.4475	4.055	0.013	1.1558	0.110	0.1125	-0.9586	-1.9488
0.568	3.65	0.0166	1.1511	0.1556	0.01442	-.8079	-1.8410
0.698	3.211	0.025	1.453	0.2174	0.0218	-.6627	-1.6615
0.856	2.66	0.0366	1.1372	0.322	0.03218	-.492144	-1.4924
1.0167	2.11	0.055	1.1244	0.4818	0.0489	-0.3171	-1.3106
1.1833	1.50	0.095	1.0965	0.788	0.0866	-0.10347	-1.0624
1.3633	0.833	0.2	1.0227	1.636	0.1955	0.21378	-0.0885
1.133	0.049	1.133	0.3617	23.112	3.13	1.36172	0.4955

Table 7.4 (continued) Hand's Correlation for Water-n-Butanol-Hexane

x_{CA}	x_{AA}	x_{CD}	x_{DD}	$\frac{x_{CA}}{x_{AA}}$	$\frac{x_{CD}}{x_{DD}}$	Log $\frac{x_{CA}}{x_{AA}}$ (Y)	Log $\frac{x_{CD}}{x_{DD}}$ (X)
0.0928	5.174	0.608	0.608	0.0179	1.16698	-1.747	-.0017406
0.0917	5.178	0.485	0.618	0.0177	0.78478	-1.752	0.17078
0.0890	5.189	0.340	0.72171	0.0171	0.4667	-1.767	0.39128
0.0848	5.206	0.1988	0.8452	0.0163	0.2352	-1.7878	0.6979
0.0790	5.230	0.1322	0.8961	0.0151	0.14763	-1.821	0.89595
0.070	5.266	0.075	0.9412	0.0133	0.07968	-1.876	1.16374
0.052	5.338	0.0532	0.9586	0.00987	0.05549	-2.00	1.32116
0.040	5.338	0.007	0.9942	0.00751	0.00704	-2.124	2.17024
0.029	5.436	0.00513	0.9962	0.00533	0.005149	02.273	2.353

Table 7.5

Ternary System

Prepared Data for Computer Analysis

Water-Acetic Acid-Hexane

Run Number	Y	X
1	-1.3872	-2.5654
2	-1.1580	-2.2518
3	-0.9586	-1.9488
4	-.8079	-1.841
5	-.6627	-1.6615
6	-.49214	-1.4924
7	-.3171	-1.3106
8	-.10347	-1.0627
9	0.21378	-.70885
10	1.36172	0.4955

TERNARY SYSTEM

Water - Acetic Acid - Hexane

Computer output gave the following result:

A plot of X vs Y with slope = 0.909788

intercept = 0.784135

That means K = 10g (.0874135)

K = 7.484

and, r = 0.90978

That gives Hand's equation for the ternary system:

$$\frac{X_{BD}}{X_{AA}} = 7.484 \left(\frac{X_{BD}}{X_{DD}}\right)^{0.909788}$$

for water - acetic acid - hexane system.

Table 7.6 Solubility Data for the Quaternary System water-acetic-n-butanol-n-hexane at 25°C. (Component B).

x_{AA}	x_{BA}	x_{DD}	x_{BD}	$\frac{x_{BA}}{x_{AA}}$	$\frac{x_{BD}}{x_{DD}}$	Y: Log $\frac{x_{CA}}{x_{AA}}$	X: Log $\frac{x_{CD}}{x_{DD}}$
4.33	0.0645	0.3224	0.0023	1.49×10^{-2}	0.702×10^{-2}	$_2$.1225	0.0219
4.67	0.2326	1.089	0.0357	4.98×10^{-2}	3.281×10^{-2}	1.5178	0.0826
5.33	0.3736	0.6956	0.0328	7.01×10^{-2}	4.721×10^{-2}	1.4848	0.1173
2.22	0.1974	0.7402	0,.0506	8.89×10^{-2}	6.835×10^{-2}	1.3007	0.1573
1.83	0.1852	0.612	0.0492	10.12×10^{-2}	8.044×10^{-2}	1.2581	0.1816
1.89	0.2463	0.5365	0.0663	13.03×10^{-2}	12.322×10^{-2}	1.0575	0.2535
1.589	0.2388	0.5582	0.0826	15.03×10^{-2}	14.841×10^{-2}	1.0128	0.2987
2.110	0.3389	0.5565	0.0777	16.06×10^{-2}	15.830×10^{-2}	1.0148	0.3189

Table 7.7 Solubility Data for the Quaternary System: Water-Acetic Acid-n-butanol-n-hexane at 25°C on mole percent basis for Component C.

x_{AA}	x_{CA}	x_{DD}	x_{DD}	$\frac{x_{CA}}{x_{AA}}$	$\frac{x_{CD}}{x_{DD}}$	Y $\text{Log}\ \frac{x_{CA}}{x_{AA}}$	X $\text{Log}\ \frac{x_{CD}}{x_{DD}}$
4.33	0.0437	0.3224	0.0064	1.010×10^{-2}	1.990×10^{-2}	0.5075	0.030
4.67	0.0724	1.089	0.0328	1.550×10^{-2}	3.013×10^{-2}	0.5144	0.0456
5.33	0.1615	0.6956	0.0327	3.03×10^{-2}	4.985×10^{-2}	0.6088	0.0802
2.22	0.1088	0.7402	0.0521	4.90×10^{-2}	7.034×10^{-2}	0.7023	0.1197
1.83	0.1654	0.612	0.0666	9.046×10^{-2}	10.875×10^{-2}	0.8318	0.1992
1.89	0.2083	0.5382	0.0662	11.021×10^{-2}	12.298×10^{-2}	0.8961	0.2332
1.589	0.2212	0.5565	0.0796	13.922×10^{-2}	13.305×10^{-2}	0.9732	0.2823
2.110	0.3120	0.4910	0.0738	14.786×10^{-6}	15.031×10^{-2}	0.9833	0.2917

Table 7.8 Hand's Correlations:

For Component B: $\frac{X_{BA}}{X_{AA}} = 7.484 \left(\frac{X_{BD}}{X_{DD}}\right)^{0.91}$

For Component C: $\frac{X_{CA}}{X_{AA}} = 0.02 \left(\frac{X_{CD}}{X_{DD}}\right)^{0.215}$

$\frac{X_{BA}}{X_{AA}} + \frac{X_{BD}}{X_{DD}}$	$\frac{X_{CA}}{X_{AA}} + \frac{X_{CD}}{X_{DD}}$	$\frac{X_{BA}/X_{AA}}{X_{BD}/X_{DD}}$	$\frac{X_{CA}/X_{AA}}{X_{CD}/X_{DD}}$
0.0219	0.0300	11.6952	0.4329
0.0826	0.0456	10.1798	0.3126
0.1173	0.0802	9.8517	0.2107
0.1572	0.1197	9.5274	0.1607
0.1816	0.1992	9.3896	0.1141
0.2525	0.2332	8.0359	0.1036
0.2987	0.2823	8.8862	0.0920
0.3189	0.2917	8.9514	0.0885

Table 7.9

Regression Statistics for Quaternary Systems

(Water - Acetic Acid - Butanol Hexane)

Component B:

Coefficient of determination (R SQ) = .991488

Coefficient of multiple correlation = .995735

Standard error of estimate = 3.05226E - 03

Regression sum of squares = 5.42566E - 03

Residual sum of squares = 4.65815E - 05

Total sum of squares = 5.47224E - 03

F - Ratio (Regression) = 291.192

Degrees of freedom = 2 and 5

Probability of chance = 0.002

Number of Cases (Subjects) = 8

Number of Independent Variables = 2

REGRESSION COEFFICIENTS

Variable	Name	Mean	S.D.	Coefficient
C	Constant			.859123
IV 1	X 1	-.854263	.383639	-.0786313
IV 2	X 2	-.912338	.375566	6.33751E - 03
DV	Y	.920513	.0279598	

Table 7.10

Regression Statistics for Quaternary Systems

(Water - Acetic Acid - Butanol Hexane)

Component C:

Coefficient of determination (R SQ)	=	.980278
Coefficient of multiple correlation	=	.99009
Standard error of estimate	=	.0632777
Regression sum of squares	=	.995125
Residual sum of squares	=	1.0515
F - Ratio (Regression)	=	124.1264
Degrees of freedom	=	2 and 5
Number of Cases (Subjects)	=	8
Number of Independent Variables	=	2

REGRESSION COEFFICIENTS

Variable	Name	Mean	S.D.	Coefficient
C	Constant			.517847
IV 1	X 1	-.854263	.386339	.70871
IV 2	X 2	-.912338	.380816	.292703
DV	Y	.354621	.380816	

7.7 Discussion of Results

7.7.1 The Ternary System

The equilibrium ternary data for the systems water-acetic acid-n-hexane and water-n-butanol-n-hexane are given in Tables (7.1) to (7.5). A triangular plot of the corresponding data were made for both systems as shown in Figures (7.2) and (7.3).

The ternary data arranged as indicated in Table (7.5) were inserted into a subroutine regression analysis in compliance with Hand's general equation. The subroutine was first tested against the data reported by Al-Saadi (2), and it showed agreement therewith. The following correlations were obtained accordingly:-

Water - Acetic Acid - n-Hexane:

$$X_{BA}/X_{AA} = 7.494\ (X_{BD}/X_{DD})^{0.91} \qquad (7.1)$$

Water-n-Butanol-n-Hexane:

$$X_{CA}/X_{AA} = 0.02\ (X_{CD}/X_{DD})^{0.215} \qquad (7.2)$$

The experimental plot of the above equations on log-log paper produced a straight line.

The plot of the experimental data against the predicted showed a straight line passing through the origin for both systems as shown in Figures (7.6) and (7.7).

It was observed that the quantities of n-hexane in the aqueous phase is very small and can be neglected and the quantity of water in the organic phase is also small and can be neglected, this is in agreement with Al-Saadi and Jeffreys stipulation (2), and also indicated that the two solvents could satisfactorily be considered immiscible.

7.7.2 Quaternary Systems

The quaternary equilibrium data for the system water-acetic acid-n-butanol were arranged as shown in Tables (7.6) to (7.10). (A multiple region subroutine analysis was used to determine the corresponding correlations of the data specified thereto and the following were obtained).

$$\frac{X_{BA}/X_{AA}}{X_{BD}/X_{DD}} = \frac{x_{BA}/x_{AA}}{x_{BD}/x_{DD}} - 7.2297 \left(\frac{X_{BA}}{X_{AA}} + \frac{X_{BD}}{X_{DD}}\right)^{-.00786} \times \left(\frac{X_{CA}}{X_{AA}} + \frac{X_{CD}}{X_{DD}}\right)^{0.0063} \qquad (7.3)$$

$$\frac{X_{CA}/X_{AA}}{X_{CD}/X_{DD}} = \frac{x_{CA}/x_{AA}}{x_{CD}/x_{DD}} + 3.295 \left(\frac{X_{BA}}{X_{AA}} + \frac{X_{BD}}{X_{DD}}\right)^{0.7087} \times \left(\frac{X_{CA}}{X_{AA}} + \frac{X_{CD}}{X_{DD}}\right)^{0.2927} \qquad (7.4)$$

These results were also checked against Al-Saadi (1, 2) data and consequently typical results and correlations were realised. When checking and evaluating the deviation of the actual experimental data against the mean value, it was found that some deviations exist which are due to analytical errors and any other errors accompanied the methods employed. In the first equation (7.3), it was observed that the value of the ternary terms is greater than the quaternary term, this means that the presence of n-butanol suppresses the distribution of acetic acid, and, in the second equation (7.4) the opposite is true showing that the presence of acetic acid favours the distribution of n-butanol and hence the ternary term is less than the corresponding quaternary, this is in agreement with Al-Saadi (1) findings for other systems (1). Again, the quantity of either solvent in the other phase is very small and can be neglected, confirming that the two solvents in the quaternary system are immiscible.

TEXT BOUND INTO

THE SPINE

Phase Equilibrium diagram for the system water – Acetic acid Hexane.

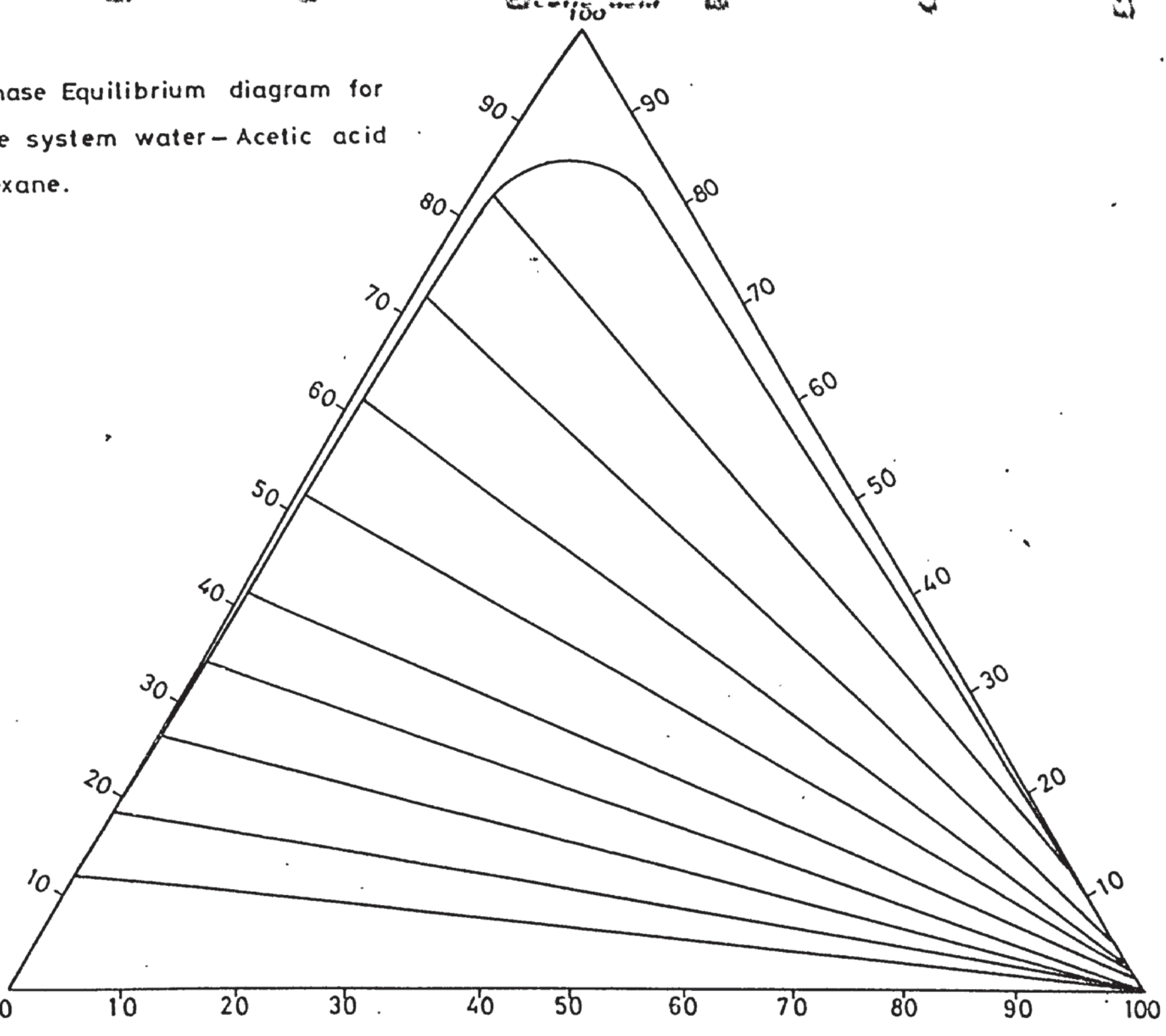

Figure 7.1

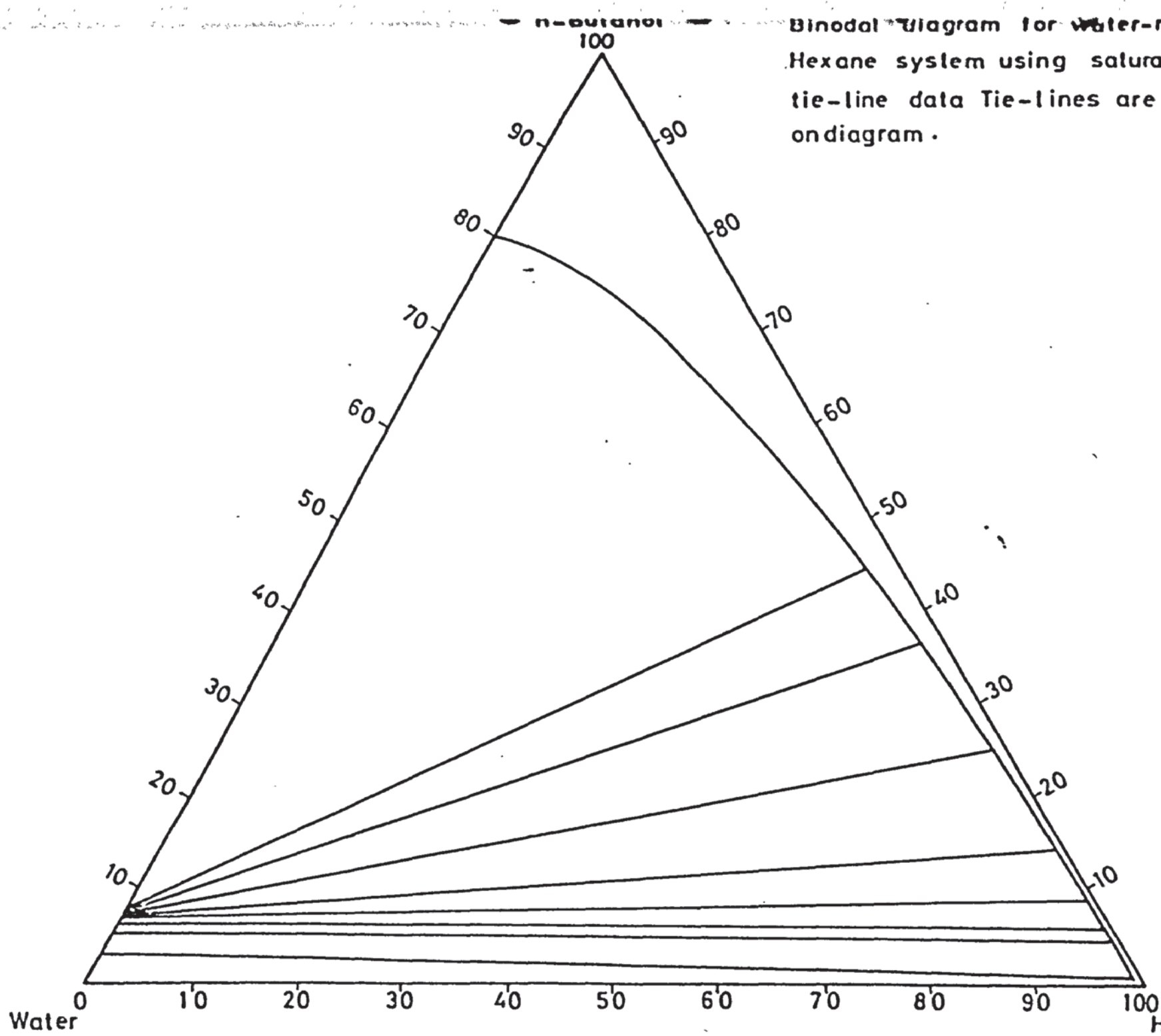

Binodal diagram for water-n.Butanol-Hexane system using saturation and tie-line data Tie-lines are shown on diagram.

Figure 7.2

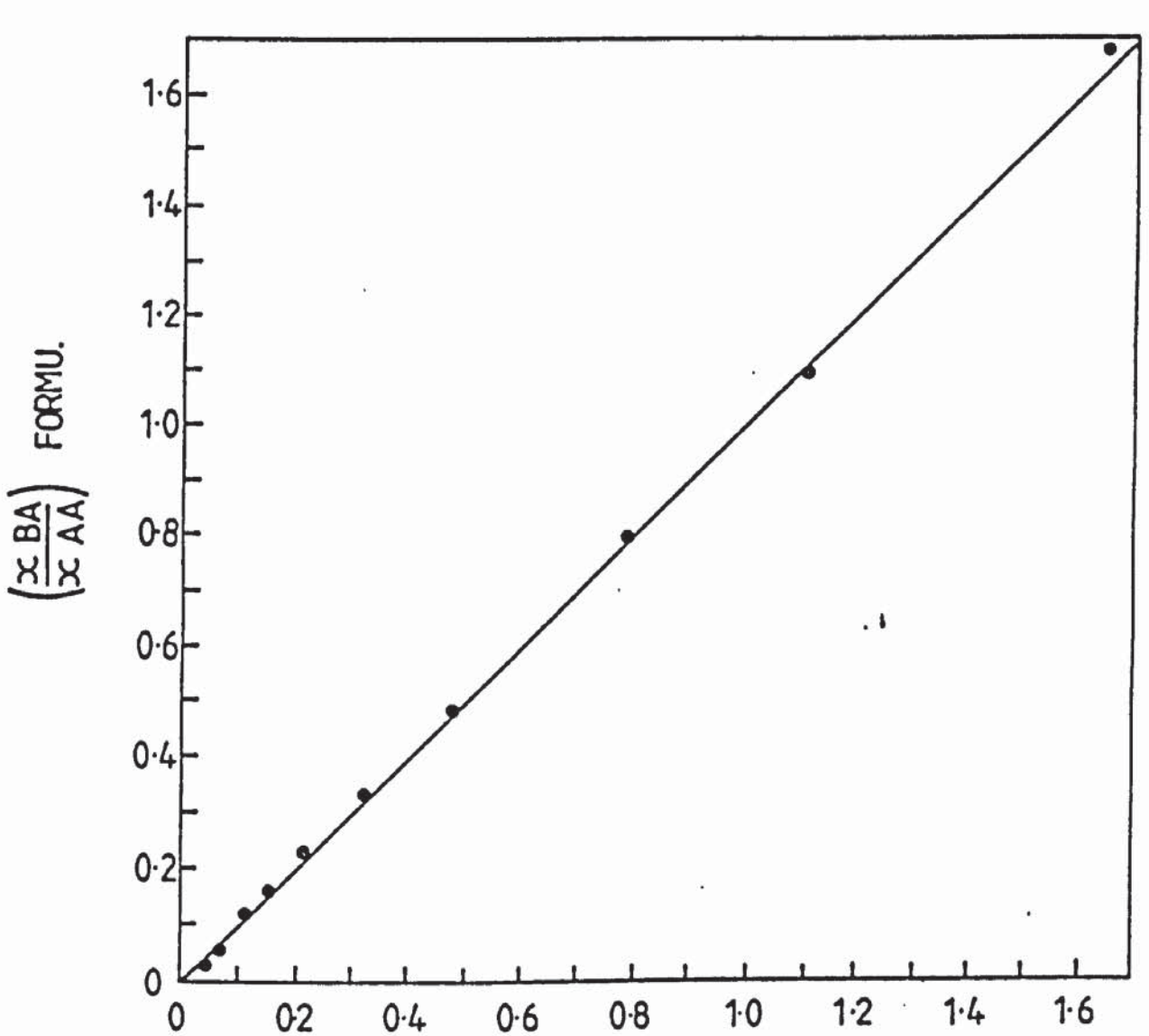

Figure 7.3 Distribution of Acetic Acid in Water-Hexane.

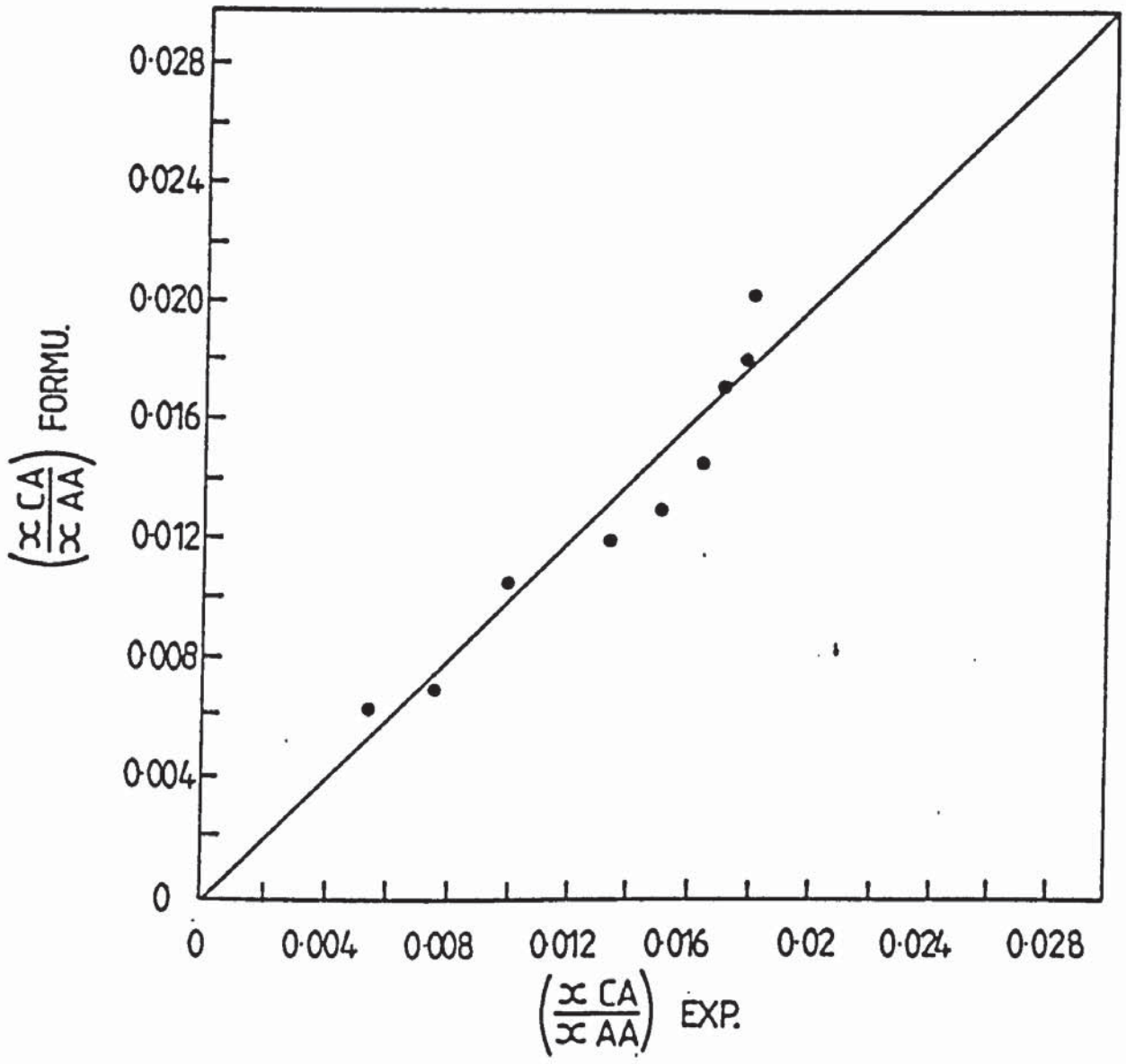

Figure 7.4 Distribution of Butanol in Water-Hexane

CHAPTER EIGHT

MATHEMATICAL MODELS

8.1 MATHEMATICAL MODELS

Simple models that neglect backmixing had been in use until recently when the effect of axial mixing on the concentration profile was observed. However, the incorporation of backmixing in equipment such as extraction columns requires the value of the axial mixing coefficients as well as the mass transfer coefficients or their predicted values. And as the effect of backmixing is important, it is given a special consideration for further study in the future for the system undertaken.

There are two basic models of backmixing. One applies to continuous or differential equipment, such as spray, RDC, and packed columns where there is smooth variation in the concentration along the column. The other model is applicable to stagewise equipment such as plate columns, mixer settlers and Scheibel columns where the concentration alters in a series of steps. The first will be referred to as diffusion model or differential backmixing model and the second as backflow model or stagewise backmixing model. The two models take into account the non-ideal flow of the phases in extraction equipment. The effect of backmixing on the performance of liquis extraction column has been dealt with; much work has been devoted to the subject (106). Alowance of back-mixing is important at both the design stage and the evaluation of the performance of an existing piece of equipment or plant.

The two models are equivalent and either can be used for both types of equipment, and if the number of stages is high, identical results could be obtained (107). Plug-flow models are approximate and assume ideality which would never be realised in actual equipment.

8.2 The Diffusion Model

In this model the solute transfers within the phase from high concentration to low concentration in a manner similar to Fick's Law of diffusion. The relevant solute concentration changes continuously along the axial distance and the mass transfer is proportional to the concentration gradient:

8.3 Mathematical Derivation

8.3.1 Assumptions

1. Both phases could be made continuous or dispersed.

2. Deviation from plug-flow can be considered for the entire column by a constant axial eddy diffusion.

3. Mean velocity concentration of each phase is constant across the column diameter.

4. The two solvents are immiscible.

5. Volume rates of solvents do not change with height for each section of the column.

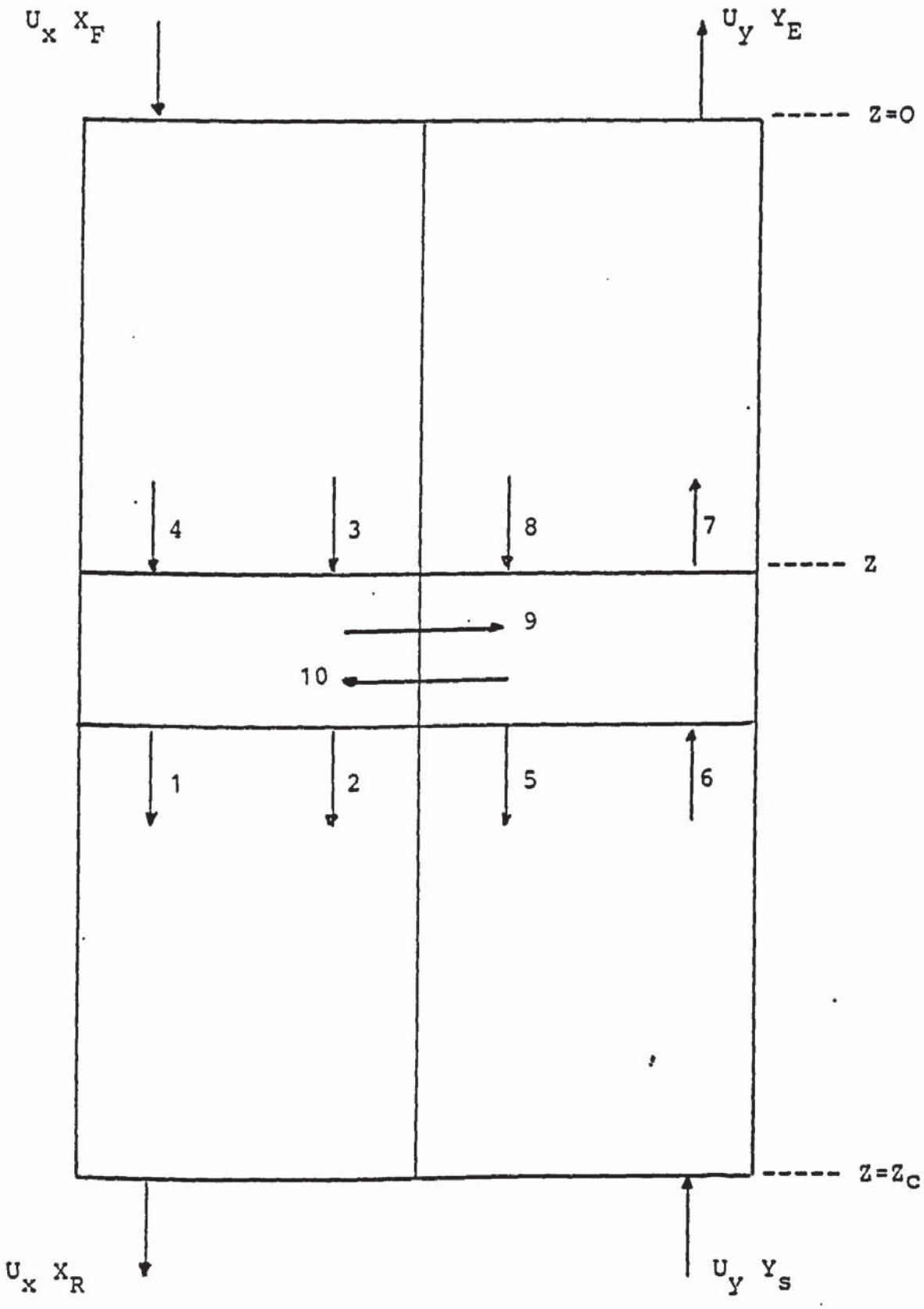

Figure 8.1 Diffusion model

1. $\left(\frac{U_x}{\Theta} X_i \right)_Z$

2. $\left(-E_x \frac{dXi}{dZ}\right)_Z$

3. $\left(-E_x \frac{dXi}{dZ}\right)_{Z+dZ}$

4. $\left(\frac{Ux}{\Theta} Xi\right)_{Z+dZ}$

5. $\left(-E_y \frac{dyi}{dZ}\right)_Z$

6. $\left(\frac{Uy}{\Theta} Yi\right)_Z$

7. $\left(\frac{Uy}{\Theta} Yi\right)_{Z+dZ}$

8. $\left(-E_y \frac{dyi}{dZ}\right)_{Z+dZ}$

9. $K_{iy}a\ (Y_i - Y_i^x)$

10. $K_{ix}a\ (X_i^x - X_i)$

6. The volumetric mass transfer coefficients (Ka) are considered constant throughout each section of the column.

7. There is smooth variation in the concentration profile.

8. Pure solvents are introduced at the column ends.

9. Equilibrium is assumed to be achieved.

8.3.2 Material Balance on each phase over a Differential volume of height dz as in Figure 8.1 yields:

8.3.3 Aqueous Phase

$$\frac{U_X}{\theta} x_i - E_X \frac{dx_i}{dZ} = \left(\frac{U_X}{\theta} x_i\right)_{Z+dZ} - \left(E_X \frac{dx_i}{dZ}\right)_{Z+dZ} + J/\theta \qquad (8.1)$$

where:

U_X = superficial velocity of the continuous phase

E_X = axial mixing dispersion coefficient

J = mass transferred

The terms on the right hand side of equation (8.1) can be expanded as follows:-

$$\left(\frac{U_X}{\theta} x_i\right)_{Z+dZ} = \frac{U_X}{\theta} x_i + \frac{U_X}{\theta} dX_i \qquad (8.2)$$

and

$$\left(E_X \frac{dx_i}{dZ}\right)_{Z+dZ} = E_X \frac{dx_i}{dZ} + E_X \frac{d^2x_i}{dZ^2} \qquad (8.3)$$

Substitute equations (8.2) and (8.3) in equation (8.1):

$$-\frac{U_X}{\theta}\frac{dx_i}{dZ} + E_X \frac{d^2x_i}{dZ^2} - J/\theta = 0 \qquad (8.4)$$

$$-U_X \frac{dx_i}{dZ} + E_X\,\theta \frac{d^2x_i}{dZ^2} - J = 0 \qquad (8.5)$$

Let $E_X\,\theta = e_X$

$$e_X \frac{d^2x_i}{dZ^2} - U_X \frac{dx_i}{dZ} - K_X (x_i - x_i^*) = 0 \qquad (8.6)$$

Define the following dimensionless group:

$$\eta = (X_i - (mY_i + q))/(X_{ii} - mY_{ii} + q)$$

$$\eta = \frac{x_i - x_i^*}{x_{ii} - x_{ii}^*} \qquad (8.7)$$

Where:

x_{ii} = concentration of component i at the interface.

From equation (8.7):

$$\eta x_{ii} - \eta x_{ii}^* = x_i - x_i^* \qquad (8.8)$$

$$x_i = \eta x_{ii} - \eta x_{ii}^* + x_i^* \qquad (8.9)$$

Differentiate equation (8.8) with respect to Z:

$$\frac{dX_i}{dZ} = \eta \frac{dX_{ii}}{dZ} + x_{ii} \frac{d\eta}{dZ} - \eta \frac{dx_{ii}^*}{dZ} - x_{ii}^* \frac{d\eta}{dZ} + \frac{dX_i^*}{dZ}$$

but $\frac{dX_{ii}}{dZ} = \frac{d_{xii}^*}{dZ} = \frac{CX_i^*}{dZ} = 0$

Therefore
$$\frac{dx_i}{dZ} = \frac{d\eta}{dZ} (x_{ii} - x_{ii}^*) \qquad (8.9)$$

Differentiate equation (8.9) with respect to Z:

$$\frac{d^2X_i}{dZ^2} = x_{ii} \frac{d^2\eta}{dZ^2} + \frac{d\eta}{dZ} \frac{dx_{ii}}{dZ} - x_{ii}^* \frac{d^2\eta}{dZ^2} - \frac{d\eta}{dZ} \frac{dX_i^*}{dZ}$$

Again

$$\frac{dx_{ii}}{dZ} = \frac{dx_i^*}{dZ} = 0$$

$$\frac{d^2x_i}{dZ^2} = \frac{d^2\eta}{dZ^2} (x_{ii} - x_{ii}^*) \qquad (8.10)$$

Substitute equation (8.9) and (8.10) into equation (8.6):

$$e_X \frac{d^2\eta}{dZ^2} (x_{ii} - x_{ii}^*) - U_X \frac{d\eta}{dZ} (x_{ii} - x_{ii}^*) = K_X (x_i - x_i^*) \qquad (8.11)$$

Define the following:

Peclet number for the X-phase:

$$(Pe)_X = \frac{U_X}{e_X} \text{ per unit length}$$

Number of transfer unit for the X-phase:

$$(NO)_X = \frac{K_X}{U_X} \text{ pet unit length}$$

Then divide equation (8.11) by U_X

$$\frac{e_X}{U_X}\frac{d^2\eta}{dZ^2}(x_{ii} - x_i^*) - \frac{d\eta}{dZ}(x_{ii} - x_i^*) - \frac{K_X}{U_x}(x_i - x_i^*) = 0$$

But, $$\frac{U_X}{e_X} = (Pe)_X \qquad (8.12)$$

$$\frac{e_X}{U_X} = \frac{1}{(Pe)_X} \qquad (8.13)$$

$$\frac{1}{(Pe)_X}\frac{d^2\eta}{dZ^2}(x_{ii} - x_{ii}^*) - \frac{d\eta}{dZ}(x_{ii} - x_{ii}^*) - (NO)_X(x_i - x_i^*) = 0 \qquad (8.14)$$

$$\frac{d^2\eta}{dZ^2}(x_{ii} - x_i^*) - (Pe)_X\frac{d\eta}{dZ}(x_{ii} - x_i^{i*}) - (Pe)_X(NO)(x_i - x_i^*) = 0 \qquad (8.15)$$

Divide equation (8.15) by $(x_{ii} - x_{ii}^*)$:

$$\frac{d^2\eta}{dZ^2} - (Pe)_X\frac{d\eta}{dZ} - (Pe)_X(NO)_X\frac{x_i - x_i^*}{x_{ii} - x_{ii}^*} = 0 \qquad (8.16)$$

Define the following terms:

$$\phi = (Y_i - Y_{ii})/(X_{ii} - (mY_{ii} + q)) \qquad (8.17)$$

$$\eta - \phi = \frac{X_i = mY_{ii} - q - mY_i + mY_{ii}}{X_{ii} - (mY_{ii} + q)}$$

$$= \frac{X_i\,(mY_i + q)}{X_{ii} - (mY_{ii} + q)} = \frac{X_i - X_i^*}{x_{ii} - x_{ii}^*} \qquad (8.18)$$

Substitute equation (8.18) into equation (8.16):

$$\frac{d^2\eta}{dZ^2} - (Pe)_X\frac{d\eta}{dZ} - (Pe)_X(NO)_X(\eta - \phi) = 0$$

$$\frac{d^2\eta}{dZ^2} - (Pe)_X\frac{d\eta}{dZ} = (NO)_X(Pe)_X(\eta - \phi) \qquad (8.19)$$

8.2.4 The Dispersed Organic Phase (Y):

$$\left(-E_Y \frac{dY_i}{dZ}\right)_{Z+dZ} + \frac{U_Y}{\theta} Y_i = \left(\frac{U_Y Y_i}{\theta}\right)_{Z=dZ} - E_Y \frac{dY_i}{dZ} + \frac{J}{\theta} = 0 \qquad (8.20)$$

By following the same procedure for the X-phase the following equation is obtained for the Y-phase:

$$e_y \frac{d^2 y_i}{dZ^2} + U_y \frac{dY_i}{dZ} + k_Y (Y_i - Y_i^*) = 0 \qquad (8.21)$$

Define the following:

$$U_y/e_y = (Pe)_Y \qquad (8.22)$$

$$F = m\, U_X/U_y \text{ extraction factor.} \qquad (8.23)$$

$$K_y (Y_i - Y_i^*) = K_x (X_i = X_i^*) \qquad (8.24)$$

From equation (8.17):

$$\phi = \frac{m(x_i - x_{ii})}{x_{ii} = x_{ii}^*} \qquad (8.25)$$

$$\frac{\phi}{m} x_{ii} - \frac{\phi}{m} x_{ii}^* = x_i - x_{ii}$$

$$x_i = \frac{\phi}{m} x_{ii} - \frac{\phi}{m} x_{ii}^* + x_{ii} \qquad (8.26)$$

Differentiate equation (8.26) with respect to Z:

$$\frac{dX_i}{dZ} = \frac{1}{m} \frac{d\phi}{dZ} (X_{ii} - x_{ii}^*) \qquad (8.27)$$

Differentiate equation (8.27) with respect to Z:

$$\frac{d^2X_i}{dZ^2} = \frac{1}{m}\frac{d^2\phi}{dZ^2}(x_{ii} - x_{ii}^*) \qquad (8.28)$$

At equilibrium:

$$Y_i = mX_i$$

$$m\frac{dX_i}{dZ} = dY_i/dZ \quad \text{or} \quad \frac{dX_i}{dZ} = \frac{1}{m}\frac{dy_i}{dZ} \qquad (8.29)$$

and,

$$m\frac{d^2X_i}{dZ^2} = d^2Y_i/dZ^2 \quad \text{or} \quad \frac{d^2X_i}{dZ^2} = \frac{1}{m}\frac{d^2y}{dZ^2} \qquad (8.30)$$

Substitute these terms in equation (8.27), (8.28):

$$dY_i/dZ = \frac{m}{m}\frac{d\phi}{dZ}(x_{ii} - x_{ii}^*) \qquad (8.31)$$

$$d^2Y_i/dZ^2 = \frac{m}{m}\frac{d^2\phi}{dZ^2}(x_{ii} - x_{ii}^*) \qquad (8.32)$$

Substitute (8.31) and (8.32) into equation (8.21):

$$e_y\frac{d^2\phi}{dZ^2}(X_{ii} - X_{ii}^*) + U_y\frac{d\phi}{dZ}(x_{ii} - x_{ii}^*) +$$

$$K_x(X_i - X_i^*) = \underline{0} \qquad (8.33)$$

$$\frac{d^2\phi}{dZ^2} + \frac{U_y}{e_y}\frac{d\phi}{dZ} + \frac{K_x}{e_y}\frac{(x_i - x_i^*)}{(x_{ii} - x_{ii}^*)} = 0 \qquad (8.34)$$

By rearrangement and substitution of equation (8.18):

$$\frac{d^2\phi}{dZ^2} + (P_e)_y \frac{d\phi}{dZ} + \frac{k_x}{U_x}\frac{U_x}{U_y}\frac{m}{m}\frac{U_y}{e_y}(\eta - \phi) = 0 \qquad (8.35)$$

$$\frac{d^2\phi}{dZ^2} + (P_e)_y \frac{d\phi}{dZ} + (N_o)_x, \frac{F}{m}, (P_e)_y (\eta - \phi) = 0 \qquad (8.36)$$

8.4 Backmixing Stage Model

A simplified version of this model with phase inlets to the end stages has been made (109). The mass transfer rate in a stage is assumed to be governed by the principle of additivity of resistances.

A constant distribution coefficient, constant flow rate and backmixing of each phase are considered. The model is described as shown in Figure (8.2). Define the following terms:

$$Q_X = K_X a\ (X_i - X_i^*) \qquad (8.37)$$

$$Q_Y = K_Y a\ (Y_i^* - Y_i) \qquad (8.38)$$

$$Q_X - Q_Y = 0 \qquad (8.39)$$

$$Y_i^* = m\ X_i^* \qquad (8.40)$$

Material Balance Round Stage j:

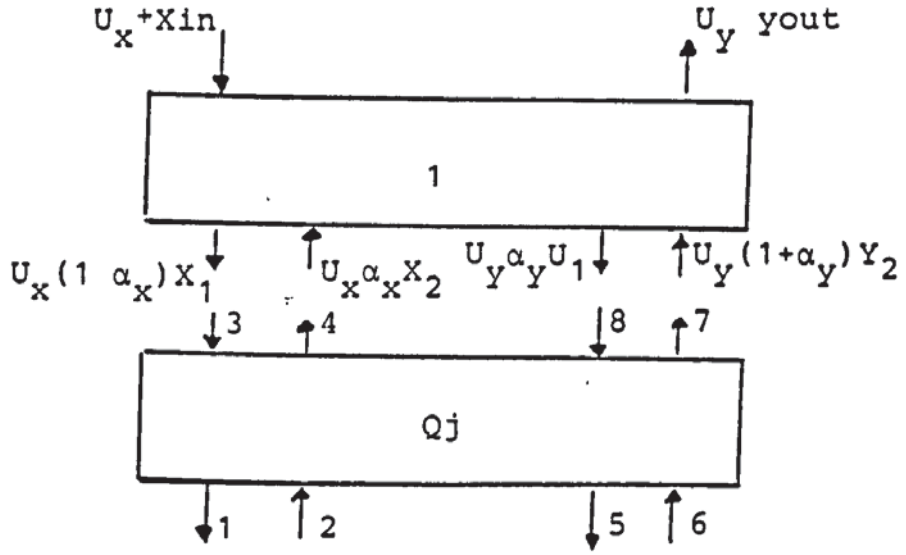

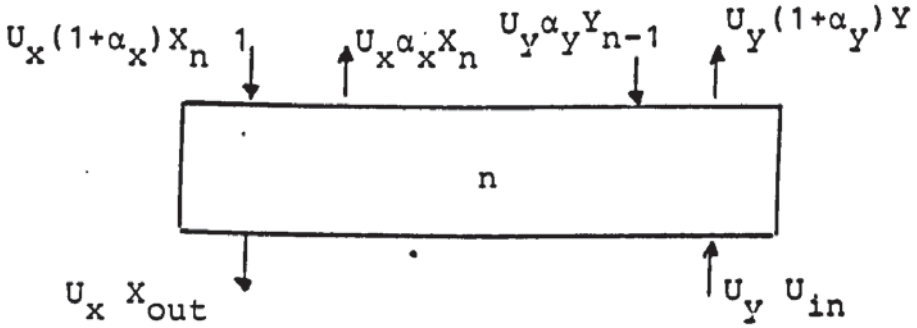

Figure 8.2 Back mixing model

1. $U_x\ (1+\alpha_x)X_j$
2. $U_x\alpha_xX_{j+1}$
3. $U_x(1+\alpha_x)j-1$
4. $U_x\alpha_xXj$
5. $U_y\alpha_yY_j$
6. $U_y(1+\alpha_y)_{j+1}$
7. $U_y(1+\alpha_y)_{yj}$
8. $U_y\alpha_yY_{j-1}$

For the aqueous phase (X-phase):

$$U_X(1 + \alpha_X)\, X_{j-1} + U_X\, \alpha_X\, X_{j+1} - U_X\alpha_X\, X_j - U_X$$

$$(1 + \alpha_X)X_j = Q_X \qquad (8.41)$$

Divide equation (8.41) by U_X and rearrange:

$$(1 + \alpha_X)X_{j-1} + \alpha_X\, X_{j+1} - \alpha_X\, X_j - (1 + \alpha_X)X_j = Q_X/U_X$$

$$(1 + \alpha_X)X_{j-1} - (1 + 2\alpha_X)X_i + \alpha_X\, X_{j+1} - Q_X/U_X = 0 \qquad (8.42)$$

Similarly for the organic phase (Y):

$$\alpha_Y\, Y_{j-1} - (1 + 2\alpha_Y)Y_j + (1 + \alpha_Y)Y_{j+1} + Q_Y/U_Y = 0 \qquad (8.43)$$

Equations (8.42) and (8.43) are applicable for:

$J = 2, \ldots\ldots\ldots, n - 1$

where n = number of stages.

For the first stage:

$$X_{i,in} - (1 + \alpha_X)X_1 + 1\ \alpha_X\, X_2 - Q_X/U_X = 0 \qquad (8.44)$$

For the last stage, i.e. stage (n):

$$Y_{i,in} - (1 + \alpha_Y)\, Y_{i,n} + \alpha_Y\, Y_{i,n-1} + Q_Y/U_y = 0 \qquad (8.45)$$

If constant interfacial area and constant mass transfer coefficients are assumed, equations (8.37) to (8.45) describe the model with four paramters (two mass transfer terms), K_Xa, K_Ya and two backmixing coefficients α_X and α_Y.

8.4.1 Determination of Mass Transfer and Backmixing Coefficients.

8.4.2 The Tracer Injection Technique

Axial mixing in each of the two phases flowing countercurrently can be determined experimentally by pulse injection of a tracer or any other type of disturbances. Runs are performed both with ascending flow, wherein the tracer is injected into the bottom compartment and descending of concentration flow, wherein the tracer is injected into the top stage and concentration detection is made some distance below. The tracer must be soluble in one of the liquid phases only. The column is made to operate without transfer of solute between the liquids until steady state is reached. Then suddenly a pulse of tracer is injected into the column. Samples are withdrawn at the specified distance and plotted on a y-t recorder connected thereto. The data obtained would be used to determine the tracer concentration and the relevant response curve.

Once the axial dispersion parameters are determined, the model would be simulated and the data obtained may be compared with the actual concentration profile to check the validity thereof.

8.4.3 The Concentration Profile Technique

Although the effect of axial mixing is important in both the design of an extraction column and its performances, the technique of its experimental determination is not well developed. The equations relating axial mixing are evaluated from either tracer injection techqniue or from the concentration profile. Both technqiues are approximate and need to be improved to represent the actual equipment.

By determining the concentration profile along the column, axial mixing could be obtained, and due to the influence of the exit boundary conditions the sample locations should be made near the column ends and not far therefrom. The accuracy with which a parameter can be estimated depends on the number of measured data, their accuracy and location of the sampling points along the column.

Hanson and Rod (109) recommended the use of solute concentration profile instead of tracer injection method. They pointed out that the method of concentration profile could be used for the deisgn stage and for an existing plant without interupting the production or imposing any impurity to the product.

Prochazka (110) showed that the column hydrodyanmics could give rise to variations in other quantities such as volumetric mass transfer and axial dispersion coefficient and therefore should be incorporated in the model.

The drop sizes, physical properties and drop velocities may change along the column due to mass transfer and change of concentrations and consequently the interfacial area will also change. As the mean drop velocity is dependent on the drop size, the mean residence time of a drop depends upon its size. The forward mixing or chanelling in the dispersed phase contributes to the spread of residence times in the dispersed phase. This causes a decrease in the effective driving force for mass transfer in comparison with that in fully mixed flow with uniform concentration in each phase and thus affected the concentration profile in the column, and hence should be incorporated in the relevant model (110).

8.5 The Stagewise Model

Modelling of countercurrent stagewise flow liquid-liquid extraction columns has proceeded from two basic models.

1. Stagewise model, with flows between completely mixed stages, and with ideal mixing.

2. Stagewise contacting model with backmixing.

It has been previously mentioned that the stagewise model with backmixing is superior to the differential one for representing such type of equipment, at least for a low number of stages of the relevant equipment, and that the two models give identical results if the number of stages is high.

The stagewise model consists of a cascade of perfectly mixed stages of equal volume, as shown in Figure (8.3).

8.5.1 Mathematical Derivation of the Stagewise Model

It is the simplest model that describes the processes in the extraction column. In this model, the column will be divided into two sections, the upper section (located above the feed stage) and the bottom section (located below the feed stage).

The model is described as shown in Figure (8.3).

In this model the following assumptions were made:

1. Perfect mixing is assumed in the stages.
2. No effect of backmixing between the stages.
3. The exit concentration of each stream from a stage is equal to the bulk concentration of each phase.
4. The equilibrium approach assumes that the mixing and calming section constitute one complete stage in which both phases are perfectly mixed.
5. Equilibrium is attained in each stage.

Taking material balance for the upper setion about stage (n), Figure (8.39):

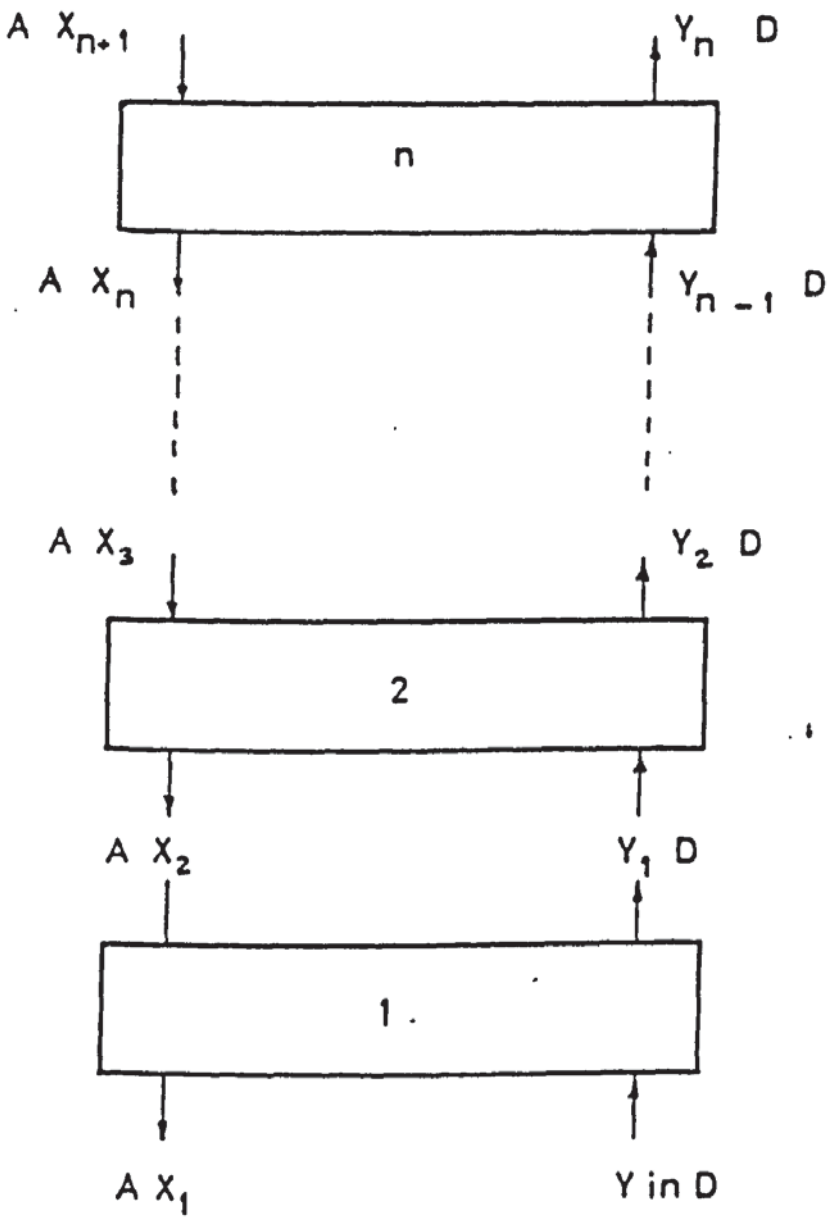

Figure 8.3(a): Upper part of the column in stage wise model

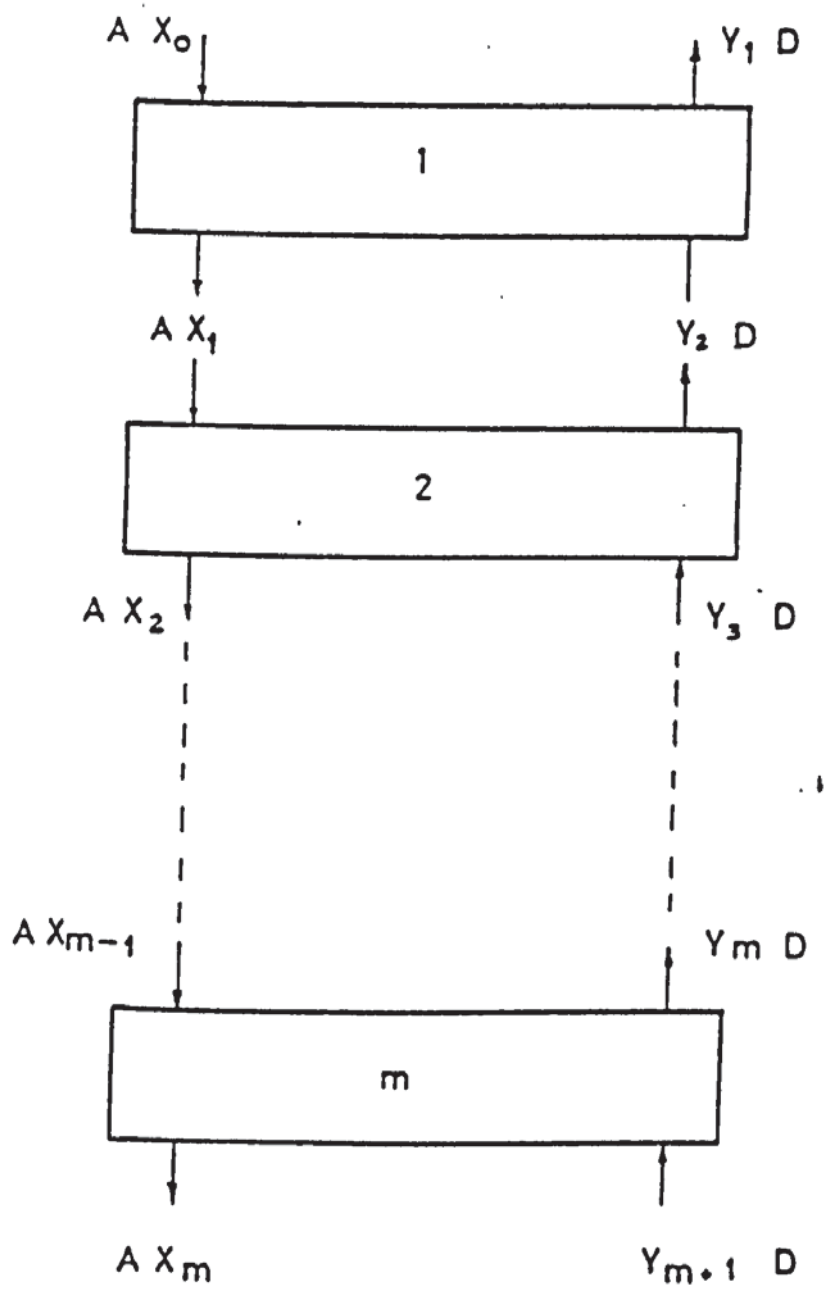

Figure 8.3(b): Lower part of the column in stage wise model

$$A X_{n+1} + DY_{n-1} = AX_n + DY_n \tag{8.46}$$

Assuming linear equilibrium relationship to prevail:

$$Y = KX \tag{8.47}$$

$$AX_{n+1} = AX_n + DY_n - DY_{n-1} \tag{8.48}$$

Divide both sides by A:

$$X_{n+1} = X_n + \frac{D}{A} Y_n - \frac{D}{A} Y_{n-1}$$

$$X_{n+1} = X_n + \frac{D}{A} KX_n - \frac{D}{A} KX_{n-1}$$

$$= X_n + \frac{D}{A} K (X_n - X_{n-1}) \tag{8.49}$$

Equation (8.49) coupled with the material balance equation is used to calculate the stage to stage concentrations for the upper section as shown in the computer program (Appendix III), and the logic flow diagram (Figure 8.4).

Taking material balance around stage m as shown in Figure 8.3b):

$$A X_{m-1} + DY_{m+1} = AX_m + DY_m \tag{8.50}$$

$$Y_m = KX_m \tag{8.51}$$

$$AX_{m-1} + DY_{m+1} = AX_m + D_m X_m$$

$$DY_{m+1} = AX_m + DKX_m - AX_{m-1}$$

Divide by D:

$$Y_{m+1} = \frac{A}{D} X_m + KX_m - \frac{A}{D} X_{m-1}$$

$$Y_{m+1} = (\frac{A}{D} + K)X_m - \frac{A}{D} X_{m-1} \qquad (8.52)$$

This equation and the material balance equation are used to calculate the stage-to stage concentrations for the lower section as shown in the computer program (Appendix III) and the logic flow diagram in Figure 8.4.

8.5.2 Stagewise Model Applied to Multifeeds Cascade With Non-Linear Equilibrium Relation:

Material balance round stage n (figure 5.6):

$$F_n + E_{n+1} + L_{n-1} = L_n + E_n \qquad (8.53)$$

Components balance

$$F_n X^F_{i,n} + E_{n+1} Y_{i,n+1} + L_{n-1} X_{i,n-1} = L_n X_{i,n} + E_n Y_{i,n} \qquad (8.54)$$

Equilibrium Relationship

According to the equilibrium data obtained on this system previously (Chapter 7):

$$X_{B,n} = 7.484 (Y_{B,n})^{0.91} \qquad (8.55)$$

$$X_{C,n} = 0.02 (Y_{C,n})^{0.215} \qquad (8.56)$$

$$\frac{X_{B,n}}{Y_{B,n}} = \frac{x_{B,n}}{y_{B,n}} - 7.2297\,(X_{b,n} + Y_{B,n})^{-0.0786}(X_{C,n} + Y_{C,n})^{0.006338} \tag{8.57}$$

$$\frac{X_{C,n}}{Y_{C,n}} = \frac{x_{C,n}}{y_{C,n}} + 3.295\,(X_{B,n} + Y_{B,n})^{0.70871}\,(X_{c,n+Y_{C,n}})^{0.2927} \tag{8.58}$$

and

$$Y_{i,n}/X_{i,n} = K_{i,n} \tag{8.59}$$

Substitute (8.59) into equation (8.54);

$$L_nX_{i,n} + E_nK_{i,n}X_{i,n} - E_{n+1}\,K_{i,n+1}\,X_{i,n+1} - L_{n-1}\,X_{i,n-1} = F_nX^F_{i,n} \tag{8.60}$$

Mass balance round envelope 1 yields:

$$E_{n+1} + F_n + F_2 + F_1 = D_1 + L_n \tag{8.61}$$

and

$$\sum_{j=1}^{n} F_j + E_{n+1} = L_n + D_1 \tag{8.62}$$

Component balance:

$$\sum_{j=1}^{n} F_jX^F_{i,j} + E_{n+1}\,K_{i,n+1}\,X_{i,n+1} = L_nX_{i,n} + D_1K_i\,X_{i,1} \tag{8.63}$$

Equation (8.60) could be re-arranged into the following matrix:

$$
\begin{bmatrix}
(L_1+D_1K_{i,1}) & (-E_2K_{i,2}) & 0 & 0 & 0 & 0 \\
(-L_1) & (L_2+E_2K_{i,2}) & (-E_3K_{i,3}) & 0 & 0 & 0 \\
0 & (-L_2) & (L_3+E_3K_{i,3}) & (-E_4K_{i,4}) & 0 & 0 \\
0 & 0 & 0 & 0 & 0 & 0 \\
0 & 0 & 0 & 0 & (-L_{n-1}) & (L_n+E_nK_{i,n}) \\
 & & & & 0 & 0
\end{bmatrix}
\begin{bmatrix} X_{i,1} \\ X_{i,2} \\ X_{i,3} \\ \\ X_{i,n} \\ X_{i,N} \end{bmatrix}
=
\begin{bmatrix} F_1X^F_{i,1} \\ F_2X^F_{i,2} \\ F_3X^F_{i,3} \\ \\ F_{n1}X^F_{i,n} \\ F_{N1}X^F_{i,N} \end{bmatrix}
\tag{8.64}
$$

8.5.2.1 Multifeed Simulation Model

The mathematical solution of the multifeed simulation model is initiated from the top of the column as follows:

* The exit concentration and rate of the light phase is given, estimated or taken from the experimental data.

* The purity of the aqueous phase is specified as well as its flow rate.

* The feed rate and composition are specified.

* The feed plate is specified as well as the number of stages.

8.5.2.2 Calculation Procedure

1. From the equilibrium relationship with both $Y_{1,B}$ and $Y_{1,C}$ the value of $X_{1,B}$ and $X_{1,C}$ are calculated from equations (8.55), (8.56), (8.57) and (8.58), the method of solution utilised the Newton Raphson technique for convergence.

2. The flow rate (L1) of the aqueous phase exiting from stage (1) is then calculated:

$$L1 = Lo/(1.0 - \sum (X_{1,B} + X_{1,C}) \qquad (8.65)$$

3. Then, the flow rate of the organic phase entering stage (1) is calculated.

$$E2 = E1 + L1 - Lo \qquad (8.66)$$

4. Then Y2,i can be calculated

$$Y2,i = (L1X1,i + E1\ Y1,i)/E2 \qquad (8.67)$$

5. The calculation will then take the following general form:

$$Ln = Ln-1\ (1.0 - \sum Xi\ (N-1))/(1.0 - \sum Xi(N)) \qquad (8.68)$$

$$E_{n+1} = E_n + L_n = L_{n-1} - F_n \qquad (8.69)$$

6. Then the organic phase concentration is calculated for the following stage as follows:

$$Y_{n+1,i} = (L_nX_{n,i} - L_{n-1}\ X_{n-1,i} + E_{n,i}\ Y_{ni} - F_n\ X_{F,i})/E_{n+1}. \qquad (8.70)$$

7. From $Y_{n+1,i}$ the equilibrium value of $X_{n+1,i}$ can be calculated by the equations in step 1.

8. The procedure is repeated until the conditions are satisfied.

In the procedure described the specified conditions from either the first top stage or the last bottom stage can be used to develop the concentration profile and the componential flow rates.

8.5.2.3 The significance and alternative formulation of the design question:

1. The simulation model procedure can be utilised to predict the final exit concentrations of either phase for a predetermined condition.

2. The number of stages could be increased or decreased to satisfy the required exit concentrations.

3. The feed location can also be adjusted as the conditions may require as well as the feed concentration.

4. The phase ratio may also be investigated and its effect on the concentration profiles and product purity could be checked.

5. Finally, the model may be adjusted to allow for backmixing effect and used for the design of counter-current liquid-liquid contactor, with single feed, multiple feeds or normal counter-current stagewise operations.

A computer program following steps 1 through to 7 has been made as shown in Appendix VI. The program generates X and Y profiles from the top of the column to the bottom. Table 8.1 shows the concentrations of each stage as generated by the simulation program. The solution is started by estimating the flow rate of the aqueous

phase exiting from the first stage by adding the componenial quantity built up to the amount of the pure solvent entering the first stage:

$$L_1 = L_o + \text{quantity extracted}$$

assuming the two solvents are compllete y immiscible i.e. no hexane is found in the aqueous phase and vice versa. The method is superior to the graphical method in calculation of stage-to-stage concentration and in determination of the number of theoretical stages. From any choice of either the first and final stage and with the specification of the conditions stated previously, the simulation may be carried out to solve the relevant design problem.

Table 8.1

Concentration Profile by the Simulation Model

Stage No.	Component B		Component C	
	X1	Y1	X1	Y1
1	.0226	.0112	.0078	.0080
2	.0534	.0334	.0113	.0155
3	.0880	.0637	.0149	.0187
4	.1216	.0977	.0183	.0216
5	.1507	.1308	.0229	.0251
6	.1358	.1133	.0199	.0226
7	.1174	.0924	.0161	.0187
8	.0917	.0660	.0121	.0126
9	.0485	.0288	.0083	.0078

Figure 8.4 Logic Diagram for Stagewise Model.

- Flow chart

(a) Stagewise model to solve for solute concentration profile along the column

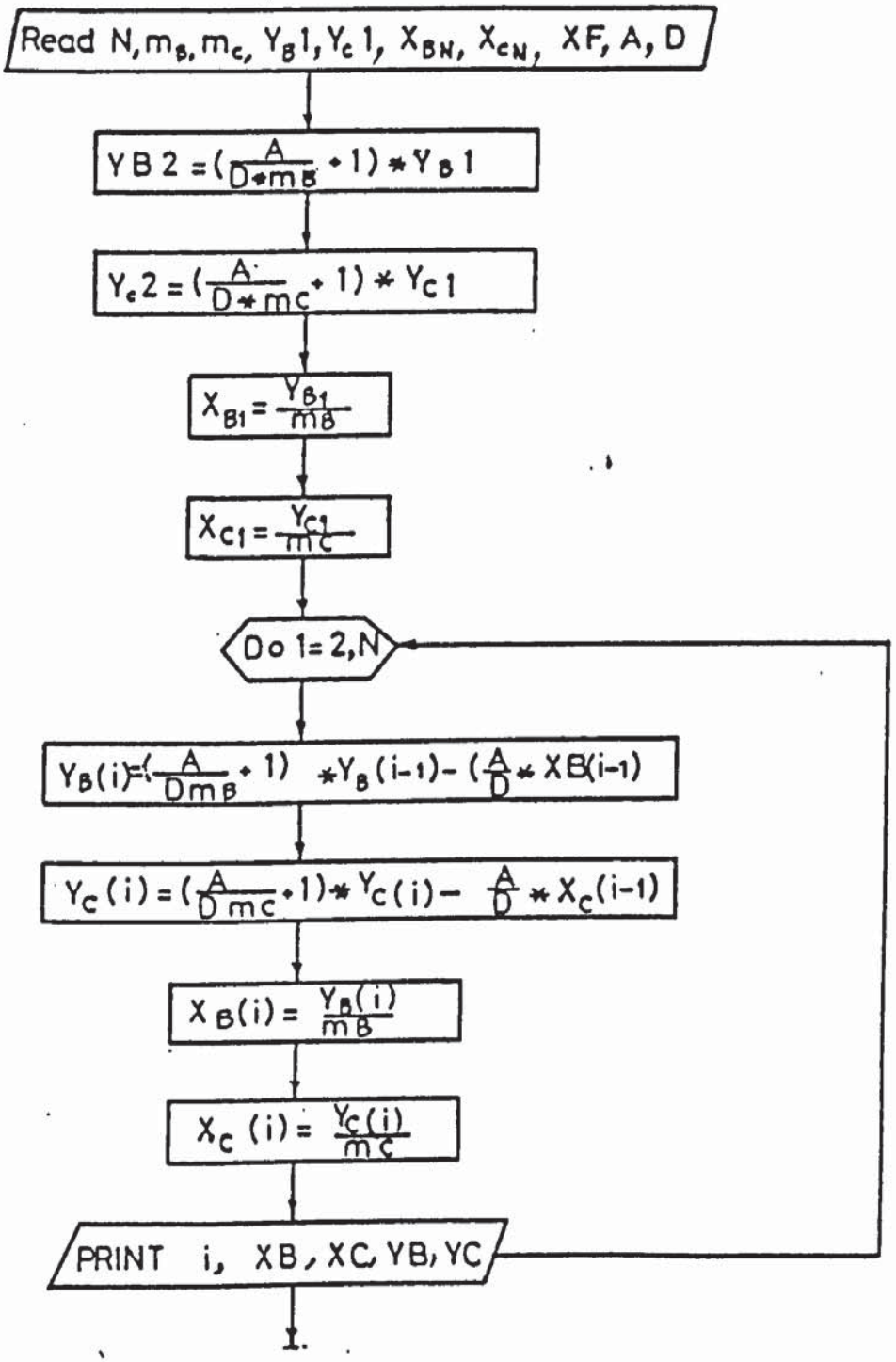

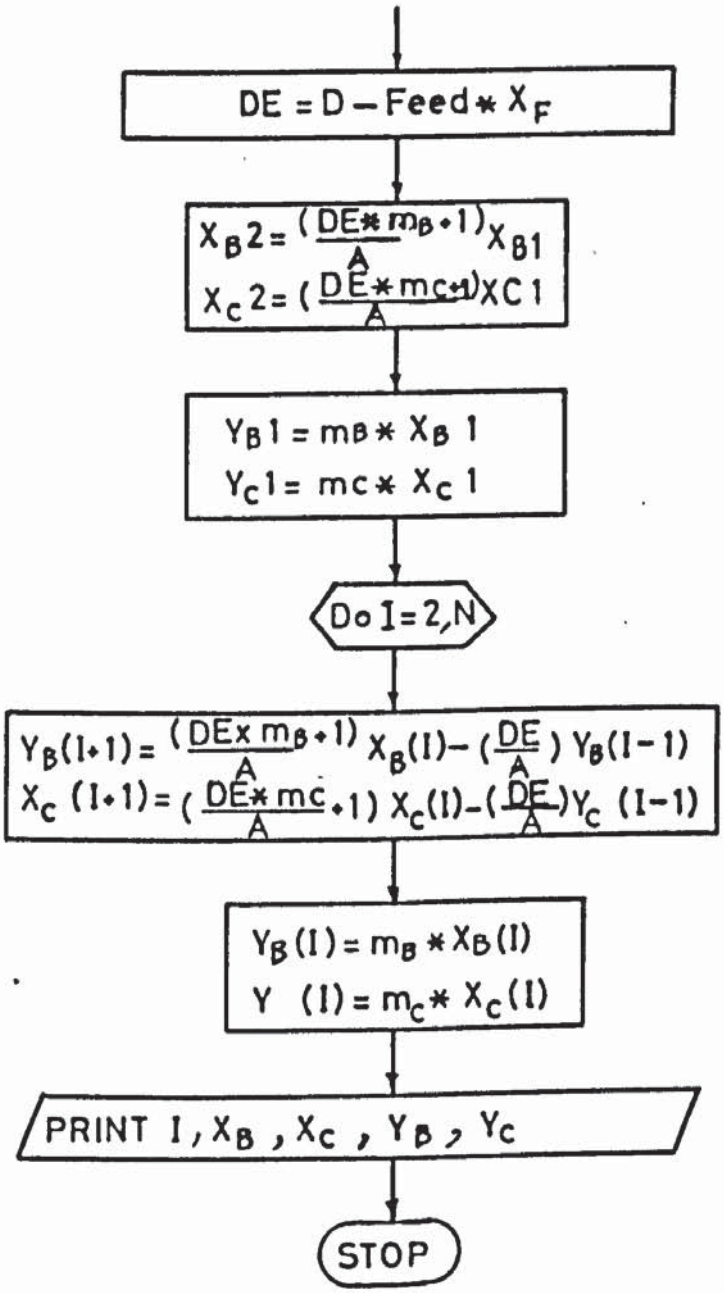
DE = D − Feed * X_F
$X_B 2 = \left(\frac{DE * m_B + 1}{A}\right) X_{B1}$
$X_C 2 = \left(\frac{DE * mc + 1}{A}\right) XC1$
$Y_B 1 = m_B * X_B 1$
$Y_C 1 = mc * X_C 1$
Do I = 2, N
$Y_B(I+1) = \left(\frac{DEx\, m_B + 1}{A}\right) X_B(I) - \left(\frac{DE}{A}\right) Y_B(I-1)$
$X_C(I+1) = \left(\frac{DE * mc}{A} + 1\right) X_C(I) - \left(\frac{DE}{A}\right) Y_C(I-1)$
$Y_B(I) = m_B * X_B(I)$
$Y(I) = m_C * X_C(I)$
PRINT I, X_B, X_C, Y_B, Y_C
STOP

CHAPTER NINE

EXPERIMENTAL INVESTIGATIONS

9.0 EXPERIMENTAL INVESTIGATIONS

9.1 Introduction

Experimental work was carried out to investigate and study the column hydrodynamics without mass transfer so that any further experimentation involving mass transfer would be limited to a reasonable safety factor away from the conditions of flooding and phase inversion. Also a two level factorial experiment was made to investigate the effect of the various factors that have the greatest influence on the column performance.

Based on the results obtained from the column hydrodynamics without mass transfer, and the results of the statistical experimentals, further investigations were designed to settle any doubt raised by the statistical analysis through a proper choice of the levels of the factors in doubt. In these studies, the factors that were confirmed to be significant were fixed and the factors which need to be further studied were varied over wider ranges. All the relevant factors which were mainly: The phase ratio, agitator speed, feed rate and feed concentration were studied and their effect on the column performance expressed as overall stage efficiency was determined.

9.2 Non-Mass Transfer Studies

Non-mass transfer experiments were conducted in order to know the capacity of the column, the flow phase ratio, the feed flow rate and the agitator speed at which flooding and phase inversion may take place. Non-mass transfer experiments are rather important for preliminary assessment of the column hydrodynamics, and some researchers believe that the difference between non-mass transfer hydrodynamics behaviour is not significantly different from hydrodynamics with mass trnasfer of the same column. This belief is rather controversial, and it may apply for some systems whose physical properties such as surface tension, viscosity and density do not vary very much with the addition of the solutes when mass transfer experiments are undertaken. However, in some cases, for special chemical systems non-mass transfer hydrodynamics may not be similar to that of mass transfer and may be misleading if used in the relevant design.

The column was filled with distilled water which was the continuous phase up to the level to be occupied by the interface, a distance of 15 cm above the top distributor. With the agitator stationary and without the continuous phase flow, the dispersed normal hexane was admitted to the column at a low flow rate. When the build up of the coalesced dispersed phase above the interface was high enough, it flowed out of the column to exit.

The water flow rate was started and fixed and the agitator then started and its speed adjusted to the required level. The column was allowed to come to steady conditions and and then the feed of pure n-hexane was introduced into the central feed stage at the specified rate. The column was allowed to attain steady conditions which took about 30 minutes. When steady state was obtained photographs were taken for drop size, distribution and hold-up volume of the dispersed phase. The water flow rate and the agitation speed were kept constant while the flow rate of normal hexane was increased until the column flooded or phase inverted, and the flow at which flooding or phase inversion occurred was observed. This procedure was repeated at different agitator speeds, namely (250, 350, 550, 650 and 750 r.p.m.), and at higher values of the continuous phase flow rate.

As the continuous phase flowed through the bottom of the column, its outflow was carefully controlled so that the interface was always maintained at the same level.

An appearance of a second interface beneath any pad inside the column is an indication of the possibility of flooding. Flooding was taken to exist when an interface appeared in the column at the opposite end from which it was being controlled and the column could no longer be operated. When the light phase was dispersed and the interface was controlled at the top of the column, the

appearance of an interface at the bottom was taken to be the flooding point. Generally a column floods when the solvent throughput is greater than can be handled at the relevant agitator speed. Flooding can be corrected by either reducing the throughput or the speed of agitation.

Flooding sometimes started at the middle of the column and proceeded to one or both ends of the column. Flooding might be detected by observing an inversion of the phase in a particular mixing stage. This should coincide with the appearance of little or no mixing in such a stage because flooding frequently results in a complete blocking of the flow of the dispersed phase. The flooding data obtained and results thereof are given in figures (9.1) to (9.3).

9.3 Flow Meters Calibration

Calibration of the flow meters was made by the traditional method of taking a measured quantity over five minutes interval and the flow rates were plotted against the relevant flow meter scale as shown in Appendix (V).

9.4 Selection of Liquid-Liquid Chemical Systems

The chemical system used in this work was selected for the following reasons:

1. Availability and cost.

2. The two solvents i.e. water and n-hexane are almost completely immiscible.

3. The physical properties of the two solvents such as surface tension, specific gravity, and viscosity are different.

4. The system is industrially important.

5. The analysis of the liquid mixtures must be reliable and can be performed on various devices such as gas liquid chromatographs, refractometer, electro-photometer as well as chemical analysis for the determination of the acetic acid transferred to the aqueous phase.

6. The solutes used have got good range of partition coefficient between the two solvents.

7. Equilibrium data could be easily obtained through experiments or could be obtained from the literature.

The system properties are shown in Table 9.1

Table 9.1

Chemical	Density ρ g/cm^3	Surface Tension Dyne/cm	Viscosity μ Cps
Acetic Acid 98% Purity	1.049	27.30	1.540
n-Butanol	0.815	24.45	2.567
n-Hexane	0.658	18.42	0.294
Distilled Water	0.997	71.97	0.890

9.5 The Factorial Experiments

Based on the column hydrodynamics made without mass transfer and the equilibrium data obtained previously in chapters (6 and 7), a two-level factorial experiment was designed to investigate the effect of each factor on the column performance, the factors are:

Factors and Their Levels

A. Flow rate ratio of heavy and light phase: Water was used as the continuous phase and hexane as the dispersed phase. Two levels were considered.

Low level - 1:2 - n-hexane/distilled water

High level - 2:3 - n-hexane/distilled water

B. Speed of Agitation:-

A mechanical agitator is often used to provide intimate contact of the two phases to provide efficient transfer. The speed of agitation has a strong effect on the process performance. Level studied:

Low Level 250 r.p.m.

High Level 650 r.p.m.

C. Feed Concentration Ratio:

Two levels of concentration of feed were considered:

Low Level 7.6% Acetic 8.4% Butanol 84% Hexane.

High Level 10% Acetic 10.4% Butanol 79.6% Hexane.

D. Feed Flow Rate:

Two levels of feed flow rate will be considered

Low Level 100 g/min

High Level 125 g/min

Design of Experiment

Factorial Experiment:

The study of the effect on a response of the K factors, each at two levels result in a 2^K factorial experiment. In this case the factors equal 4 and hence there are 16 treatment combinations. The lower levels of each factor is denoted by (1). The higher level of the factors was denoted by a positive sign, and the lower level of each factor by a negative sign.

The factorial experiment allows the effect of each and every factor to be estimated and tested independently through the usual analysis of variance. In addition, the interaction effects are easily assessed. The disadvantage with the factorial experiment is the excessive amount of experimentation that is required. The following table shows the sequence of treatment combination.

FACTORIAL EXPERIMENTS

Factors:-

A = speed of agitation

B = feed concentration

C = phase ratio organic/aqueous

D = feed flow rate

Each factor will be replicated at two levels as follows:

Table 9.2

Treatment Combination	FACTORS A	B	C	D
(1)	-	-	-	-
a	+	-	-	-
b	-	+	-	-
ab	+	+	-	-
c	-	-	+	-
ac	+	-	+	-
bc	-	+	+	-
abc	+	+	+	-
d	-	-	-	+
ad	+	-	-	+
bd	-	+	-	+
abd	+	+	-	+
cd	-	-	+	+
acd	+	-	+	+
bcd	+	+	+	+
abcd	+	+	+	+

Table 9.3 Operating Lines Data

Heavy Phase

Treatment Combination	$X_{B,out}$	$X_{B,in}$	$X_{C,out}$	$X_{C,in}$
1*	0.042	0.0	0.0302	0.0
A	0.0185	0.0	0.02765	0.0
B	0.044	0.0	0.02720	0.0
AB	0.0147	0.0	0.01863	0.0
C	0.0578	0.0	0.01605	0.0
AC	0.0243	0.0	0.0111	0.0
BC	0.0680	0.0	0.1005	0.0
ABC	0.0200	0.0	0.01763	0.0
D	0.0406	0.0	0.03325	0.0
AD	0.0180	0.0	0.02503	0.0
BD	0.0430	0.0	0.0292	0.0
ABD	0.0190	0.0	0.02015	0.0
CD	0.052	0.0	0.0214	0.0
ACD	0.0205	0.0	0.0171	0.0
BCD	0.0564	0.0	0.0168	0.0
ABCD**	0.0450	0.0	0.01338	0.0

Light Phase

Treatment Combination	$Y_{B,in}$	$Y_{B,out}$	$Y_{C,in}$	$Y_{C,out}$
1*	0.0	0.0123	0.0	0.07234
A	0.0	0.0100	0.0	0.049923
B	0.0	0.0110	0.0	0.07338
AB	0.0	0.0094	0.0	0.051985
C	0.0	0.0148	0.0	0.07896
AC	0.0	0.0134	0.0	0.05678
BC	0.0	0.0113	0.0	0.08108
ABC	0.0	0.0156	0.0	0.05340
D	0.0	0.0120	0.0	0.09200
AD	0.0	0.0105	0.0	0.06410
BD	0.0	0.0117	0.0	0.09340
ABD	0.0	0.0141	0.0	0.06660
CD	0.0	0.0239	0.0	0.09823
ACD	0.0	0.0202	0.0	0.06924
BCD	0.0	0.0227	0.0	0.09980
ABCD	0.0	0.0188	0.0	0.07123

* All factors at their low levels
** All factors at their high levels

Table 9.4

Analysis of the Results of the Factorial Experiments:

Sum of Variation	Sum of Squares	Degrees of Freedom	Mean Square	
Main Effect				
A	7.15×10^{-3}	1	7.15×10^{-3}	39**
B	5.46×10^{-5}	1	5.46×10^{-5}	0.3
C	7.7×10^{-4}	1	7.7×10^{-4}	4.246**
D	5.15×10^{-5}	1	5.15×10^{-5}	0.284
Two Factor				
AB	3.655×10^{-5}	1	3.655×10^{-5}	0.201
AC	3.1878×10^{-4}	1	3.178×10^{-4}	1.757*
AD	4.656×10^{-5}	1	4.656×10^{-5}	0.2567
BC	7.7×10^{-6}	1	2.7×10^{-6}	0.424
BD	9.1125×16^{-7}	1	0.1125×10^{-7}	5.02×10^{-3}
CD	2.145×10^{-5}	1	2.145×10^{-5}	0.11827
Three Factor				
ABC	2.016×10^{-5}	1	2.016×10^{-5}	0.111
ABD	2.278×10^{-5}	1	2.278×10^{-5}	0.1256
ACD	3.57×10^{-5}	1	3.57×10^{-5}	0.1968
BCD	6.6×10^{-7}	1	6.6×10^{-7}	0.1968
Four Factor				
ABCD	2.7×10^{-5}	1	2.7×10^{-5}	0.149
Error	2.9016×10^{-3}	16	1.8135×10^{-4}	
Total	0.011466	31		

Using the variance ratio test for significances of the above source variation.

$$f_{0.05} = 4.49$$

$$f_{0.10} = 3.09$$

* Significant
** Highly Significant

9.6 Results and Discussion

9.6.1 Column Hydrodynamics

Experiments were carried out to investigate the various factors on column hydrodynamics without mass transfer. Drop size and drop size distribution were studied at different agitator speeds (250 - 650 r.p.m.) at specified feed rates and phase ratios. The results indicated that the drop size decreased with agitator speed which is in agreement with all previous work. Initially, large drop sizes were dominant at low speeds, but smaller drop sizes appeared, such drops might be due to the fact that these were the smallest drop (smaller than the packing voids) which did not undergo any change as their sizes were already established and could not be further subdivided into smaller drops. However, upon increasing the agitator speed, the smaller size droplets become dominant and increased in population; this decrease in drop size continued to increase with the speed of agitation, until a maximum speed was reached (650 r.p.m.) when the drop size could no longer be reduced. Any further increase in the agitator speed made the system milky and hazy and at further speeds flooding occurred. This is shown in Tables (9.5) to (9.7). Figure (9.1) shows the effect of phase ratio and speed of agitation on flooding point determination at different feed rates when the organic phase was dispersed/water continuous and water dispersed/organic continuous.

From Figure (9.2) it is seen that flooding was specified by the phase ratio n-hexane/water. In all cases i.e. at all feed rates, phase ratios with either phase dispersed, the agitator speed played a controlling point with regard to the flooding determination and as the phase ratio increased, flooding occurred at a comparatively lower speed, the same effect was realised with the feed rate i.e. as the feed rate increased, flooding occurred at a lower agitator speed. However, a difference was clearly seen, when comapring the agitator speed at which flooding occurred with respect to each dispersion, and when water was dispersed flooding ocurred at a higher speed than that producing flooding when hexane was dispersed at the same conditions. This was because the agitator speed required more energy to disperse the heavy phase than that required to disperse the light phase, hence flooding ocurred at a higher speed. The centrifugal action of the impeller in the mixing compartment tended to make the light phase flow to the centre of the column and when the heavy phase was dispersed, it was necessary to overcome the centrifugal action by setting up a high velocity flow pattern to bring the heavy phase into the area in which the agitator was effective. Hence, the speed required to disperse the heavy phase into the light phase was much higher than that required to disperse the light phase into the heavy one.

Examination of Figure (9.1) shows that, as the phase ratio is increased flooding ocurred at a lower speed. The opposite was also true i.e. as the phase ratio decreased, flooding occurred at a lower speed. At flooding, both the phase ratio or the agitator speed may be used to get the column back to its normal operating conditions. This could either be made by reducing the phase ratio or by lowering the agitator speed. However, if lowering the agitator speed does not eliminate flooding appearance, the phase ratio must be lowered or both the phase ratio and the agitator speed shall be lowered to eliminate flooding.

9.6.2 Statistical Analysis

A series of factorial experiments was carried out to investigate the effect of the various parameters on the Scheibel column performance.

The factors were:

A : Solvent Flow Ratio

B : Feed Concentration

C : Speed of Agitation

D : Feed Flow Rate

The results shown in Table (9.4) indicate that the effects of the solvent flow ratio n-hexane/water is highly significant, thus increasing the ratio will increase

extraction efficiency. This is obvious, as either phase preferentially extracts one of the two solutes with some traces of the other. This ratio, although highly significant, should be treated with care, as the specified ratio was taken below the flooding conditions of the column. The other points to consider is the amount of the organic phase that was introduced with the feed mixture, as the flow rate of the organic phase would be increased by the amount introduced, and the upper section of the column will be affected, and in fact behaved differently from a hydrodynamic point of view with respect to the lower section. Drop size, flooding, phase inversion and hence relevant hold-up would all be different. This would be expected since a high concentration in the feed will lead to a large difference in the driving force, particularly if the solvents introduced pure. However, on close examination it was found that the column hydrodynamics i.e. drop size, hold-up and flooding were affected by the relevant increase in concentration indicating that the concentration of the solutes in the feed is an important factor in the determination of the column hydrodynamics, particularly with regard to the upper section, and that the results obtained from experiments made without mass transfer should be reconsidered. However, it was found that the speed of agitation was significant. This was expected, as the speed of agitation affects drop size, interfacial area and consquently the

rate of mass transfer. As the speed was increased to a higher level its effect on the droplets size is dominant, but partiuclar consideration should be given to the column hydrodyanmics as the column approaches flooding.

It appears that by increasing the agitator speed, the droplet size decreases and the relevant dispersion is improved (smaller drop diameter) and consequently the mass transfer increases and so does the number of theoretical stages. However, a further increase in the agitator speed (650 - 750 r.p.m.) did not increase the interfacial area per unit volume considerably because, within this range, a uniform drop size had been established. This effect is somewhat different in the upper section, where the flow rate of the organic phase was increased by the amount introduced with the feed, and where a greater load resulted, hence stable drop size was obtained at a lower speed of agitation than at which it occurred in the lower section (600 - 650 r.p.m.). However, the effect of mixing at the lower range of agitator speed may be much improved by increasing the impeller diameter and by use of baffles, which would break-up the smooth swirling motion at column boundary set by agitation and reduce the drop size at this part of the column.

It was thought that the feed rate and feed concentration are highly significant, thus their levels were chosen to be limited, however the results have shown otherwise.

Backmixing between the stages has not a considerable effect due to the packing between the stages. It was found that the hydrodynamics behaviour in each stage in either section did not differ very much from each other. Hence photographs for the remaining experiments were only taken from the central feed stage and the two stages above and below it, in either section of the column.

GXGT ANN.20

*** D R O P S I Z E D I S T R I B U T I O N ***

ROTOR SPEED = 250 RPM

RUN NO. # 1 (Without Mass Transfer) :

DM	DA	F	FV	FCV
2.1400	1.2585	2	2.0879	.0006
2.5900	1.5235	4	9.4906	.0096
3.1400	1.8471	3	19.3839	.0104
3.7000	2.1765	6	51.7573	.0336
5.3500	3.1471	7	165.9375	.0402
6.1800	3.6353	8	367.0722	.1407
7.0100	4.1235	10	734.0043	.2567
7.2800	4.2824	9	1103.5906	.7954
7.5600	4.4471	8	1472.0933	.7635
7.8400	4.6118	10	1985.4034	1.0644
8.1100	4.7706	7	2383.1370	.8553
8.3900	4.9353	8	2927.9348	1.1297

SAUTER MEAN DIAMETE = 4.2958117

Table 9.5.1.

DM = Measured Dia.

DA = Actual Dia.

F = Number Of Drops

FV = Comulative Volume

$$FVC = \frac{dFV}{dDA}$$

@XQT ANN.20

*** D R O P S I Z E D I S T R I B U T I O N ***

ROTOR SPEED = 350 RPM

RUN NO. # 2 (Without Mass Transfer) :

DM	DA	F	FV	FCV
2.0400	1.2000	4	3.6173	.0014
3.1400	1.8471	6	23.4039	.0144
3.7000	2.1765	3	39.5906	.0232
4.8000	2.8235	9	145.6131	.0773
5.3500	3.1471	12	341.3506	.2855
5.9000	3.4706	8	516.3666	.2553
6.1800	3.6353	10	767.7850	.7203
6.4600	3.8000	6	940.0830	.4936
7.0100	4.1235	8	1233.6287	.4281
7.5600	4.4471	5	1463.7554	.3356
8.1100	4.7706	6	1804.5699	.4972
8.3900	4.9353	5	2119.2183	.9012

SAUTER MEAN DIAMETE = 3.8958138

Table 9.5.2.

@XGT ANN.20

*** D R O P S I Z E D I S T R I B U T I O N ***

ROTOR SPEED = 550 RPM

RUN NO. # 3 (Without Mass Transfer) :

DM	DA	F	FV	FCV
2.0400	1.2000	13	11.7562	.0094
3.1400	1.8471	9	41.4361	.0441
3.7000	2.1765	10	95.3917	.1575
4.2500	2.5000	8	160.8084	.1944
4.8000	2.8235	7	243.2703	.2450
5.3500	3.1471	4	308.5162	.1939
6.1800	3.6353	8	509.6509	.3960
7.0100	4.1235	4	656.4237	.2890
7.5600	4.4471	3	794.4997	.4103
8.1100	4.7706	2	908.1379	.3377
8.3900	4.9353	1	971.0476	.3672
8.6600	5.0941	1	1040.2283	.4187

SAUTER MEAN DIAMETE = 3.4804287

Table 9.5.3

@XQT ANN.20

*** D R O P S I Z E D I S T R I B U T I O N ***

ROTOR SPEED = 650 RPM

RUN NO. # 4 (Without Mass Transfer) :

DM	DA	F	FV	FCV
1.4900	.8765	20	7.0473	.0309
2.0400	1.2000	15	20.6121	.1612
2.5900	1.5235	20	57.6256	.4397
3.1400	1.8471	8	84.0078	.3134
3.7000	2.1765	12	148.7546	.7555
4.2500	2.5000	3	173.2858	.2914
4.8000	2.8235	2	196.8463	.2799
5.3500	3.1471	1	213.1578	.1938
5.9000	3.4706	1	235.0348	.2599
6.1800	3.6353	1	260.1766	.5867

SAUTER MEAN DIAMETE = 2.0943058

Table 9.5.4.

Table 9.6

Determination of Flooding Point - Without Mass Transfer

a) Feed Rate : 600 g/min
Phase Ratio : n-hexane/distilled water

Run No.	Phase Ratio wt/wt	Hold-Up at Flooding	Agitator Speed at Flooding
1	1:0.833	0.167	900 r.p.m.
2	1:1.000	0.178	875 r.p.m.
3	1:1.250	0.184	825 r.p.m.
4	1:1.500	0.191	775 r.p.m.

b) Feed Rate: 500 g/min

Run No.	Phase Ratio wt/wt	Hold-Up at Flooding	Agitator Speed at Flooding
1	1:0.833	0.154	1000 r.p.m.
2	1:1.000	0.156	925 r.p.m.
3	1:1.250	0.157	900 r.p.m.
4	1:1.500	0.166	850 r.p.m.

c) Feed Rate: 400 g/min

Run No.	Phase Ratio wt/wt	Hold-Up at Flooding	Agitator Speed at Flooding
1	1:0.833	0.130	1100 r.p.m.
2	1:1.000	0.144	1025 r.p.m.
3	1:1.250	0.147	975 r.p.m.
4	1:1.500	0.153	925 r.p.m.

d) Feed Rate: 300 g/min

Run No.	Phase Ratio wt/wt	Hold-Up at Flooding	Agitator Speed at Flooding
1	1:0.833	0.115	1250 r.p.m.
2	1:1.000	0.121	1200 r.p.m.
3	1:1.250	0.118	1100 r.p.m.
4	1:1.500	0.127	775 r.p.m.

Table 9.7

Relation Between Flow Rates at Flooding

Feed rate 600 gm/min
Agitator Speed 900 r.p.m.
Without Mass Transfer.

Run No.	Flow Rate of Dispersed Phase (g/min)	Flow Rate of Continuous Phase (g/min)
1	833	1000
2	900	900
3	1100	880
4	1200	800

DAMAGED TEXT IN ORIGINAL

Figure (9.1) Determination of Flooding Point At Different Phase Ratios and Various Feed Rate Vs. The Speed of Agitation

Without Mass Transfer

$F_1 < F_2 < F_3 < F_4$ F = Feed Rate

Water Dispersed

Hexane Dispersed

Phase Ratio Hexane/Water

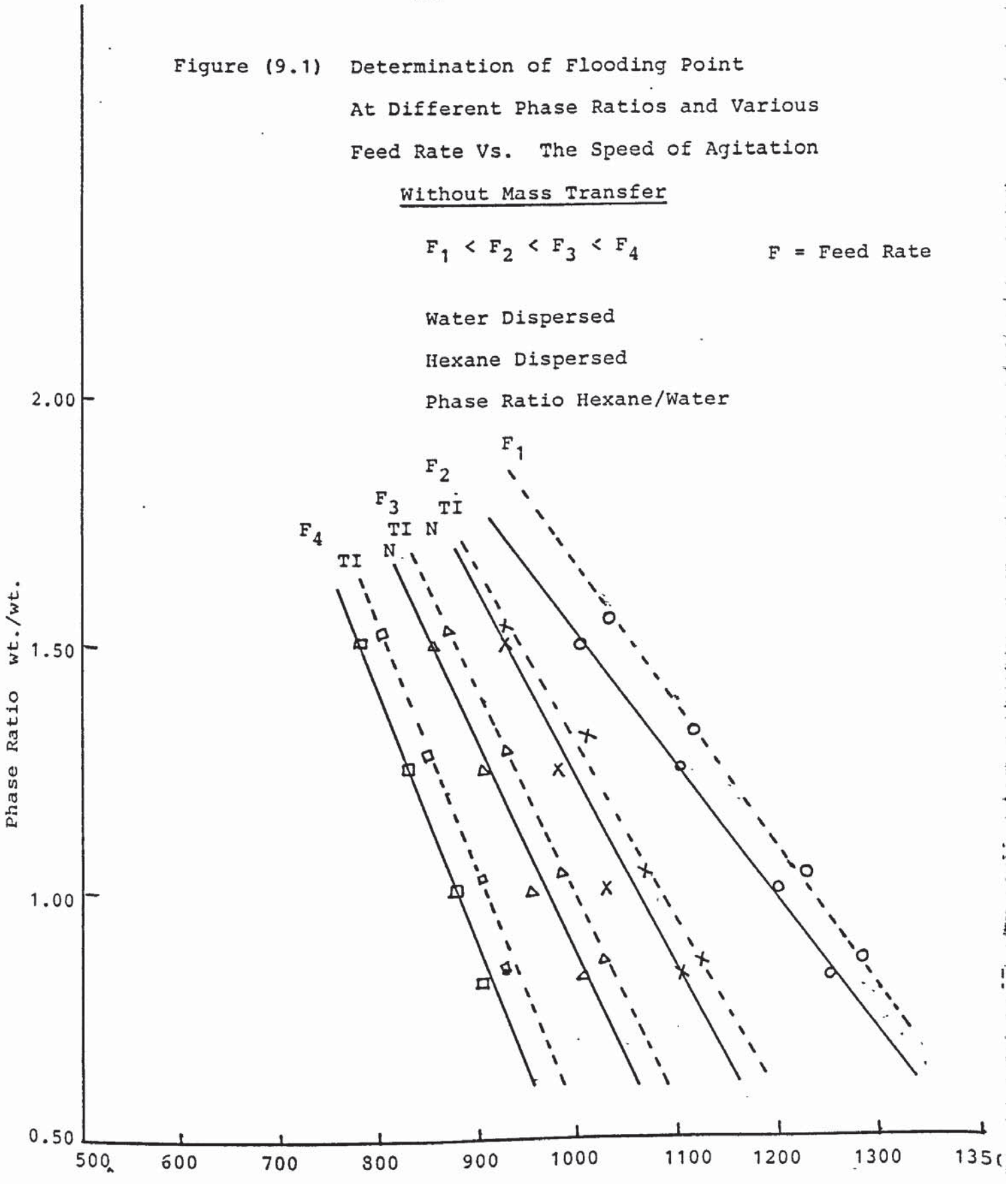

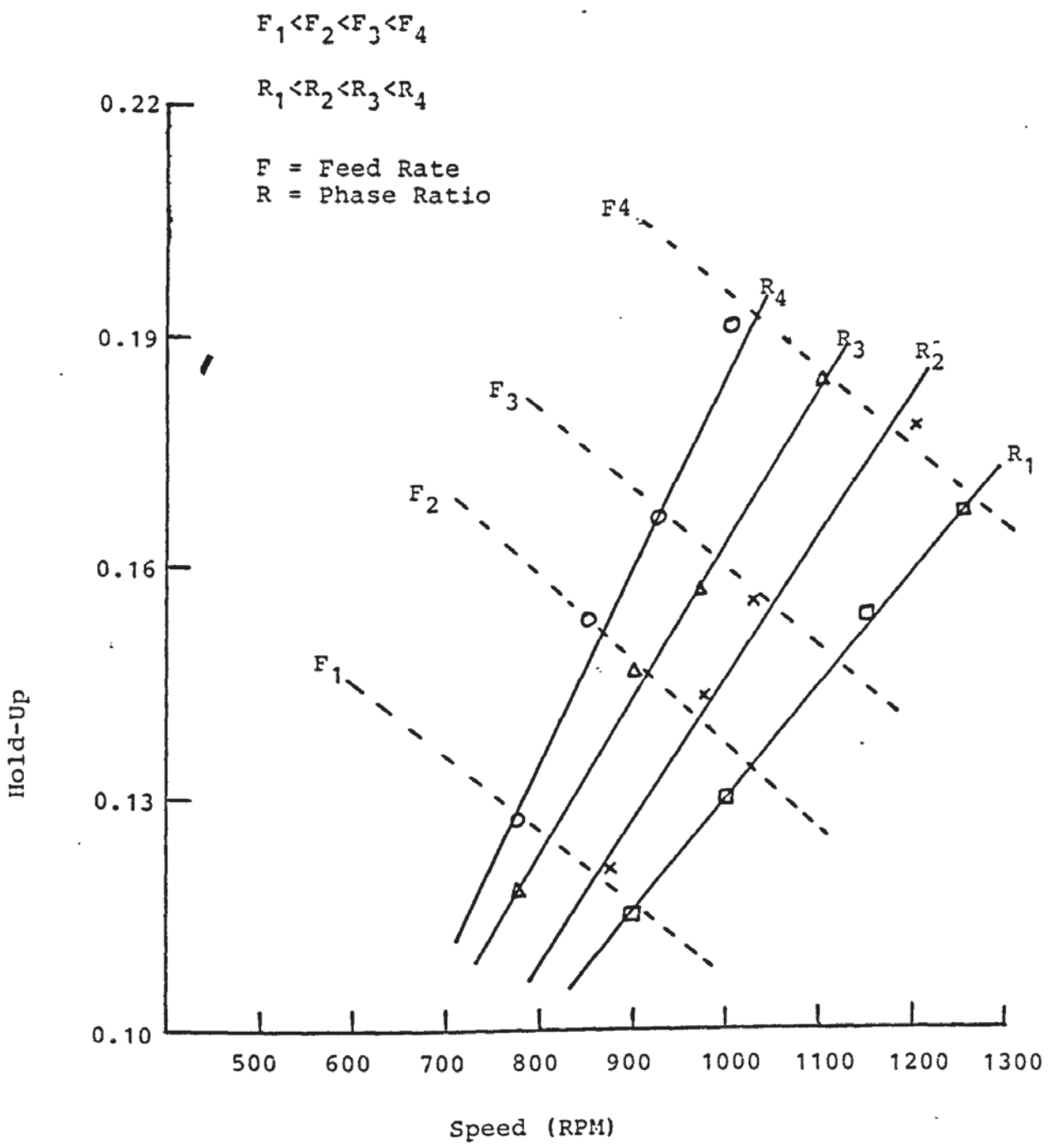

Figure 9.2 Hold-Up At Flooding vs Agitator Speed

$F_1 = 300$ g/min. $R_1 = 1:0.833$

$F_2 = 400$ g/min. $R_2 = 1:1$

$F_3 = 500$ g/min. $R_3 = 1:1.25$

$F_4 = 600$ g/min. $R_4 = 1:1.5$

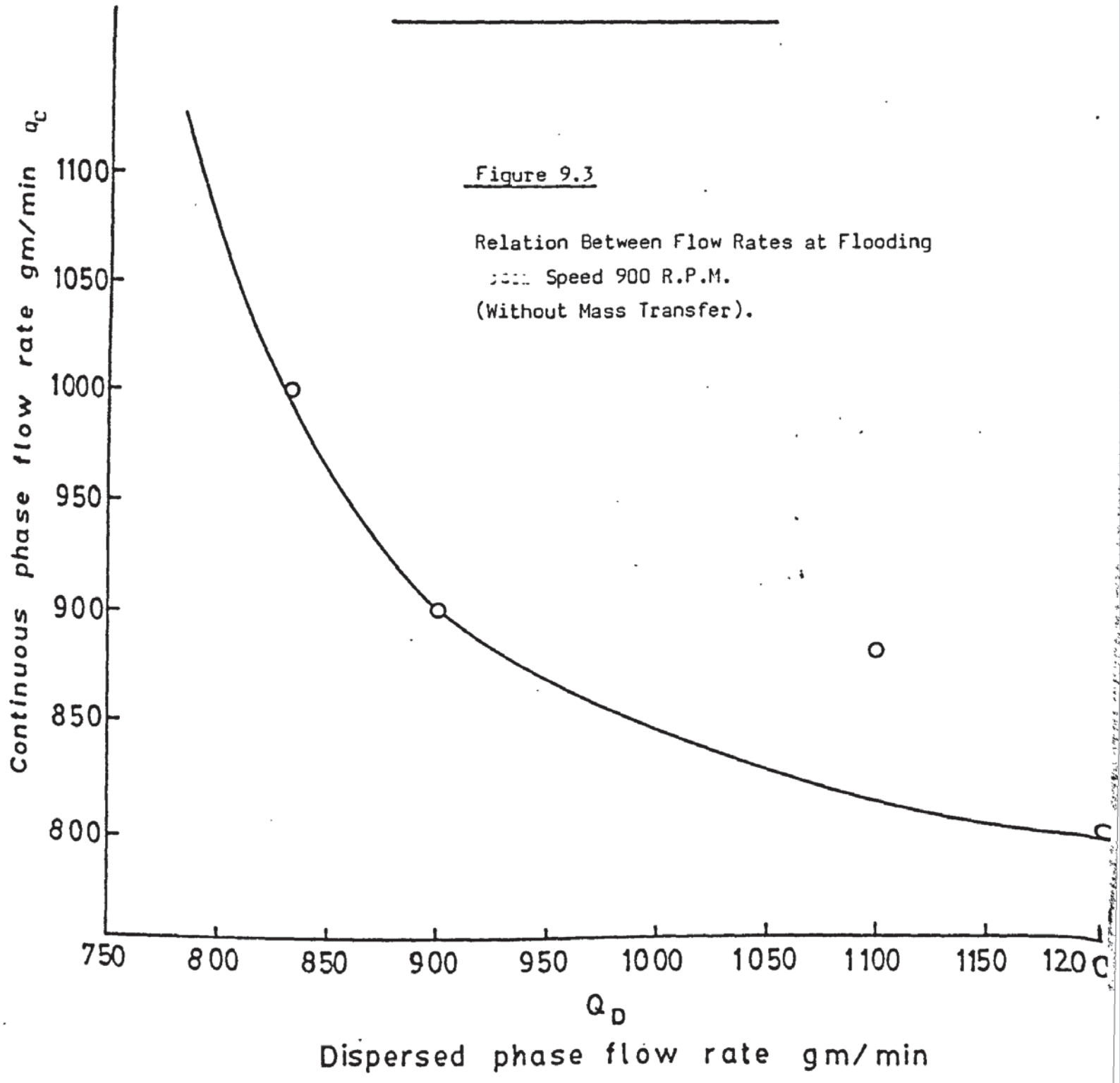

Figure 9.3

Relation Between Flow Rates at Flooding
Speed 900 R.P.M.
(Without Mass Transfer).

CHAPTER 10

MASS TRANSFER STUDIES

10.0 MASS TRANSFER STUDIES

10.1 Factors Investigated

10.1.1 Solvent Flow Ratio

The ratio of the two solvents is generally established on the basis of equilibrium data and the column hydrodynamics. This was studied at the levels specified previously in Chapter 9.4. The statistical analysis of the factorial experiments indicated that the solvent flow ratio (hexane to water) was highly significant, and as this ratio increased so the degree of extraction would also be increased, but at the expense of a more diluted product. This is obvious since each solvent will preferentially extract one of the two solutes mainly with only a small amount of the other. This ratio, although highly significant should be treated carefully as it is limited by column hydrodynamics such as flooding, phase inversion and the relevant cost of solvent recovery. The effect of phase ratio was previously investigated against agitator speed and feed rate for cases where there was no mass transfer, and its effect on the determination of flooding is seen in Figure 9.1. The amount of solvent introduced at the feed stage should be considered as it increases the quantity of the light phase flow rate. The upper section of the column will be influenced by the

amount of solvent introduced with the feed and might behave differently from a hydrodynamic point of view with respect to the lower section. However, at high feed flow rates the drop size, flooding, phase inversion and consequently the column hold-up in both sections of the column would be affected. This is due to changes in the system properties, i.e. density, surface tension and viscosity. However, there is a maximum possible flow rate of one of the solvents in respect of a specified flow rate of the other at which flooding and phase inversion would take place, as it is illustrated in Figure 9.3, for non-mass transfer runs. The column flooded at both ends, a fact that depends on the solvent properties, the internal design of the column, the rate of mixing and the solvent flow ratio (hexane to water). If the maximum flow ratio is exceeded in favour of one solvent, the other solvent would be rejected by the system and the system is said to flood. When the maximum phase ratio is exceeded, the following may occur:

(i) Entrainment of the dispersed phase into the continuous phase, this will decrease the rate of extraction and will be indicated by flooding.

(ii) Phase inversion may occur, a case wherein the dispersed phase changes into continuous and the continuous changes into dispersed. In such a situation the hydrodynamic equilibria between coalescence and redispersion would be disturbed.

(iii) Formation of other interface boundary beneath the packing.

At flooding the total throughput of the dispersed and continuous phases are a maximum; this ratio could be adjusted in favour of either solvent, depending on the particular case under consideration and also of the relevant system properties at such a ratio. In factional extraction each section of the cascade behaves differently and flooding would occur in the upper section first, and this would be a determining factor with regard to column hydrodynamics. This would depend on which of the two solvents is to be introduced with the solutes, the amount of solvent introduced and the direction of its flow i.e. up or down the cascade, the influence of the solvent and the system properties. However, it is usual to introduce the solutes with the light phase, and in this case the upper section would be very more liable to flood at a high feed flow rate, the mass transfer rate would be different and influenced by the change in the relevant driving force.

10.1.2 Speed of Agitation

The optimum agitator speed is the speed at which maximum stage efficiency is obtained. This depends on the system properties, back mixing effects and the rate

of mass tranfser. In addition to its variation with the system properties, the agitator speed varies with the phase ratio and with feed flow rate. This was investigated with respect to non-mass transfer cases, and the effect of the speed of agitation is indicated in figure 9.1. From the statistical analysis in the preceding chapter it was concluded that the agitator speed was significant, a fact that was convincing, and this was due to the range of speeds at which the experiments were conducted, such speeds were high enough to produce a considerable change in the drop size, the interfacial area and the mass transfer rate. Hence it was decided to further investigate the speed of agitation at various values not previously considered. The effect of the agitator speed on the drop size, drop size distribution, the dispersed phase hold-up and the stage efficiency were all studied and carefully investigated.

10.1.3 Feed Concentration

The feed composition in all runs consisted of n-hexane, acetic acid and n-butanol at different concentrations.

10.1.4 Feed Flow Rate

The change of feed flow rate will favour the light phase-increase in the upper section of the column,

it will also increase the solutes quantities per unit time. It is clear that the amount of the light solvent per unit time in the upper section is greater than the amount introduced at the bottom of the column by the quantity introduced in the feed and it would be imagined that the effect on the column hydrodynamics, and on the system properties such as surface tension, viscosity and density in that part of the cascade. The significance of this factor was confirmed in the factorial experiment discussed in chapter nine, and its effect on the column hydrodynamics at various phase ratios and speed of agitation for non-mass trnasfer is indicated in figures 9.1 and 9.2. It may be concluded that this factor affected the specification of the point at which flooding took place and it was a controlling factor with respect to the column hydrodynamics.

Different feed flow rates were taken, starting at 300 g/min and increasing this up to 600 g/min with an increment of 100 g/min for each run. The phase ratio (hexane/water) and the feed concentration were kept constant at the pre-specified levels. In every run the exit concentrations of either phase was measured.

10.2 Experimental Study

A flow diagram of the apparatus is shown in Figure 10.1. The column had nine stages consisting of a packed

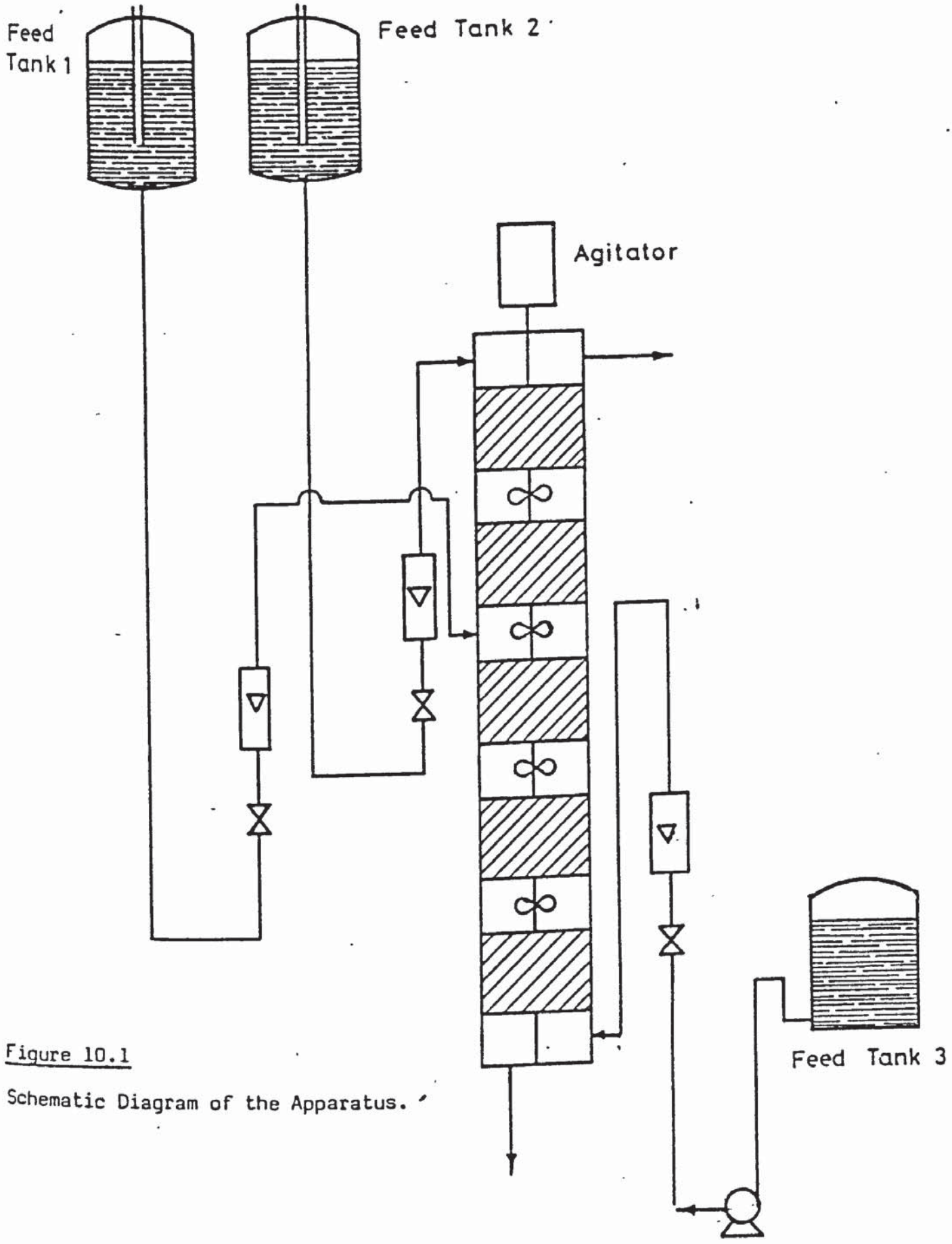

Figure 10.1

Schematic Diagram of the Apparatus.

section and mixing section, both comprising one actual stage. The feed stage was located at the middle of the column, the light phase (n-hexane) was introduced at the bottom, the heavy phase (distilled water) was introduced at the top of the column an the samples were collected from the exitting points of the heavy and light phase. Photographs were taken from the middle compartments and hold-up volume was measured by the simultaneous shut-off method as the column configuration would not allow the sampling technique application. The photographic technique was used to measure drop size and drop size distribution. To measure the actual drop size a scale was fixed on the column at the middle compartment so that the relevant magnification would be taken into account. After the photographs were taken the drop size was measured on the particle size analyser, TG23, No. 4866, made by Option, of West Germany. Flooding rates for non-mass transfer experiments have been specified previously (9.3) for different agitator speeds, and although those rates are different from those with mass transfer, they give a basis for conducting mass transfer experiments less than the flooding rates. Hence, flow ratio of the relevant solvents was fixed and the feed flow rate and agitator speed were varied outside the range that may approach flooding conditions.

10.2.1 Experimental Procedure

Hexane dispersed/water was continuous:

- The overhead tank was filled with distilled water and the meter valve closed.
- The feed tank 1 was filled with the feed admixture of n-hexne, n-butanol and acetic acid at the specified concentration.
- The feed tank 3 was filled with n-hexane.
- The distilled water flow meter valve was opened and the column was filled to the required level.
- The agitator was set at a specified speed.
- The n-hexane was introduced and its flow rate was adjusted to the required value.
- The feed admixture was introduced at specified flow rate with the exit valve at the bottom of the column closed until an interface established.
- The water flow rate was started at a specified value and the interface established was kept at the same level by adjusting the water exit valve at the bottom of the column.
- The column was allowed to attain steady conditions (about 35 minutes, then photographs were taken).
- Samples were collected from the exiting dispersed and continuous phases for the relevant analysis.
- All exit and inlet valves were closed simultaneously and hold-up was measured.

- The procedure was repeated at various speeds of agitation: 250, 350, 550, 650 and 750 r.p.m. keeping the feed admixutre flow rate and the solvent ratio (hexane/water) constant all through.
- The procedure was repeated at different feed admixture flow rate,: 300, 400, 500 and 600 g/min.

10.3 Graphical Representation of the Theoretical Number of Stages

The complete calculation of a fractional liquid extraction column required a matching of the components at the feed and this was made by plotting either the concentration or the quantity of each component against the stage number above and below the feed stage. The point at which the curves for all individual components coincide was obtained by inspection of the graph and only such a point is possible, as shown by Appendix (III). However, sometimes the change within one theoretical stage is very small. In this case the concentration might be taken for every five stages or even more. The opposite is also true when the change of concentration in a stage is high and in such a case a fraction of stage should be considered. The method of stage matching may be convenient for up to four components, but for more than four componets it is tedious and might not be practical.

10.4 Calculation of the Number of Theroetical Stages

The method of equilibrium stage calculations will be considered by two different approaches, one considers a linear equilibrium relationship and the other introduces non-linearity of the equilibrium data.

The required equilibrium data were reported in Chapters (6 and 7), and the relevant correlations have been derived, as shown by equations (7.1 - 7.4). The material balance for each section of the column was made considering a linear case and the following equations were obtained:

For the top section n + 1:

$$Y_{i,n+1} = \frac{\left(\frac{A_n}{D_n m_i}\right)^{n+1} - 1}{\frac{A_n}{D_n m_i} - 1} Y_{i,p} \qquad (10.1)$$

For the bottom section

$$X_{i,m+1} = \frac{\left(\frac{D_m m_i}{A_m}\right)^{m+1} - 1}{\frac{D_m m_i}{A_m} - 1} X_{iB} \qquad (10.2)$$

The above equations hold for each component and as the mutual solubility between the two contacting solvents is

very small it can be neglected. The concentration will be expressed on the basis of a unit quantity of the relevant solvent rather than on the basis of mole or mass fraction. In addition, it is considered that the quantity of each solvent in the column is constant, bearing in mind that the quantity of the light phase will be increased by the amount introduced with the feed. Therefoere, either mole ratios, weight ratios, mole or weight per unit volume of solvent can be used in the above equations. These equations are applicable to ideal systems wherein the distribution coefficients do not vary with concentration, the assumption of ideality can also be assumed for very dilute solutions; otherwise the application is just an approximation. However, the method of calculation is straight forward and, for dilute solutions, the average distribution coefficients at various concentration give reliable results.

Scheibel (11, 12) carried out stagewise calculations for non-ideal systems in which the distribution coefficients varied with concentration. He plotted the relevant distribution coefficeints (m_i) against the mole fraction of a solute in the organic phase at various concentrations as well as the equilibrium curves versus the same ratios. The calculations were started at the top or bottom of the column iteratively using these plots. He then plotted the quantities of the solutes, instead of concentrations, to match up with the feed stage.

This method is suitable for non linear systems and can be modified by the correlation of both the distribution coefficients and the equilibirium data. Once the relevant correlations are made the stage equilibrium calculations could be performed by computer. As stated previously the equilibrium data for the quaternary system (water-acetic acid-n-butanol-n-hexane) were experimentally determined and correlated by the method proposed by (1, 2) for single binary quaternary systems together with Hand's correlations for the corresponding ternaries. These correlations were used in the equilibrium stage calculations using the Newton-Raphson method of convergeance as stated in the attached program (VI). The same calculations were carried out using the linear distribution coefficients relation.

10.5 Determination of Sauter Mean Diameter and Hold-Up Correlation

Photographs were taken to determine the mean drop size and the drop size distribution of the dispersed phase as well as the specific interfacial area thereof. The drop sizes and the drop size distribution depend on the solvent ratio, the method of formation, nature of interactions with other drops, the internal of the vessel, the physical properties of the system, the type of agitator and its speed of agitation.

Generally the dispersion of one fluid in other takes placed in three stages:

(i) When the mixing process is started, large lumps of fluid are already present.

(ii) These large lumps are deformed into long filaments that break up into drops.

(iii) These drops may be further broken up due to viscous shear and dynamic fluctuation introduced by velocity difference and mixing turbulence.

This process continues until a dynamic equilibria is attained between the relevant forces generated in the turbulent continuous phase and the opposite forces of interfacial tension that attempt to retain the drop in its spherical shape.

However, practically the drop size and drop size distribution in an agitated dispersion is determined by both break-up and coalescence occurring simultaneously. The calming section in the Scheibel column acts as a coalescer wherein the drops grow in size and are forced by the bouyancy forces to "drip out" into the mixing section. The mixing section is provided with the agitator that breaks up the drops exiting from the calming section into ones smaller size. It is claimed that drop size varies with location, being smaller in the vicinity of the impeller and larger at the circulation zones where mixing

shear effects are not effective and coalescence might take place in these conditions. It has been confirmed that the drop sizes were greatly influenced by the presence of solute transfer; this is due to the effect of solute transfer, on the rate of coalescence. Many workers (20) claimed that mass transfer enhances coalescence when the solute is transferred from the dispersed to the continuous phase, and retards coalescence when it is transferred in the opposite direction i.e from the continuous phase to the dispersed phase. This is due to the interfacial tension gradients created in the region in between the drops approaching each other. For most systems with immiscible solvents, the presence of a solute in either phase will alter the surface tension and the physical properties thereof. When mass transfer takes place from the relevant drop, the concentration of the solute in the vicinity between the two approaching drops rapidly attains equilibrium with the drop and this will lead to a decrease in the interfacial tension in the film which will cause the interface in that vicincity to reduce the intervening film, a fact that promotes coalescence. Alternatively when solute is transferred from the continuous phase into the drop, the case would be the reverse and material from the bulk continuous phase is drawn into the vicinity between the approaching

drops. This will hinder the film drainage and thereby stabilise the drops. This indicates that coalescence is influence by the direction of mass transfer.

In the determination of hold-up volume of the dispersed phase there are several methods available, but the most suitable for this study was simultaneous shut-off-displacement method, other methods have been discussed in preceeding chapters.

10.6 Determination of Stage Efficiency:

The efficiency in the Scheibel column depends on many parameters, these parameters include:

(1) The packing height and type.

(2) The agitator speed.

(3) Phase ratios: organic/aqueous.

(4) Feed concentration and feed flow rate.

In the Scheibel column wherein perfect mixing is considered in the mixing section, either Murphree stage efficiency or the overall stage efficiency would be used, since the point efficiency is not likley to be applied in a case of high rate if agitation. These were calculated by assuming perfect mixing in both the continuous and dispersed phase. The Murphree stage efficiency describes

the efficiency of a single stage. It was originally defined for distillation but is easily applied in a typical manner to liquid extraction. The light phase coming to the relevant stage is assumed to be thoroughly mixed in that stage and of uniform composition, this phase is in equilibrium with the heavy liquid leaving at the bottom of such stage. The Murphree stage efficiency is defined in terms of the light phase for ecah components (i) as:

$$E_L = \frac{Y_{n,i} - Y_{n-1,i}}{K_{n,i} X_{n,i} - Y_{n-1,i}} \qquad (10.3)$$

And in terms of the heavy phase for each component (i):

$$E_H = \frac{X_{n-1,i} - X_{n,i}}{X_{n-1,i} - Y_{n,i}/K_{n,i}} \qquad (10.4)$$

The value of the Murphree stage efficiency may approach 100% if ideal conditions are provided. Overall stage efficiency is determined by interstage mixing which depends on the mass transfer rate and the factors that govern it. These factors are: the speed of agitation and the type of drop produced, i.e. rigid, circulating or oscillating, the solvents ratio, feed concentration and feed rate. The overall stage efficiency is simply defined as the ratio of the number of equilibrium stages calculated for a given separation to the number of actual stages required for the separation. Thus the overall stage efficiency:

$$E_o = \frac{\text{Number of equilibrium stages calculated}}{\text{Number of actual stages required}}$$

The overall efficiency was investigated against the speed of agtitation at various feed flow rates, as indicated by Figure (10.2).

10.7 Discussion of Results

The performance of liquid-extraction columns have been the subject of considerable research and data on different equipment and systems are available. However, the lack of complete success of all these equipment is evident by the fact that in spite of the recognised advantages of fractional extraction over distillation, no large industrial applications have been made in competitive field with distillation.

In this study experiments have been conducted in a 7.6×10^{-2}m diameter, 1.82m height Scheibel column provided with nine stages as shown in Figure (10.1). The aim was to study the effect of feed flow rate and agitator speed on the solute transfer from the dispersed phase (n-hexane) to the continuous phase (water) and vice versa for n-butanol. The data were used to determine the mean drop size distribution, dispersed phase hold-up volume and the overall efficiency.

Close examination of the data shown in Tables (10.1 to 10.4) and the relevant plots (Figure (10.2) indicate that as the feed flow increases the overall efficiency increases to a considerable extent indicating that changing the feed flow will bring with it more solute quantities, and this quantity would be definitely in favour of the aqueous phae wherein the flow rate is not changed at the feed stage. On the other hand increase of feed flow rate increases the flow rate of the organic phase in the top section of the column which will strengthen the relevant solvent capacity. However, such an increase is limited by the column capacity and hydrodynamics. If the feed consists of a smaller quantity of the solvent (n-hexane) this effect would be very obvious on the overall efficiency. The fact that the overall efficiency was increased by the increase in the feed flow rate should be carefully investigated, particularly when the quantity of the solvent accompanying the feed is as high as in this special case. The presence of either solvent in the feed in large quantity makes the separation somewhat difficult and at infinite dilution it might be very difficult if not impossible to achieve any feasible separation.

The feed flow rate was increased to 600 g/min at which the column operates optimumly at a high separation

efficiency. The determination of feed flow rate maximisation or optimisation is based on the experience obtained from the column hydrodynamics made previously without mass transfer. This would be governed by the capacity of the column, the speed of agitation, the solvents ratio, the feed concentration, feed stage location and the overall system properties as well as the internal design geometry of the relevant column.

A study of tables (10.5 to 10.8) representing the drop diameter at various speeds of agitation, showed that the drop size (d_{32}) is appreciably affected by agitator speed. The visual assessment of the drop sizes and column hydrodynamics supported by the relevant photographs and the corresponding analysis thereof indicated that at low speed large drops were observed in the mixing chamber, and at high agitator speed, when the mixing effect is adequate the drop size decreases. At higher values discrete drops could not be identified and the appearance of the system becomes milky. This phenomena of haziness for this system takes place when the column operates at 750 r.p.m. and at higher speeds at all feed flow rates. The plots of the drop diameter against the drop cummulative volume percent confirmed that the drop size distribution is affected by, both the speed of agitation and the feed flow rate. Figures (10.3 -

10.6) give the distribution of the drop sizes and it is seen that the dominant drop size, indicated by the maximum number of drops, experience an appreciable decrease with increase of speed of agitation, while the frequency of small drops occurring does not show any considerable change. This is because the small drops may pass through the packing section without coalescence and change in size and may not be further reduced or subdivided into smaller drops, hence their numbers will be constant or increased by a small value. The main change of drop size actually observed was on large drops coming from the packing section by bouyancy forces by a drip point mechanism. These drops constitute the major drops exiting from the packing section and their sizes are reduced by redispersion in the mixing section. This was particularly noticeable at high agitation speeds (650 r.p.m.).

10.8 Mass Transfer Results

The dispersion in the mixing compartment of the Scheibel column is dependent on the limits of the agitator speed, but is generally made up of circulating and oscillating drops with negligible fraction of stagnant drops as shown in figures (10.7 - 10.10). The most reliable single-drop models that predict the dispersed and continuous phase mass transfer coefficient are summarised in appendix (IV).

These have been applied to estimate a composite overall mass transfer coefficient. They were calculated on the basis of stagant, circulating and oscillating drops co-existing in the drop swarms in proportion to their volume fraction (51) by applying Tayeban and Rowe (1963) for stagant drops, Kronig and Brink (1960), Garner and Ford, Tayeban (1959) for circulating drops and Rose, Kintner (1966) for oscillating drops. The rate of mass transfer during drop formation was calculated by applying Heertjes et al equation quoted by Johnson et al (115):

$$E_f = \frac{20}{d}\sqrt{\frac{D\theta}{\pi}} \qquad (10.5)$$

where E_f = fraction approach to equilibirum

$$= \frac{C_1 - C_o}{C - C^*}$$

d = drop diameter

θ = time of formation

D = diffusion coefficient

C - C* could correspond to 100% efficiency.

The experimental stage-to-stage mass transfer coefficient was calculated by applying the mass transfer rate equation:

$$N_A = Ka\ \Delta C_{LM} \qquad (10.6)$$

A comparison has been made between the experimental overall mass transfer coefficient, calculated composite overall mass transfer coefficient and the mass transfer coefficient on the basis that all the drops were oscillating and also all drops were circulating at various stage efficiencies in terms of the speed of agitation and the results are shown in Tables 10.9 - 10.12.

Examination of these results show that after allowing for mass transfer at drop formation and a stage efficiency between 60% - 70% an experimental mass transfer greater than the calculated composite mass transfer coefficient becomes much larger as the efficiency approached 100%. However, if it is assumed that all drops are oscillating, the ratio of the average mass transfer coefficient of the oscillating drops to the experimental K_{Os}/K_{Exp} is in the neighbourhood of unity at efficiencies between 60% - 70%. This would be expected because the turbulence induced by the agitator would induce even the smaller drops in the high shear zone in the vicinity of the agitator to oscillate at Reynolds number greater than 200 as shown in Tables 10.9 - 10.12. Furthermore this oscillation could probably be maintained by collision with each other and against the packing surface and the walls of the column. The drops were in fact observed to be oscillating at very high frequencies by the centrifugal acceleration of the agitator.

The agreement between the experimental mass transfer coefficient with that of the oscillating drop $K_{Exp}:K_{OS}$ suggests that all the drops oscillate at the agitator speeds studied. The results also suggest that the average mass transfer coefficient may be calculated by the oscillating drop model for the Scheibel column and probably any similar agitated extractor. The rate of mass transfer during drop formation of the dispersed phase emerging from the wire mesh packing has been shown to be small and may be neglected for the system studied, as shown in Table 10.13.

Figure 10.2 shows the the effect of agitator speed and feed flow rate on the overall efficiency. It is seen that by increasing the speed of agitation the drops oscillate at higher frequencies; hence a higher mass transfer rate and a higher overall efficiency will be realised. The maximum overall stage efficience obtained was 87% at agitation speed of 650 r.p.m. Any increase above 650 r.p.m. resulted in a decrease in the overall efficiency. This would be expected since, at higher speed stagnant drops were produced and these are believed to resist oscillation, and the oscillation would be damped out leading to reduction in the overall efficiency.

Table 10.1

Represents the Over All Efficiency at Different Agitator Speeds at Feed Flow Rates at 300 gm/min

No.	Agitator Speed R.P.M.	Number of Theoretical Stages	Over All Stages Efficiency
1	0.0	--	--
2	250	1.5	16.67%
3	350	3.92	43.56%
4	550	6.2	68.89%
5	650	7.0	77.78%
6	750	3.70	41.11%

Table 10.2

Represents the Over All Efficiency at Different Agitator Speeds, at Feed Flow Rates at 400 gm/min

No.	Agitator Speed R.P.M.	Number of Theoretical Stages	Over All Stages Efficiency
1	0.0	0 2	2.22%
2	250	1.60	17.78%
3	350	4.1	45.56%
4	550	7.0	77.78%
5	650	8.0	88.89%
6	750	5.8	64.44%

Table 10.3

Represents Over All Efficiency at Different Agitation Speeds, at Feed Flow Rate = 500 gm/min

No.	Agitator Speed R.P.M.	Number of Theoretical Stages	Over All Stages Efficiency
1	0.0	0.5	5.56%
2	250	2.5	27.78%
3	350	5.5	61.11%
4	550	7.1	78.89%
5	750	6.0	66.67%

Table 10.4

Represents the Over All Efficiency at Different Agitator Speeds, at Feed Flow Rate = 600 gm/min

No.	Agitator Speed R.P.M.	Number of Theoretical Stages	Over All Stages Efficiency
1	0.0	1.7	18.89%
2	250	2.8	31.11%
3	350		
4	550	7.7	85.56%
5	650		
6	750	7.8	86.67%

Table 10.5

Drop Size Distribution

Agitator Speed 250 R.P.M.

Run No. 1 (With Mass Transfer)

DM	DA	F	FV	FCV
1.4900	.8765	3	1.0571	.0003
2.0400	1.7000	3	3.7700	.0018
2.5900	1.5235	4	11.1728	.0049
3.4200	2.0118	5	32.4777	.0093
3.7000	2.1765	5	59.4555	.0348
6.1800	3.6353	6	210.3065	.0220
7.100	4.1235	11	613.9318	.1757
7.2800	4.7824	8	942.7196	.4400
7.5600	4.4471	10	1402.9730	.5939
7.8400	4.6118	7	1762.2901	.4637
8.1100	4.7706	8	2216.8427	.6083
8.3900	4.9353	7	2657.2105	.5682
8.6600	5.0941	12	3487.3795	1.1109
8.9400	5.2388	16	4705.1464	1.5714

Sauter Mean Diameter 4.6681710 mm

Table 10.6

Drop Size Distribution

Agitator Speed 350 R.P.M.

Run No. 2 (With Mass Transfer)

DM	DA	F	FV	FCV
2.5900	1.5235	1	1,8507	.0007
3.1400	1.8471	7	24.9351	.0392
3.7000	2.1765	8	68.0996	.0719
4.2500	2.5000	10	149.8704	.1387
4.8000	2.8235	8	244.1126	.1599
5.1900	3.0529	7	348.3520	.2494
3.3500	3.1471	24	739.8271	2.2833
6.4600	3.8000	15	1170.5723	.3621
7.0100	4.1235	9	1500.8112	.5603
7.5600	4.4471	3	1638.8872	.2343
8.1100	4.7706	2	1752.5253	.1928
8.6600	5.0941	1	1821.7061	.1174

Sauter Mean Diameter = 3.5028832 mm

Table 10.7

Drop Size Distribution

Agitator Speed 550 R.P.M.

Run No. 3 (With Mass Transfer)

DM	DA	F	FV	FCV
2.5900	1.5253	14	25.9095	.0275
3.1400	1.8471	10	58.8872	.1650
3.1700	1.8647	17	116.5716	5.2900
3.7000	2.1765	10	170.5272	.2801
4.2300	2.4882	12	267.2734	.5022
5.3500	3.1417	1	283.5849	.0401
5.9000	3.4706	5	392.9699	.5472
6.4600	3.8000	4	507.8353	.5643
7.0100	4.1235	3	617.9149	.5506

Sauter Mean Diameter = 2.7697867 mm

Table 10.8

Drop Size Distribution

Agitator Speed 650 R.P.M.

Run No. 4 (With Mass Transfer)

DM	DZ	F	FV	FCV
1.4900	.8765	25	8.8091	.0422
2.0400	1.2000	18	25.0868	.2112
2.4200	1.4323	10	40.1834	.2835
2.5900	1.5235	21	79.0476	1.6315
3.1400	1.8471	11	115.3231	.4707
3.1700	1.8647	9	145.8619	7.2645
3.7000	2.1765	7	183.6309	.5086
4.2500	2.5000	4	216.3392	.4244
5.9000	3.4706	1	238.2162	.0946

Sauter Mean Diameter = 1.7890367 mm

Table 10.9 Mass Transfer Results - Stage Efficiency 60%

Stage	$K_{Exp}:K_{Cal}$	$K_{Exp}:K_{Os}$	$K_{Exp}:K_{Cir}$	Re_{drop}	Re_{ag}	ϕ D	Agitator Speed r.p.m.
2	2.65	2.65		405.9	2054	0.049	250
	1.28	1.00	5.43	192.60	2681	0.062	550
	2.03	0.57	3.48	92.03	2056	0.08	650
3	2.71	2.71		405.9	2054	0.049	250
	1.26	0.98	5.10	192.60	2681	0.062	550
	2.59	0.55	3.36	92.03	2056	0.08	650
4	1.62	1.62		405.9	2054	0.049	250
	1.26	0.98	5.32	192.60	2681	0.062	550
	2.54	0.54	3.30	92.03	2056	0.08	650
6	0.98	0.98		405.9	2054	0.049	250
	0.82	0.63	3.44	192.60	2681	0.062	550
	1.65	0.35	3.15	92.03	2056	09.08	650
7	1.83	1.83		405.9	2054	0.049	250
	0.65	0.50	2.73	192.60	2681	0.062	550
	1.74	0.37	2.26	92.03	2056	0.08	650

Table 10.10 Mass Transfer Results - Stage Efficiency 70%

Stage	$K_{Exp}:K_{Cal}$	$K_{Exp}:K_{Os}$	$K_{Exp}:K_{Cir}$	Re_{drop}	Re_{ag}	ϕ D	Agitator Speed r.p.m.
2	4.1	4.1		405.9	2054	0.049	250
	1.93	1.50	8.16	192.6	2681	0.062	550
	4.12	0.90	5.35	92.03	2056	0.08	650
3	4.18	4.18		405.4	2054	0.049	250
	1.84	1.46	7.79	192.6	2681	0.062	550
	4.01	0.85	5.22	92.03	2056	0.08	650
4	4.18	4.18		405.9	2054	0.049	250
	1.94	1.51	8.19	192.6	2681	0.062	550
	3.89	0.83	5.06	92.03	2056	0.08	650
6	2.66	2.60		405.9	2054	0.049	250
	1.24	0.96	6.50	192.6	2681	0.062	550
	2.50	0.54	3.25	92.03	2056	0.08	650
7	2.73	2.73		405.9	2054	0.049	250
	1.31	1.02	5.54	192.6	2681	0.062	550
	2.61	0.56	3.39	92.03	2956	0.08	650

Table 10.11 Mass Transfer Results - Stage Efficiency 80%

Stage	$K_{Exp}:K_{Cal}$	$K_{Exp}:K_{Os}$	$K_{Exp}:K_{Cir}$	Re_{drop}	Re_{ag}	ϕ D	Agitator Speed r.p.m.
2	6.92	6.92		405.9	2054	0.049	250
	3.54	2.74	14.94	192.6	2681	0.062	550
	7.13	1.51	8.63	92.03	2056	0.08	650
3	7.24	7.24		405.4	2054	0.049	250
	3.37	3.36	14.19	192.6	2681	0.062	550
	6.80	1.44	8.24	92.03	2056	0.08	650
4	13.25	13.25		405.9	2054	0.049	250
	3.21	2.55	13.86	192.6	2681	0.062	550
	6.53	1.38	7.92	92.03	2056	0.08	650
6	4.43	4.43		405.9	2054	0.049	250
	2.11	1.64	8.91	192.6	2681	0.062	550
	4.11	0.89	5.11	92.03	2056	0.08	650
7	4.57	4.57		405.9	2054	0.049	250
	2.17	1.68	9.13	192.6	2681	0.062	550
	3.35	0.92	5.27	92.03	2956	0.08	650

Table 10.12 Mass Transfer Results - Stage Efficiency 90%

Stage	$K_{Exp}:K_{Cal}$	$K_{Exp}:K_{Os}$	$K_{Exp}:K_{Cir}$	Re_{drop}	Re_{ag}	ϕ D	Agitator Speed r.p.m.
2	5.98	5.98		405.9	2054	0.049	250
	7.68	5.96	32.39	192.6	2681	0.062	550
	5.33	3.26	18.61	92.03	2056	0.08	650
3	2.73	2.73		405.4	2054	0.049	250
	7.14	5.54	30.13	192.6	2681	0.062	550
	15.32	3.26	18.61	92.03	2056	0.08	650
4	10.00	10.00		405.9	2054	0.049	250
	7.31	5.57	30.83	192.6	2681	0.062	550
	14.93	3.18	18.12	92.03	2056	0.08	650
6	9.99	9.99		405.9	2054	0.049	250
	4.59	3.55	19.63	192.6	2681	0.062	550
	9.47	2.01	11.49	92.03	2056	0.08	650
7	10.02	10.02		405.9	2054	0.049	250
	4.66	3.61	19.63	192.6	2681	0.062	550
	9.45	2.01	11.47	92.03	2956	0.08	650

Table 10.13 Mass Results: Comparison Between Mass Transfer Rate During Drop Release from the Wire Mesh packing and the Experimental Mass Transfer Rate in Each Stage.

Stage	Experimental Mass Transfer Rate $N_{A\ Exp}$	Predicted Mass Transfer Rate Dispersed Phase Ndf	Predicted Mass Transfer Rate Continuous Phase N_{cf}	$N_{A\ Exp}$: Ndf
2	0.2039	2.097×10^{-3}	5.962×10^{-3}	97.23
3	0.0786	1.632×10^{-4}	4.640×10^{-4}	481.62
4	0.1198	2.311×10^{-4}	6.573×10^{-4}	518.39
6	0.1549	4.89×10^{-4}	1.384×10^{-3}	31.77
7	0.221	6.789×10^{-4}	1.93×10^{-3}	325.10

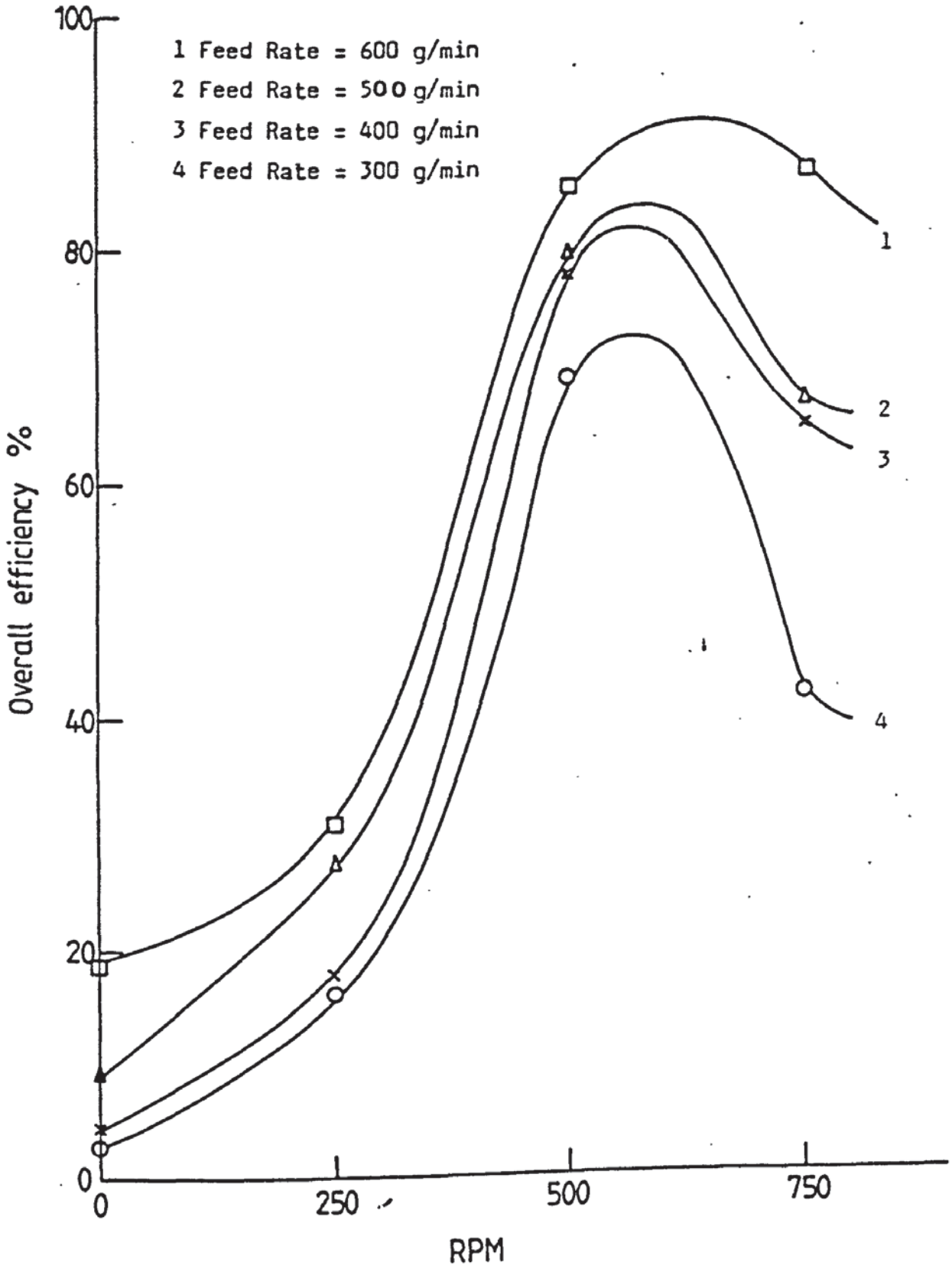

Figure 10.2 Overall Efficiency vs R.P.M.

```
@ED,U ANN.5
CASE UPPER ASSUMED
ED 16R1C. MON-05/06/85-09:41:13-(11,12)
EDIT
0:
       1:250 1
       2:1.7 15
       3:1.49 3
       4:2.04 3
       5:2.59 4
       6:3.42 5
       7:3.70 5
       8:6.18 6
       9:7.01 11
      10:7.28 8
      11:7.56 10
      12:7.84 7
      13:8.11 8
      14:8.39 7
      15:8.66 12
      16:8.94 16
EOF:16
0:
END ED. LINES:16 FIELDATA
KEC08A*ANN(1).5(12)


@xqt saut.20
```

*** D R O P S I Z E D I S T R I B U T I O N ***

ROTOR SPEED = 250 RPM

RUN NO. # 1 (With Mass Transfer):

DM	DA	F	FV	FCV
1.4900	.8765	3	1.0571	.0003
2.0400	1.2000	3	3.7700	.0018
2.5900	1.5235	4	11.1728	.0049
3.4200	2.0118	5	32.4777	.0093
3.7000	2.1765	5	59.4555	.0348
6.1800	3.6353	6	210.3065	.0220
7.0100	4.1235	11	613.9318	.1757
7.2800	4.2824	8	942.7196	.4400
7.5600	4.4471	10	1402.9730	.5939
7.8400	4.6118	7	1762.2901	.4637
8.1100	4.7706	8	2216.8427	.6083
8.3900	4.9353	7	2657.2105	.5682
8.6600	5.0941	12	3487.3795	1.1109
8.9400	5.2588	16	4705.1464	1.5714

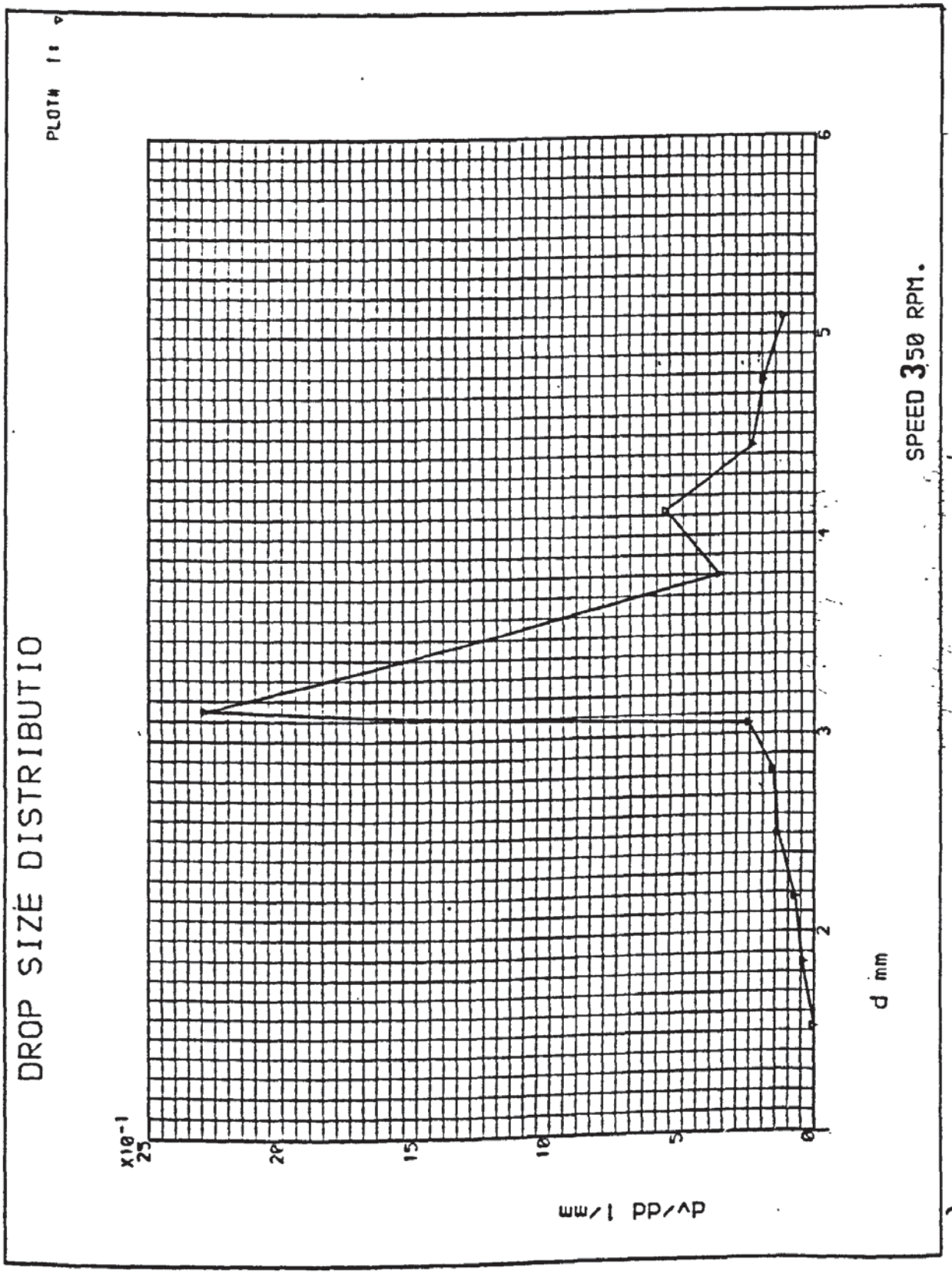

Figure 10.4 Drop Size Distribution

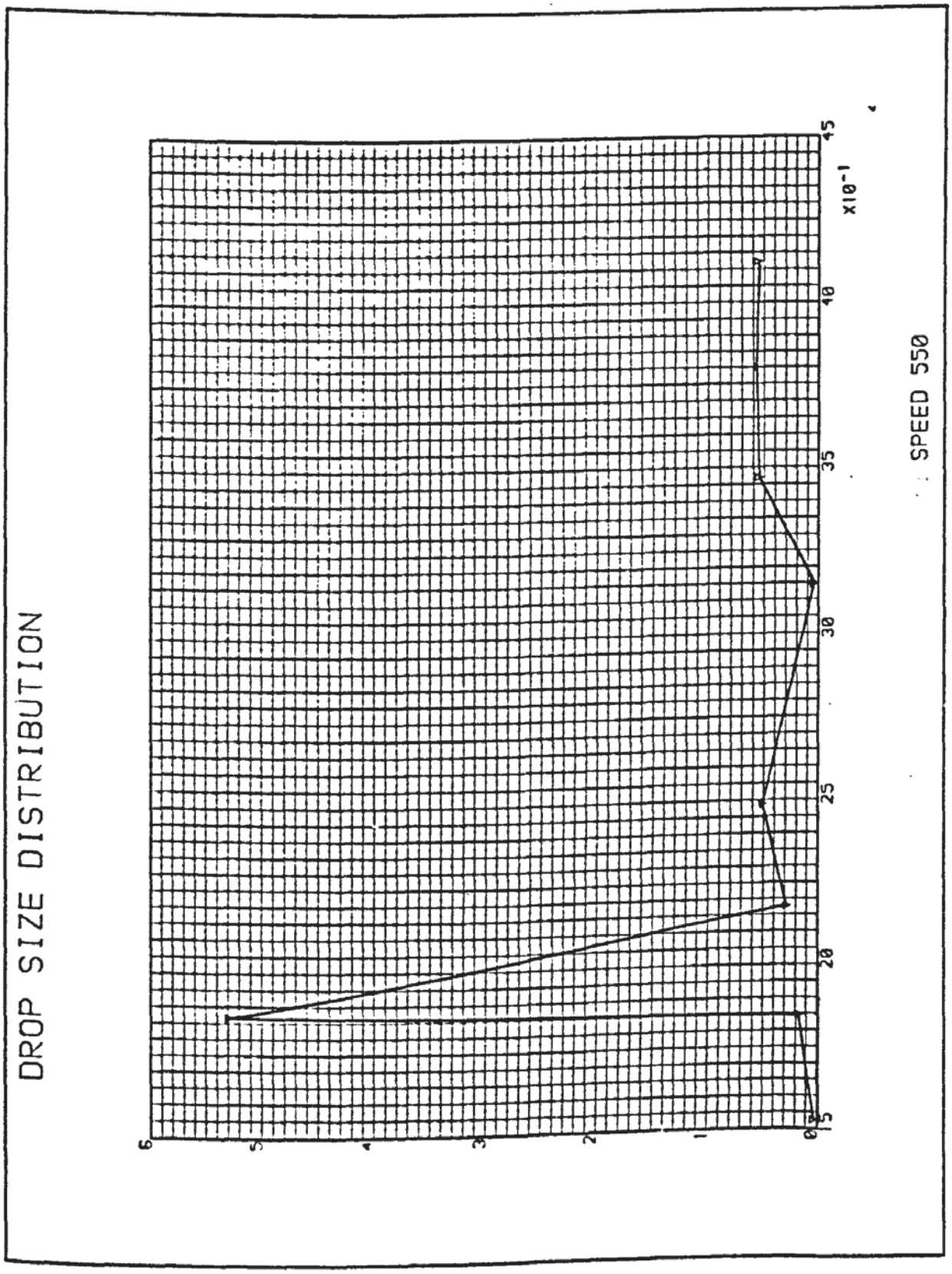

Figure 10.3 Drop Size Distribution

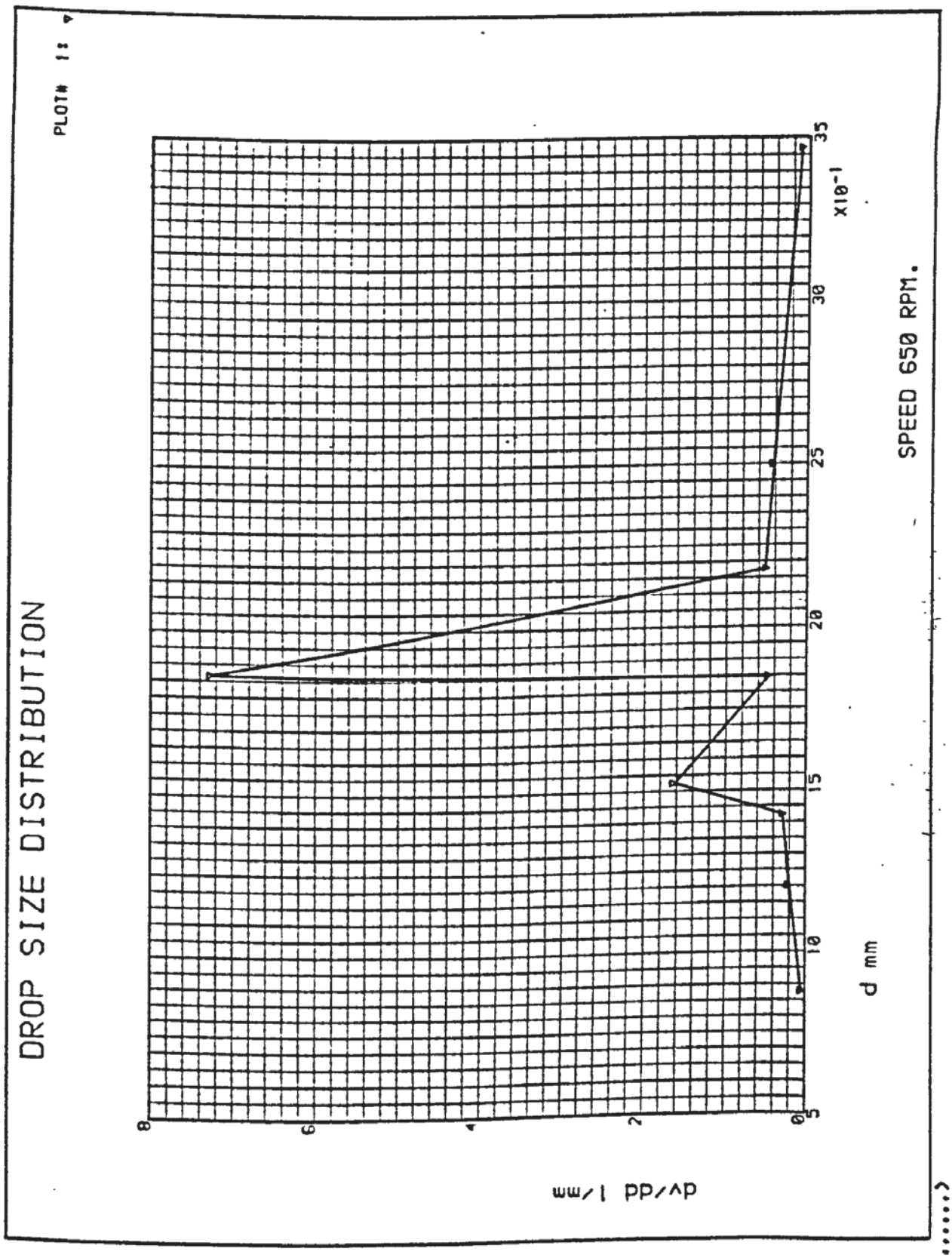

Figure 10.6 Drop Size Distribution

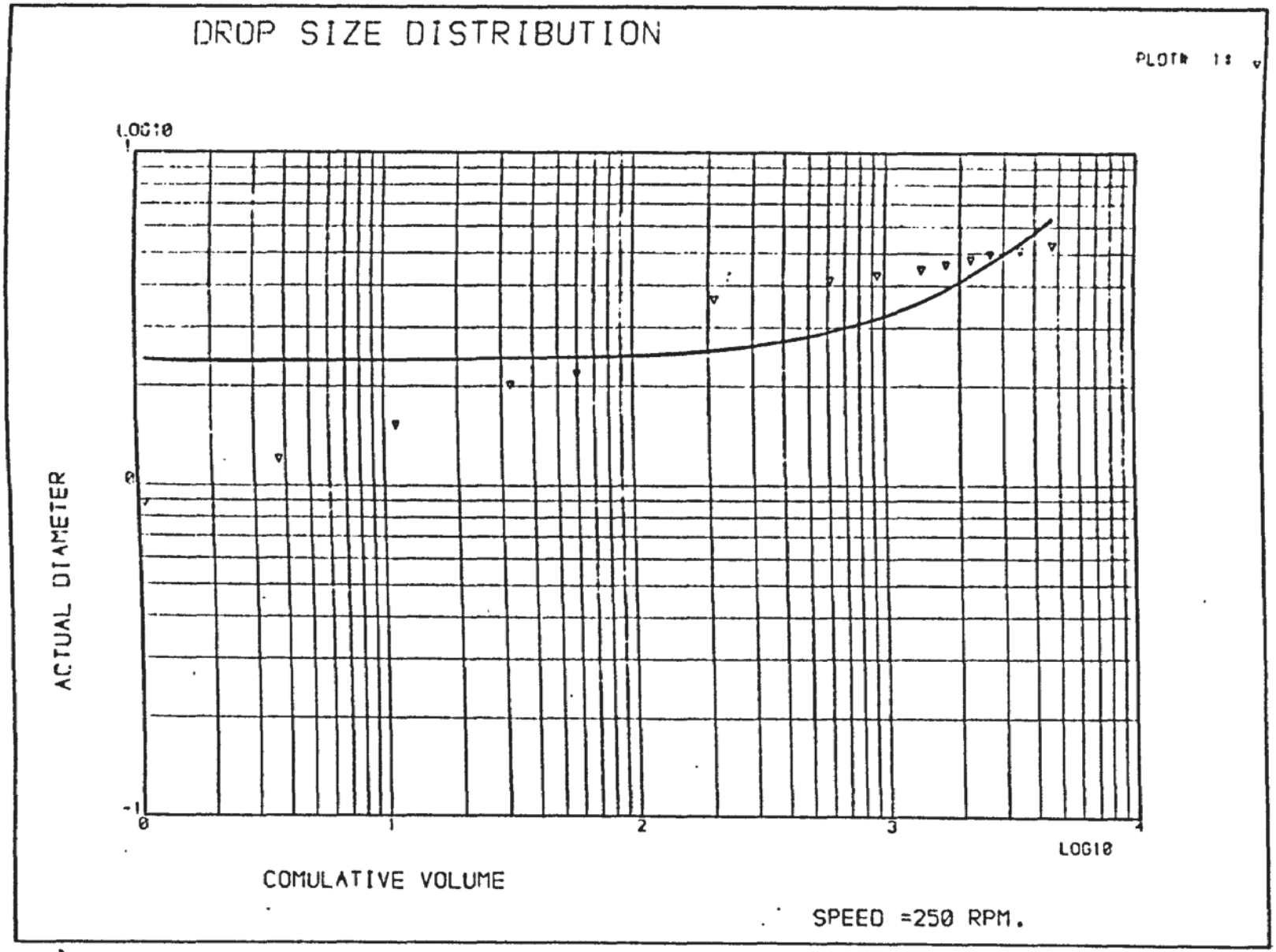

Figure 10.7 Drop Size Distribution

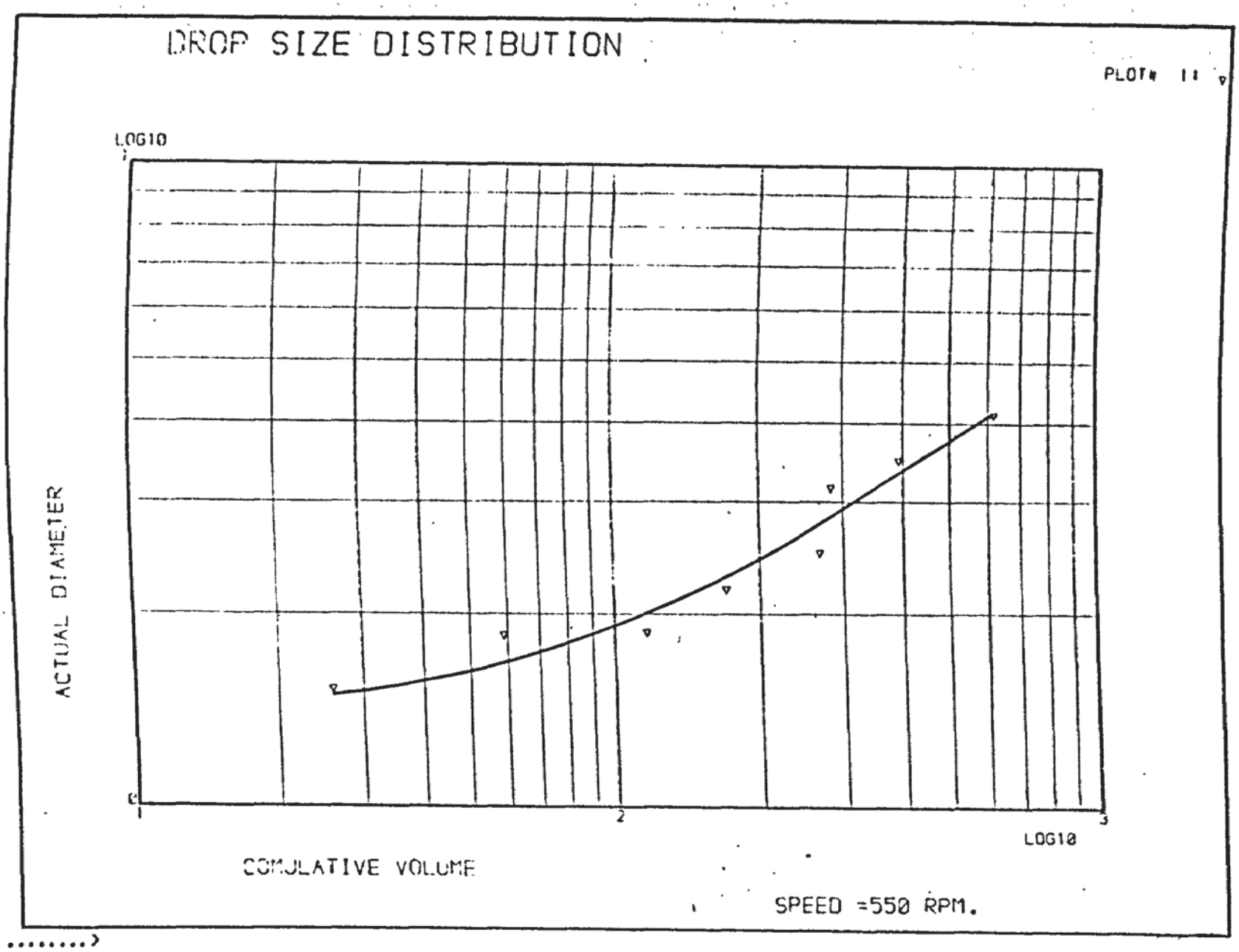

Figure 10.9 Drop Size Distributions

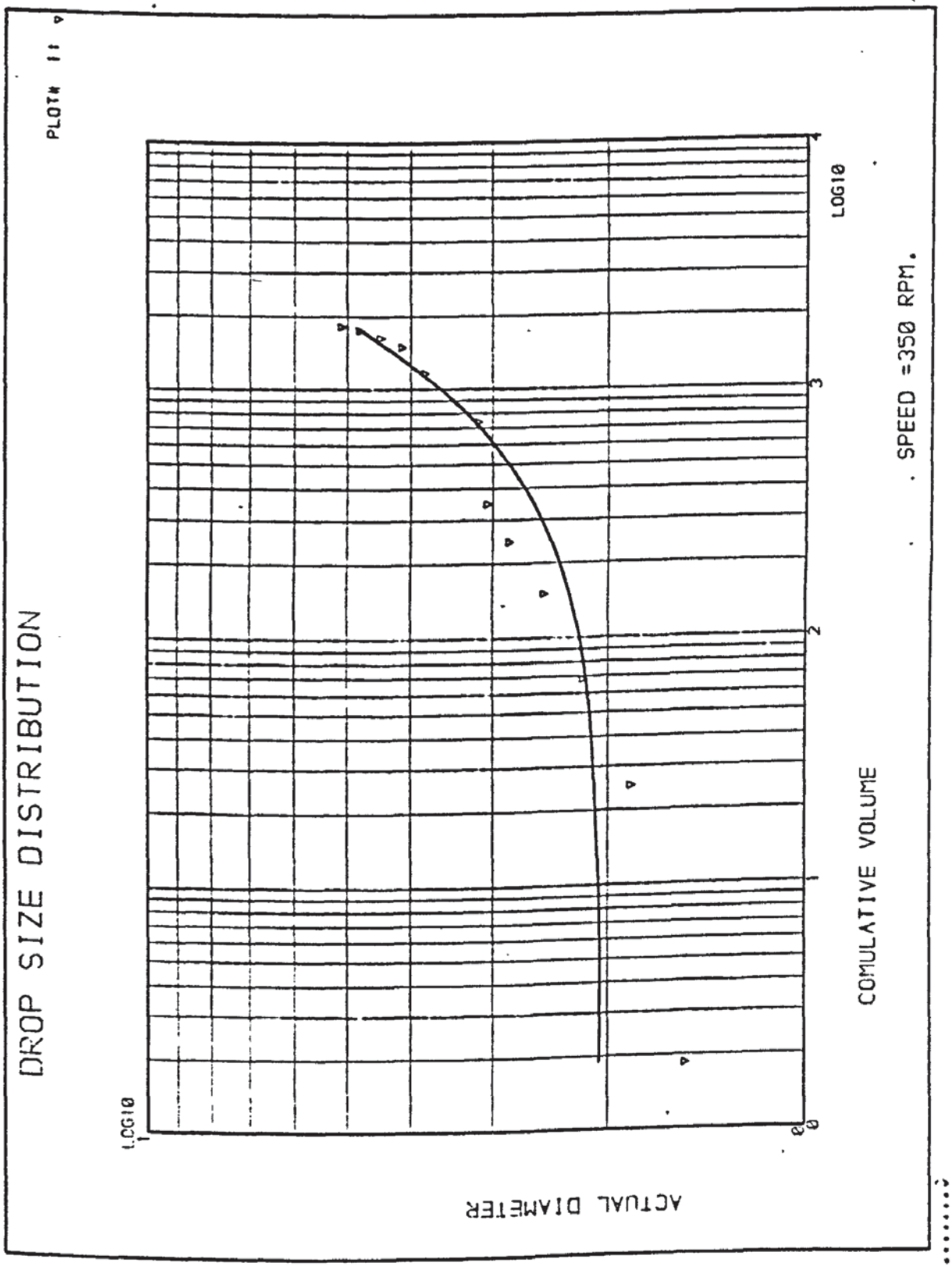

Figure 10.8 Drop Size Distributions

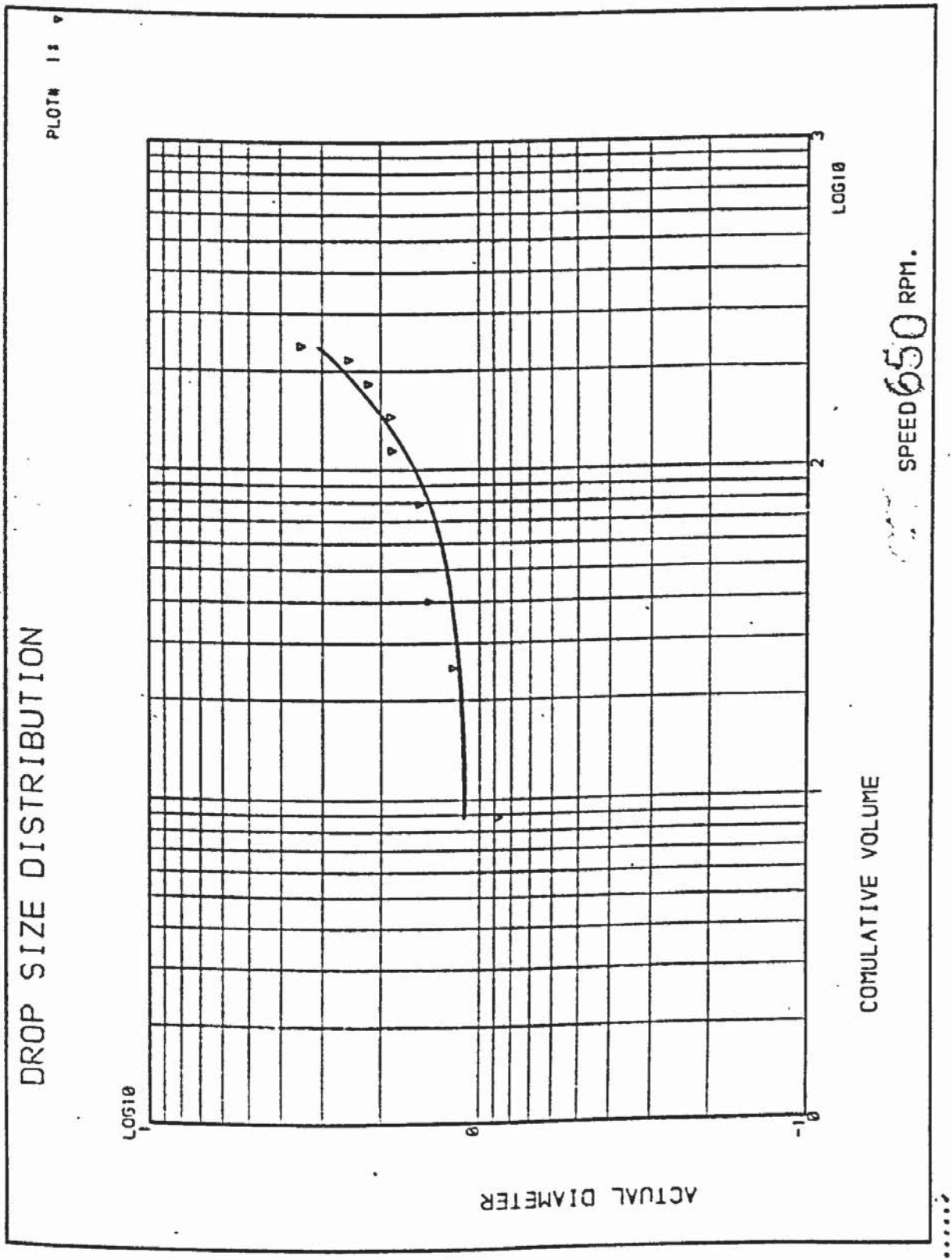

Figure 10.10 Drop Size Distributions

CHAPTER 11

CONCLUSION AND RECOMMENDATION

11.1 Conclusion

(1) Liquid-liquid equilibrium data can be predicted from binary experimental data, from binary and limited erxperimental data points of the ternary and quaternary systems. However, the reproducibility of such data at all range of concentrations were not always realised. It is believed that if the time devoted to these prediction models is devoted to the improvement of the experimental cell, comparison and verification thereof would be more practical.

(2) The presence of a solute in the relevant chemical system affected the system hydrodynamics considerably, and the hydrodynamics predictions made in the absence of solute might be misleading and should be reconsidered.

(3) The overall column efficiency is mainly controlled by the speed and its mixing effectiveness only to a certain value, after which it may either remain constant or further drops from a maximum to a lower value.

(4) Fractional extraction is an effective fractionation process and could compete with distillation and in cases wherein the chemical system is affected by temperature it will be superior.

11.2 Recommendation for Further Work:

(1) The present available Scheibel column should be modified to allow for sampling points at each mixing and packing compartment. This is important for back-mixing parameter determination and for the check-up and comparison of the back-flow model against the experimental concentration profile.

(2) The investigation of the performance of the Scheibel column for the relevant system was only made with the organic phase dispersed, further work could be made when the organic phase is continuous and the aqueous phase dispersed. This is important for the effect of mass transfer direction i.e. from dispersed to continuous and vice versa.

(3) Study of further chemical systems at the same conditions.

(4) A comparative study could be made for liquid-liquid fractional extraction in the Scheibel column against distillation of the same system in the bubble cap column of similar dimension and capacity.

NOMENCLATURE

The symbols shall have the following meaning, unless stated otherwise in the text:

A = Total interfacial area

A = Surface area of an oscillating drop

a = Interfacial area per unit packed volume, cm^2/cm^3

a' = Distribution parameter

b = Vertical radious of sperhoid in equation (4.19)

Δc = Concentration driving force

C = Solute concentration g/cm^3

C^* = Equilibrium solute concentration

D = Molecular diffusivity cm^2/sec

D = Binary diffusivity in equation (4.10)

D = Outside diameter of the agitator, ft, in equation (3.20)

D_1 = Impeller diameter, m, in equation (3.6)

D_m = Maximum stable drop size

D_N = Nozzle inside diameter in equation (4.9), cm.

d = Diameter of drop, cm

d_e = Drop equivalent diameter, cm

d_p = Peak drop diameter, cm

d_{32} = Sauter mean drop diameter, cm

E = Mass flow rate of organic phase in Figure (8.3), g/min

E = Axial mixing coefficient

E_m = Extraction efficiency

e = Eddy diffusivity, cm^2/sec

F_n = Feed rate, g/min introduced to stage n

g, g_c = Acceleration due to gravity, cm/sec^2

g^E = Gibbs free energy

H_E = Effective column height, cm

H_m = Stage Height, cm

K = Overall mass trnasfer coefficient, cm/sec

K_c = Individual mass transfer coefficient with respect to continuous phase.

k_d = Individual mass transfer coefficient with respect to the dispersed phse.

K_{HB} = Mass transfer coefficient calculated by means of Bandlos and Baron, cm/sec

L = Distance of drop fall, cm

L = Mass flow rate of the aqueous phase, in Figure (8.3), g/min

m = Equilibrium distribution coefficient

N = Agitator speed, rev/sec

n = Compartment number

P = Power input, ft.lb/sec

Q = Volumetric flow rate, cm^3/sec

r = Radius of sphere of volume equal to that of a drop, cm.

t = Time, sec

t_f = Time of drop formation

$\bar{t}$ = Mean coalescence time, sec

V_c = Volumetric flow rate of the continuous phase, cm^3/sec

V_d = Volumetric flow rate of the dispersed phase, cm^3,sec

V_g = Geometrical mean

X = Solute concentration in the aqueous phase g/g

X_1 = Liquid composition, mole fraction

Y = Solute concentration in the dispersed phase g/g

Y_1 = Vapour composition, mole fraction

Z = Effective length measured from the feed entry to exit.

μ = Viscosity, g/cm.sec

ν = Kinematic viscosity, cm^2/sec

ρ = Density, g/cm^3

$\Delta\rho$ = Density difference, g/cm^3

σ = Interfacial tension

ω = Frequency of oscillation, sec^{-1}

π = 3.1416, constant

Subscripts

A,B,C = Components, A,B,C .... etc. respectively

A = Water

B = Acetic acid

C = n-butanol

D = n-hexane

C = Continuous

d = Dispersed

X_{BA} = Mole ratio of B in A rich phse

X_{CA} = Mole ratio of C in A rich phase

X_{AA} = Mole ratio of A in A rich phase

X_{DD} = mole ratio of D in D rich phase

Dimensionless Groups:

N_p = Power Number = $\dfrac{P}{N^3 D^5 \rho}$

$(Pe)_c$ = Peclet Number = $\dfrac{V_c H}{E_C}$ for continuous phase

$(Pe)_d$ = Peclet Number = $\dfrac{V_d H}{E_d}$ for the dispersed phase

Re = Droplet Reynolds Number = $\dfrac{dV_o \rho}{\mu}$

Re = Column Reynolds Number = $\dfrac{V_d H \rho d}{\mu x}$

Sh = Sherwood Number = $\dfrac{Kd}{D}$

We = Agitator Weber Number = $\dfrac{N^2 D_r^3 \rho_c}{\sigma}$

Greek Letters:

α = Backflow coefficient

γ = Activity coefficient

γ = Surface tension, dyne/cm

δ = Uniformity distribution parameter

$\bar{\varepsilon}$ = Energy input per unit mass and time

ϕD = Fractional hold-up of dispersed phase

APPENDICES

APPENDICES

APPENDIX 1

CHEMICAL METHOD OF ANALYSIS

CHEMICAL METHOD:

Normality of NaOH = 0.1

10 ml of aqueous exit phase required 35.3 ML of 0.1 N NaOH

Apply the material balance equation:

$$V_1 \times N_1 = V_2 \times N_2$$

Therefore $$N_1 = \frac{V_2 \times N_2}{V_1}$$

$$= \frac{35.2 \times 0.1}{10.0} = 0.353$$

Weight of 1N Acetic Acid = 60.05 g/L

Therefore Weight of Acetic Acid in the aqueous solution

$$= \frac{0.353}{1} \times 60.05 = 21.1977 \text{ g/L}$$

$$= 0.0212 \text{ g/mL}$$

Volumetric flow rate of the exit aqueous phase = 1000.2 mL/min

Therefore componential flow rate of the acetic acid in the aqueous phase = 1000.2 X 0.0212 = 21.204 g/min

Therefore the componential flow rate of acetic acid in the organic phase = FX_B - 21.204

= 30.0 - 21.204 = 9.008 g/min

Componential flow rate of acetic acid in the organic phase

$$= \frac{9.008}{1235} = \underline{0.0073} \text{ g/mL}$$

APPENDIX II

CALIBRATION OF THE REFRACTOMETER

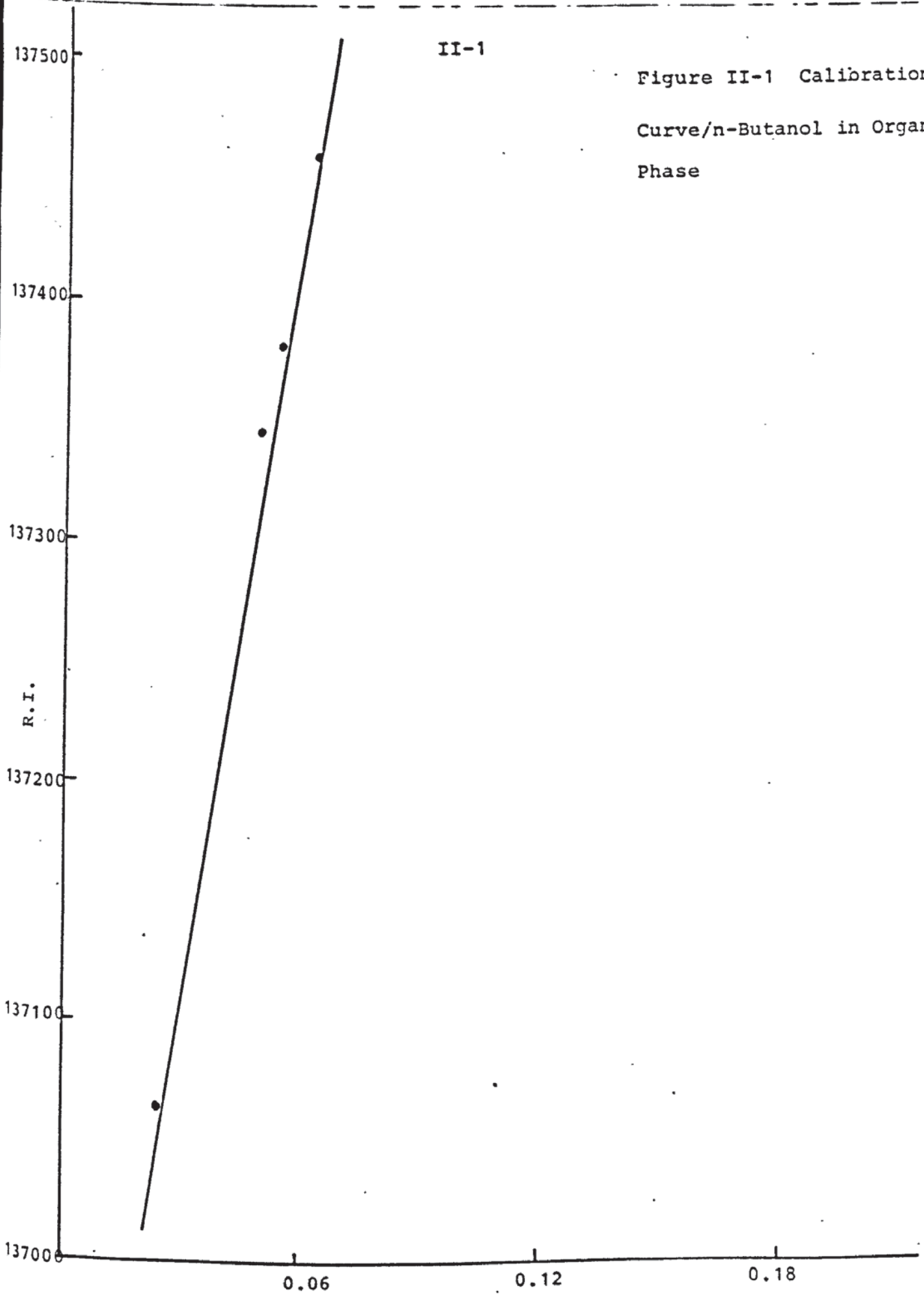

Figure II-1 Calibration Curve/n-Butanol in Organic Phase

APPENDIX III

COMPUTER PROGRAM FOR STAGE-TO-STAGE CALCULATIONS AND STAGE MATCHING RESULTS

TEXT BOUND INTO

THE SPINE

```
)U ANN.1S
:E UPPER ASSUMED
)ORIC. TUE-06/11/85-14:54:51-(11,12)
:T

 1:            DIMENSION YB(40),YC(40),XB(40),XC(40),YUB(40),YUC(40),
 2:     # XUB(40),XUC(40),FEED(40),D(40)
 3:            REAL MB,MC,MB1,MC1
 4:            PRINT*,'NO. OF ITERATION '
 5:C*** STAGE TO STAGE CALCULATION
 6:C----THIS PROGRAM CALCULATES THE STAGE-TO-STAGE CONCENTRATION
 7:C-------------------------------------------------------
 8:C
 9:            READ(5,*)N
10:            PRINT*,'YB,YC'
11:            READ(5,*)YB(1),YC(1)
12:            PRINT*,'MB,MC'
13:            READ(5,*)MB,MC
14:            PRINT*,'MB1,MC1'
15:            READ(5,*)MB1,MC1
16:            PRINT*,'XUB,XUC,XF'
17:            READ(5,*)XUB(1),XUC(1),XF
18:            PRINT*,'A,D'
19:C-----------------CALCULATION FOR TOP COLUMN ------------------
20:            PRINT*,'===========CALCULATION FOR TOP OF COLUMN ==========='
21:            DO 45 J=1,7
22:            READ(5,*)A,D(J)
23:55          READ(5,*)FEED(J)
24:            PRINT*,'FEED(',J,')=',FEED(J),'D(',J,')=',D(J)
25:            IF (A.EQ.0.)GO TO 99
26:            YB(2)=(A/(D(J)*MB1)+1.)*YB(1)
27:            YC(2)=(A/D(J)*MC1+1.)*YC(1)
28:            XB(1)=YB1/MB1
29:            XC(1)=YC(1)/MC1
30:            DO 1 I=2,N
31:            YB(I+1)=(A/D(J)*MB1+1.)*YB(I)-(A*XB(I-1)/D(J))
32:            YC(I+1)=(A/D(J)*MC1+1.)*YC(I)-(XC(I-1)/D(J))
33:            XB(I)=YB(I)/MB1
34:            YC(I)=YC(I)/MC1
35:1           CONTINUE
36:            PRINT*,'-----------------------------------------'
37:            PRINT*,'  I    :   XB    :    XC    :    YB    :    YC '
38:            PRINT*,'-----------------------------------------'
39:            DO 88 I=1,N
40:88          WRITE(6,13)I,XB(I),XC(I),YB(I),YC(I)
41:13           FORMAT(2X,I2,2X,2X,E10.3,2X,E10.3,2X,E10.3,2X,E10.3)
42:            PRINT*,'======== CALC. FOR BOTTOM OF COLUMN ========'
43:            DE=D(J)-FEED(J)*XF
44:            XUB(2)=((DE*MB/A)+1.)*XUB(1)
45:            XUC(2)=((DE*MC/A)+1.)*XUC(1)
46:            YUB(1)=XUB(1)*MB
47:            YUC(1)=XUC(1)*MC
48:            DO 44 I=1,N
49:            XUB(I+1)=((DE*MB/A)+1.)*XUB(I)-(DE*YUE(I-1)/A)
50:            XUC(I+1)=((DE*MC/A)+1.)*XUC(I)-(DE*YUC(I-1)/A)
51:            YUB(I)=XUB(I)*MB
52:44           YUC(I)=XUC(I)*MC
```

```
53:
54:           PRINT*,'-------------------------------------------------'
55:           PRINT*,' I  :    XB     :     XC     :     YB     :     YC'
56:           PRINT*,'-------------------------------------------------'
57:77         DO 77 I=1,N
58:61         WRITE(6,6*)I,XUB(I),XUC(I),YUB(I),YUC(I)
59:45         FORMAT(2X,I2,E10.3,3X,E10.3,2X,E10.3,2X,E10.3)
60:99         CONTINUE
61:           PRINT*,'----------END OF CALCULATION-----------'
62:           STOP
:62           END

ED. LINES:62 FIELDATA
COBA*ANN(1).15(12)
```

TABLE III-1

Typical Results of the Concentration Profile for Stage-To-Stage Matching

```
&ED,U SH.5
CASE UPPER ASSUMED
ED 16R1A-MON-12/17/84-12:42:01-(5,6)
EDIT
C:
      1:10
      2:.0111 .008
      3:1000. 1088.
      4:.8339 1.3309
      5:.8339 1.3309
      6:.0151 .0065 .85
      7:300.
      8:0.
EOF:C
C:
END ED. LINES:8 FIELDATA


&XQT SH.3
NO. OF ITERATION
YB,YC
A,D
MB,MC
MB1,MC1
XUB,XUC,XF
==========   CALC TOP OF TOWER  ==============
-------------------------------------------------
  I    :   XB      :      XC     :     YE     :  YC     :
-------------------------------------------------
  1     .133-001     .601-002     .111-001     .800-002
  2     .280-001     .102-001     .233-001     .135-001
  3     .442-001     .130-001     .368-001     .173-001
  4     .620-001     .150-001     .517-001     .200-001
  5     .816-001     .164-001     .681-001     .218-001
  6     .103+000     .173-001     .861-001     .231-001
  7     .127+000     .180-001     .106+000     .239-001
  8     .153+000     .184-001     .128+000     .245-001
  9     .182+000     .187-001     .152+000     .249-001
 10     .214+000     .189-001     .179+000     .252-001
=========   CALC BOTTOM OF TOWER ====================
FEED(              1) =  300.00000
-------------------------------------------------
  I   :    XB      :      XC     :     YE     :  YC     :
-------------------------------------------------
  1     .181-001     .650-002     .151-001     .865-002
  2     .307-001     .137-001     .256-001     .182-001
  3     .394-001     .217-001     .329-001     .289-001
  4     .455-001     .306-001     .379-001     .407-001
  5     .497-001     .404-001     .414-001     .537-001
  6     .526-001     .513-001     .439-001     .682-001
  7     .546-001     .633-001     .456-001     .843-001
  8     .561-001     .767-001     .467-001     .102+000
  9     .570-001     .915-001     .476-001     .122+000
 10     .577-001     .108+000     .481-001     .144+000
---------- CALC IS FINISHED ----------
```

Table III-1

Mass Transfer Results

Run No. 1

Feed Flow Rate = 300 g/min

Speed R.P.M.	Component	Organic Phase Product		Aqueous Phase Product		Total	
		gm	%	gm	%	gm	%
Zero	Acetic Acid	14.0	64.8	15.7	68.9	29.7	66.9
	n-Butanol	7.6	35.2	7.1	3.1	14.7	33.1
	Total	21.6	100.8	22.8	100.0	44.4	100.0
250	Acetic Acid	9.90	51.10	18.10	73.6	30.22	66.7
	n-Butanol	9.5	48.9	6.50	26.4	15.10	33.3
	Total	19.40	100.0	24.6	100.0	45.32	100.0
350	Acetic Acid	10.80	53.20	10.00	77.6	29.8	66.5
	n-Butanol	9.50	46.80	5.50	22.4	15.0	33.5
	Total	20.30	100.0	29.50	100.0	44.8	100.0
550	Acetic Acid	12.12	58.5	20.1	80.00	29.7	66.3
	n-Butanol	8.6	41.5	5.0	20.00	15.1	33.7
	Total	20.72	100.0	25.1	100.0	44.8	100.0
650	Acetic Acid	8.4	43.8	22.0	83.3	30.4	66.7
	n-Butanol	10.8	56.2	4.40	16.7	15.2	33.3
	Total	19.2	100.0	26.4	100.0	45.6	100.0
750	Acetic Acid	09.6	48.5	19.80	78.9	29.7	66.7
	n-Butanol	10.1	51.3	5.30	21.1	14.8	33.3
	Total	19.7	99.8	25.10	100.0	44.5	100.0

Feed Concentration:

Acetic Acid = 10%

n-Butanol = 2%

Concentration of n-butanol in inlet water = 1.5%

In all runs stated in Tables III-1 to III4

Table III-2

Mass Transfer Results

Run No. 2

Feed Flow Rate = 400 g/min

Speed R.P.M.	Component	Organic Phase Product		Aqueous Phase Product		Total	
		gm	%	gm	%	gm	%
Zero	Acetic Acid	18.5	63.4	22.10	70.3	40.60	67.0
	n-Butanol	10.7	36.6	24.34	29.7	20.04	33.0
	Total	29.2	100.0	31.44	100.0	60.64	100.0
250	Acetic Acid	15.10	55.0	24.8	74.3	39.9	66.1
	n-Butanol	11.90	44.1	8.6	25.7	20.5	33.9
	Total	27.00	100.0	33.4	100.0	60.4	100.0
350	Acetic Acid	14.0	51.3	26.4	80.2	40.4	67.2
	n-Butanol	13.3	48.7	6.5	19.8	19.8	32.8
	Total	27.3	100.0	32.9	100.0	60.2	100.0
550	Acetic Acid	12.10	44.6	29.8	83.7	41.9	66.8
	n-Butanol	15.0	55.4	5.8	16.3	20.8	33.2
	Total	27.10	100.0	35.6	100.0	62.7	100.0
650	Acetic Acid	10.7	40.1	30.3	87.8	41.0	67.0
	n-Butanol	16.0	59.9	4.2	12.2	20.2	33.0
	Total	26.7	100.0	34.5	100.0	61.2	100.0
750	Acetic Acid	12.5	47.3	26.5	81.5	39.0	66.2
	n-Butanol	13.9	52.7	6.0	18.5	19.9	33.8
	Total	26.4	100.0	32.5	100.0	58.9	100.0

Table III-3

Mass Trarsfer Results

Run No. 3

Feed Flow Rate = 500 g/min

Speed R.P.M.	Component	Organic Phase Product		Aqueous Phase Product		Total	
		gm	%	gm	%	gm	%
Zero	Acetic Acid	23.10	61.4	29.4	72.2	52.5	67.0
	n-Butanol	14.50	38.6	11.30	27.8	25.8	33.0
	Total	37.6	100.0	40.7	100.0	78.3	100.0
250	Acetic Acid	19.8	55.0	33.10	76.1	52.9	66.5
	n-Butanol	16.2	45.0	10.40	23.9	26.6	33.5
	Total	36.0	100.0	43.5	100.0	79.5	100.0
350	Acetic Acid	15.10	46.6	30.5	79.2	45.6	64.3
	n-Butanol	17.30	53.4	8.0	20.8	25.3	35.7
	Total	32.4	100.0	38.5	100.0	70.9	100.0
550	Acetic Acid	14.30	43.7	35.5	83.1	49.8	66.0
	n-Butanol	18.40	56.3	7.2	16.9	25.6	34.0
	Total	32.7	100.0	42.7	100.0	75.4	100.0
650	Acetic Acid	8.5	29.3	43.0	93.5	51.5	68.7
	n-Butanol	20.5	70.7	3.0	6.5	23.5	31.3
	Total	20.0	100.0	46.0	100.0	75.0	100.0
750	Acetic Acid	16.5	48.10	32.5	80.4	49.0	66.3
	n-Butanol	17.8	51.90	7.9	19.6	24.9	33.7
	Total	34.3	100.0	40.4	100.0	73.9	100.0

Table III-4

Mass Transfer Results

Run No. 4

Feed Flow Rate = 600 g/min

Speed R.P.M.	Component	Organic Phase Product		Aqueous Phase Product		Total	
		gm	%	gm	%	gm	%
Zero	Acetic Acid	24.8	58.4	34.2	74.0	59.0	66.5
	n-Butanol	17.7	41.6	12.0	26.0	29.7	33.5
	Total	42.5	100.0	46.2	100.0	88.7	100.0
250	Acetic Acid	23.20	55.9	37.8	76.7	61.0	67.2
	n-Butanol	18.30	44.1	11.5	23.3	29.8	32.8
	Total	41.50	100.0	49.3	100.0	90.8	100.0
350	Acetic Acid	16.6	44.1	42.4	83.0	58.5	66.3
	n-Butanol	21.0	55.9	8.7	17.0	29.7	33.7
	Total	37.6	100.0	51.1	100.0	88.2	100.0
550	Acetic Acid	13.7	37.1	45.7	86.2	59.4	66.1
	n-Butanol	23.2	62.2	7.3	13.8	30.5	38.9
	Total	36.9	100.0	53.0	100.0	89.9	100.0
650	Acetic Acid	6.8	19.8	54.6	96.3	61.4	67.4
	n-Butanol	27.6	80.2	2.1	3.7	29.7	32.6
	Total	34.4	100.0	56.7	100.0	91.1	100.0
750	Acetic Acid	18.1	45.3	42.4	68.3	60.5	67.2
	n-Butanol	21.9	54.7	8.6	31.7	30.5	32.8
	Total	40.0	100.0	51.0	100.0	90.0	100.0

From the computer oputput the stage matching can be made by matching the concentration of component B in each phase:

From Table III-1:

From top of the column to feed stage:

	X_B	Y_B
At stage 3	0.0442	0.0368

From bottom of the column to feed stage

	X_B	Y_B
At stage 4	0.0455	0.0379

Therefore the feed stage was at stage number 3 from the top of the column and at sage number 4 from the bottom.

Total number of theoretical stage = 7

But the feed stage was calculated twice, hence the number of theoretical stages = 7 - 1 = 6

Total overall efficiency:

$$= \frac{\text{No. of theoretical stages}}{\text{No. of actual stages}}$$

$$= \frac{6}{9} \times 100 = \underline{66.67\%}$$

This is in agreement with that found from the matching inspection plot as seen in Table (10.11) :

for run 4 at speed of 550 R.P.M.

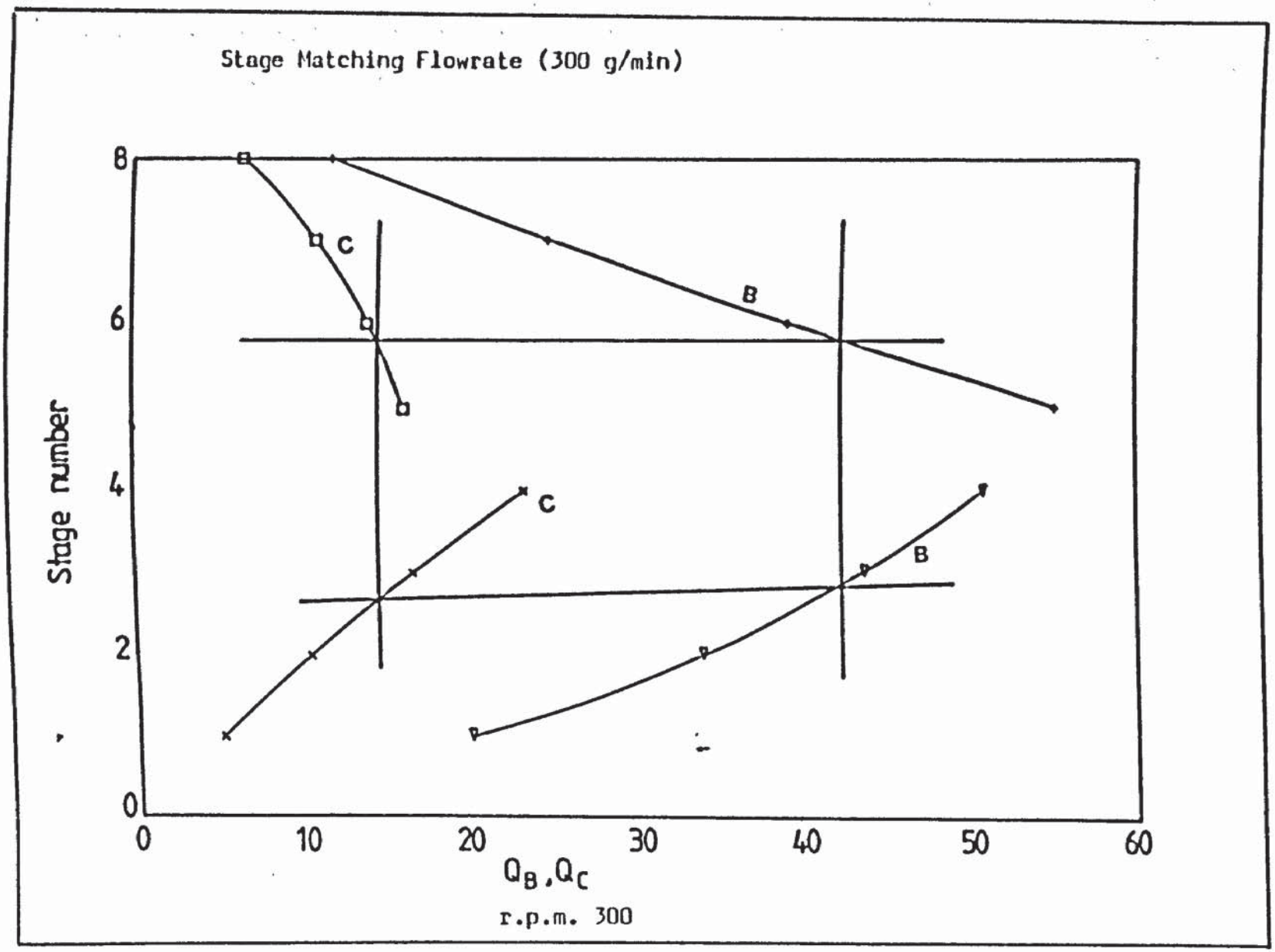
Stage Matching Flowrate (300 g/min)
Stage number
8
6
4
2
0
0
10
20
30
40
50
60
C
B
C
B
Q_B, Q_C
r.p.m. 300

Figure III-1

Stage Matching Flowrate = 300 g/min
Stage number
10
8
6
4
2
0
0
20
40
60
80
Q_B, Q_C
r.p.m. 550
B
B
C
C

Figure III-2

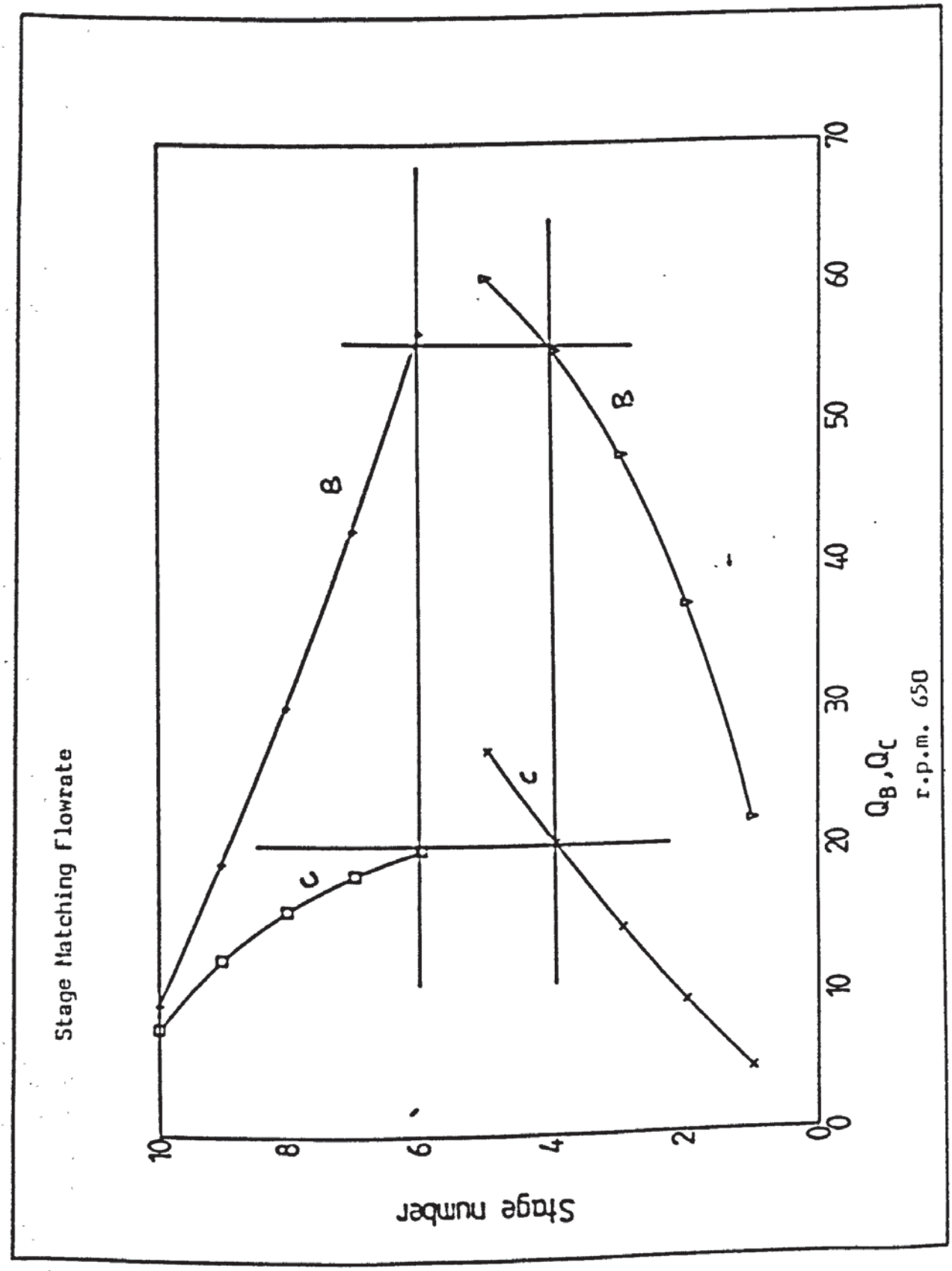
Stage Matching Flowrate
Stage number
10
8
6
4
2
0
0
10
20
30
40
50
60
70
Q_B, Q_C
r.p.m. 650
B
B
C
C

Figure III-3

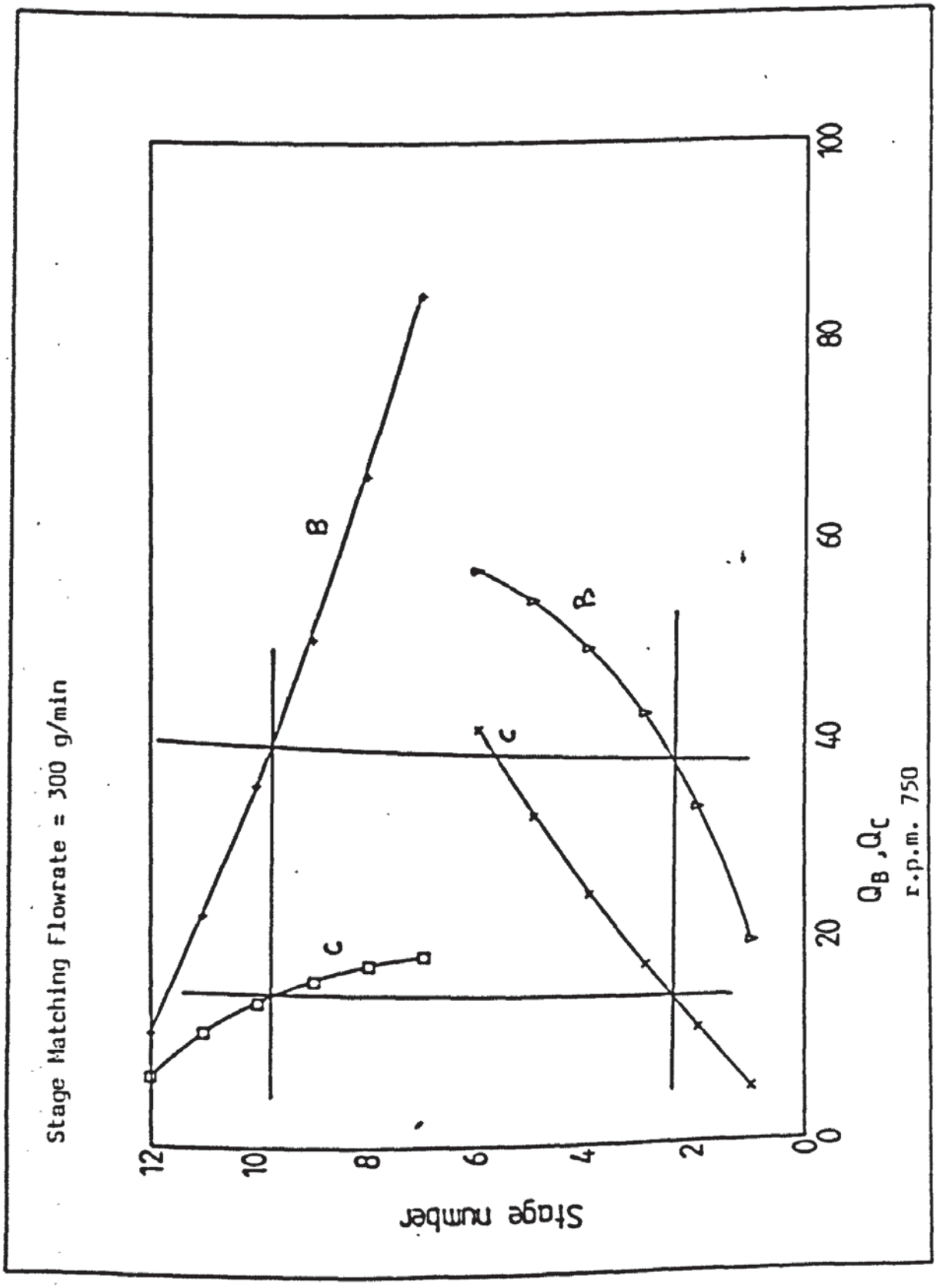
Stage Matching Flowrate = 300 g/min
Stage number
12
10
8
6
4
2
0
0
20
40
60
80
100
Q_B , Q_C
r.p.m. 750
B
B
C
C

Figure III-4

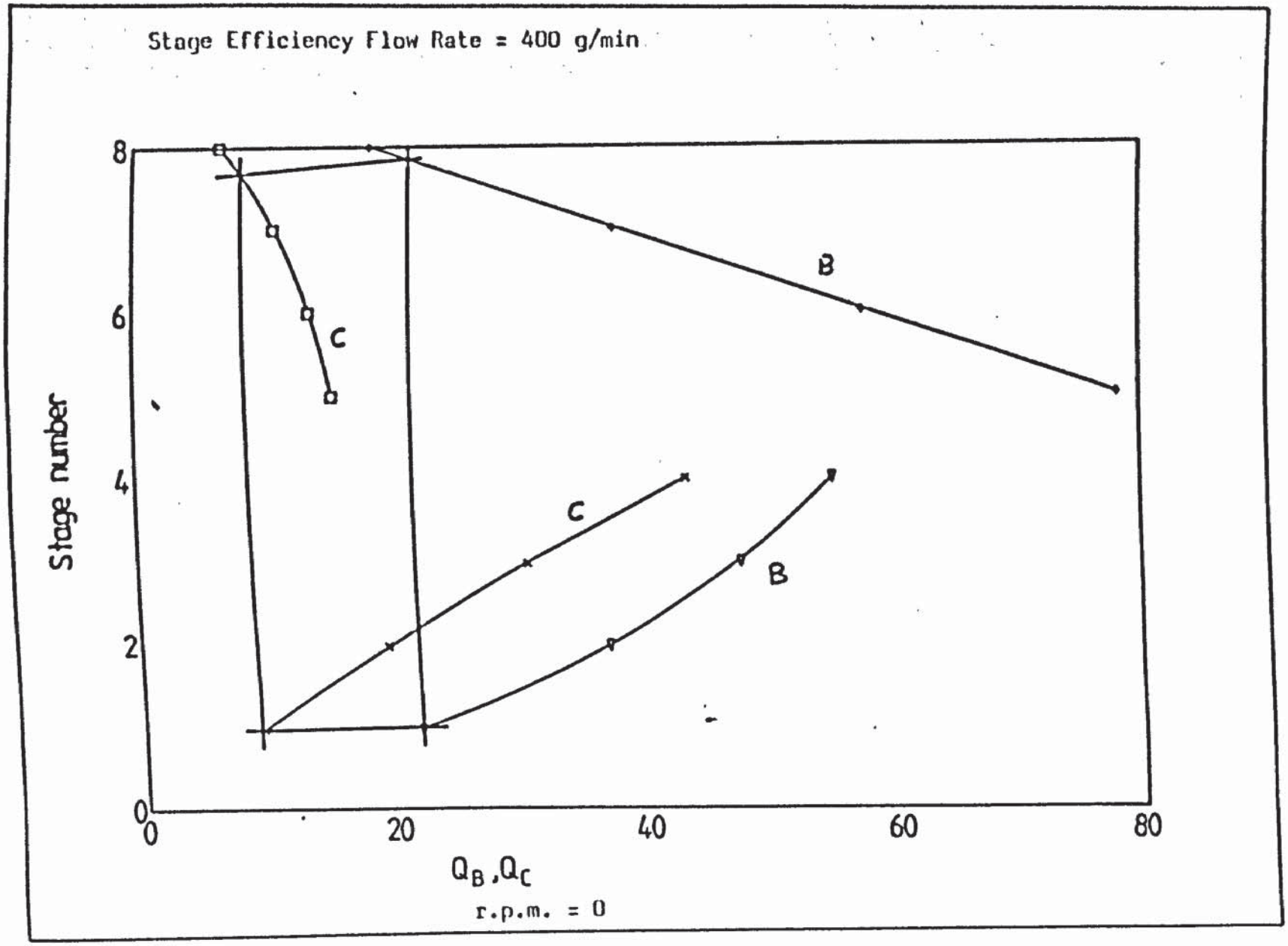
Stage Efficiency Flow Rate = 400 g/min
Stage number
8
6
4
2
0
0
20
40
60
80
B
C
C
B
Q_B, Q_C
r.p.m. = 0

Figure III-5

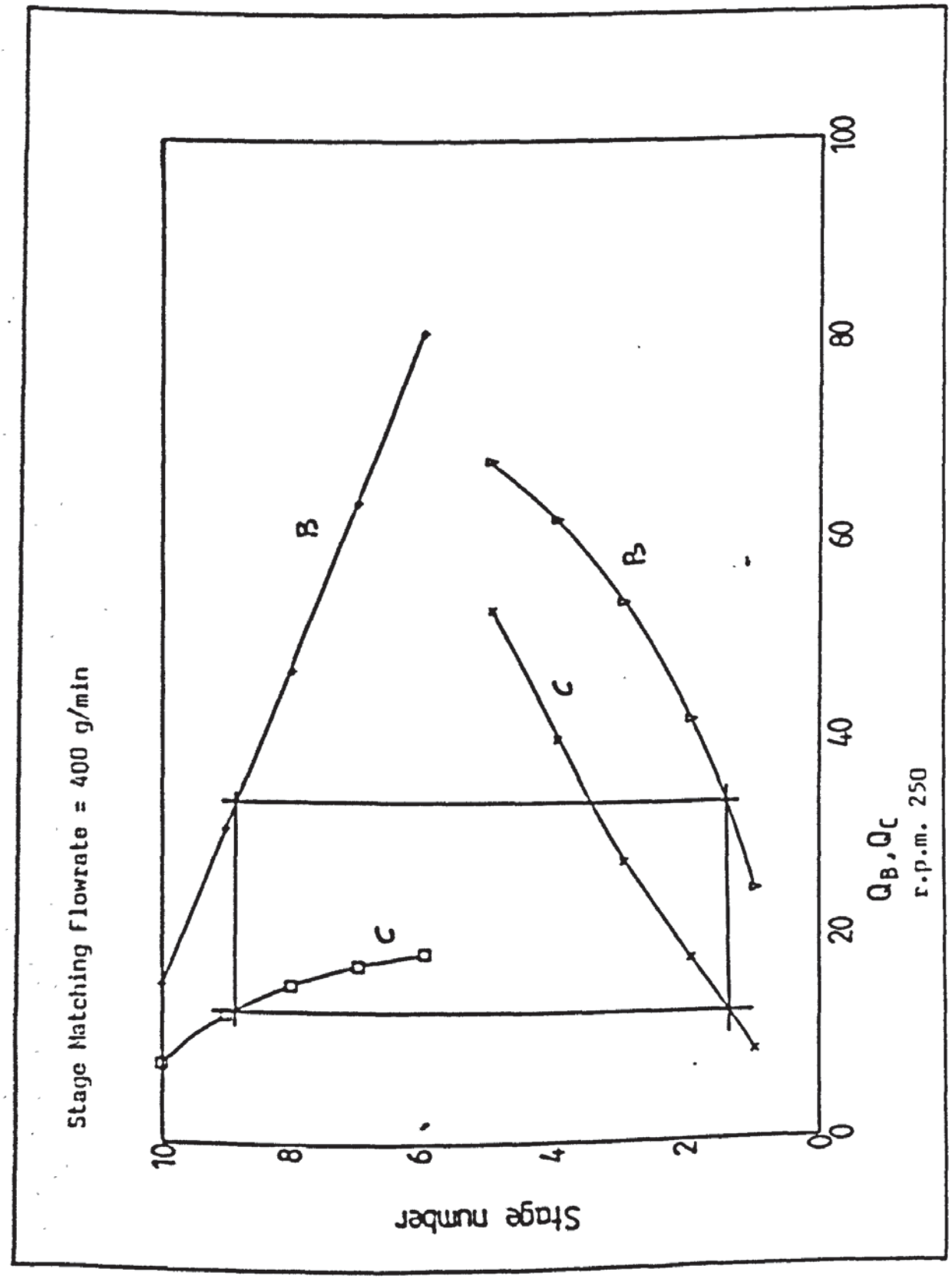
Stage Matching Flowrate = 400 g/min
Stage number
10
8
6
4
2
0
0
20
40
60
80
100
Q_B, Q_C
r.p.m. 250
B
B
C
C

Figure III-6

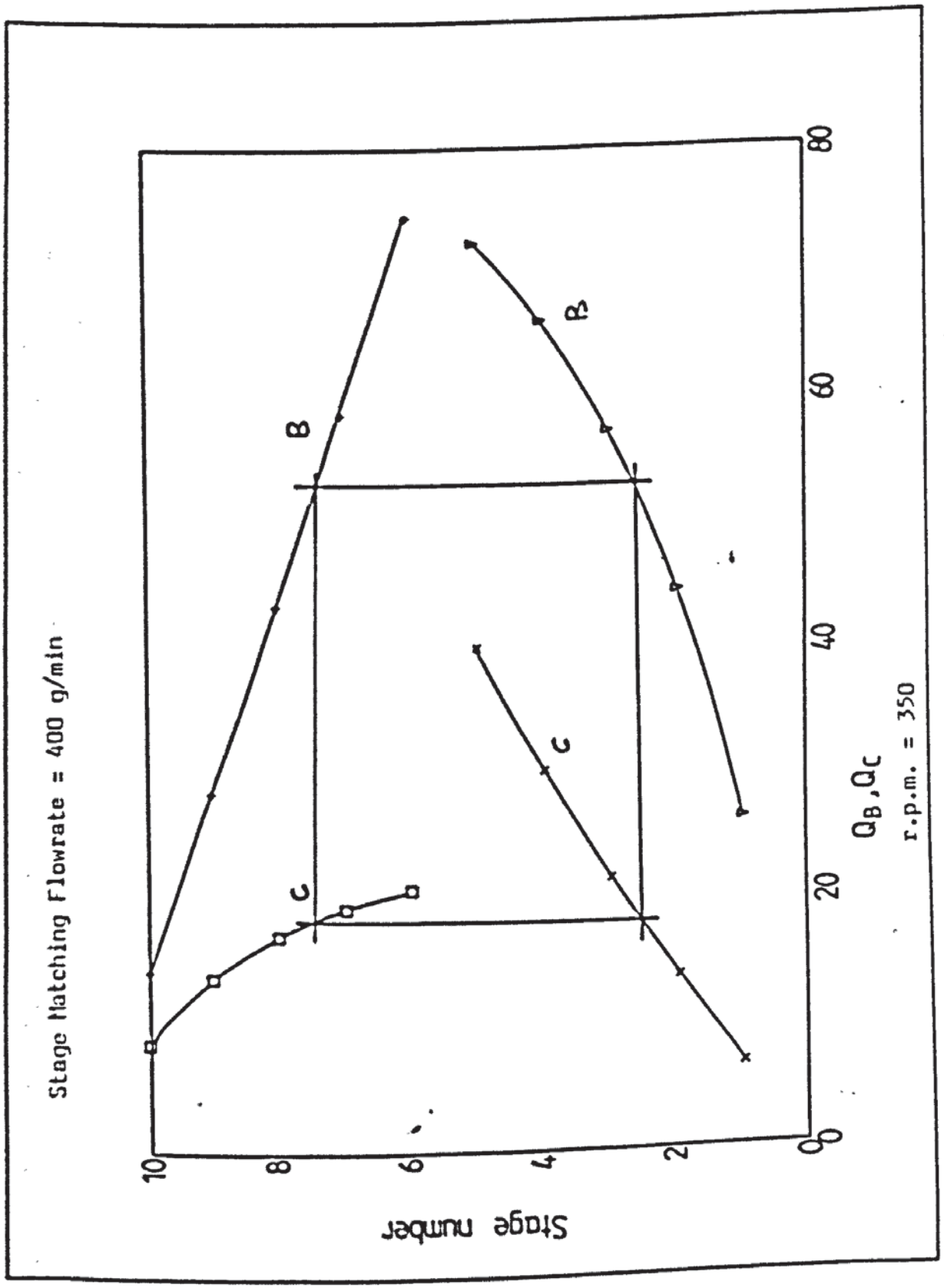
Stage Hatching Flowrate = 400 g/min
r.p.m. = 350
Q_B, Q_C
Stage number
0
20
40
60
80
2
4
6
8
10
B
B
C
C

Figure III-7

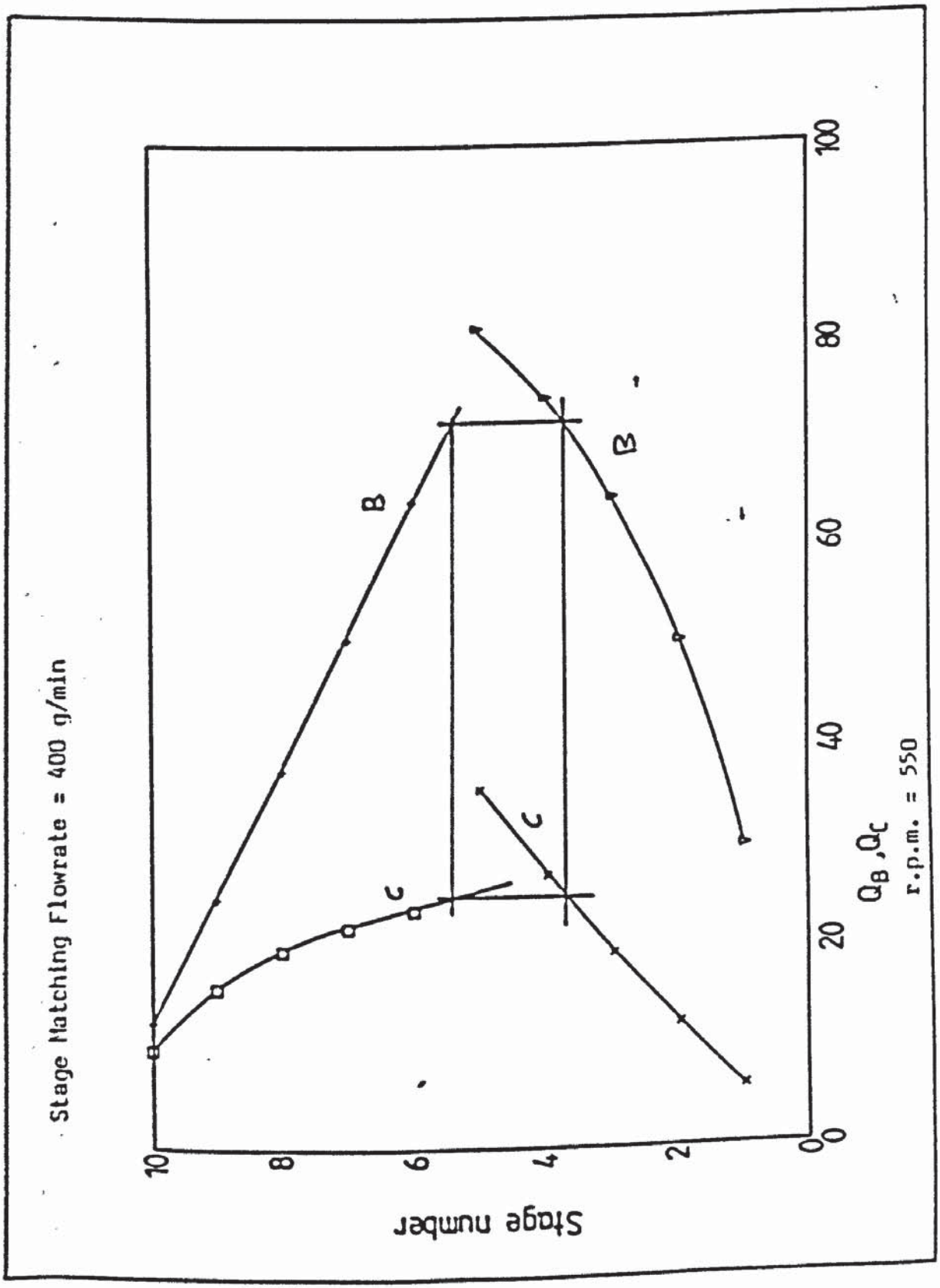
Stage Matching Flowrate = 400 g/min
Stage number
10
8
6
4
2
0
0
20
40
60
80
100
Q_B, Q_C
r.p.m. = 550
B
B
C
C

Figure III-8

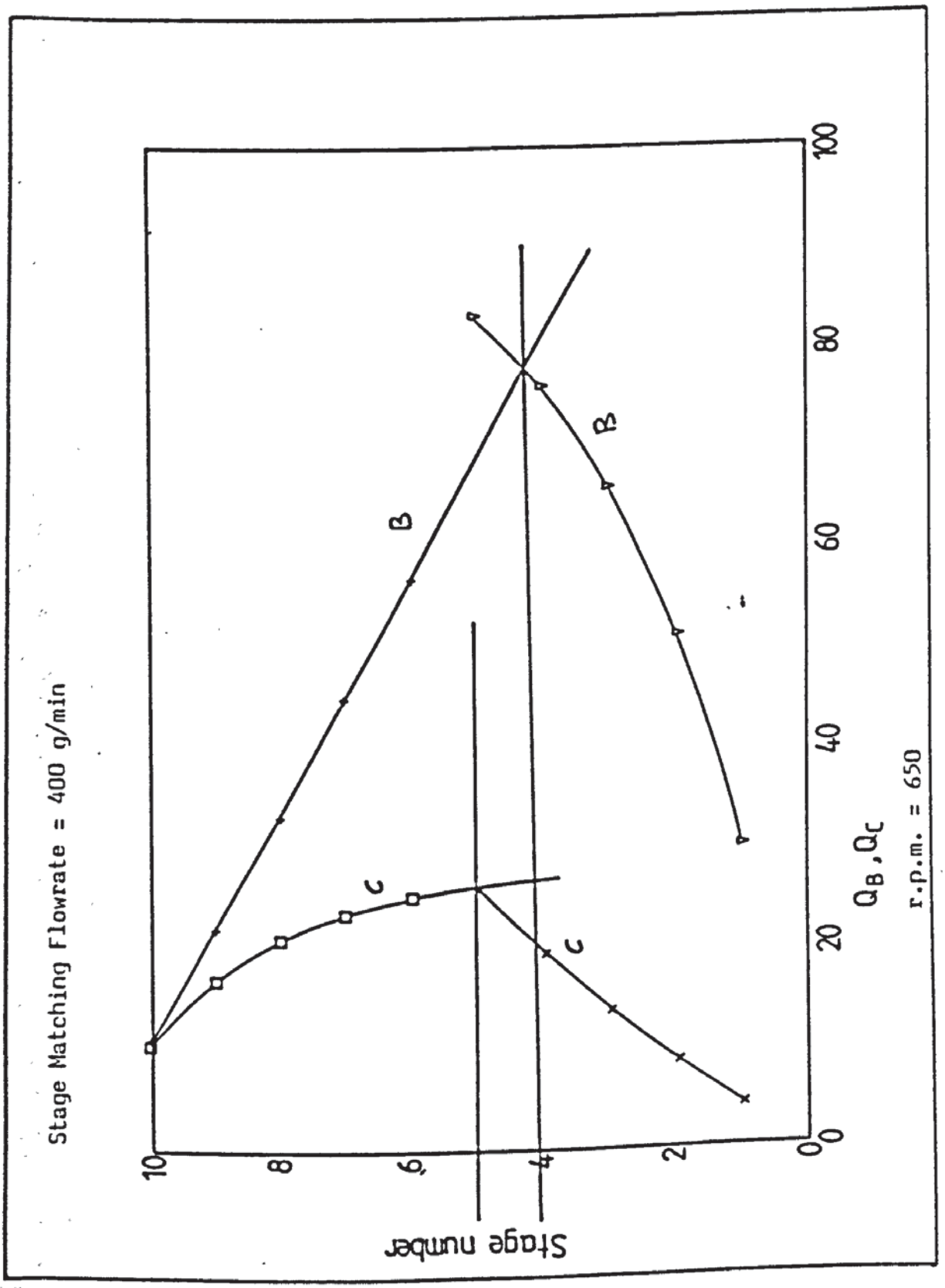
Stage Matching Flowrate = 400 g/min
r.p.m. = 650
Stage number
Q_B, Q_C
B
B
C
C
0
20
40
60
80
100
2
4
6
8
10

Figure III-9

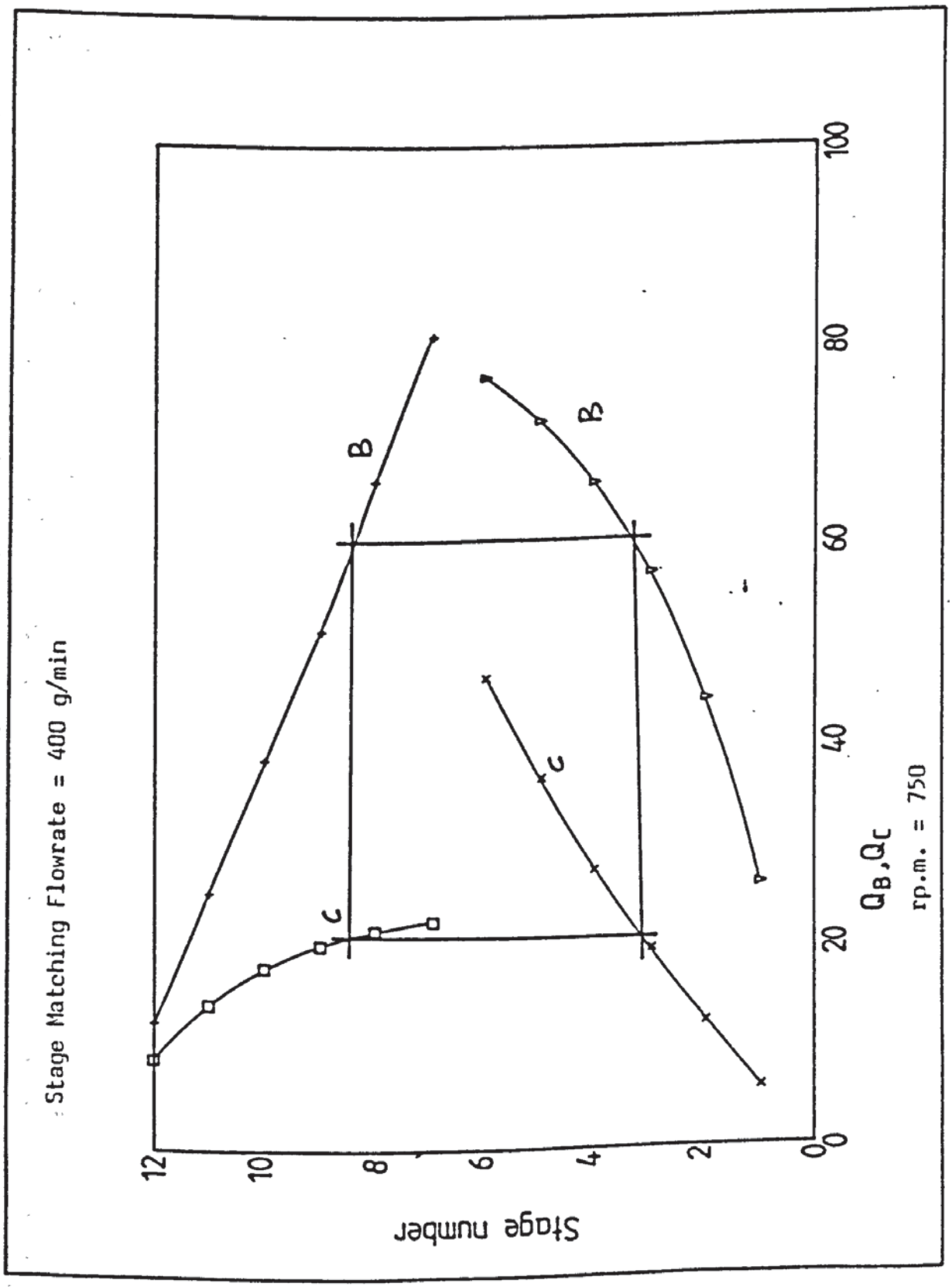

Figure III-10

Figure III-11

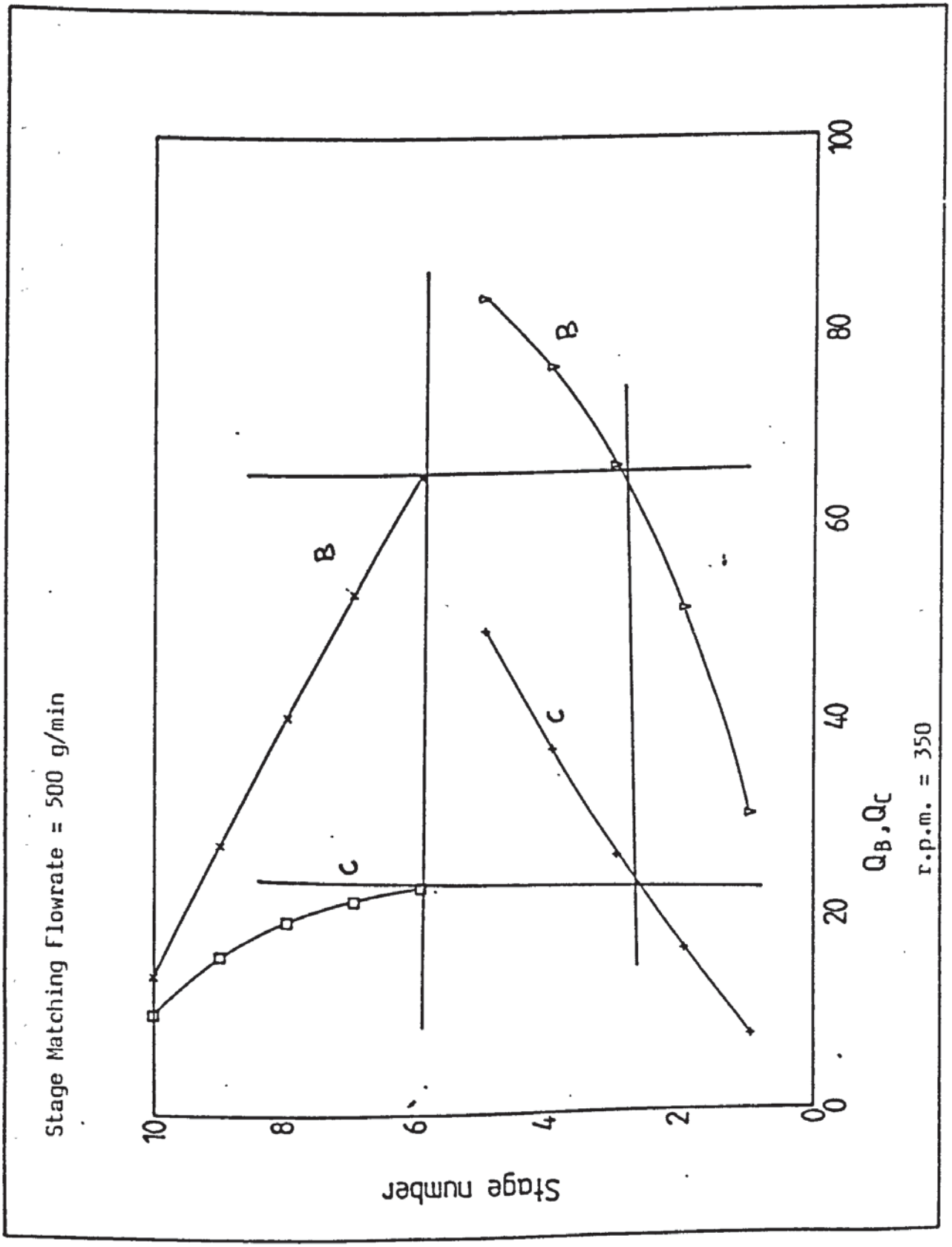

Figure III-12

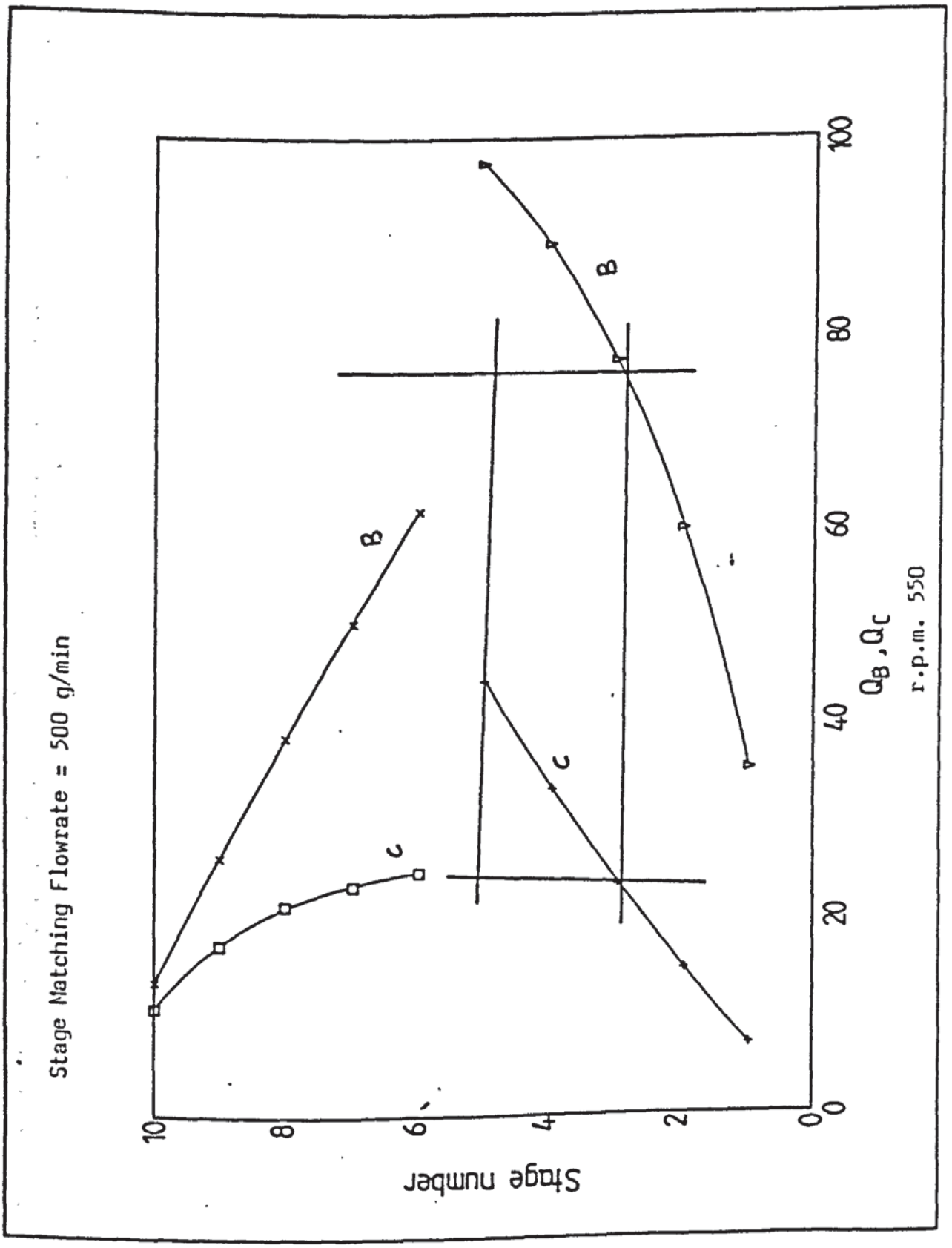

Figure III-13

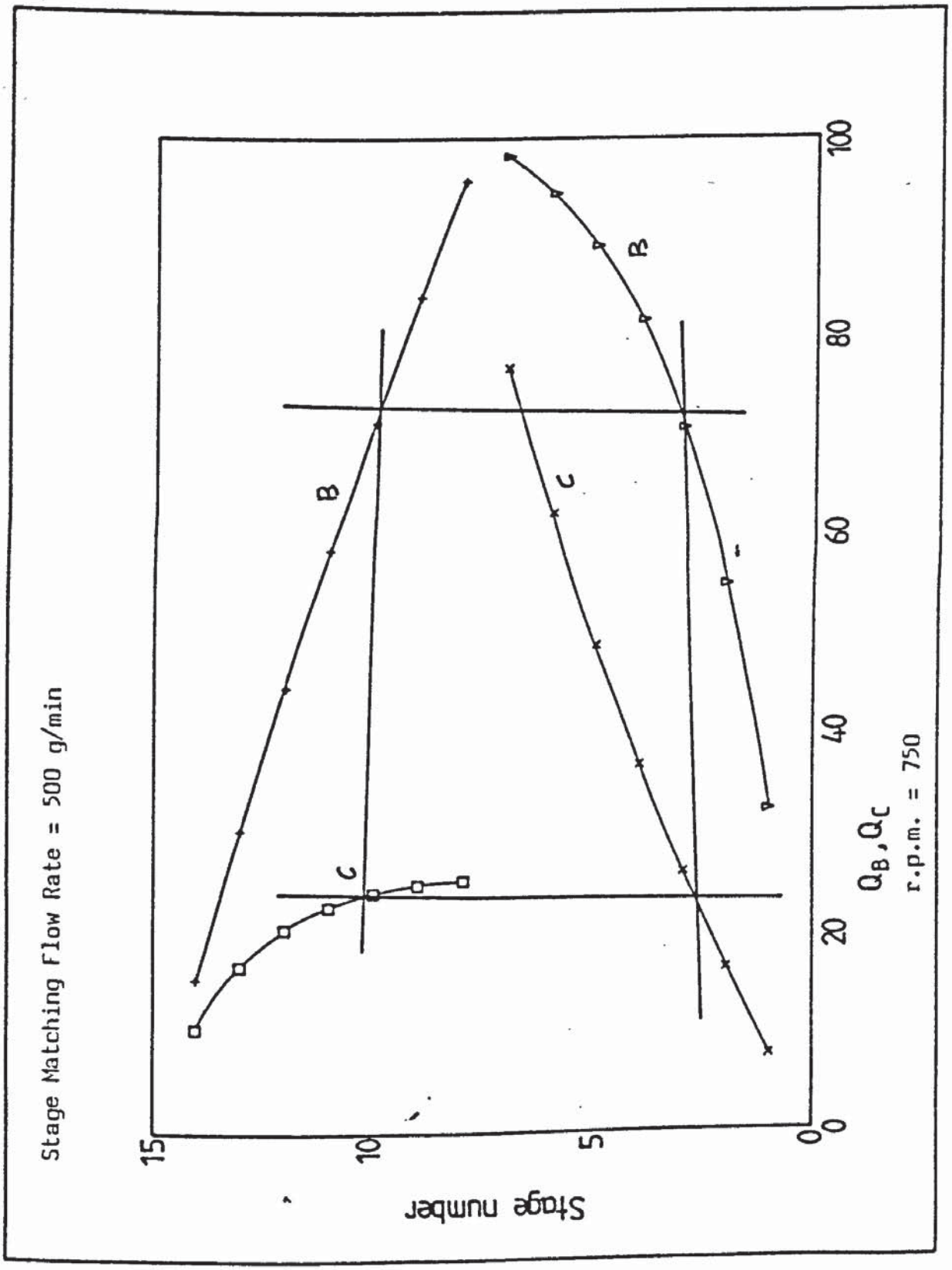

Figure III-14

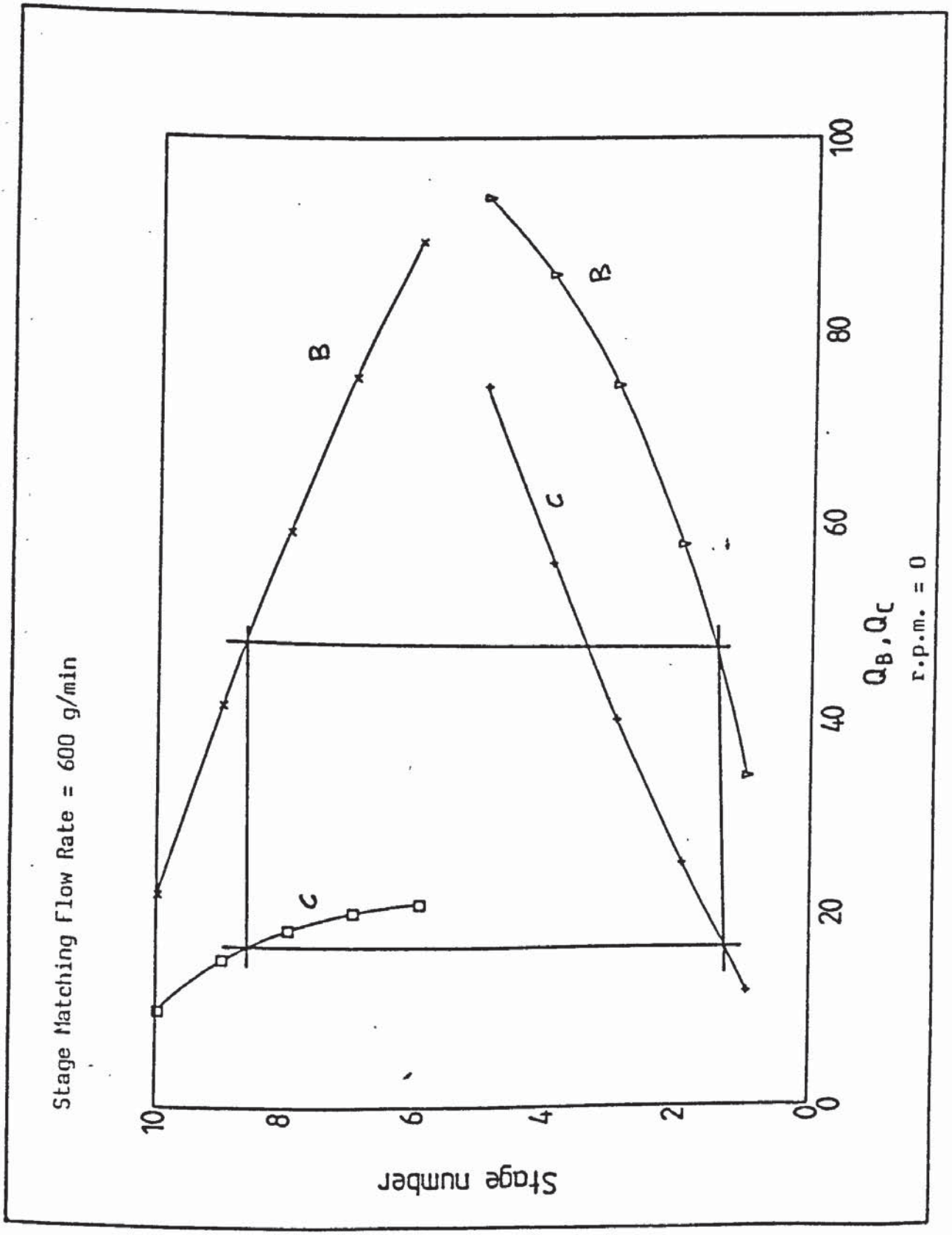

Figure III-15

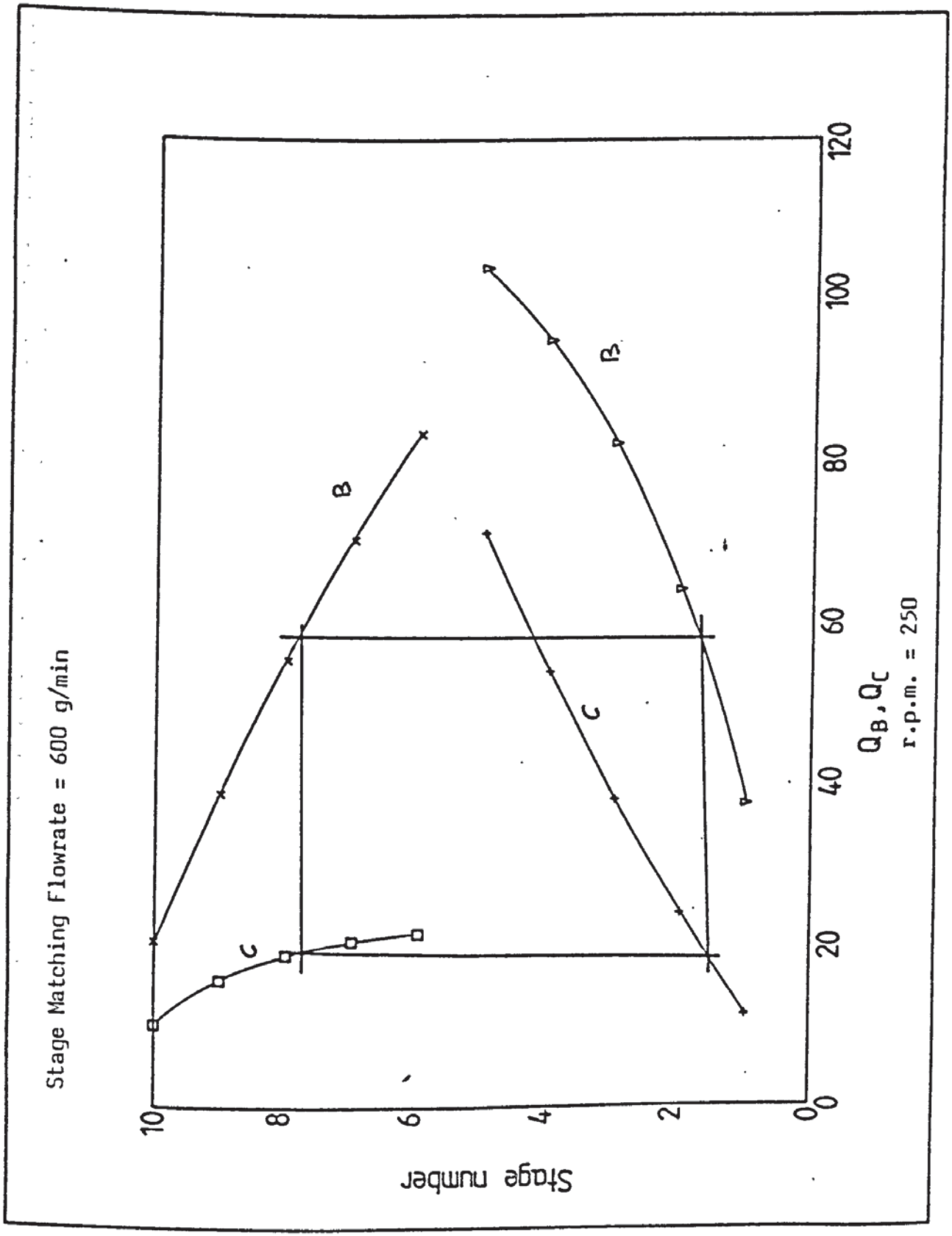

Figure III-16

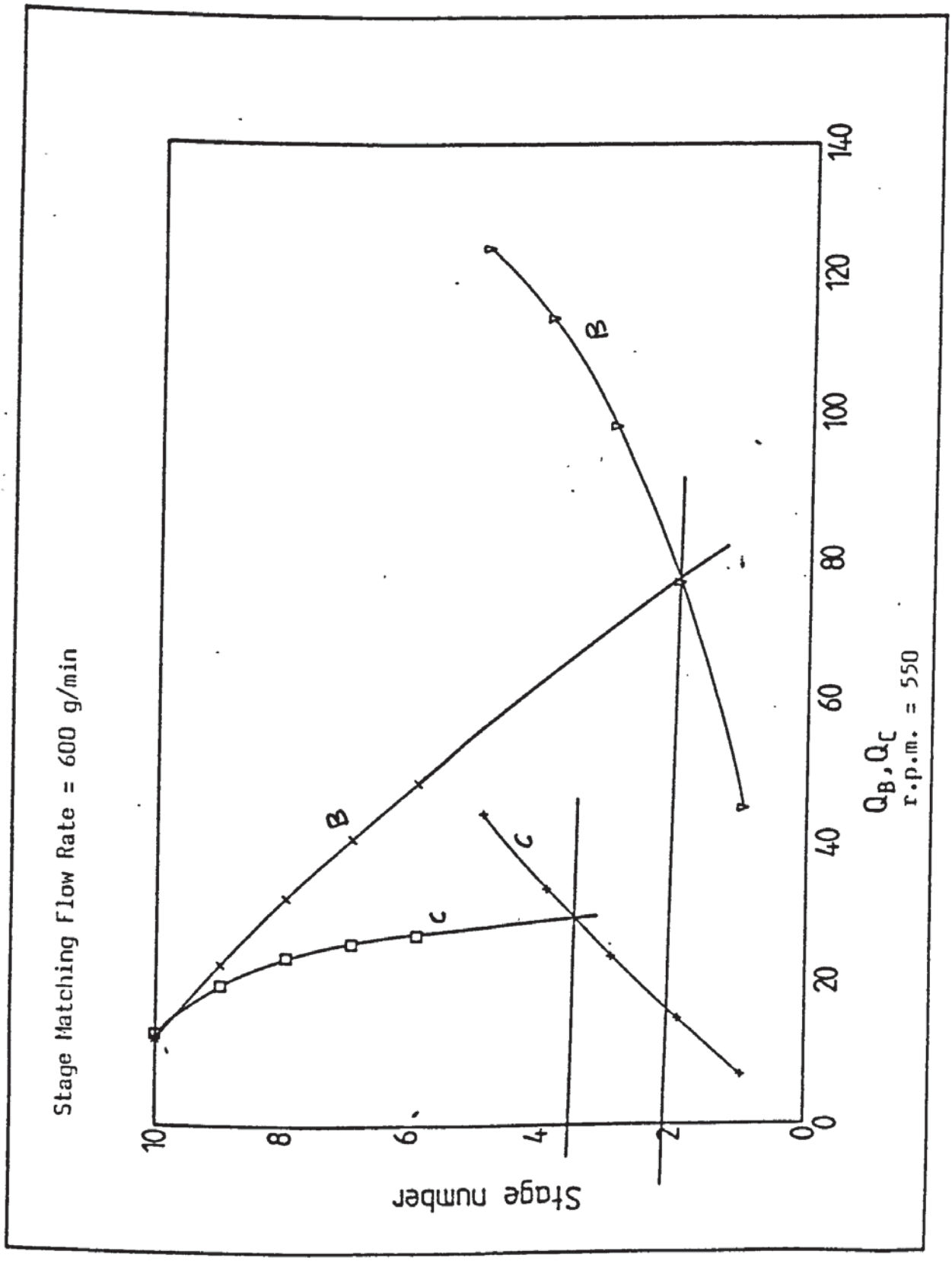

Figure III-17

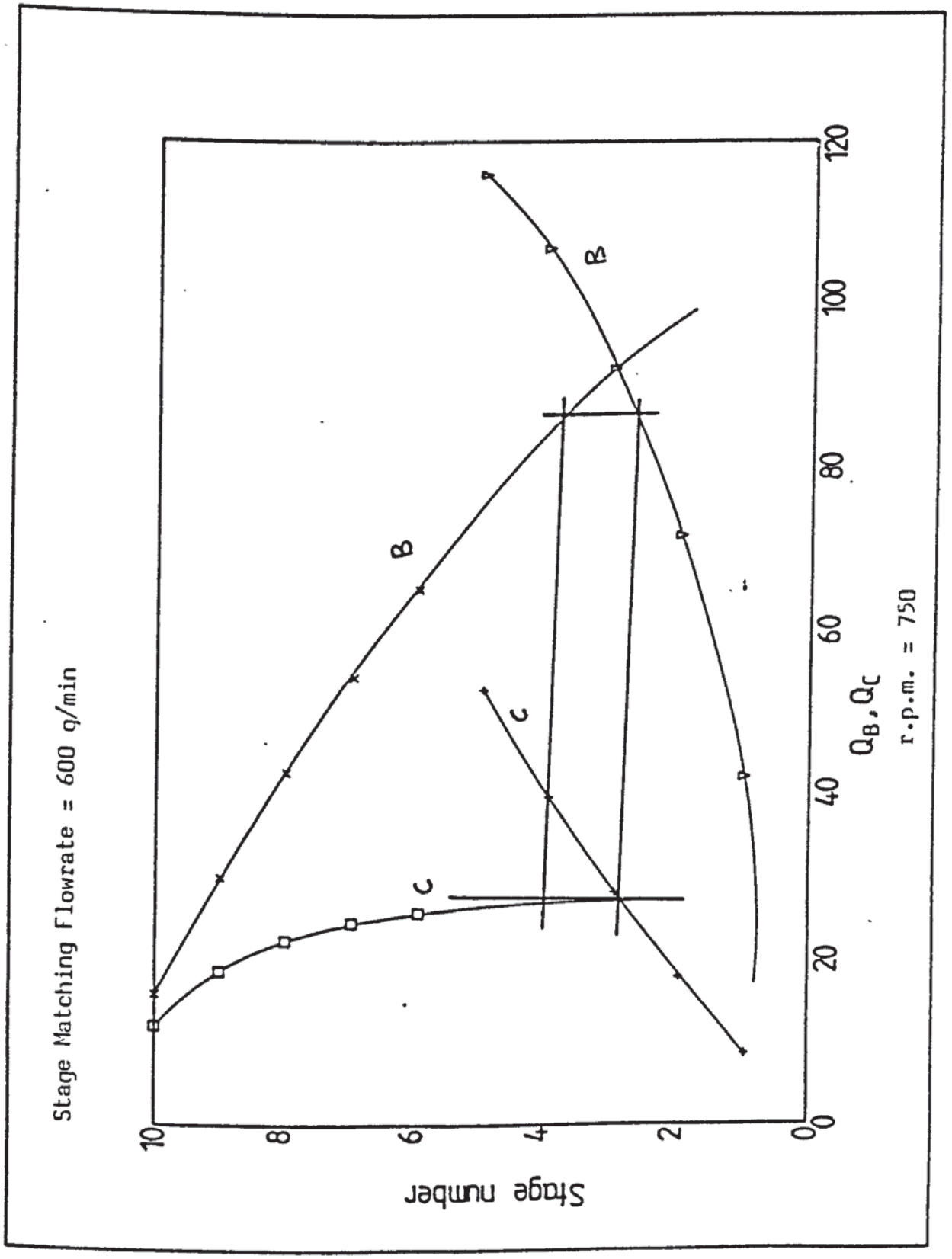

Figure III-18

APPENDIX IV

DROP SIZE DISTRIBUTION COMPUTER PROGRAM AND MASS TRANSFER COEFFICIENT CALCULATIONS

DROP SIZE DISTRIBUTION

Actual drop diameter:

$$d_{actual} = \frac{d\ measured}{Magnification}$$

Cummulative drop volume:

$$V = \sum n_i \left(\frac{\pi}{6} d_i^3 \right)$$

Cummulative drop volume fraction:

$$= \frac{V_i}{V_{Total}} \times 100$$

Total Cummulative drop volume:

$$V_{Total} = 4705.1464$$

$$V_1 = 1.0571$$

$$V_1/V_{Total} = 1.0571/4705.1464$$

$$= \underline{0.003}$$

$$d_{32} = \frac{\sum n_i\ d_i^3}{\sum n_i\ d_i^2}$$

$$\frac{dv}{dd} = \frac{V_i = V_{i-1}}{d_i - d_{i-1}}$$

d_{32} for run ! :

$$= \underline{4.2958117\ mm}$$

Table IV-1

Drop Size Distribution

Rotor Speed 650 r.p.m.

Run No. 4 (With Mass Transfer)

DM	DA	F	FV	
1.4900	.8765	25	8.8091	.0422
2.0400	1.2000	18	25.0868	.2112
2.4200	1.4235	10	40.1834	.2835
2.5900	1.5235	21	79.0476	1.6315
3.1400	1.8471	11	115.3231	.4707
3.1700	1.8647	9	145.8619	7.2645
3.7000	2.1765	7	183.6309	.5086
4.2500	2.5000	4	216.3392	.4244
5.9000	3.4706	1	238.2162	.0946

Sauter Mean Diameter = 1.7980367

From Table IV:

$$\text{Stagnant Drops} = \frac{40.1834}{238.2162} \times 100 = \underline{16.87\%}$$

Circulating Drops = 73.95%

Oscillating Drops = 9.18%

d_s = 0.1214 cm

d_c = 0.2326 cm

d_o = 0.450 cm

EXPERIMENTAL MASS TRANSFER COEFFICIENT CALCULATIONS:

Table IV-4

Run No. 4

Stage	X_B	Y_B	X_C	Y_C	Y_B^*	$Y_B^* - Y_B$	ΔY_{BLM}
1	0.172	0.14275	0.0021	0.0028	0.143	2.5×10^{-4}	
2	0.169	0.1405	0.0044	0.0059	0.141	5.0×10^{-4}	3.61×10^{-4}
3	0.165	0.1364	0.0070	0.0093	0.137	6.0×10^{-4}	5.48×10^{-4}
4	0.159	0.1312	0.0098	0.0131	0.132	8.0×10^{-4}	6.95×10^{-4}
5	1.150	0.1237	0.0130	0.0174	0.125	1.3×10^{-3}	1.03×10^{-3}
6	0.137	0.1123	0.0166	0.0220	0.114	1.7×10^{-3}	1.49×10^{-3}
7	0.119	0.0965	0.0205	0.0272	0.0991	2.6×10^{-3}	2.12×10^{-3}
8	0.0925	0.0734	0.0248	0.0330	0.0772	3.62×10^{-3}	3.08×10^{-3}
9	0.0546	0.04095	0.0296	0.0394	0.0455	4.55×10^{-3}	4.07×10^{-3}

Feed Flow Rate = 600 g/min

Feed Concentration = 40% Acetic Acid
59.5% n-Hexane
0.5% n-Butanol

Water Flow Rate = 1000 ml/min
Hexane Flow Rate = 13.43 ml/min
Concentration of Butanol in inlet water = 3.5%

$Y_B^* = 0.743\ X_B$

The specific interfacial area

$$a = 6 \times \frac{\phi D}{d_{32}}$$

$d_{32} = 0.1798$ cm

$\phi D = 0.08$

$$\text{Therefore } a = \frac{6 \times 0.08}{0.1798} = 2.67\ cm^2/cm^3$$

Column cross sectional area

$$A = \frac{\pi D^2}{4} = \frac{\pi \times (7.6)^2}{4} = 45.36\ cm^2$$

Effective stage height = 15.875 cm

(Packing + Mixing)

Total interfacial area per stage

$= a \times V_K$

where V_K = effective volume of the k^{th} stage

$A_T = 45.36 \times 15.875 \times 2.67 = 1922.65\ cm^2$

$$\text{Mass Transfer Rate } N = \dot{V}_D\ (Y_{B,in} - Y_{B,out})$$
$$= \dot{V}_C\ (X_{B,out} - X_{B,in})$$

$$\text{For Stage No. 1} = \frac{1343}{60} \times (0.14275 - 0.1405)$$

$$= 0.050\ g/sec$$

$$K_{Exp} = \frac{N}{A\ \Delta Y_{LM}}$$

$$= \frac{0.050}{1922.64 \times 3.61 \times 10^{-4}} = 7\ 2 \times 10^{-2}\ \text{cm/sec}$$

Calculated Mass Transfer Coefficient:

The calculated mass transfer coefficients were computed from the equation summarised in Table IV-3.

Dispersed phase flow rate = 1343 cm^3/min

Vertical velocity of the dispersed phase

$$U_d = \frac{1343}{45.36 \times 60} = 0.49\ \text{cm/sec}$$

Continuous phase flow rate = 1000 cm^3/min

Vertical velocity of the continuous phase

$$U_c = \frac{1000}{60 \times 45.36} = 0.367\ \text{cm/sec}$$

The vertical velocity of drops is determined by applying equation (3.5) for the relative velocity determination:

$$U_s = \frac{U_c}{1 - \phi_D} + \frac{U_d}{\phi_D}$$

$$= \frac{0.367}{1 - 0.08} + \frac{0.49}{0.08} = 6.52\ \text{cm/sec}$$

Table IV-3

State of Droplet	Reynolds Number	Dispersed Phase Coefficient Model	Eq. No.	Continuous Phase Coefficient Model	Eq. No.
Stagnant	Re 10	$K_{ds} = \frac{4\pi^2 D_d}{3d_s}$	(1)	$Sh_{cs} = 2.076\ (Re)^{0.5}(Sc)^{0.3}$	(2)
		Treybal (1963)		Rowe (1965)	
Circulating	10 Re 200	$K_{dc} = \frac{17.9 D_d}{d_c}$	(3)	$Sh_{cc} = -126 + 1.8\ (Re)^{0.5}(Sc)^{0.42}$	(4)
		Kronig & Brink (1960)		Garner-Ford Tayeban (1959)	
Oscillating	Re 200	$k_{do} = 0.45(\omega D_d)^{0.5}$	(5)	$Sh = 50 + 0.0085\ (Re)(Sc)^{0.7}$	(7)
		Rose & Kintner (1966)		Garner-Tayeban (1960)	
		$Kd_o = \sqrt{\frac{4\omega D_d(1+\varepsilon)}{\pi}}$	(6)		
		Where $\varepsilon_o = \varepsilon + \frac{3}{8}\varepsilon^2$			
		Angelo-Lightfoot (1966)			

The maximum diameter of stagnant drops in the drop population occurred at a drop Reynold's number equal to 10.0

$$Re = \frac{ds\ \rho c\ Us}{\mu}$$

$$d_s = \frac{\mu_c\ Re}{\rho_c\ Us} = \frac{0.0089 \times 10}{0.997 \times 6.52}$$

$$= 0.0137 \text{ cm}$$

The maximum diameter of circulating drops occurred at a drop Reynold's number equal to 200.0

$$d_c = \frac{0.0089 \times 200}{0.997 \times 6.52} = 0.274 \text{ cm}$$

Therefore the drop swarm consists of:

Stagnant drop of $d_s = 0.137$ mm

Circulating drop of $0.137 < d_c < 2.74$ mm

Oscillating drops of $d_o > 2.74$ m

The drop distribution diagram of Figure 10.10 and Table IV-3 shows the portion fraction of each drop pattern.

(a)(i) Dispersed phase mass transfer coefficient for stagnant drops was estimated by Tayeban equation (1963) indicated in Tble IV-3:

$$k_{ds} = \frac{4\ \pi\ ^2D_d}{3ds}$$

$$= \frac{4\ \pi^{2} \times 6.11 \times 10^{-5}}{3 \times 0.1214} = 1.99 \times 10^{-2}\ \text{cm/sec}$$

(ii) The continuous mass transfer coefficient for stagnant drops was estimated by Rowe equation (1965) indicated in Table IV-3 above.

$$Sh = 2.076\ (Re)^{0.5}\ (Sc)^{0.3}$$

$$Sc = \frac{0.0089}{0.997 \times 1.366 \times 10^{-5}} = 653.5$$

$$Re = \frac{0.997 \times 0.1214 \times 102.1}{0.0089} = 1388.5$$

$$Sh = 136.67$$

$$\frac{K_{cs} d_m}{D_c} = 540.85$$

$$K_{cs} = \frac{540.85 \times 1.366 \times 10^{-5}}{0.1214} = 6.08 \times 10^{-3}\ \text{cm/sec}$$

Overall mass transfer coefficient for stagnant drops

$$\frac{1}{K_{os}} = \frac{1}{K_{ds}} + \frac{m}{K_{cs}}$$

$$= \frac{1}{1.99 \times 10^{-2}} + \frac{0.743}{5.08 \times 10^{-3}}$$

Therefore $K_{os} = 6.13 \times 10^{-3}$ cm/sec

(b) Mass Transfer Coefficient for circulating drops

(i) Dispersed phase estimated by Kronig and Brink equation indicated in Table IV-3 above:

$$K_{dc} = \frac{17.9\ D_d}{d_c}$$

$$= \frac{17.9 \times 6.11 \times 10^{-5}}{0.2326} = 4.70 \times 10^{-3} \text{ cm/sec}$$

(ii) Continuous phase mass transfer coefficient was estimated by Garner et al. equation indicated in Table (IV-3) above.

$$\frac{K_{cc}\ d_c}{D_c} = -126 + 1.8\ Re^{0.5}\ Sc^{0.42}$$

$$\text{Velocity of drop } U_d = \pi\ DN = \frac{\pi\ (3.0)650}{60}$$

$$= 102.10 \text{ cm/sec}$$

$$Re = \frac{0.997 \times 0.2326 \times 102.10}{0.0089} = 2660.4$$

$$Sc = 653.5$$

$$Sh = 785.0$$

$$\frac{K_{cc}\ d_{cc}}{D_c} = 785.0$$

$$K_{cc} = \frac{785.0 \times 1.366 \times 10^{-5}}{0.2326}$$

$$= 4.61 \times 10^{-3} \text{ cm/sec}$$

(c) Oscillating Drops:

(i) Dispersed Phase mass transfer was estiamted by Rose and Kintner equation indicated in Table V-3 above.

$$K_{do} = 0.45\ (D_d w)^{0.5}$$

Where,

$$w^2 = \frac{\sigma\ b}{r^3} \qquad \frac{n(n-1)(n+1)(n+2)}{(n+1)\ \rho_d + n\rho}$$

$n = 2$

$$b = \frac{d_o^{0.225}}{1.242}$$

$d_o = 0.45$ cm

$b = 0.673$

$r = 0.225$ cm

$\sigma = 18.42$ dyne/cm

$w = 81.13\ sec^{-1}$

$$k_d = 0.45\ (6.11 \times 10^{-5} \times 81.13)^{0.5}$$

$$= 3.16 \times 10^{-2}\ cm/sec$$

(ii) Continuous phase mass transfer coefficient was estimated by Garner et al equation indicated in Table IV-3 above.

$$\frac{K_{co}\ d_o}{D_c} = 50 + 0.0085\ Re\ Sc^{0.7}$$

$$Re = \frac{0.997 \times 0.45 \times 102.1}{0.0089}$$

$$= 5146.96$$

$$\frac{K_{co}\, d_o}{D_c} = 4146.96$$

$$K_{co} = \frac{4146.96 \times 1.366 \times 10^{-5}}{0.45}$$

$$= 0.1258 \text{ cm/sec}$$

Overall mass transfer coefficient for the oscillating drops.

$$= 2.67 \times 10^{-2} \text{ cm/sec}$$

Composite overall mass transfer coefficient

$$K_{cal} = K_s P_s + K_c P_c + K_{os} P_{os}$$

where P_s, P_c, P_{os} are the volume fraction of drops in the stagnant, circulating and oscillating drop regimes.

$$K_{Cal} = 0.167 \times 6.13 \times 10^{-3} + 0.7389 \times 4.37 \times 10^{-3} + 0.0918 \times 2.67 \times 10^{-2}$$

$$= 5.68 \times 10^{-3} \text{ cm/sec}$$

Calculation of theoretical mass transfer rate during drop release from the wire mesh packing:

The mass transfer rate during drop release from the wire mesh packing was estimated by Heertjes et al quoted from Johnson et al (115):

$$\frac{C_1 - C_2}{C_1 - C^*} = \frac{20.6}{d}\sqrt{\frac{d\theta}{\pi}}$$

where D = the diffusion coefficient

θ = time of drop formation = 100 ms

C_1, C_2, C^* = inlet, outlet and equilibrium concentration in one stage.

For Run No.4

Stage 3 $C_4 - C^* = 0.1312 - 0.1320$

$= 5.4 \times 10^{-4}$ g/min

$$\frac{C_4 - C_3}{C_4 - C^*} = \frac{2.0}{0.496} \quad \frac{(6.11 \times 10^{-5} \times 0.1)}{\pi}$$

$= 0.0562$

Therefore $C_4 - C_3 = 4.721 \times 10^{-5}$ g/cm^3

Total number of drops released at a time interval of 100 ms = 14 drops.

Volumetric flow of the drops released

$$= \frac{\pi D^3 \times 14}{6 \quad 0.1} =$$

$$= \frac{\pi (0.496)^3 \times 14}{0.6} = 10.22 \text{ cm}^3/\text{sec}$$

Therefore mass transfer rate during drop release from dispersed to continuous:

$$N_{df} = 10.22 \times 4.721 \times 10^{-5}$$

$$= 4.825 \times 10^{-4} \text{ g/sec}$$

Experimental mass trnasfer rate for stage No. 3

$$= \frac{1343}{60} (0.1364 - 0.1312)$$

$$= 0.11388 \text{ g/sec}$$

Percent of mass trnasfer rate during drops released from the wiremesh packing with respect to the experimental mass transfer rate

$$= \frac{4.825 \times 10^{-4}}{11.388 \times 10^{-2}} \times 100 = 0.42\%$$

This shows that the mass transfer rate during drop relese was very small and may be neglected.

TEXT BOUND INTO

THE SPINE

```
NN.20
PER ASSUMED
C. MON-05/06/85-11:49:10-(34,35)


1:C         CALCULATION OF CUMULATIVE VOLUME & DROP SIZE DISTRIBUTION
2:C         MIXING COMPARTMENT
3:C         SHEIBEL COLUMN
4:C           SAUTER MEAN DIAMETER
5:C
6:C         DM IS THE MEASURED .DROP DIAMETER
7:C         DA IS THE ACUAL DROP DIAMETE
8:C         RF IS THE MAGNIFICATION FACTOR
9:C         F IS THE NUMBER OF DROPS WITHIN THE GROUP OF DROPS
0:            DIMENSION DM(50),DA(50),F(50),C(50),V(50),VD(50),VV(50),
1:       $DD(50),FCV(50),FV(50),VC(50),S(50),RS(50),RC(50)
2:            SUMRS=0.
3:            SUMRC=0.
4:            READ(5,*)N,L
5:            WRITE(6,80)N,L
6:80       FORMAT(////8X,'***  D R O P   S I Z E   D I S T R I B U T I O N'
7:       $,'  ***'//5X,'ROTOR SPEED = ',I5,'  RPM',//5X,'RUN NO. # ',I2///)
8:            WRITE(6,10)
9:10       FORMAT(7X,' DM ',9X,'DA ',7X,'F',8X,' FV ',11X, 'FCV ')
0:            READ(5,*)RF,K
1:            VSUM =0.0
2:            DA(1) =0.0
3:            VD(1) =0.0
4:            DO 30 I =2,K
5:            READ(5,*)DM(I),F(I)
6:            DA(I) =DM(I)/RF
7:            S(I)=DA(I)**2
8:            C(I) =DA(I)**3
9:            RS(I)=S(I)*F(I)
0:            RC(I)=C(I)*F(I)
1:            SUMRS =SUMRS+RS(I)
2:            SUMRC =SUMRC +RC(I)
3:            V(I)=(3.14/6.0)*C(I)
4:            VD(I) =V(I)*F(I)
5:            VSUM =VSUM+VD(I)
6:            FV(I) =VSUM
7:   30       CONTINUE
8:            DO 40 I =2,K
9:            VC(I)= FV(I)/VSUM
0:            VV(I)=VC(I)-VC(I-1)
1:            DD(I)=DA(I)-DA(I-1)
2:            FCV(I)= VV(I)/ DD(I)
3:            WRITE(6,123)DM(I),DA(I),INT(F(I)),FV(I),FCV(I)
4:123         FORMAT(5X,F7.4,5X,F7.4,5X,I2,5X,F10.4,5X,F7.4)
5:   40          CONTINUE
6:            SMD =SUMRC/SUMRS
7:            PRINT*,' SAUTER MEAN DIAMETE = ',SMD
8:            STOP
9:            END

. LINES:49 FIELDATA
```

APPENDIX V

CALIBRATION OF FLOW METERS

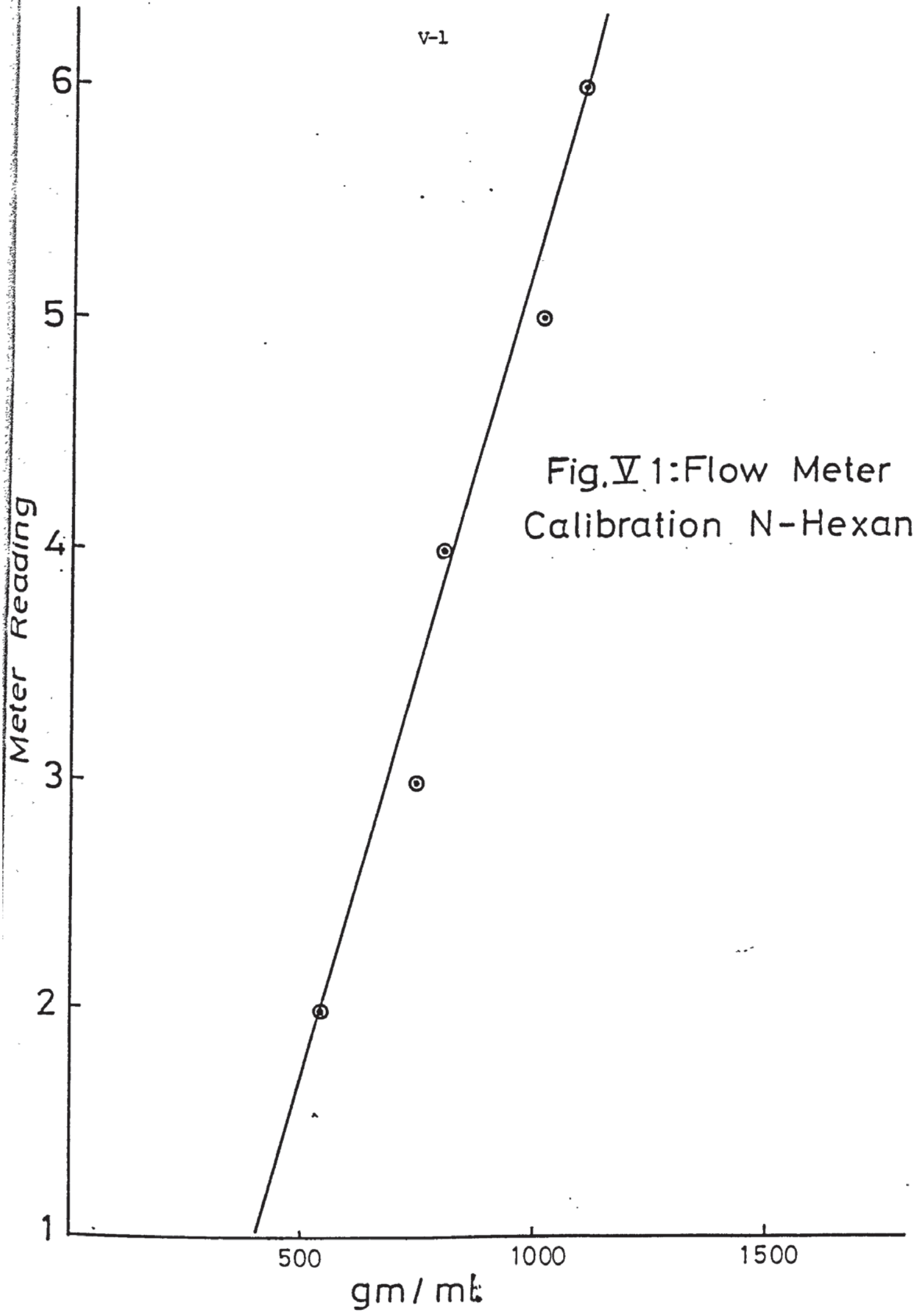

Fig. V 1: Flow Meter Calibration N-Hexane

Fig. V-2: Calibration Curve
Feed Admixture

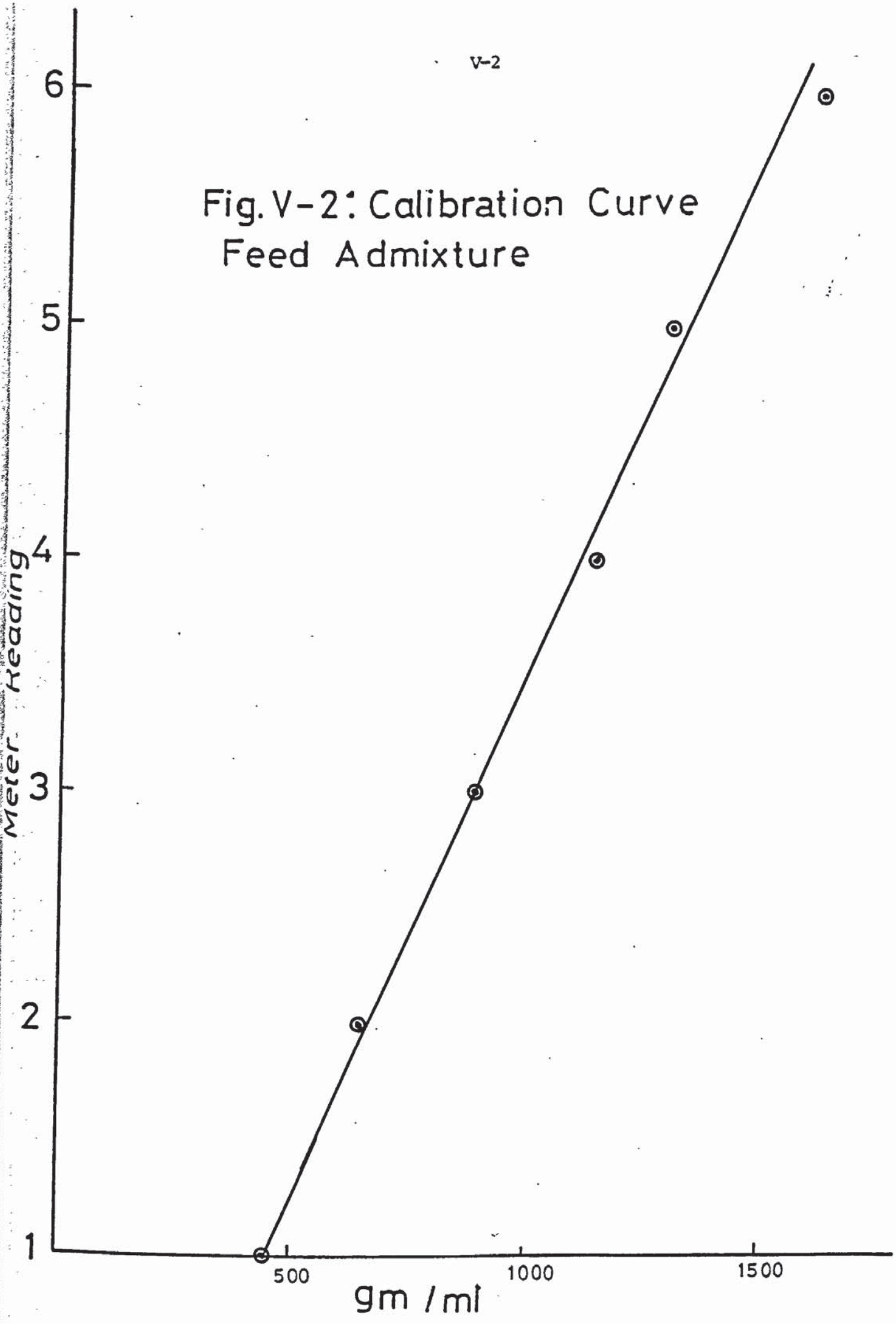

Fig.V 3:Flow Meter Calibration
Water

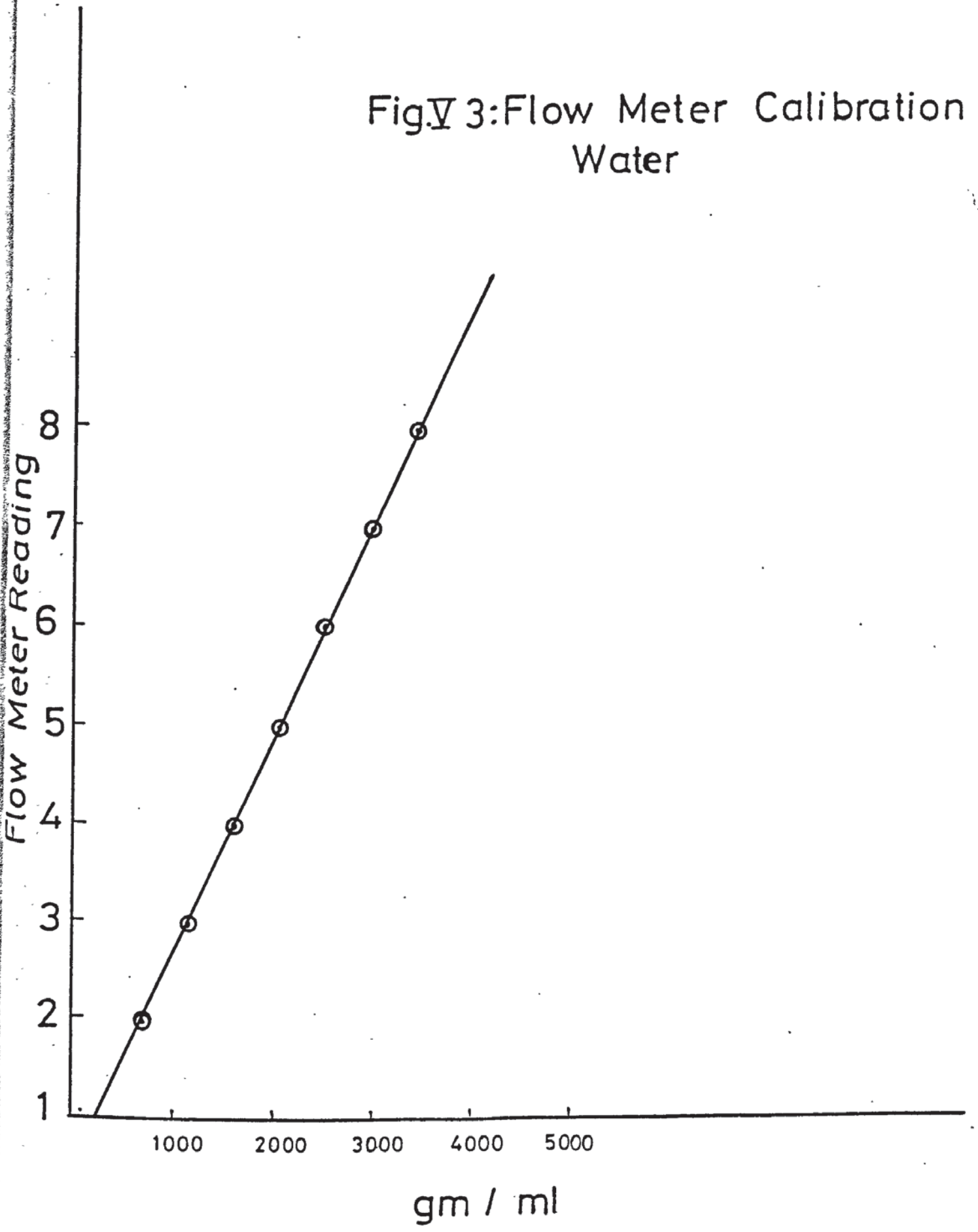

APPENDIX VI

MODEL SIMULATION COMPUTER PROGRAM

```
&ED,U SHA.2
CASE UPPER ASSUMED
ED 16R1C. TUE-05/28/85-12:30:05-(23,24)
EDIT
C:
     1:            DIMENSION XN(20,4),X(20,4),Y(20,4),SUMX(20),B(4)
     2:C           SIMULATION MULTISTAGE MODEL
     3:C           FRACTIONAL EXTRACTION
     4:C           SCHEIBEL COLUMN
     5:            REAL L(30),E(30),K(30,4),HLO,F(30),XF(30,4)
     6:            READ(5,*)N,M
     7:            READ(5,*)HLO,E(1)
     8:            DO 1 J=1,M
     9: 1          READ(5,*)Y(1,J)
    10:            READ(5,*)A1,A2,A3,A4,A5
    11:            READ(5,*)A6,A7,A8,A9,A10
    12:            DO 50 I=1,N
    13:  50        READ(5,*)F(I),XF(I,1),XF(I,2)
    14:            READ(5,*)DIM,UL,VD,DDD
    15:            I=1
    16:            SUMX(1)=0.
    17:            DO 2 J=1,M
    18:            CALL XCALC(X,XN,Y,A1,A2,A3,A4,A5,A6,A7,A8,A9,A10,I)
    19:            K(1,J)=Y(1,J)/X(1,J)
    20: 2          SUMX(1)=SUMX(1)+X(1,J)
    21:            L(1)=HLO/(1.-SUMX(1))
    22:            E(2)=E(1)+L(1)-HLO
    23:            DO 21 J=1,M
    24:  21        Y(2,J)=(L(1)*X(1,J)+Y(1,J)*E(1))/E(2)
    25:            DO 3 I=2,N
    26:            SUMX(I)=0.
    27:            DO 4 J=1,M
    28:            CALL XCALC(X,XN,Y,A1,A2,A3,A4,A5,A6,A7,A8,A9,A10,I)
    29:            SUMX(I)=SUMX(I)+X(I,J)
    30:            K(I,J)=Y(I,J)/X(I,J)
    31:  4         CONTINUE
    32:            DO 32 J=1,M
    33:            L(I)= L(I-1)*(1.-SUMX(I-1))/(1.-SUMX(I))
    34:            E(I+1)=E(I)+L(I)-L(I-1)-F(I)
    35:            Y(I+1,J)=((L(I)*X(I,J)-L(I-1)*X(I-1,J))+E(I)*Y(I,J)
    36:     $      -F(I)*XF(I,J))/E(I+1)
    37:  32        CONTINUE
    38:  3         CONTINUE
    39:            DO 5 J=1,M
    40:            WRITE(6,150)J
    41: 150        FORMAT(///15X,'COMPONENT  NO. ',I2/)
    42:            PRINT*,'-------------------------------------------'
    43:            PRINT*,'STAGE NO.  COMPONENT          XI          YI          KI'
    44:            PRINT*,'-------------------------------------------'
    45:            DO 6 I=1,N
    46:            PRINT12,I,J,X(I,J),Y(I,J),K(I,J)
    47:  12        FORMAT(4X,I2,11X,I2,9X,F5.4,6X,F5.4,1X,F7.4)
    48:            PRINT*,'-------------------------------------------'
    49: 6          CONTINUE
    50:  5         CONTINUE
    51:            STOP
    52:            END
```

```
      SUBROUTINE XCALC(X,XN,Y,A1,A2,A3,A4,A5,A6,A7,A8,A9,A10,I)
      DIMENSION XN(20,4),X(20,4),Y(20,4)
    9 SS=(X(I,1)+Y(I,1))
      SA=(X(I,2)+Y(I,2))
      XN(I,1)=A1*(Y(I,1))**A2
      XN(I,2)=A3*(Y(I,2))**A4
      F1=XN(I,1)+A5*(SS**A6)*(SA**A7)*Y(I,1)-X(I,1)
      F2=XN(I,2)+A8*(SS**A9)*(SA**A10)*Y(I,2)-X(I,2)
      DF1XB=A5*A6*(SS**(A6-1.))*(SA**A7)*Y(I,1)-1.
      DF1XC=A5*A7*(SS**A6)*(SA**(A7-1.))*Y(I,1)
      DF2XB=A8*A9*(SS**(A9-1.))*(SA**A10)*Y(I,2)
      DF2XC=A8*A10*(SS**A9)*(SA**(A10-1.))*Y(I,2)-1.
      DD=(DF1XB*DF2XC-DF1XC*DF2XB)
      DXB=(-F1*DF2XC+F2*DF1XC)/DD
      DXC=(-F2*DF1XB+F1*DF2XB)/DD
      X(I,1)=X(I,1)+DXB
      X(I,2)=X(I,2)+DXC
      IF(ABS(DXB).GT.1.E-9.AND.ABS(DXC).GT.1.E-9)GOTO 9
      RETURN
      END
      SUBROUTINE KCALC(II,JJ,X,Y,DDD,VD,DIM,UL,B,E,M)
      REAL YS(20,4),B(4),X(20,4),Y(20,4),FN(4),E(20),LL
      S=3.1416*UL*(DIM/2.)**2.
      SMALLA=6.*VD/DDD
      BIGA=SMALLA*S
      PRINT*,'FIRST STAGE =',II,'     ','LAST STAGE =',JJ
      DO 203 J=1,M
      FN(J)=E(1)*(Y(JJ,J)-Y(II,J))
      YS(II,J)=B(J)*X(II,J)
      DYTOP=YS(II,J)-Y(II,J)
      YS(JJ,J)=B(J)*X(JJ,J)
      DYBOTT=YS(JJ,J)-Y(JJ,J)
  203 CONTINUE
      SUMDYO=0.
      SUMDYE=0.
      LL=(JJ-II+1)
      DO 201 J=1,M
      HHH=(Y(JJ,J)-Y(II,J))/(LL)
      DO 200 I=II+1,JJ-1,2
      YS(I,J)=B(J)*X(I,J)
      DYO=YS(I,J)-Y(I,J)
      SUMDYO=SUMDYO+DYO
  200 CONTINUE
      DO 204 I=II+2,JJ-2,2
      YS(I,J)=B(J)*X(I,J)
      DYE=YS(I,J)-Y(I,J)
      SUMDYE=SUMDYE+DYE
  204 CONTINUE
      DYMEAN=HHH*(DYE*2.+DYO*4.+DYTOP*DYBOTT)/3.
      YK=FN(J)/(BIGA*DYMEAN)
      YK=ABS(YK)
      PRINT*,'K MEAN =',YK,'       ','J=',J
  201 CONTINUE
      RETURN
      END
  107
```

```
@ED,U ANN.11
CASE UPPER ASSUMED
ED 16R1C. TUE-05/28/85-12:28:12-(33,34)
EDIT
0:
       1:9 2
       2:1000. 1004.36
       3:.0112
       4:.008
       5:7.484 .91 .02 .215 -7.2297
       6:-.0786 .0063 3.295 .7087 .2927
       7:0. 0. 0.
       8:0. 0. 0.
       9:0. 0. 0.
      10:0. 0. 0.
      11:300. .30 .05
      12:0. 0. 0.
      13:0. 0. 0.
      14:0. 0. 0.
      15:0. 0. 0.
      16:.076 1.8388 .108 4.668171E-3
EOF:16
0:
END ED. LINES:16 FIELDATA
KEC08A*ANN(1).11(34)


@xqt sha.2
```

COMPONENT NO. 1

STAGE NO.	COMPONENT	XI	YI	KI
1	1	.0226	.0112	.4946
2	1	.0534	.0334	.6255
3	1	.0880	.0637	.7236
4	1	.1216	.0977	.8033
5	1	.1507	.1308	.8684
6	1	.1358	.1133	.8339
7	1	.1174	.0924	.7873
8	1	.0917	.0663	.7197
9	1	.0485	.0288	.5938

COMPONENT NO. 2

STAGE NO.	COMPONENT	XI	YI	KI
1	2	.0078	.0080	1.0266
2	2	.0113	.0155	1.3723
3	2	.0145	.0187	1.2929
4	2	.0182	.0216	1.1856
5	2	.0229	.0251	1.0956
6	2	.0199	.0226	1.1370
7	2	.0161	.0187	1.1598
8	2	.0121	.0136	1.1244
9	2	.0083	.0079	.9501

APPENDIX VII

APPLICATIONS OF THE NRTL FOR CONCENTRATION PROFILE

FOUR COMPONENT SYSTEM THREE FEED CASE RUN NO. 17
COMPONENTS (1)BUTANOL (2) ACETIC-ACID (3) HEXANE (4) WATER
DILUENT SOLUTE BOTTOM SOLVENT TOP SOLVEN

TOTAL NUMBER OF STAGES	9
NUMBER OF COMPONENTS	4
EXTRACT REFLUX CODE	0
NUMBER OF SPECIFICATIONS	0

TOLERANCES ON COMPUTED VARIABLES
COMPOSITIONS .005000
FLOW RATES .005000

MAXIMUM FRACTIONAL CHANGE IN FLOW RATES PER ITERATION .500000

NUMBER OF FEED STREAMS	3
SOLVENT FEED IS	3

FEED	STAGE
1	1
2	5
3	9

COMP	FD 1	FD 2	FD 3
1	.000	.160	.000
2	.000	.300	.000
3	1.000	.540	.000
4	.000	.000	1.000
TOT	1.000	1.000	1.000

ITERATION NUMBER 46

DESCRIPTION	STAGE	RATE
RAFFINATE PRODUCT	9	1.648
EXTRACT PRODUCT	1	1.352

STAGE	RAF RATE	EXT RATE
1	1.092	1.352
2	1.203	1.444
3	1.495	1.555
4	.775	1.847
5	1.601	1.127
6	1.641	.953
7	1.655	.993
8	1.655	1.007
9	1.648	1.007

STAGE NUMBER 1

COMP	RAF FRAC	EXT FRAC	RAF RATE	EXT RATE
1	.0000010	.0263592	.000	.036
2	.0000010	.0166942	.000	.023
3	.9999970	.0000098	1.092	.000
4	.0000010	.9569369	.000	1.294
TOT	1.0000000	1.0000000	1.092	1.352

STAGE NUMBER 2

COMP	RAF FRAC	EXT FRAC	RAF RATE	EXT RATE
1	.0019384	.0231331	.002	.033
2	.0052509	.0146510	.006	.021
3	.9928087	.0000087	1.194	.000
4	.0000021	.9622073	.000	1.390
TOT	1.0000000	1.0000000	1.203	1.444

STAGE NUMBER 3

COMP	RAF FRAC	EXT FRAC	RAF RATE	EXT RATE
1	.0038757	.0198876	.006	.031
2	.0105007	.0125956	.016	.020
3	.9856203	.0000076	1.474	.000
4	.0000032	.9675092	.000	1.504
TOT	1.0000000	1.0000000	1.495	1.555

STAGE NUMBER 4

COMP	RAF FRAC	EXT FRAC	RAF RATE	EXT RATE
1	.0058131	.0166228	.005	.031
2	.0157505	.0105279	.012	.019
3	.9784320	.0000065	.758	.000
4	.0000044	.9728428	.000	1.797
TOT	1.0000000	1.0000000	.775	1.847

STAGE NUMBER 5

COMP	RAF FRAC	EXT FRAC	RAF RATE	EXT RATE
1	.0077508	.0133390	.012	.015
2	.0209998	.0084463	.034	.010
3	.9712437	.0000055	1.555	.000
4	.0000057	.9782092	.000	1.102
TOT	1.0000000	1.0000000	1.601	1.127

STAGE NUMBER 6

COMP	RAF FRAC	EXT FRAC	RAF RATE	EXT RATE
1	.0114483	.0132578	.019	.013
2	.0244036	.0000000	.040	.000
3	.9636258	.0001658	1.581	.000
4	.0005223	.9865764	.001	.940
TOT	1.0000000	1.0000000	1.641	.953

STAGE NUMBER 7

COMP	RAF FRAC	EXT FRAC	RAF RATE	EXT RATE
1	.0122698	.0079368	.020	.008
2	.0309419	.0018294	.051	.002
3	.9566232	.0000653	1.583	.000
4	.0001651	.9901685	.000	.983
TOT	1.0000000	1.0000000	1.655	.993

STAGE NUMBER 8

COMP	RAF FRAC	EXT FRAC	RAF RATE	EXT RATE
1	.0135625	.0033798	.022	.003
2	.0367498	.0008744	.061	.001
3	.9496788	.0000581	1.572	.000
4	.0000089	.9956878	.000	1.003
TOT	1.0000000	1.0000000	1.655	1.007

STAGE NUMBER 9

COMP	RAF FRAC	EXT FRAC	RAF RATE	EXT RATE
1	.0154998	.0000010	.026	.000
2	.0419996	.0000010	.069	.000
3	.9424906	.0000010	1.553	.000
4	.0000100	.9999970	.000	1.007
TOT	1.0000000	1.0000000	1.648	1.007

FINAL MATERIAL BALANCE

INPUT SUMMARY

	COMP 1	COMP 2	COMP 3	COMP 4	TOTAL
FEED 1	.000	.000	1.000	.000	1.000
FEED 2	.160	.300	.540	.000	1.000
FEED 3	.000	.000	.000	1.000	1.000
TOTAL	.160	.300	1.540	1.000	3.000

OUTPUT SUMMARY

	COMP 1	COMP 2	COMP 3	COMP 4	TOTAL
RAF PROD	.026	.069	1.553	.000	1.648
EXT PROD	.036	.023	.000	1.294	1.352
TOTAL	.061	.092	1.553	1.294	3.000

REFERENCES

1. Al-Saadi, A.N., and Jeffreys, G.V., A.I.Ch.E.J., 27, 5, 754 (1981).

2. Al-Saadi, A.N., PhD Thesis, University of Aston in Birmingham (1979).

3. Renon, H. and Prausnitz, J.M., A.I.Ch.E.J., 14, 135, (1968).

4. Renon, H. and Prausnitz, J.M., Ind. Eng. Chem. Proc. Des. Devel., 8, 413 (1969).

5. Fredenslund, A., Jones, R.L. and Prausnitz, J.M., A.I.Ch.E.J., 21, 1086 (1975).

6. Fredenslund, A., Gmehling, J. and Rasmussen, P., Elsevier, Amsterdam, (1977).

7. Abrams, D.S. and Prausnitz, J.M., A.I.Ch.E.J., 21, 62 (1975).

8. Pratt, H.R.C., Ind. Eng. Chem., 30, 475, 597 (1954).

9. Oliver, E.D., Differential Separation Processes, John Wiley, New York, p362, (1966).

10. Teh, C., Malcomn, H.I. and Hanson, C., Handbook of Solvent Extraction, John Wiley and Sons Press, (1983).

11. Scheibel, E.G., Chem. Eng. Prog. 44, 681 (1948).

12. Scheibel, E.G., A.I.Ch.E.J., 2, 74 (1956).

13. Scheibel, E.G., Ind. Eng. Chem, 42, 74 (1950).

14. Honekamp, J.R. and Burkhart, L.E., Ind. Eng. Chem. Proc. 39, 1932 (1947).

15. Piper, H.B., PhD Thesis, University of Manchester (1969).

16. Lewis, J.B., Jones, I. and Pratt, H.R.C., Trans. Inst. Chem. Eng., 129, 126 (1951).

17. Bonnet, J.C., PhD Thesis, University of Aston in Birmingham (1982).

18. Gayler, R., Roberts, M.W. and Pratt, H.R.C., Trans. Inst. Chem. Eng., 31, 57 (1953).

19. Gayler, R. and Pratt, H.R.C., Trans. Inst. Chem. Eng. 29, 110 (1951).

20. Jeffreys, G.V., Davies, G.A. and Piper, H., I.S.E.C., 71. The Hague, (1971).

21. Reman, G.H., U.S. Patent 21, 601, 674, (June 24, (1952)).

22. Stienour, H.H., Ind. Eng. Chem., 36, 618 (1944).

23. Lapidus, L. and Elgin, J.C., A.I.Ch.E.J., 19, 851, (1957).

24. Uhl, V.W., "Mixing Theory and Practice", Academic Press, (1966).

25. Sitaramayya, T. and Ladha, G.S., Chem. Eng. Sci., 13, 263, (1961).

26. Treybal, R.E., Ind. Eng. Chem., 47, 2435, (1955).

27. Jeffreys, G.V., Chemical Engineering Practice, Volume 9, Ed. Cremer and Warner, Butterworths, (1965).

28. Arashmid, M. and Jeffreys, G.V., A.I.Ch.E.J., 26, 1 p51-55.

29. Thornton, J.D. Bouyoatiotes, B.A., Chem. Eng. Symposium Series, 26, 43, (1967).

30. Clarks, S.I. and Sawistowski, H., Trans. Inst. Chem. Eng., 56, 50, (1978).

31. Luhning, R.W. and Sawistowski, H., Proc. I.S.E.C., Volume 11, 873, (1971).

32. Quin, J.A., and Sigloh, D.B., Cand. J. Chem. Eng., 15, 41, (1963).

33. Strand, C.P., Olney, R.B. and Ackerman, G.H., A.I.Ch.E.J., 8, 252, (1962).

34. Al-Hassan, T.S., PhD Thesis, University of Aston in Birmingham, U.K., (1979).

35. Pratt, H.R.C. and Baird, M.H.L., Handbook of Solvent Extraction, John Wiley and Sons Press, 199, (1983).

36. Hanson, C., Ed. Recent Advances in Liquid-Liquid Extraction, Pergammon Press, New York, (1971).

37. Kolmogoroff, A.N., Dokl. Akad. Nauk. USSR, 66, 825, (1949).

38. Hinze, J.O., A.I.Ch.E.J., 1, 289 (1955).

39. Sterling, G.V. and Seriven, L.E., A.I.Ch.E.J., 5, 514, (1959).

40. Davies, J.T., Turbulence Phenomena, Academic Press, New York, (1972).

41. Cockbain, E.G. and McRoberts, T.S., J. Colloidal Sci., 8, 440, (1953).

42. Gillespie, T. and Rideal, E.K., Faraday Soc., 52, 1973, (1956).

43. Neilsen, L.E., Wall, R., and Adams, G., J. Coll. Sci., 13, 441, (1958).

44. Groothuis, H. and Zuiderweg, F.J., Chem. Eng. Sci. 12, 288, (1960).

45. Treybal, R.E., Liquid Extraction, 2nd Ed. McGraw Hill, New York (1963).

46. Al-Hemiri, A.A.A., PhD Thesis, University of Aston in Birmingham, U.K., (1976).

47. Sarkar, PhD Thesis, University of Aston in Birmingham, U.K. (1976).

48. Arnold, D.R., PhD Thesis, University of Aston in Birmingham, U.K. (1974).

49. Jordan, D.G., Chemical Process Development, Paret 2, Interscience, New York, (1968).

50. Masters, K. Spray Drying, George Godwin, Halstead Press, (1976).

51. Jeffreys, G.V., Al-Aswad, K and Mumford, C.J. Sep. Sci. and Tech., 1619, p1217-1245, (1981)

52. Klee, A.J. and Treybal, R.E., A.I.Ch.E.J., 2, 444, (1956).

53. Reman, G.H. and Olney, Chem. Eng. Progr. 51, 141, (1955).

54. Olney, R.B., A.I.Ch.E.J., 10, 827, (1964).

55. Mugele, R.A. and Evans, H.D., Ind. Eng. Chem., 43, 1317, (1951).

56. Chartes, R.H. and Korchinsky, W.J., Transact. Inst. Chem. Eng., 53, 247, (1975).

57. Korchinsky, W.J. and Azinadeh-Khataylo, Chem. Sci. 31, 871, (1976).

58. Davies, G.A. and Jeffreys, G.V., Filtr. Sep., 6, 349, (1969).

59. Licht, W. and Pansing, W.F., Ind. Eng. Chem., 45, 1885, (1953).

60. Coulson, Z.M. and Skinner, S.J., Chem. Eng. Sci., L971, (1952).

61. Popovitch, A.T., Jervis, R.E. and Trass, O., Chem. Eng. Sci., L9, 357, (1964).

62. Hu, S. and Kintner, R.C., A.I.Ch.E.J., 1, 42, (1955)

63. Litch, W., and Narasimhamurthy, G.S.R., A.I.Ch.E.J., 1, 336, (1955).

64. Klee, A.J., and Treybal, R.E., A.I.Ch.E.J., 2, 444, (1956).

65. Krishna, P.M., Venkateswarlu, D., and Narasimhamurthy, G.S.R., J. Chem. Eng. Data., 4, 336, 340, (1959).

66. Devatta, S. and Chandrasekharan, Paper No. H_2-21, C.H.I.S.A. Conference, The Prague, (1978).

67. Pratt, H.R.C., Handbook of Solvent Extraction, John Wiley and Sons, New York, (1983), Interphase Mass Transfer, p91.

68. Higbie, R., Transact. A.I.Ch.E.J., 31, 365, (1935).

69. Linton, M. and Sutherland, Chem. Eng. Sci., 12, 214, (1960).

70. Rowe, P.N, et al., Trans. Inst. Chem. Eng., 42, 14, (1965).

71. Kinard, G.E., Manning, F.S., and Manning, W.P., Brit. Chem. Eng., 8, 326, (1963).

72. Boussinesq, J., C.R. Acad. Sci., Paris, 156, 983, 1035, 1124, (1913).

73. Garner, F.H. and Tayeban, H., An. R. Soc., Esp. Quim., 56B, 479, (1960).

74. Hughmark, G.A., Ind. Eng. Chem. Funds., 6, 408, (1967).

75. Korchinsky, W.J., and Cruz-Pinto, J.J.C., Chem. Eng. Sci., 34, 55, (1979).

76. Johnson, A.I., and Hamielec., A.I.Ch.E.J., 6, L45, (1960).

77. Brunson, R.J. and Wellek, R.M., Cand. J. Chem. Eng., 48, 267, (1970).

78. Skelland, A.H.P. and Welleck, R.M., A.I.Ch.E.J., 10, 491, (1964).

79. Rose, P.M. and Kintner, R.C., A.I.Ch.E.J., 12, 530, (1960).

80. Crank, J., The Mathematic of Diffision, Oxford University Press, London, (1956).

81. Anon, Pet. Processes, 10, 230, (1955).

82. Newman, A.B., Transact. Inst. Chem. Eng., 27, 310, (1931).

83. Treybal, R.E., chem. Eng. Progr. 62, 9, 67, (1966).

84. Kronig, R. and Brink, J.C., App. Sci. Res., A-2, 142, (1960).

85. Handlos, A.E. and Baron, T., A.I.Ch.E.J., 3, 127, (1957).

86. Olander, D.R., A.I.Ch.E.J., 12, 1018, (1966).

87. Gunn, R., J. of Geophys. RMs, 54, 383, (1949).

88. Schoeder, R.R. and Kintner, R.C., A.I.Ch.E.J., L1, 5, (1965).

89. Lamb, H., (Hydrodynamics), Cambridge University, (1957).

90. Garner, F.H., Jenson, V.C. and Keey, R., T.I.C.E., 37, 197, (1957).

91. Linton, M. and Sutherland., Chem. Eng. Sci, 17, 214, (1960).

92. Heertjes, P.M., and De Nie, L.H., "Mass Transfer to Drops", Recent Advances in Liquid-Liquid Extraction., Ed. Hanson, C., Pergammon Press, (1971).

93. Jeffreys, G.V. and Ellis, E.M.R., C.H.I.S.A., (1962).

94. Misek, T. and Rod, V., Paper presented on C.H.I.S.A., II Congress, Marienbad, Czechoslovakia, (1965).

95. Garner, F.H. and Hole, A.R., Chem. Eng. Sci., 20, 737, (1965).

96. Treybal, R.E., Ind. Eng. Chem. 36, 875, (1944).

97. Campbell, J.A., Ind. Eng. Chem., 36, 1158, (1944).

98. Banker, A.V., Hunter, T.G. and Nash, A.W., Ind. Eng. Chem., 12, 35, (1940).

99. Bashman, L., Ind. Eng. Chem., 12, 38, (1940).

100. Bancroft, W.D., J. Phys. Rev., 3, 21, 114, 193, (1985).

101. Othmer, D.F. and Tobias, P.E., Ind. Eng. Chem., 34, 693, (1942).

102. Hand, D.B., J. Phys. Chem. 34, 1961, (1930).

103. Wilson, G.M., J. Am. Chem. Soc., 86, 127, (1964).

104. Abrams, D.S. and Prausnitz, J.M., A.I.Ch.E.J., 21, 62, (1975).

105. Freden, A., Jones, R.L. and Prausnitz, J.M., A.I.Ch.E.J., 21, 1086, (1975).

106. Rod, V., Chem. Eng. Sci., 11, 483, (1966).

107. Sheikh, A.R., Ingham, J. and Hanson, C., Transact. Inst. Chem. Eng., 50, 199, (1972).

108. Wakao, N., K aguei, S. and Smith, J.M., J. Chem. Eng., Japan, 12, 481, (1979).

109. Rod, V., Recent Advances in Liquid-Liquid Extraction, Ed. C. Hanson, (1971).

110. Prochazka, J. and Jirichy, V., Chem. Eng. Sci., 31, 179, (1979).

111. Scheibel, E.G., Ind. Eng. Chem., 46, 16, (1954).

112. Ladha, G.S. and Degaleesan, T.E., Transport Phenomena in Liquid Extraction, Tata Mc Graw Hill, New Delhi, (1976).

113. Reid, R.C., Prausnitz, M.J. and Sherwood, K.T., The Properties of Gases and Liquids, McGraw Hill, (1977).

114. Van Dijeck, W.J.D., U.S. Patent 2011, 186 (1935)

115. Johnson, A.I. and Hamielec, A.E., A.I.Ch.E. Journal 6, 145, (1960).